

**School of Molecular and Life Sciences**

**Chemical Characterisation and Source Attribution of Inorganic  
Nitrate-based Homemade Explosives**

**Joshua D'Uva**

**0000-0002-4629-2120**

**This thesis is presented for the Degree of  
Doctor of Philosophy  
of  
Curtin University**

**November 2022**

## **Declaration**

To the best of my knowledge and belief this thesis contains no material previously published by any other person except where due acknowledgments has been made.

This thesis contains no material which has been accepted for the award of any other degree or diploma in any university.

This thesis aims to address many of the fundamental knowledge gaps surrounding select inorganic based HMEs in order to improve our understanding of how explosive precursors are sourced and prepared and to determine the maximum amount of identifying and discriminatory information that can be gained from an array of analytical techniques.

Signature:

Date: 24/11/2022

## **Abstract**

Homemade explosives (HMEs) and improvised explosive devices (IEDs) are responsible for some of the most devastating explosive attacks that have occurred throughout history and continue to pose a legitimate threat as precursors, materials and ‘how-to’ internet guides have become increasingly more accessible. Although any explosive has the potential to be homemade, HMEs are often based on inorganic nitrate salts as they are easily prepared from commercially available products with little knowledge of chemical synthesis. Within the forensic investigation of a HME incident, the successful recovery, analysis, and identification of the explosive material summarise the core objectives of the forensic scientist, as this information can be used to generate leads and establish links based on previously gathered evidence. However, once the explosive has been identified, further forensic examination of the explosive residues is often left incomplete, with no attempt to identify what precursors were used, where they were sourced and how the explosive was prepared. To improve the investigative and analytical protocols and respond to the critical operational need to increase the understanding of nitrate based HMEs, an investigative strategy was developed and used for the complete forensic characterisation, identification and source attribution of several nitrate based HMEs. The information presented is a significant addition to the forensic intelligence literature as well as providing a basis for the continuous improvement of forensic chemical analysis and source determination procedures.

The explosives investigated in this work include nitrate based party sparklers, ammonium nitrate (AN), urea nitrate (UN) and nitrourea (NU). A comprehensive investigation was performed on each explosive that involved three main stages: a market study of alternative precursor sources and synthesis from commercial ingredients, the complete forensic characterisation using routine and non-routine analytical techniques, and an investigation into the source attribution using chemometrics on pre- and post-blast residues. This strategy resulted in a substantial amount of information that applies to forensic case procedures within law enforcement, as well as forensic and military agencies that rely on gathered intelligence for HME disruption and prevention.

As party sparkler based HMEs make up the majority of explosive-related casework in Western Australia (WA), investigations were first performed on the characterisation and source attribution of 19 distinct party sparkler products that were sourced within Australia. Analysis with routine instrumentation including ion chromatography (IC), scanning electron microscopy (SEM) and infrared spectroscopy (IR) revealed that although the primary oxidiser and fuel components can be identified, no further discriminatory information could be obtained. Analysis of unburnt and burnt residues from eight out of the 19 brands by inductively coupled plasma mass spectrometry (ICPMS) found that each had a highly characteristic elemental profile, which was used to effectively discriminate between them when combined with principal component analysis (PCA) and linear discriminant analysis (LDA). Subsequent studies applying the same analytical and chemometric procedures to post-blast sparkler residues were also performed, where intact post-blast material was recovered from several IEDs prepared using party sparklers from four brands. Despite being collected from an exploded device, the source of the post-blast residues from all four brands could be identified as full separation of samples was achieved within the PC scores plots. Results from chemometric analysis indicate that ICPMS coupled with PCA-LDA is extremely effective at discriminating between party sparkler products and can potentially identify the source of party sparkler material from analysis of post-blast debris. This information is potentially highly beneficial to forensic casework involving the investigation of party sparkler based devices and in that it may further assist in establishing links between a seized device and the person/s responsible.

AN has also been frequently used as a HME despite restrictions imposed on obtaining high-purity forms across many countries. Nine distinct AN products were sourced and prepared from commercial ingredients and separated into two groups: 'pure form' and homemade. Products that were sourced in their original form and did not require any further extraction or synthesis were classed as 'pure form', and products that were synthesised from ammonium sulfate and calcium nitrate were classed as homemade. It was shown that all analytical techniques employed were capable of distinguishing between pure and homemade AN. This demonstrates that some source information can be quickly obtained using several routine instruments. The source determination capabilities of using data from IR, X-ray diffraction (XRD) and ICPMS were further assessed in combination with PCA-LDA. It was found that some additional source

information could be accurately obtained using spectral data and diffraction patterns, however, the use of trace elemental data proved highly effective as all AN products could be distinguished. These results show that in addition to discerning between pure form sources such as lab grade and explosive grade AN, a homemade product can potentially be linked back to the commercial ingredients used within synthesis as well as specific brands of fertilisers.

UN is often compared with AN as both are fertiliser, nitrate based HMEs with comparable explosive properties. UN can easily be prepared from urea, which remains unregulated and so could become the preferred choice as a fertiliser based HME. Eight distinct UN products were prepared from a diverse range of commercial ingredients and a substantial amount of characteristic data was collected from IR and Raman spectroscopy, XRD, SEM, IC and ICPMS. Again, PCA-LDA performed with elemental data proved to be highly effective as all products were discerned using the concentration data from four elements, indicating that UN explosive can be traced back to several distinct sources of urea as well as specific brands of urea fertiliser. Characteristic data was also reported for NU products that were synthesised from homemade UN. Chemometric analysis demonstrated the capacity to distinguish between NU products based on the minor variation within elemental profiles, however, they did not correlate to their respective UN precursors. Source attribution capabilities were further assessed on post-blast residues collected from firings of five charges containing 200g each of a different UN product. Across these post-blast experiments, it was discovered that UN was detonator sensitive, which greatly contributes to the forensic intelligence of UN as an HME as this characteristic is often used to classify explosives into certain groups and will also improve our understanding of the different ways UN based devices can be functioned. Source attribution results from post-blast investigations were mostly inconclusive, however, the experimental design and recovery and analysis protocols will aid in future research involving the chemical analysis of residues from high-order explosives.

## **Acknowledgment of Country**

We acknowledge that Curtin University works across hundreds of traditional lands and custodial groups in Australia, and with First Nations people around the globe. We wish to pay our deepest respects to their ancestors and members of their communities, past, present, and to their emerging leaders. Our passion and commitment to work with all Australians and peoples from across the world, including our First Nations peoples are at the core of the work we do, reflective of our institutions' values and commitment to our role as leaders in the Reconciliation space in Australia.

## Acknowledgments

I would like to take this opportunity to express my gratitude and appreciation to the many people within my life and across collaborating agencies, as without their guidance and support, this research would not have been possible.

Firstly, to Simon Lewis, I consider myself extremely fortunate to have had you as my supervisor for the last six years and I cannot thank you enough for your ongoing mentorship and support throughout my studies. Your persistence in showing me the value of my work and teaching me to be proud of my achievements no matter how small they may seem, was hugely motivating for me. I am certain that the skills and knowledge I have gained under your guidance will continue to have a positive impact in my future studies, work, and research.

To David DeTata, thank you for being a major supporter of me and my work from the first day we met. Throughout the last four years you have given me an enormous amount of invaluable personal and professional guidance that I am forever grateful for. The range days you were able to organise were by the far the best part of the project, and so I thank you for the opportunity to not only witness actual explosions, but also the professional and personal relationships I was able to build with the people involved. How many students can say they threw a Molotov cocktail during their project? And thank you for adding all my works to the highly exclusive trophy cabinet at ChemCentre, my contribution to science will forever be known thanks to you.

To everyone at ChemCentre, thank you for being so welcoming and supportive of me during my research. A large portion of this research would not be possible without access to the ChemCentre laboratories and instrumentation. To Matt Freeman, thank you for putting up with my constant requests to use your one and only ICPMS, a major portion of this work would not have been possible without your contribution. To Chris May, thank you for assisting me with ICPMS analysis, and for being a major contributor in my first published journal article from this work. To Kari Pitts, thank you teaching me all about SEM and XRD, and for the ongoing support throughout many areas of this work. To Ryan Fillingham and Robert Dunsmore, I am extremely grateful for the time you spent assisting me in all aspects of this project during the last four years. Your guidance with instrumentation, designing experiments and data

analysis (just to name a few) was invaluable. A special thank you also to Melissa Davies for your continuous support and encouragement throughout the project.

To all the members in the WABRU, a big thank you for giving me the opportunity to perform several field work experiments. I am extremely grateful for the time and resources you spent on assisting me in collecting data for my project, the post-blast experiments would never have been possible without your ongoing contribution and support. A special thank you also for the knowledge you provided on all things explosive and allowing me to participate in several range days and workshops outside of my project.

To the Forensic and Analytical Research Group, I could not have asked for a better group of colleagues and friends to have by my side throughout my research. I would like to thank all past and present members for the collective knowledge and support you gave me. And a big thank for the fun times shared at morning tea, pub lunches, conferences, and Christmas parties. To Georgina, who always made time to review my work and assist me with chemometrics. A very special mention to Rhiannon, who was always there to give me a helping hand and was a constant source of entertainment throughout the day, and I wish you all the best in Canada and in your future studies. A special mention also to Talia, Jemmy, Aaron and Anna, you guys made the last conference trip one to remember!

To all my colleagues and friends at Curtin, I could always rely on the fun times spent together at morning tea and lunch, to get me through the day. A special thank you to Lee, David, Brad and Alex, I am grateful to have gone through my undergraduate, Honours and PhD studies with all of you, and thank you for all the great times shared together in and outside of work.

To my family, for the endless amount of support during both my PhD and previous studies. To Mum and Dad, thank you for always believing in me and for your constant love and support, no matter how busy you were with your own work and problems, you were always there to help me when I needed it most, which I am forever grateful for. A special thank you to my brothers Nathan and Ryan, and my sister Sara, for your ongoing support throughout my studies.



Finally, to my partner Rhiannon, thank you for always being by my side throughout the last five years of my studies. Thank you for being there during the late nights, early mornings, and always being my number one supporter, no matter the circumstance. I and forever grateful for your ongoing love and support as I cannot imagine being able to have completed this thesis without you in my life.

This research was supported by an Australian Government Research Training Program (RTP) scholarship.

## Contribution to Others

The following have contributed to the thesis, with contributions being listed in the form of CRediT (Contributor Roles Taxonomy) statements for each chapter (see <https://www.elsevier.com/authors/journal-authors/policies-and-ethics/creditauthor-statement>)

Chapters 1 to 7:

Professor Simon W. Lewis (Principal Supervisor): Project administration, Supervision, Conceptualisation, Writing – Review & Editing

Dr David DeTata (Co-Supervisor): Supervision, Conceptualisation, Resources, Writing – Review & Editing

Chapter 3:

Portions of this chapter have been published in *Analytical methods* see Appendix for details.

Dr Chris May, Ryan Fillingham, Robert Dunsmore: Methodology, Investigation, Resources, Writing – Review & Editing

Chapter 4:

Portions of this chapter have been published in *Forensic Chemistry* see Appendix for details.

Ryan Fillingham, Robert Dunsmore: Methodology, Investigation, Writing – Review & Editing

Chapter 5:

Portions of this chapter have been published in *Forensic Chemistry* see Appendix for details.

Ryan Fillingham: Methodology, Investigation, Writing – Review & Editing

## Publications

This dissertation contains work which has been submitted for publication in the following peer reviewed journals:

**Joshua A. D’Uva**, David DeTata, Christopher D. May, Simon W. Lewis. Investigations into the source attribution of party sparklers using trace elemental analysis and chemometrics. *Analytical methods* **2020** 12, 4939-4948

➤ Front cover article

**Joshua A. D’Uva**, David DeTata, Ryan Fillingham, Robert Dunsmore, Simon W. Lewis. Synthesis and characterisation of homemade urea nitrate explosive from commercial sources of urea. *Forensic Chemistry* **2021** 26, 1-9 DOI: <https://doi.org/10.1016/j.forc.2021.100369>

**Joshua A. D’Uva**, David DeTata, Simon W. Lewis. Source determination of homemade ammonium nitrate using ATR-FTIR spectroscopy, trace elemental analysis and chemometrics. *Forensic Chemistry* **2022** 28, 1-11 DOI: <https://doi.org/10.1016/j.forc.2022.100411>

➤ Front cover article

In addition, the following book chapters were published during the course of this dissertation:

**Joshua A. D’Uva**, David DeTata. Improvised explosive devices. *Encyclopedia of Forensic Sciences*. 3<sup>rd</sup> ed; Elsevier Ltd; 2022. p. 224-231.

David DeTata, Ryan Fillingham, **Joshua A. D’Uva**. Overview of explosives. *Encyclopedia of Forensic Sciences*. 3<sup>rd</sup> ed; Elsevier Ltd; 2022. p. 356-390.

## Conference Presentations

Selected aspects of the work contained within this thesis have been presented, or have been accepted for the presentation, at the following conferences:

### Oral Presentations

Source attribution of party sparklers; comparison between pre-blast, burnt and post-blast residues, *Curtin University School of Molecular and Life Sciences Symposium*, Perth, 2020

Characterisation, identification and source attribution of homemade explosives and their precursors, *Australian and New Zealand Forensic Science Society – Western Australian Forum*, Perth, 2021 (**Invited speaker**)

Source determination of party sparkler based improvised explosive devices, *Florida International University Annual Forensic Science Symposium*, 2021 (**Online**)

Characterisation, identification and source attribution of homemade explosives and their precursors, *Australian and New Zealand Forensic Science Society 25<sup>th</sup> International Symposium*, Brisbane, 2022

- 1<sup>st</sup> place presentation prize

### Poster Presentations

Preliminary investigations into the source attribution of party sparklers using trace elemental analysis and chemometrics, *Royal Society of Chemistry Twitter Conference*, 2019 (**Online**)

Preliminary investigations into the source attribution of party sparklers using trace elemental analysis and chemometrics, *Royal Australian Chemical Institute of Research and Development Topics Conference*, Adelaide, 2019

- 1<sup>st</sup> place poster presentation prize

Source attribution of party sparklers; comparison between pre-blast, burnt and post-blast residues, *Royal Society of Chemistry Twitter Conference*, 2021 (**Online**)

Source determination of homemade ammonium nitrate using ATR-FTIR spectroscopy, trace elemental analysis and chemometrics, *Curtin University School of Molecular and Life Sciences Symposium*, Perth, 2021

# Table of Contents

Declaration .....	i
Abstract .....	ii
Acknowledgment of Country .....	v
Acknowledgments.....	vi
Contribution to Others .....	ix
Publications .....	x
Conference Presentations .....	xi
Table of Contents .....	xiii
List of Figures .....	xxi
List of Tables.....	xxix
List of Abbreviations.....	xxxii
Chapter 1. Introduction .....	1
1.1 Introduction .....	2
1.2 Explosives .....	3
1.2.1 Types of explosives .....	4
1.2.2 Improvised explosive devices .....	7
1.2.3 Forensic investigation of incidents involving explosives .....	10
1.3 Nitrate based HMEs – preparation and market availability of precursors .....	11
1.3.1 Ammonium nitrate .....	16
1.3.1.1 Manufacture and commercial use .....	16
1.3.1.2 Homemade ammonium nitrate .....	16
1.3.1.3 Additional fuel sources .....	17
1.3.2 Urea nitrate .....	17
1.3.2.1 Legitimate manufacture and uses .....	17
1.3.2.2 Homemade urea nitrate .....	18

1.3.2.3 Nitrourea and analogues.....	19
1.3.3 Pyrotechnics.....	20
1.3.3.1 Legitimate uses and manufacture.....	20
1.3.3.2 Homemade pyrotechnic compositions and market availability .....	20
1.3.3.3 Use of pyrotechnics as a HME.....	21
1.4 Forensic chemical analysis of HMEs .....	21
1.4.1 Spectroscopy .....	22
1.4.2 Microscopy and X-ray techniques .....	23
1.4.3 Separation methods.....	24
1.5 Application of chemometrics in explosives analysis.....	25
1.5.1 Chemometric techniques.....	26
1.5.1.1 Principal component analysis.....	26
1.5.1.2 Linear discriminant analysis.....	27
1.5.2 Discrimination and source attribution of HMEs involving chemometrics	28
1.6 Forensic intelligence of HMEs .....	29
1.7 Summary and aims .....	30
Chapter 2. Experimental methods and instrumentation .....	34
2.1 Introduction .....	35
2.2 Experimental considerations .....	35
2.3 Preparation of homemade explosives.....	36
2.3.1 Ammonium nitrate.....	36
2.3.1.1 Synthesis from commercial sulfate of ammonia fertiliser and laboratory reagents .....	36
2.3.1.2 Synthesis from Black Marvel and African Violet Food.....	37
2.3.2 Urea nitrate .....	37
2.3.2.1 Synthesis using chemical grade urea and urea fertiliser .....	37

2.3.2.2 Synthesis using urea based cold packs .....	37
2.3.2.3 Synthesis using diesel exhaust fluid.....	38
2.3.2.4 Synthesis using alternative fertiliser mixtures .....	38
2.4 Instrumentation.....	38
2.4.1 Infrared spectroscopy.....	38
2.4.2 Raman spectroscopy .....	39
2.4.3 Ion chromatography .....	39
2.4.4 Scanning electron microscopy .....	40
2.4.5 Gas chromatography mass spectrometry .....	40
2.4.6 X-ray diffraction .....	41
2.4.7 Inductively coupled plasma mass spectrometry .....	41
2.4.8 Chemometric methods.....	42
2.4.8.1 Chemometric analysis using spectral data from ATR-FTIR spectroscopy .....	42
2.4.8.2 Chemometric analysis using X-ray diffraction patterns.....	42
2.4.8.3 Chemometric analysis using elemental concentration data from ICP- MS .....	43
2.4.8.4 ANOVA based feature selection.....	43
Chapter 3. Multi-technique analysis of homemade explosives containing commercial party sparklers .....	45
3.1 Introduction .....	46
3.2 Experimental .....	48
3.2.1 Party sparkler collection .....	48
3.2.2 Infrared spectroscopy.....	51
3.2.3 Gas chromatography mass spectrometry .....	51
3.2.4 Ion chromatography .....	52
3.2.5 Scanning electron microscopy .....	52



3.2.6 Inductively coupled plasma mass spectrometry .....	53
3.2.7 Chemometrics and feature selection .....	53
3.2.7.1 Chemometric analysis using spectral data from infrared spectroscopy .....	53
3.2.7.2 Feature selection and element reduction .....	53
3.2.7.3 Chemometric analysis using elemental concentration data from ICPMS .....	54
3.3 Results and Discussion .....	54
3.3.1 Physical analysis .....	54
3.3.2 Preliminary investigations .....	54
3.3.3 Characterisation of party sparklers .....	55
3.3.3.1 Infrared spectroscopy .....	55
3.3.3.2 Gas chromatography mass spectrometry .....	57
3.3.3.3 Ion chromatography .....	59
3.3.3.4 Scanning electron microscopy .....	63
3.3.3.5 Inductively coupled plasma mass spectrometry .....	63
3.3.4 Source attribution of party sparklers with chemometrics .....	66
3.3.4.1 Discrimination of party sparklers by ATR-FTIR spectroscopy .....	66
3.3.4.2 Discrimination of party sparklers using trace elemental data .....	77
3.4 Conclusions .....	86
Chapter 4. Preparation, characterisation, and source attribution of homemade ammonium nitrate as an explosive precursor .....	88
4.1 Introduction .....	89
4.2 Methodology .....	92
4.2.1 Sources of ammonium nitrate and precursors.....	92
4.2.2 Preparation of ammonium nitrate products .....	93
4.2.3 Infrared spectroscopy .....	94

4.2.4 Raman spectroscopy .....	95
4.2.5 Ion chromatography .....	95
4.2.6 Scanning electron microscopy .....	95
4.2.7 X-ray diffraction .....	95
4.2.8 Inductively coupled plasma mass spectrometry .....	95
4.2.9 Chemometrics .....	96
4.2.9.1 Chemometric analysis using spectral data from infrared spectroscopy .....	96
4.2.9.2 Chemometric analysis using X-ray diffraction patterns.....	96
4.2.9.3 Chemometric analysis using elemental concentration data from ICPMS.....	96
4.3 Results and Discussion .....	96
4.3.1 Preliminary assessment of ammonium nitrate products .....	96
4.3.2 Characterisation of ammonium nitrate products.....	98
4.3.2.1 Infrared and Raman spectroscopy .....	98
4.3.2.2 Ion chromatography .....	101
4.3.2.3 Scanning electron microscopy .....	102
4.3.2.4 X-ray diffraction.....	105
4.3.2.5 Inductively coupled plasma mass spectrometry.....	107
4.3.3 Source attribution of ammonium nitrate with chemometrics .....	110
4.3.3.1 Discrimination of ammonium nitrate by ATR-FTIR spectroscopy ..	110
4.3.3.2 Discrimination of ammonium nitrate using X-ray diffraction .....	123
4.3.3.3 Discrimination of ammonium nitrate using trace elemental data .....	126
4.4 Conclusions .....	131
Chapter 5. Investigations into the preparation and source attribution of homemade urea nitrate and nitrourea explosive .....	133
5.1 Introduction .....	134

5.2 Experimental .....	136
5.2.1 Sources of urea.....	136
5.2.2 Preparation of urea nitrate products.....	137
5.2.3 Infrared spectroscopy.....	138
5.2.4 Raman spectroscopy .....	138
5.2.5 Ion chromatography.....	138
5.2.6 Scanning electron microscopy.....	139
5.2.7 X-ray diffraction .....	139
5.2.8 Inductively coupled plasma mass spectrometry .....	139
5.2.9 Chemometrics .....	139
5.2.9.1 Chemometric analysis using spectral data from infrared spectroscopy .....	139
5.2.9.2 Chemometric analysis using X-ray diffraction patterns.....	140
5.2.9.3 Chemometric analysis using elemental concentration data from ICPMS.....	140
5.3 Results and discussion.....	140
5.3.1 Preliminary assessment of urea nitrate prepared from urea.....	140
5.3.2 Characterisation of urea nitrate.....	142
5.3.2.1 Infrared and Raman spectroscopy .....	142
5.3.2.2 Scanning electron microscopy .....	148
5.3.2.3 X-ray diffraction.....	150
5.3.2.4 Ion chromatography .....	151
5.3.2.5 Inductively coupled plasma mass spectrometry.....	151
5.3.3 Source attribution of urea nitrate using chemometrics .....	154
5.3.3.1 Discrimination of urea nitrate by ATR-FTIR spectroscopy .....	154
5.3.3.2 Discrimination of urea nitrate with X-ray diffraction .....	165

5.3.3.3 Discrimination of urea nitrate by ICPMS .....	167
5.4 Preparation and source attribution of homemade nitrourea .....	171
5.4.1 Synthesis of nitrourea using urea nitrate and sulfuric acid .....	171
5.4.2 Preliminary assessment of nitrourea products .....	172
5.4.3 Infrared spectroscopy .....	173
5.4.2 Inductively coupled plasma mass spectrometry .....	174
5.5 Conclusions .....	177
Chapter 6. Recovery and source attribution of post-blast residues from party sparkler and UN-based improvised explosive devices .....	179
6.1 Introduction .....	180
6.2 Experimental .....	184
6.2.1 Party sparkler experiments.....	184
6.2.1.1 Materials.....	184
6.2.1.2 Preparation of party sparkler based IEDs.....	185
6.2.1.3 Preparation of party-sparkler based pipe bombs.....	186
6.2.1.4 Sample processing and analysis .....	187
6.2.1.5 Chemometric analysis .....	188
6.2.2 Urea nitrate experiments.....	188
6.2.2.1 Materials.....	188
6.2.2.2 Experimental design.....	188
6.2.2.3 Recovery and storage of post-blast residues .....	189
6.2.2.4 Collection and analysis of post-blast residues .....	190
6.2.2.5 Chemometric analysis .....	190
6.3 Results and discussion.....	190
6.3.1 Preliminary considerations when performing post-blast experiments.....	190
6.3.2 Party sparkler experiments.....	191

6.3.2.1	Functionality of sparkler based IEDs .....	191
6.3.2.2	Analysis of post-blast residues by ICPMS .....	193
6.3.2.3	Discrimination of party sparklers using trace elemental data .....	196
6.3.3	Urea nitrate experiments .....	201
6.3.3.1	Preliminary trials .....	202
6.3.3.2	Functionality of urea nitrate IEDs .....	203
6.3.3.3	Characterisation of post-blast residues.....	205
6.3.3.4	Discrimination of urea nitrate using trace elemental data.....	207
6.4	Conclusions and further work .....	209
Chapter 7.	Conclusions and future work .....	211
7.1	Conclusions .....	212
7.1.1	Characterisation and source attribution of nitrate based HMEs .....	213
7.1.1.1	Party sparklers .....	214
7.1.1.2	Ammonium nitrate .....	215
7.1.1.3	Urea nitrate.....	216
7.1.2	Recovery and source attribution of nitrate based IEDs .....	217
7.1.2.1	Sparkler based IEDs .....	218
7.1.2.2	Urea nitrate based IEDs .....	218
7.2	Future work and applications .....	219
7.3	Summary .....	221
Appendix A –	Supplementary figures.....	223
Appendix B –	Supplementary table data.....	232
Chapter 8.	References .....	236

## List of Figures

<b>Figure 1.1:</b> Chemical structures of some military, commercial and homemade explosives.....	6
<b>Figure 1.2:</b> High energy density materials that can be prepared from nitrourea.....	19
<b>Figure 2.1:</b> Equations used to calculate f-ratios. The between class variance (1) is divided by the within class variance (2) to give the f-ratio for a selected element (3). .....	44
<b>Figure 3.1:</b> ATR-FTIR spectra of party sparkler samples from full and refined sample set. Six sparklers of varying colours from the Artwrap brand (a) and eight uncoated sparklers from different brands purchased from online and local Australian retail stores (b). No discernible difference was observed between or within brands. Spectra has been offset for better visualisation of individual samples. ....	56
<b>Figure 3.2:</b> ATR-FTIR spectra of sparkler material from an unburnt and burnt PC sparkler. Spectra of burnt material can be discerned from an unburnt sparkler based on the absence of nitrate ( $3900 - 1800 \text{ cm}^{-1}$ region removed as no information was present as seen in Figure 3.1).....	57
<b>Figure 3.3:</b> Chromatograms from GCMS analysis of eight different party sparklers including a silver WLP, an uncoated T2P and six coloured Artwrap sparklers (offset for better visualisation of peaks). ....	59
<b>Figure 3.4:</b> Average concentration of elements within unburnt and burnt samples. Elements that were present at concentrations $> 1 \text{ ppm}$ (a) and $< 1 \text{ ppm}$ (b).....	65
<b>Figure 3.5:</b> 2-D scores plots generated from PCA performed on party sparklers from full and refined sample sets. The classification of samples and number of classes differs in each scores plot: (a) was generated using the full sparkler sample set with each sparkler classified as an individual brand (19 classes, 190 samples), (b) was generated using the full sparkler sample set with coloured variants of the same brand grouped into a single class (eight classes, 190 samples), (c) was generated using the refined sample set with each sparkler classified as an individual brand (eight classes, 80 samples), (d) was generated using samples from within the Korbond brand (seven classes, 70 samples). ....	68

<b>Figure 3.6:</b> 3-D scores plot from PCA of the refined sparkler sample set using the trace concentration data from 22 elements. Distribution of sample data shows three distinct classes including the T2P, FC and FF samples. ....	78
<b>Figure 3.7:</b> 2-D scores plot from PCA of the refined sparkler sample set after elements with a f-ratio < 200 were removed. Distribution of sample data shows five distinct classes including the T2P, FC, FF, Artwrap and WLP samples. ....	79
<b>Figure 3.8:</b> 3-D scores plot from PCA of the refined sparkler sample set using a refined 7-element profile that shows five distinct classes and three with minimal separation (a), repeated PCA on the highlighted cluster reveals full discrimination between the three classes across the first two PCs (b). ....	81
<b>Figure 3.9:</b> 3-PC factor loadings plot for elemental data acquired from PCA performed on refined sparkler sample set using a 7-element profile. ....	82
<b>Figure 3.10:</b> 3-D scores plot from PCA using a 6-element profile showing the distribution of burnt sparkler samples that shows full discrimination between the eight classes.....	84
<b>Figure 4.1:</b> Sources and precursors used to prepare AN: (a) explosive grade AN, (b) AN based cold packs, (c) commercial ammonium sulfate fertiliser, (d) hydroponic nutrient product containing calcium nitrate, (e) Black Marvel fertiliser containing 11.7% w/w NH <sub>4</sub> and (f) African Violet Food containing 10.5% w/w NH <sub>4</sub> . ....	93
<b>Figure 4.2:</b> ATR-FTIR spectra of a typical pure form AN product (explosive grade AN) and homemade AN product (synthesised from Richgro sulfate of ammonia and commercial calcium nitrate). Identifiable peaks are labelled across both spectra. ....	98
<b>Figure 4.3:</b> Raman spectra of a typical pure form AN product (chemical grade AN) and homemade AN product (synthesised from Baileys sulfate of ammonia and commercial calcium sulfate). Close-up view of 350 – 700 cm <sup>-1</sup> region (b) and 1020 – 1070 cm <sup>-1</sup> region (c) highlights bands associated with the sulfate ion present in the homemade AN products.....	100
<b>Figure 4.4:</b> Scanning electron microscopy back-scattered electron image of AN products: chemical grade (a), explosive grade (b), cold pack (c), synthesised from chemical reagents (d), synthesised from Richgro ammonium sulfate (e), synthesised	

from Baileys ammonium sulfate (f), synthesised from SREDA ammonium sulfate (g) and synthesised from Black Marvel Food (h). ..... 104

**Figure 4.5:** X-ray diffraction pattern of chemical grade AN. Overlaid is the typical diffraction pattern associated with synthetic gwihabaite (ammonium nitrate). Close-up view of the 45-49° 2 $\Theta$  region (b) is also displayed..... 106

**Figure 4.6:** X-ray diffraction pattern of homemade AN products (baseline has been offset for better visualisation). Close-up view of the 17-18.5° 2 $\Theta$  region that shows an additional reflection in the Richgro product (b), and a close-up view of the 28-29.2° 2 $\Theta$  region that shows an additional reflection in the SREDA product (c). .... 106

**Figure 4.7:** 2-D scores plot from PCA showing the distribution of samples using ATR-FTIR spectral data. The circled group contains all pure form products including the chemical grade, explosive grade and cold pack samples. .... 111

**Figure 4.8:** 2-D scores plot from PCA performed on the samples included in the pure form (a) and homemade (b) classes. Some sample clusters have been highlighted in each plot to show class discrimination. .... 112

**Figure 4.9:** PC factor loadings plot for ATR-FTIR spectra acquired from the PCA performed on all AN products. Shaded areas indicate the regions which have strong contribution to the separation of samples across PC1 (red) and PC2 (blue)..... 114

**Figure 4.10:** 3-D scores plot from PCA showing the distribution of pure form and homemade AN samples using X-ray diffraction patterns. Distribution of sample data shows distinct groupings of all homemade products while all pure form products are positioned in a single tight cluster..... 124

**Figure 4.11:** 2-D scores plot from PCA performed on the cluster of pure form AN samples. No additional discrimination was achieved with repeated PCA. .... 125

**Figure 4.12:** PC factor loadings plot for X-ray diffraction patterns acquired from PCA performed on all AN products. Shaded areas indicate the regions which have strong contribution to the separation of samples across PC1 (red) and PC2 (blue). 126

**Figure 4.13:** 3-D scores plot from PCA showing the distribution of pure form and homemade AN samples using trace elemental data. Distribution of sample data shows full discrimination of all homemade products and all pure form samples grouped together in a single tight cluster. .... 127



<b>Figure 4.14:</b> 2-D scores plot from PCA performed on the highlighted cluster of pure form AN samples in Figure 4.13. Repeated PCA allowed for the full discrimination of the pure form samples across 2 PCs. ....	129
<b>Figure 4.15:</b> PC factor loadings plots for elemental data acquired from PCA performed on all AN products (top) and the pure form cluster (bottom).....	130
<b>Figure 5.1:</b> Urea products used to prepare UN: (a) chemical grade urea, (b) fertiliser urea, (c) cold pack urea, (d) DEF, (e) Osmocote fertiliser mixture, (f) Green Boost fertiliser mixture.....	137
<b>Figure 5.2:</b> UN prepared from different fertilisers containing urea: from left to right, Osmocote purchased in May 2020, Osmocote purchased in November 2020 and Green Boost fertiliser. ....	142
<b>Figure 5.3:</b> ATR-FTIR spectra of UN prepared from chemical grade urea (a) and overlay of all UN samples (b) (baseline has been offset for better visualisation of individual spectra). Labelled peak in (b) suggests presence of sulfate within product prepared from Osmocote fertiliser. ....	144
<b>Figure 5.4:</b> ATR-FTIR spectra of chemical grade urea (top) and select pellets from the Osmocote fertiliser mixture (bottom). A sample of the mixture (a) and the two pellets primarily composed of urea is shown (b). ....	145
<b>Figure 5.5:</b> Raman spectra of UN prepared from chemical grade urea (a) and overlay of all UN products (b) (baseline has been offset for better visualisation of individual spectra). ....	147
<b>Figure 5.6:</b> SEM BSE image of UN products: chemical grade (a), cold pack (b), DEF (c), Richgro fertiliser (d), SREDA fertiliser (e), Baileys fertiliser (f), Osmocote (blue product) (g), Osmocote (yellow product) (h).....	149
<b>Figure 5.7:</b> X-ray diffraction pattern of all UN products (baseline has been offset for better visualisation of individual patterns). ....	150
<b>Figure 5.8:</b> Scores plot from PCA showing the distribution of UN samples using ATR-FTIR spectral data: 2-D scores plot with all UN samples (a) and 3-D scores plot of sample cluster (b). Highlighted groups in both plots show separated classes. ....	156

**Figure 5.9:** PC factor loadings plot for ATR-FTIR spectra acquired from PCA performed on all UN products (a) and highlighted cluster (b). Shaded areas indicate regions that have strong contribution to the separation of samples across PC1 (blue), PC2 (red) and PC3 (yellow). ..... 158

**Figure 5.10:** 2-D scores plot from PCA showing the distribution of UN samples using X-ray diffraction patterns (a) and PC factor loadings showing regions which have strong contribution to the separation of samples across PC1 and PC2 (b). ..... 166

**Figure 5.11:** Scores plot from PCA showing the distribution of UN samples using trace elemental data: 2-D scores plot with all UN samples (a) and 2-D scores plot of highlighted cluster (b). Highlighted groups show separated classes. .... 169

**Figure 5.12:** PC factor loadings plot for elemental data acquired from the PCA performed on all urea nitrate products (top) and sample cluster (bottom). ..... 170

**Figure 5.13:** ATR-FTIR spectra of NU prepared from Richgro UN, chemical grade UN. Spectra of chemical grade UN is shown for comparison. Labelled peaks are aligned with those reported in Oxley *et al* (75). ..... 174

**Figure 5.15:** 2-D scores plot showing the distribution of NU samples projected on the UN scores plot with refined elemental profile. Highlighted group shows one separated class containing UN and NU samples prepared from the same urea source. .... 177

**Figure 6.1:** Example of party sparkler device prepared and used within post-blast experiments. A single sparkler was placed at the top of the device to act as the fuse, which was ignited using a gas lighter. The design and construction were modelled after devices typically seized within WA casework. .... 185

**Figure 6.2:** Experimental set up for functioning and collecting residues from party sparkler based IEDs. Sparkler device was positioned on a wooden plank which protruded from a collection bucket. A wooden box surrounded the scene to contain the explosion and minimise damage done to surroundings. .... 186

**Figure 6.3:** Example of the experimental set-up for functioning party sparkler based pipe bombs. A single sparkler was placed at the top of the device to act as the fuse, which was ignited using a gas lighter. Devices were placed over a bucket of water so that it could be dropped and rendered safe if a misfire occurred. .... 187

**Figure 6.4:** Example of the sample grid for post-blast UN experiments with witness plates of varying materials placed both perpendicular and beneath the charge. The charge was suspended on a wire approximately 1.5m from the ground and detonated using an electric detonator. .... 189

**Figure 6.5:** Examples of the damage caused, and debris produced from a functioned sparkler based IEDs: initial attempts where devices melted instead of rupturing (a), CO<sub>2</sub> canister recovered after rupturing (b), CO<sub>2</sub> canister embedded into wooden box surrounding the initial device (c), damaged bucket after device was functioned (d). .... 192

**Figure 6.6:** Comparison of average concentration of elements detected in post-blast samples from devices constructed using Party Central branded sparklers against unburnt samples from the same brand. Figure separated based on elements present at concentrations > 1ppm (a) and < 1 ppm (b). .... 195

**Figure 6.7:** ATR-FTIR spectra of unburnt, burnt and post-blast party sparkler material from the Party Central brand. .... 196

**Figure 6.8:** 3-D scores plot from PCA performed on the post-blast samples collected from devices prepared using four different party sparkler brands. Distribution of samples reveals four distinct groups indicating complete separation of brands. .... 197

**Figure 6.9:** PC factor loadings plot for elemental data acquire from the PCA performed on post-blast samples, highlighting elemental contributions across the first three PCs. .... 198

**Figure 6.10:** 3-D scores plot from PCA performed on the post-blast samples using the elemental profile that distinguished between unburnt samples. Distribution of samples reveals two distinct groups with the remaining samples overlapping. .... 199

**Figure 6.11:** 2-D scores plot from PCA performed on the post-blast samples collected from all ten devices. Distribution of samples reveals four distinct groups with samples from different canister types grouped together with remaining Artwrap samples. .... 200

**Figure 6.12:** Images depicting the damage of UN based IEDs explosion and damage caused to surrounding witness plates. Explosion resulting from functioning the device (a), damaged metal witness plate placed perpendicular to the charge with

visible holes (b), damaged metal witness plate placed beneath the charge (c), and damaged corflute witness plate placed perpendicular to the charge (d). .....205

**Figure 6.13:** 2-D scores plot from PCA performed on the post-blast samples collected from various witness plates. Samples were collected from five devices that had been constructed with urea nitrate prepared from different source of urea.....208

**Figure A.1:** Images of party sparkler products used throughout this study. Party sparklers have been photographed in the packet as they were purchased (top row) and individually (bottom row). Party sparklers have been labelled according to their sample name as detailed in Table 3.1 .....224

**Figure A.2:** ATR-FTIR spectra of party sparkler from the PC brand. Spectra of five two cm sections of a single sparkler (a) and of five individual sparklers from the same packet (b). Both show no discernible difference between samples. Spectra has been offset for better visualisation of individual samples.....225

**Figure A.3:** Mass spectra of the terephthalic acid (PTA) peak (25.1 minutes) detected from GCMS analysis of the blue, pink, purple and green Artwrap branded party sparklers. ....226

**Figure A.4:** Mass spectra of the paraxylene peak (7.6 minutes) detected from GCMS analysis of gold coated Artwrap branded party sparkler.....226

**Figure A.5:** Mass spectra of the 2-bornanone peak (12.1 minutes) detected from GCMS analysis of silver coated Artwrap branded party sparkler.....227

**Figure A.6:** ATR-FTIR spectra of AN prepared from African Violet Food fertiliser product. The presence of several additional peaks allowed for the product prepared from this fertiliser to be discerned from other homemade AN products. ....228

**Figure A.7:** ATR-FTIR spectra of all pure form and homemade AN products. Stacked spectra highlights additional peaks present within the homemade products within the 1100 – 600  $\text{cm}^{-1}$  region. (baseline has been offset for better visualisation of individual spectra).....228

**Figure A.8:** ATR-FTIR spectra of commercial (Richgro brand) sulfate of ammonia fertiliser. Labelled peaks align closely with those observed in the homemade AN products. ....229

<b>Figure A.9:</b> Raman spectra of all AN products (baseline has been offset for better visualisation). Stacked spectra highlights additional peaks present within the homemade products within the 1100 – 700 cm <sup>-1</sup> region. ....	229
<b>Figure A.10:</b> X-ray diffraction patterns of pure form AN products (baseline has been offset for better visualisation). ....	230
<b>Figure A.11:</b> Scree plot associated with the discriminant model generated using ATR-FTIR spectral data collected from eight AN products. The plot shows the cumulative variance accounted for by each successive PC. ....	230
<b>Figure A.12:</b> ATR-FITR spectrum of the UN product prepared from Green Boost fertiliser. The presence of several additional peaks allowed for the product prepared from this fertiliser to be discerned from other synthesised UN products. ....	231
<b>Figure A.13:</b> Scree plot associated with the discriminant model generated using ATR-FTIR spectral data collected from seven UN products. The plot shows the cumulative variance accounted for by each successive PC. ....	231

## List of Tables

<b>Table 1.1:</b> Historical attacks involving the use of IEDs which incorporated fertiliser, peroxide or inorganic based HMEs.....	8
<b>Table 1.2:</b> A summary of freely accessible precursors and commercial products used in the synthesis of HMEs and preparation of explosive and pyrotechnic compositions. ....	13
<b>Table 3.1:</b> Full sample set that includes 19 different sparklers purchased from a variety of local and online Australian retail stores. Sparklers were collected from eight different brands with additional coloured sparklers collected from within the Artwrap and Korbond brand. Throughout this study, specific sparklers are referred to by the sample name listed. Brand, distributor and main distinguishing feature is also detailed. ....	49
<b>Table 3.2:</b> Refined sample set that includes sparklers collected from eight different brands. All samples within the refined set have no distinguishing features or additional coatings and only differ by their manufacturer/brand. Throughout this study, specific sparklers are referred to by the sample name listed. Place of purchase is also detailed. ....	51
<b>Table 3.3:</b> Concentration of cations and anions (ppm) in 100 mg of unburnt and burnt sparkler material from different brands. Species that are reported < 5 ppm were present within the sample at concentrations below the lower limit of the calibration range. (ions not detected in samples are labelled as n.d). ....	61
<b>Table 3.4:</b> Classification and validation results from LDA on the full sparkler sample set using the first six PCs with equal probabilities assumed. Discriminant model was generated with ten samples from 19 classes and validated using an independent dataset that contained five samples from each class (95 samples total). Number of correct vs incorrect classifications is shown.....	71
<b>Table 3.5:</b> Classification and validation results from LDA on the refined sparkler sample set using the first six PCs with equal probabilities assumed. Discriminant model was generated with 10 samples from eight classes and validated using an independent dataset that contained five samples from each class (40 samples total). Number of correct vs incorrect classifications is shown.....	73

<b>Table 3.6:</b> Discriminant values of samples within the independent data set used for validation. Discriminant values and predictions represent the samples within Table 3.5. Shaded cells indicate correct (green) and incorrect (red) predictions. ....	74
<b>Table 3.7:</b> F-ratio values calculated for each element and ranked in ascending order. Elements with a high f-ratio contribute most to the separation of classes. ....	79
<b>Table 3.8:</b> Number of correct vs incorrect classifications from validation of a four PC LDA model. Discriminant model was constructed using trace concentration data from the refined 7-element profile or using a combined profile that included elements within the refined burnt profile. ....	85
<b>Table 4.1:</b> Source and average yield information of AN products and their precursors. Products are separated into ‘pure form’ and ‘homemade’ groups based on how they were prepared or obtained. ....	94
<b>Table 4.2:</b> Concentration of cations and anions (ppm) in 10 mg of AN from different sources (ions not detected in samples are labelled as n.d). ....	102
<b>Table 4.3.</b> Average concentration (ppb) of elements within 200 mg of each AN product. (elements not detected in samples are labelled as n.d). ....	108
<b>Table 4.4.</b> Number of correct vs incorrect classifications from the validation set using a five-PC LDA model with each AN product treated as an individual class. ....	116
<b>Table 4.5.</b> Number of correct vs incorrect classifications from validation set using a stepwise five-PC model with each AN samples classified as either a pure form or homemade product before its source is predicted. ....	117
<b>Table 4.6.</b> Discriminant values of samples within the independent data set used for validation. Discriminant values and predictions represent the products within Table 4.5. Shaded cells indicate correct (green) and incorrect (red) predictions. ....	119
<b>Table 5.1:</b> Source and yield information of UN samples used throughout this study. ....	138
<b>Table 5.2:</b> Concentration of cations and anions (ppm) in 10 mg of UN prepared from different sources (ions not detected in samples are labelled as n.d). ....	151
<b>Table 5.3:</b> Average concentration (ppb) of detected elements within 200 mg of UN products. ....	153

**Table 5.4:** Number of correct vs incorrect classifications from the validation set using a five-PC LDA model with each UN product treated as an individual class. 160

**Table 5.5:** Number of correct vs incorrect classifications from the validation set using a three part stepwise five –PCA-LDA model..... 160

**Table 5.6:** Discriminant values of samples within the independent data set used for validation. Discriminant values and predictions represent the products within Table 5.4. Shaded cells indicate correct (green) and incorrect (red) predictions. .... 162

**Table 5.7:** Yield information of nitrourea samples prepared from different UN products..... 172

**Figure 5.14:** 2-D scores plot from PCA showing the distribution of NU samples using trace elemental data. No separation of classes was observed..... 176

**Table 6.1:** Number of correct vs incorrect classifications from validation set using a five-PCA model constructed with combined unburnt and post-blast elemental profile. .... 201

**Table 6.2:** Average concentration (ppb) of some elements detected on witness plates positioned perpendicular of directly below the charge. .... 207

**Table B.1:** Concentration of barium and nitrate ions within 100 mg of sparkler material from the ASilver brand. Eight samples were prepared and analysed from ground and unground material. .... 233

**Table B.2:** ICP-MS analysis of refined sparkler sample set that shows the average concentration (ppb) of elements found in 100 mg of unburnt sparkler residue. Elements that were present due to contamination or present below the calibration range were removed resulting in the concentration of 22 elements being reported. 234



## List of Abbreviations

2 / 3-D	2 / 3-Dimensional
AFP	Australian Federal Police
AN	Ammonium Nitrate
ANFO	Ammonium Nitrate Fuel Oil
ANOVA	Analysis of Variance
APCI	Atmospheric Pressure Chemical Ionisation
ATR-FTIR	Attenuated Total Reflectance Fourier Transform Infrared
AUD	Australian Dollar
AUS	Australia
BSE	Back Scattered Electron
CAN	Calcium Ammonium Nitrate
CE	Capillary Electrophoresis
DCM	Dichloromethane
DEF	Diesel Exhaust Fluid
DINGU	1,4-Dinitroglycouril
DV	Discriminant Value
ESI	Electronspray Ionisation
FESEM	Field Emission Scanning Electron Microscope
FINEX	Forensic International Network for Explosive Investigations
GC	Gas Chromatography

GCMS	Gas Chromatography Mass Spectrometry
GSR	Gunshot Residue
HEDM	High Energy Density Material
HHTDD	Hexanitrohexaazatricyclododecanione
HME	Homemade Explosive
HMTD	Hexamethylene Triperoxide
HMX	Cyclotetramethylene Tetranitramine
HPLC	High Performance Liquid Chromatography
IC	Ion Chromatography
ICPMS	Inductively Coupled Plasma Mass Spectrometry
IED	Improvised Explosive Device
IMS	Ion Mobility Spectrometry
IR	Infrared
IRMS	Isotope Ratio Mass Spectrometry
LC	Liquid Chromatography
LCMS	Liquid Chromatography Mass Spectrometry
LDA	Linear Discriminant Analysis
MEK	Methyl Ethyl Ketone
MS	Mass Spectrometry
MSA	Methanesulfonic Acid
NATO	North Atlantic Treaty Organisation

NIPALS	Non-linear Iterative Partial Least Squares
NU	Nitrourea
PC	Principal Component
PCA	Principal Component Analysis
P-DMAC	P-dimethylaminocinnamaldehyde
PETN	Pentaerythritol Tetranitrate
PLSDA	Partial Least Squares Discriminant Analysis
PPE	Personal Protective Equipment
RDX	Cyclotrimethylene Trinitramine
SDS	Safety Data Sheet
SEM	Scanning Electron Microscopy
SEM-EDS	Scanning Electron Microscopy Energy Dispersive X-ray spectroscopy
SSAN	Security Sensitive Ammonium Nitrate
TATP	Triacetone Triperoxide
TNGU	1,3,4,6-Tetranitroglycouril
TNT	2,4,6-Trinitrotoluene
TWGFEX	Technical Working Group for Fires and Explosions analysis
UK	United Kingdom
UN	Urea Nitrate
USA	United States of America
VOD	Velocity of Detonation

WA	Western Australia
WABRU	Western Australia Bomb Response Unit
XRD	X-ray Diffraction
XRF	X-ray Fluorescence
ZBP	Zero Background Plate

# **Chapter 1. Introduction**

## 1.1 Introduction

A homemade explosive (HME) is any explosive that is not produced for military or commercial purposes. They are often prepared in ‘backyard’ or clandestine laboratories using freely accessible products and used within illegitimate or criminal activities (1, 2). HMEs encompass an extremely large and diverse group of explosive and pyrotechnic compositions that have unforeseeable and unpredictable effects as their destructive potential is limited only by the capability and creativity of their maker (3, 4). As access to information surrounding HMEs is readily accessible, new approaches to sourcing, preparing and functioning HMEs will continue to emerge. The HME threat is therefore ongoing and continuously changing.

The forensic investigation of a HME incident presents many investigative and analytical challenges that requires the collaboration of skilled personnel from a variety of highly specialised disciplines due to the large range of potential scenarios, scenes and evidence types that may be encountered (5-8). Regardless of the type of incident, the primary goal at a pre- or post-blast explosive scene is to identify the explosives present and potentially reconstruct any device used and the series of events that led to its ignition (6, 9). However, the forensic examination of pre- and post-blast residues is often left incomplete once the explosive has been identified. In some scenarios this may be unavoidable, as explosives residue can be minimal and often require complex recovery and extraction protocols that are susceptible to many sources of contamination (8, 10). Alternatively, a lack of consideration of how an explosive can be sourced and prepared as well as the information that can be gathered from additional discriminatory analytical procedures can also limit the investigative process. The complete characterisation, identification and subsequent source attribution of an unknown explosive sample vastly improves its evidential value and generates a significant amount of information that can be used to establish links and introduce or eliminate specific lines of enquiry based on previous evidence gathered (10-12). This is particularly vital for the investigation of HMEs as a substantial amount of intelligence can potentially be obtained from identifying the type and brand of products used.

A large proportion of explosive forensic research focusses on developing and improving methods for the timely and accurate identification of explosives within pre-

and post-blast residues. Despite the importance of these studies, there is a high forensic need to conduct investigations on the preparation, analysis and source attribution of HMEs (1, 13-16). This thesis aims to address many of the fundamental knowledge gaps surrounding select inorganic based HMEs in order to improve our understanding of how explosive precursors are sourced and prepared and to determine the maximum amount of identifying and discriminatory information that can be gained from an array of analytical techniques. This work will assist many stages of the investigative and analytical process within casework to improve identification and source determination capabilities of HMEs, current and emerging. These investigations are also highly relevant to the broader forensic community, law enforcement, manufacturers and military agencies who rely on gathered intelligence for the purpose of recreating HME compositions and explosive devices as well as disrupting their commercial preparation and ignition (14).

## **1.2 Explosives**

An explosive is any substance that is capable of producing an explosion (17, 18). Explosions are characterised based on how they are produced and have been separated into four basic types which include mechanical, chemical, nuclear and electrical (19). A chemical explosion is described as a sudden and violent release of energy resulting from a chemical reaction and is often accompanied by heat, light and sound (19-21). Chemical explosions are produced either by the decomposition of a unimolecular substance containing both oxidiser and fuel components, or by a multi-molecular redox reaction proceeding throughout a mixture (17, 22). Individual compounds that produce chemical explosions often contain a high number of nitrite or nitrate groups which separate and react with oxidisable elements (fuels) such as carbon and hydrogen to produce a large amount of heat and gas (22). Alternatively, a solid or liquid mixture containing separate fuel and oxidiser components will react to produce an explosion. For military and industrial applications, and within the literature, chemical explosives and explosive mixtures are commonly classified according to their velocity of detonation (VOD) as this provides an indication of their relative performance (17, 22). High order explosives detonate producing a shockwave that propagates through the material and progresses faster than the speed of sound, whereas low order explosives

combust on ignition and deflagrate to produce a subsonic shockwave that progresses slower than the speed of sound (19, 22-24).

High explosives are further categorised based on their sensitivity to detonation. Primary explosives are readily ignited and detonated by weak stimuli such as heat, friction and shock (17, 25, 26). Secondary explosives are mostly insensitive to similar stimuli and require a shockwave produced by a primary explosive to detonate (3). Due to their extreme sensitivity, primary explosives are mainly used to initiate secondary explosives which generally have more destructive potential. Low explosives are mostly used as propellants in pyrotechnic mixtures, fireworks, rockets and firearm ammunition (17, 27). These explosives are highly combustible and will only deflagrate under confinement (27). High and low explosives can further be categorised based on their source, use or application, which is detailed below. Figure 1.1 shows the chemical structure of some of the explosives discussed in the next section.

### 1.2.1 Types of explosives

Military explosives are those used for military purposes and typically consist of organic compounds that contain nitrogen and oxygen groups (17). These explosives need to meet strict requirements in terms of detonation performance, functionality, and sensitivity (17). In the present-day only a limited number of explosives qualify for military use, the most common being cyclotrimethylene trinitramine (RDX), pentaerythritol tetranitrate (PETN), 2,4,6-trinitrotoluene (TNT) and cyclotetramethylene tetranitramine (HMX) (17, 28, 29). These are often plasticised by adding inert binders to form mouldable plastic explosives that are extremely insensitive and have high detonation velocities, such as C-4 or SEMTEX (17, 29).

Commercial explosives are used for legitimate purposes primarily within mining and quarrying industries (30). An ideal commercial explosive is water resistant, has a high detonation pressure and produces minimal toxic fumes (30). Currently, ammonium nitrate (AN) based formulations are amongst the few 'permitted explosives' that can be used commercially. Ammonium nitrate fuel oil (ANFO) is the most used commercial explosive which is prepared from a high porosity form of AN and fuel oil (30, 31). Alternatively, AN can be modified with metallic fuels and gelling agents to prepare slurry or emulsion explosives (3, 17, 30). Other explosives that are used



legally for nonmilitary purposes include detonating cords (to initiate or link charges), propellants (firearm ammunition) and fireworks (17, 31).

If an explosive is not produced for military or commercial purposes, it is then categorised as a HME. Any explosive could potentially be homemade, however HMEs generally refer to those that are easily prepared using commercially available ingredients and freely accessible precursors with minimal knowledge of chemical synthesis (1, 3, 32, 33). Many ingredients that can be repurposed for preparing HMEs have legitimate uses and so it is difficult to impose restrictions or develop systems that would alert authorities to their potential misuse. The complexity and destructive potential of HMEs is highly variable and can range from simple low order inorganic fuel/oxidiser mixtures to powerful high order peroxide or fertiliser based explosives that contain both oxidiser and fuel components within a single molecule (3, 32).

The attempted use of peroxide based explosives including triacetone triperoxide (TATP) and hexamethylene triperoxide diamine (HMTD) has been reported on numerous occasions with TATP thought to be the main charge used in the July 2005 London bombings (34). Both are listed as primary explosives and so can be used in a standalone charge or to detonate other explosives. TATP is prepared from acetone and hydrogen peroxide in the presence of an acid such as hydrochloric or sulfuric acid and HMTD is prepared from hexamine and hydrogen peroxide in the presence of citric acid, all readily available ingredients (1). Aside from their high detonation power, they pose an additional risk as they are extremely sensitive and an explosion can easily occur during synthesis, which has been reported on numerous occasions (35).

Fertiliser based HMEs including AN and urea nitrate (UN) are powerful secondary high explosives that have been used in several explosive attacks including the bombing of the World Trade Centre in 1993 (1). Although many countries have imposed restrictions on highly pure forms of AN, it can still be prepared with ammonium sulfate and a nitrate salt which is sourced from common garden products. UN is prepared from a urea source such as a fertiliser and nitric acid, which can also be synthesised using household products. AN and UN are highly stable energetic materials and preparing bulk amounts has minimal risk (36). The drawback of their use is that a primary explosive is required for them to reliably detonate, which are typically much more difficult to source or prepare.

Physical mixtures containing a fuel and oxidiser component are low order explosives that can be used for both legal and illicit purposes. They are primarily used as propellants or to prepare consumer fireworks. When ignited the mixture will burn rapidly due to the liberated oxygen reacting with the fuel to produce a large volume of gas (20, 37). When contained, the build-up of gas and pressure eventually overcomes the structural integrity of the container resulting in an explosion (37, 38). Common oxidisers include nitrate, chlorate and perchlorate salts as these are rich in oxygen and have a high heat of combustion (10, 20). Effective fuels will have low melting points, a small particle size and high combustion temperatures, such as aluminium, carbon, sulfur and phosphorus (20).

Although some HMEs can be initiated with heat or impact, to achieve reliable detonation or deflagration the HME will subsequently be used to prepare an improvised explosive device (IED). This involves containment of the HME mixture with additional fuel or binding components. Secondary explosives such as AN and UN will also need additional primary explosive to reach detonation.

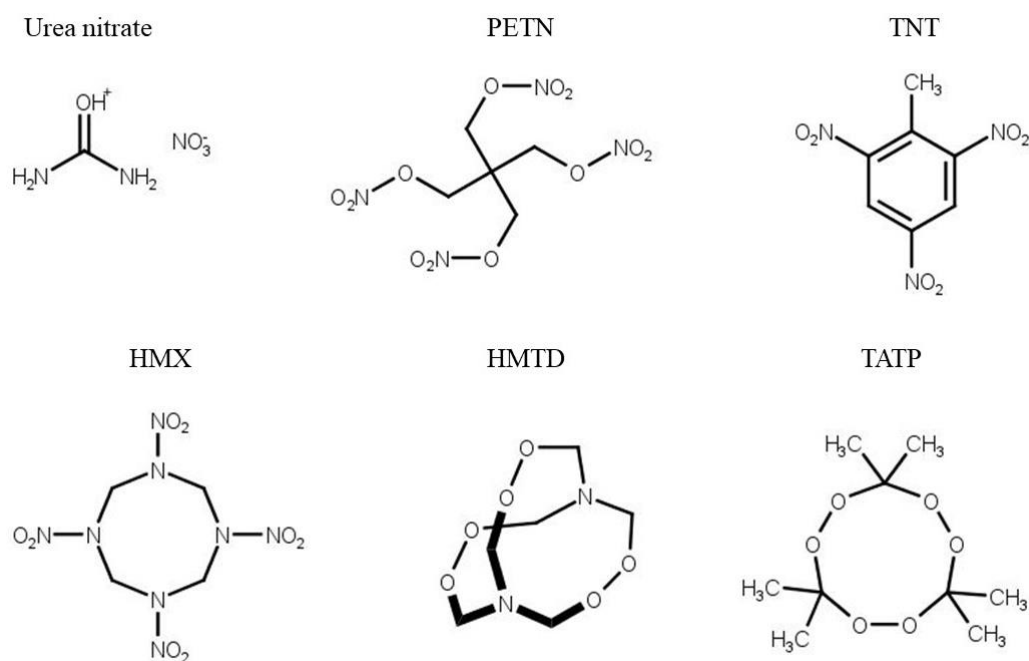


**Figure 1.1:** Chemical structures of some military, commercial and homemade explosives.

### 1.2.2 Improvised explosive devices

IEDs have become synonymous with discussions of terrorism and explosive attacks due to their frequent use by terrorist extremist groups and insurgents in areas of war such as Iraq, Pakistan and Afghanistan (39, 40). Although, a substantial number of domestic IED attacks have also been reported in many countries and so continue to be a global threat (36, 39, 41, 42). The primary explosive mixture used within IEDs is often homemade and therefore many similarities exist regarding the ongoing effort to improve forensic analysis protocols as well as disrupting their preparation and use (39). A summary of significant IED attacks which incorporated HMEs is included in Table 1.1 below.

**Table 1.1:** Historical attacks involving the use of IEDs which incorporated fertiliser, peroxide or inorganic based HMEs.

<b>Explosive incident</b>	<b>Location</b>	<b>Date</b>	<b>Type of explosive</b>	<b>Quantity</b>
<b>Sterling hall bombing (43)</b>	Wisconsin, USA	August 24 <sup>th</sup> , 1970	ANFO	~900 kg
<b>Bishopsgate bombing (44)</b>	London, UK	April 24 <sup>th</sup> , 1993	AN and nitromethane	~1000 kg
<b>World trade centre bombing (45)</b>	New York, USA	February 26 <sup>th</sup> , 1993	UN	~550 kg
<b>Oklahoma City bombing (46)</b>	Oklahoma City, USA	April 19 <sup>th</sup> , 1995	ANFO	~2300 kg
<b>Bali nightclub bombing (10)</b>	Kuta, Bali	October 12 <sup>th</sup> , 2002	Potassium chlorate, sulfur and aluminium	~900 kg
<b>2005 London train bombings (42)</b>	London, UK	July 7 <sup>th</sup> , 2005	TATP	~10 kg
<b>Oslo bombing (1, 47)</b>	Oslo, Norway	July 22 <sup>nd</sup> , 2011	AN and aluminium powder	~900 kg
<b>2015 Paris attacks (42)</b>	Paris, France	November 13 <sup>th</sup> , 2014	TATP	~10 kg
<b>Manchester arena bombing (48)</b>	Manchester, UK	May 22 <sup>nd</sup> , 2017	TATP	~20 kg

Improvised devices are highly characteristic and have enormous destructive potential as they are only limited by the capacity to obtain the necessary precursors which are mostly unrestricted (3, 4). Although being incredibly diverse, IEDs can be broken down and distinguished by differences observed within its main components such as

the initiation and delivery system, degree of sophistication, container, explosive ingredients and its overall design purpose (49, 50). There is no clear consensus on the definition of an IED between military/law enforcement agencies and the academic/research community, as a device can be defined based on a number of characteristics. The North Atlantic Treaty Organisation (NATO) provided a broad definition by describing an IED as a “device placed or fabricated in an improvised manner incorporating destructive, lethal, noxious, pyrotechnic, or incendiary chemicals and designed to destroy, incapacitate, harass, or distract” (36, 49). An alternative description that better reflects the homemade nature of IEDs and encapsulates their preparation and function is described by Thurman, which defines an IED as:

A combination of items or components that are neither designed nor produced to be used in conjunction with each other and that, when placed together or assembled, constitute a mechanism that has the capability of exploding and causing personal injuries and property damage ... an IED can be constructed with almost any item that provides for the two basic overall components: the main charge explosive and the fusing system. However, many devices employ additional components, such as an external concealment container, in which to hide the device from observation and discovery (51).

Regardless of the many varied definitions presented, all IEDs are prepared using two basic elements: the explosive and the initiation system. These are discussed below along with additional components that are often observed (32).

Any legitimate or homemade high or low explosive can be used in an IED. Some explosive formulations have a long history of use and are well established within anarchist and bomb-making literature (27). The most commonly encountered explosives used within IEDs are fertiliser based, peroxide based, and inorganic fuel/oxidiser mixtures, which have previously been discussed (1, 27, 32). These are prepared in ‘home-made’ clandestine or ‘backyard’ laboratories using increasingly accessible internet guides and videos detailing the synthetic procedures and commercial products required. Other secondary high explosives such as RDX or HMX have been used in IEDs, however homemade forms are not often encountered and are instead illegally acquired by various means from military and commercial sources.

The form of initiator required is dependent upon the nature of the explosive, intent of the bomber and relative availability (32, 51). A simple flame can be used to ignite a primary high explosive or low order pyrotechnic, while a shockwave is required for secondary high explosives. A flame can be supplied by mechanical or electrical means, whereas a shockwave is produced by detonators, which are made from primary explosives (27, 32). The method of initiation can further be categorised into delay, victim or command initiation. Delay initiation systems often involve timer and electrical components that allows for a pre-set delay time upon activation (32, 51). Victim initiation systems incorporate triggering mechanisms that cause the ignition of an IED after a specific pressure induced or mechanical action has been completed, such as the opening of a box (32, 51). Command initiation involves remote activation of the charge and contains elements of both delay and victim trigger systems (32).

The type of container used will also impact whether a low order explosive will reach deflagration or simply combust, providing a large amount of evidential value if parts are seized before or after an explosion has occurred (51). Additional materials such as glue, tapes, wire, plastics and textiles that are used for binding purposes will often survive an explosion and can be used to reconstruct the device to provide evidence within an investigation (32, 52). If a specific effect is desired to further enhance the explosive impact of the device, components such as shrapnel, incendiary or hazardous chemicals can also be added. Within the forensic investigation of a post-blast scene, the initiation system as well as the components listed above are critical in identifying the type of device used. Furthermore, as the initiation system and container are in close proximity to the explosive, they can be targeted for the recovery of biological material such as fingerprints or DNA to generate investigative leads and establish connections between the device used and the people involved (9, 53-57).

### 1.2.3 Forensic investigation of incidents involving explosives

The forensic investigation of an explosive incident encompasses an enormous range of potential scenarios, scenes and types of evidence (5-8). Within the investigation of HMEs and improvised devices, the successful recovery, analysis, and identification of explosive material and construction of any devices used summarises the core objectives of the forensic scientist (6, 9, 58). These objectives provide a wide range of

information that are used by investigators to generate leads and establish links between persons, places and/or objects of interest (8).

The typical approach undertaken by a forensic chemist involves the analysis of intact material or trace residues left behind from an exploded device to find traces of the original unconsumed material (8, 52, 59). With low order explosives, a large amount of unconsumed residue may be available for analysis as well as fragments from the improvised device (1, 8, 60). High-order explosives detonate leaving minimal residue which is dispersed over a large area and so residues are often extracted from collected fragments or witness materials expected to have a high density of explosive material (8, 52, 60). Collection of residues from high explosives presents additional challenges as they often reside in complex matrices and are subject to many potential sources of contamination (60).

Upon successful recovery of forensic items from a scene, the exhibits undergo preliminary examination before being subjected to a suite of advanced analytical techniques with the aim of identifying any explosive material (1, 61). Within the investigation of an explosives manufacturing lab where a device has yet to be constructed, forensic chemists will focus on analysing potential explosive samples and identifying any precursors or products being used within the synthesis. Profiling of potential precursors could be used to identify their source or the purchase location which is similar to the source attribution of components recovered from an improvised device.

### **1.3 Nitrate based HMEs – preparation and market availability of precursors**

Although HMEs are extremely variable, those based on nitrate or mixtures containing nitrate salts continue to be the cause of many explosive incidents ranging from destruction of property to mass casualty events. Peroxide based HMEs are considerably more powerful and have a high destruction potential, however, as the synthesis and successful ignition present extreme risk, explosives such as TATP and HMTD are rarely used (1). The precursors and products required to prepare nitrate based HMEs such as AN or UN are low cost and would raise minimal suspicion as they have legitimate uses. If prepared correctly they are often highly stable and are

extremely safe to handle and transport, however additional primary explosive or sufficient confinement is still required to achieve detonation or deflagration. A summary of potential products and precursors that are used to prepare HMEs is shown in Table 1.2 (42, 62).



**Table 1.2:** A summary of freely accessible precursors and commercial products used in the synthesis of HMEs and preparation of explosive and pyrotechnic compositions.

<b>Precursor</b>	<b>Sourced/extr-acted from</b>	<b>Availability</b>	<b>Illicit use</b>	<b>Precursor</b>	<b>Sourced/extr-acted from</b>	<b>Availability</b>	<b>Illicit use</b>
<b>Acetone</b>	Polish remover, commercial solvent	Hardware/drug stores	Synthesis of TATP	Barium nitrate	Party sparklers, consumer fireworks	Retail stores, internet suppliers	Pyrotechnic compositions
<b>Aluminium</b>	Aluminium powder, spray paint	Hardware/grocery stores	Common fuel in explosive compositions	Calcium hypochlorite	Water treatment products	Garden stores	Synthesis of chlorate salts
<b>Ammonium nitrate</b>	Fertiliser, cold packs	Garden/drug stores	Preparation of ANFO	Calcium nitrate	Hydroponic nutrients	Hydroponic/fertiliser stores	Synthesis of AN
<b>Ammonium sulfate</b>	Sulfate of ammonia fertiliser	Garden stores	Synthesis of AN	Citric acid	Cleaning products	Grocery stores	Synthesis of TATP
<b>Diesel oil</b>	Diesel oil	Hardware/auto-motive stores	Preparation of ANFO	Hydrochloric acid	Muriatic/hydrochloric acid	Hardware/cleaning product stores	Nitric acid synthesis

<b>Copper</b>	Copper metal, copper powder	Hardware stores, internet suppliers	Nitric acid synthesis	Magnesium	Magnesium powder	Health and wellness stores	Common fuel in explosive compositions
<b>Hexamine</b>	Camp stove tablets	Camping/ hardware stores	Synthesis of HMTD	Methyl ethyl ketone (MEK)	MEK solvent	Hardware/ speciality solvent stores	Synthesis of MEK peroxide (MEKP)
<b>Hydrogen peroxide (dilute)</b>	H <sub>2</sub> O <sub>2</sub> solutions	Drug stores	Peroxide based explosives	Nitric acid	Nitric acid	Specialty chemical stores	Preparation of UN
<b>Hydrogen peroxide (concentrate)</b>	Hair dyes/contact lens cleaners, hair bleach	Drug stores, specialty product stores	Peroxide based explosives	Nitromethane	Model car and plane fuels	Hobby stores	Explosive or fuel component
<b>Potassium chlorate</b>	Fireworks, matches	Firework/ grocery stores	Preparation of pyrotechnic compositions	Sodium nitrate	Speciality fertiliser, fireworks	Garden/ firework stores	Pyrotechnic compositions
<b>Potassium chloride</b>	Salt products	Grocery stores	Synthesis of potassium chlorate	Sugar	Icing sugar	Grocery stores	Used as a fuel

<b>Potassium nitrate</b>	Commercial stump remover, fireworks	Firework/ garden stores, internet suppliers	Pyrotechnic compositions		Sulfuric acid	Battery acid	Automotive stores	Synthesis of nitrourea
<b>Sodium hydroxide</b>	Garden products	Garden/ hardware stores	Synthesis of potassium chlorate		Urea	Urea fertiliser	Garden stores	Synthesis of UN
<b>Sodium hypochlorite</b>	Bleach, liquid chlorine	Grocery/ pool product stores	Synthesis of potassium chlorate					

### 1.3.1 Ammonium nitrate

#### 1.3.1.1 Manufacture and commercial use

AN is one of the most important chemicals used within agricultural and mining industries. It is manufactured in industry by reacting gaseous ammonia with concentrated nitric acid and distributed in different grades depending on its use (33). Commercial AN is primarily used to prepare ANFO, with Australia alone producing approximately 1.8 million tonnes annually (63, 64). Large scale AN manufacturers typically produce nitric acid and ammonia on site to prepare an extremely pure form of AN (~99.9%) (33). Ammonia is produced by reacting atmospheric nitrogen with natural (methane) gas. Industrial synthesis of nitric acid involves the oxidation of ammonia to form nitric oxide which is further oxidised and reacted with water to afford dilute nitric acid, which is purified by distillation (33, 64, 65). Once the solid AN is produced it is processed into prills for bulk storage and transportation. This process will vary depending on the desired use, as technical grade AN used for ANFO production will be more porous and less dense than fertiliser grade.

#### 1.3.1.2 Homemade ammonium nitrate

The shortest path to preparing an effective AN based HME is to source products containing solid AN. AN fertiliser containing low percentage forms of AN remains commercially available in many countries and is easily repurposed as a HME without any further modifications. In Australia, government issued licenses are required for the purchase, sale, manufacture, transport and storage of security sensitive ammonium nitrate (SSAN) which is any product that contains more than 45% AN (66). Regardless, products that are not classified as SSAN are unavailable in the majority of commercial retail stores. Alternatively, solid AN can be sourced from AN based cold packs, which contain high purity AN prills.

If pure AN cannot be sourced, it can be prepared from ammonium sulfate and a nitrate salt. This method involves a simple double displacement reaction whereby each component is dissolved in water and then combined to produce aqueous AN, which affords highly pure solid AN once excess water is evaporated. Calcium nitrate or sodium nitrate are effective reagents and can be sourced from hydroponic nutrient and

specialty fertiliser mixtures. Ammonium sulfate can be purchased in bulk quantities from sulfate of ammonia fertiliser products. This method is low risk and has the potential to produce extremely large quantities of AN requiring minimal knowledge of chemical synthesis. Furthermore, as the reaction relies on aqueous ammonium, any fertiliser product containing a relatively high percentage of ammonium could potentially be used to prepare AN.

#### 1.3.1.3 Additional fuel sources

Homemade AN can be combined with a range of commercial ingredients to improve explosive power and create extremely destructive devices. Homemade ANFO is easily achievable by mixing solid AN with diesel oil, typically forming mixtures containing 4-6% oil (1, 67). AN has also shown increased explosive performance with the addition of aluminium or magnesium powders (2, 30, 32). Aluminium can be purchased in a variety of forms including aluminium powder, spray paint or aluminium foil, while magnesium powder is used in dietary supplements. AN/sugar mixtures are also easily prepared and been shown to produce an effective high explosive (2). Optimal results are attributed to the sugar component having a small particle size and being sufficiently mixed with the AN, making products such as icing sugar an effective and affordable additive. Local experimental firings of AN/nitromethane mixtures, another commercially available fuel, were proven to enhance the destructive power of AN, however this was highly dependent on an optimal ratio as initial attempts using large amounts of nitromethane were mostly ineffective. AN can essentially be modified with any commercially available fuel source, however the fuels mentioned above have seen continuous use as they are readily available and are proven to consistently and reliably improve the explosive properties of AN.

#### 1.3.2 Urea nitrate

##### 1.3.2.1 Legitimate manufacture and uses

UN is an energetic salt that shares comparable explosive characteristics to AN. It is used in the manufacture of urethane, however, has no other legitimate commercial uses and is primarily used illicitly as a HME or in IEDs. UN is prepared by reacting nitric acid and urea, which are both used heavily within industry (68). The industrial

synthesis of urea involves the reaction between ammonia and carbon dioxide at high temperature and pressure (33, 69). The molten urea is then cooled and manufactured into small prills which are subsequently used for large scale fertiliser production or alternative products such as diesel exhaust fluid (DEF) (33, 69). Global urea production is significantly higher than AN due to its widespread use as a fertiliser and fuel and also highly accessible to consumers within a number of products (70, 71).

#### 1.3.2.2 Homemade urea nitrate

Products containing pure UN are not produced commercially and so cannot directly be obtained by consumers. However, there is essentially no restrictions imposed on purchasing or storing bulk urea products. A global response has been seen to restrict or desensitise AN products after their frequent use in explosive attacks, however the preparation of UN from commercial ingredients is unchallenged despite its continuous use as a HME (34, 66, 72-74)

Homemade UN can be prepared by reacting aqueous urea (~46% w/w) with concentrated nitric acid (68). The process presents minimal risk and affords a large amount of a highly stable solid UN as the theoretical yield is double the mass of urea used. Urea can be purchased in a number of forms including solid prills from urea fertiliser or urea based cold packs. Aqueous urea is also sold as DEF which is used to reduce harmful emissions expelled by trucks and diesel cars and is often sold in large 1-10L containers. Furthermore, comparable to homemade AN production, any fertiliser product containing urea could potentially be used to prepare UN if it can be extracted into an aqueous solution.

Nitric acid is harder to source but can be purchased at high concentrations as a cleaning supply products. Alternatively, a homemade product can be prepared with more accessible ingredients using a number of methods such as by reacting a nitrate salt with copper, or by distillation of a nitrate salt and sulfuric acid. Additionally, as a key step to the preparation of many explosives is nitration, nitric acid synthetic procedures and how-to guides have become increasingly more available on the internet. The production of homemade UN would likely be limited by the amount of concentrated nitric acid that can be obtained or prepared, however, as there are numerous methods

that all incorporate commercially accessible ingredients and materials, large scale production of both nitric acid and urea nitrate is possible.

### 1.3.2.3 Nitrourea and analogues

Fuels previously discussed that improve the explosive performance of homemade AN mixtures can also be used with UN. Metal powders, sugars and nitromethane could potentially modify the explosive characteristics of UN to improve its explosive properties. Unlike AN, UN can be used as a precursor in the synthesis of a powerful explosive compound known as nitrourea (NU), which is prepared by reacting aqueous UN with sulfuric acid, another commercially available product (75). NU can subsequently be used to prepare a whole range of high energy density materials (HEDM) with extremely high VODs such as those shown in Figure 1.1 (76-78). However, many of these compounds are unstable in water and so have little practical application. Numerous studies have reported the synthesis of hydrolytically stable energetic materials based on N-nitrourea, although these compounds require complex reagents and materials making them much less attainable for an individual with minimal knowledge of chemical synthesis (76, 77, 79). Nevertheless, the number of HEDMs possible highlights the enormous potential of UN as an explosive and explosive precursor.

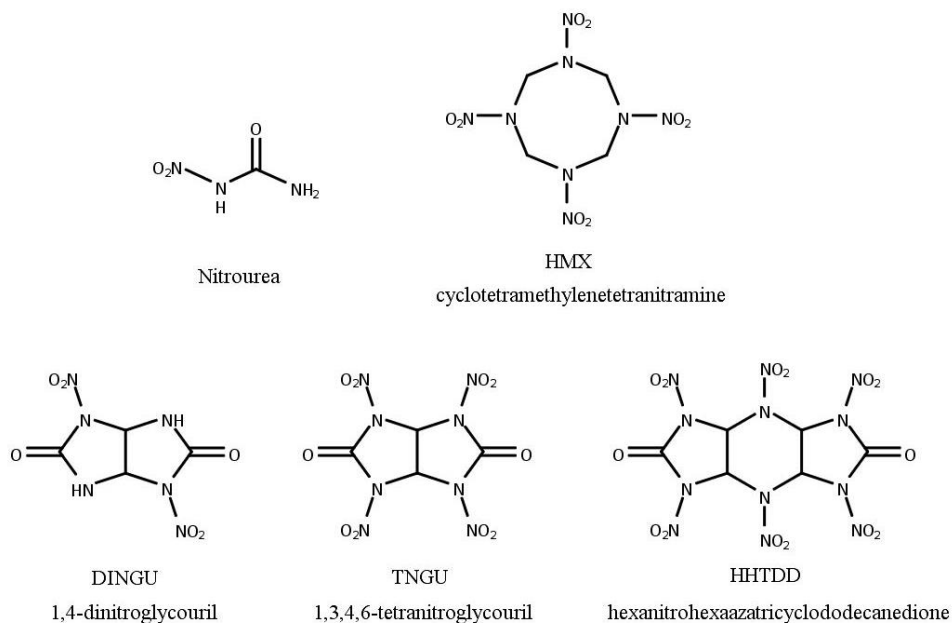


**Figure 1.2:** High energy density materials that can be prepared from nitrourea

### 1.3.3 Pyrotechnics

#### 1.3.3.1 Legitimate uses and manufacture

A pyrotechnic composition is a substance or mixture that is designed to burn in a self-sustaining exothermic reaction producing a combination of heat, colour, smoke, and noise (80-82). All pyrotechnic compositions are prepared by mixing an oxidiser and a fuel and often contain binding materials and other additives to achieve desired properties (80, 83). Pyrotechnics have had many legitimate uses and continue to have a number of military and commercial applications. Heat-generating pyrotechnics are heavily used as a component in fuses and primers in gun propellants, projectiles and fireworks (80, 84, 85). The manufacture of consumer fireworks is the most common commercial use of pyrotechnic mixtures and can be prepared with an assortment of smoke and light-generating compositions that produce specific effects based on the type and amount of metals used (84, 86). Metals such as strontium, titanium and zirconium are used within signal flares as they produce intense coloured and white light at high temperatures (84).

#### 1.3.3.2 Homemade pyrotechnic compositions and market availability

Any product containing a pyrotechnic composition has the potential to be incorporated into a HME. Commercially available pyrotechnics are highly variable in their composition but are typically based on nitrate, chlorate or perchlorate salts (83, 87). In most countries, consumer fireworks are the most accessible product containing a pyrotechnic mixture and typically include potassium chlorate or perchlorate as the primary oxidising agent (88). Although a significant decrease in chlorate-based mixtures has been observed due to them being highly reactive in certain compositions (83, 89). In Australia, the vast majority of firework products cannot be legally purchased, and so party sparklers are the most accessible and used pyrotechnic within the community (90). Furthermore, party sparklers typically contain a nitrate salt as their primary oxidising agent and so these products heavily contribute to commercially accessible nitrate based HMEs.



### 1.3.3.3 Use of pyrotechnics as a HME

Pyrotechnics are often incorporated into HMEs or used to prepare IEDs as they are low cost, readily accessible and require minimal modification to be used as a HME. They are also often used as fuses to ignite or link charges. Many factors affect reaction rate and effectiveness of a pyrotechnic product, which also applies to its use as an explosive. The burning rate and desired pyrotechnic effect are heavily dependent on particle size and mixture homogeneity as intimate contact between the oxidiser and fuel is required for an efficient reaction (83). If the intent is to produce an explosion, the pyrotechnic composition must be contained, which is often observed in the form of sparkler based or pipe bombs. As the confined mixture burns a large volume of gas is produced and will result in an explosion once the increasing pressure overcomes the structural integrity of the container (91). Pipe bombs can further be modified with additional fragmenting materials such as nails or ball bearings to improve the destructive potential. Although typically not as destructive as fertiliser based HMEs, pipe bombs and sparkler based bombs are the most common type of device encountered by law enforcement in many countries including Australia and the USA and so pose an ongoing threat while the precursors remain readily available (92).

## 1.4 Forensic chemical analysis of HMEs

There are many stages and investigative processes within the forensic investigation of explosives from the initial response to the presentation of evidence for the courts. The forensic chemical analysis of debris from an explosion is a crucial and challenging process that involves a systematic and rigorous analytical protocol to identify the chemical residues present. The knowledge gained may then aid in generating investigate leads, establishing links, supporting other forms of evidence and contributing to the forensic intelligence of explosives. Due to the inherent variability of explosives, a range of techniques may be employed to characterise and identify an unknown explosive sample. The analytical procedure carried out is also highly dependent on the location, in-tact or post-blast residues, contamination, sample substrate and render-safe procedures. The technical working group for fire and explosions analysis (TWGFEX) established and published a set of guidelines to aid in the forensic analysis of explosives which separates techniques based on the amount of structural and elemental information they provide (93, 94). This framework outlines

recommended techniques for the identification of in-tact explosives and post-blast residues which is used to infer the analytical protocol adopted for the analysis of forensic samples.

The forensic examination of HMEs typically involves the detection and identification of the inorganic ions present as they are often prepared from fertiliser products and pyrotechnic mixtures (1). The ongoing use of devices such as pipe bombs, sparkler bombs and other pyrotechnic compositions has resulted in a significant amount of research focussed on developing and improving methods for the detection of inorganic based HMEs (95-102). This includes the improvement of on-site analysis for preliminary identification, and attribution methods for the discrimination of fuel/oxidiser mixtures (95, 97, 103, 104). Although a range of techniques have proven effective in explosives analysis, those which are routine and commonly used within investigations are detailed below.

#### 1.4.1 Spectroscopy

Infrared (IR) and Raman spectroscopy have been widely used for the detection of organic and inorganic explosives as they can provide rapid and accurate identification and are commonplace in most forensic laboratories (105, 106). The addition of microscope or stand-off based systems also allow for on-site analysis and identification of microscopic explosive residues (105). Portable instruments are often used to provide a preliminary assessment of unknown samples at an explosion scene, which can also be used by personnel with minimal analytical training (106). IR and Raman techniques have been proven to reliably identify the oxidising agents within consumer fireworks and other fuel/oxidiser mixtures commonly used to prepare HMEs (103, 105, 107). Both techniques provide characteristic spectral signatures and thus can identify the oxidising salts within inorganic based HMEs.

Attenuated total reflectance Fourier transform infrared (ATR-FTIR) spectroscopy has been shown to discriminate between a number of nitrate, chlorate, perchlorate, sulfate and ammonium salts common in HME mixtures (102). As the anion provides a characteristic spectral signature according to the vibrational modes of their covalent bonds, discrimination of salts can be achieved. Furthermore, ATR-FTIR is capable of identifying salt species within post-blast residues attributed to a variety of firework

components which highlights the potential value of using IR on both in-tact particles and residues from functioned devices (103). Zapata *et al.* conducted a comprehensive investigation into the discrimination of 72 commercially available nitrate, chlorate and perchlorate salts (95). The study showed that the unequivocal identification of 44 salts was achievable using Raman, IR or a combination of both. Salts containing the same anion but different metal cations could also be distinguished based on the trace spectral contributions from different metals. Identifications made using spectroscopic techniques can further be supported using complementary techniques such as scanning electron microscopy (SEM), capillary electrophoresis (CE) and ion chromatography (IC).

#### 1.4.2 Microscopy and X-ray techniques

Scanning electron microscopy energy dispersive X-ray spectroscopy (SEM-EDS) is a non-destructive technique that can be used for the analysis of in-tact explosive particles. It is routinely used in the analysis of HMEs as it identifies metal particles as well as elemental components such as carbon and sulfur, hence it is often used for confirming the presence of black powder within a mixture (87, 107, 108). If used in sequence with spectroscopic techniques, both oxidiser and fuel components can be identified within many mixtures, making it extremely useful for pyrotechnic compositions and inorganic based HMEs. It can also be useful within the analysis of AN or UN mixtures when metal fuels have been added.

X-ray techniques including X-ray diffraction (XRD) and X-ray fluorescence (XRF) can also be used for the analysis of in-tact explosive particles (105, 109, 110). Both techniques generally enable the non-destructive analysis of a sample and require minimal sample preparation. XRF measures the characteristic wavelengths of emitted radiation induced by X-rays to identify the major elemental constituents (111). XRD is based on the elastic scattering of X-ray radiation and can identify and provide structural information of bulk crystalline materials by comparing the generated diffraction patterns to standard reference patterns (112). Both techniques rely on a flat, homogenous sample of solid crystalline particles, making them well-suited for fertiliser based HMEs such as AN and UN.

### 1.4.3 Separation methods

Separation methods are heavily relied upon for the analysis of explosives as they permit the isolation and identification of species from complex matrices and trace samples (113). Extraction techniques including liquid-liquid extraction and solid phase extraction are used for initial sample clean up before more advanced separation techniques such as gas chromatography (GC), liquid chromatography (LC), ion chromatography (IC) and capillary electrophoresis (CE) are used to separate and identify individual components from complex mixtures (113). Mass spectrometry (MS) is also commonly used post separation as a means of confirming the identity of separated analytes.

IC and CE are the most used techniques for inorganic explosives, providing the best sensitivity and selectivity for the analysis of ionic species (96, 113). CE separates ions based on their electrophoretic mobility within a capillary that has a high voltage applied across both ends. CE has been used to identify a number of anions and cations within pre and post-blast residues from inorganic based HMEs (96, 98, 114). Saiz *et al.* reported using CE for the concurrent determination of ionic species within consumer fireworks, highlighting its application to fuel/oxidiser mixtures and pyrotechnic products (100). IC has similar applications within explosive analysis and is routinely used for the analysis of homemade mixtures and IEDs due to its high specificity and sensitivity for ionic species (88, 97, 115). IC separates ions and polar molecules based on their affinity to the ion-exchange resin within the anion and cation columns. A substantial number of analytes have been characterised within pyrotechnic compositions, black powder mixtures, ANFO slurries and inorganic based IEDs (97). Simultaneous separation and detection of common ions has also been performed within post-blast residues, which can be used in parallel with CE for to obtain complementary results (97). To confirm the identity of peaks presented from separated species, IC and CE are often coupled with MS techniques to provide a positive identification.

GC and LC methods combined with electrospray ionisation (ESI) or atmospheric pressure chemical ionisation (APCI) MS apply mostly to the analysis and identification of nitro-based military and commercial explosives. However, application to UN has also been reported, being used to provide the unequivocal

identification of the in-tact salt species to confirm its presence within pre and post-blast residues. The decomposition products of AN and UN have a high degree of overlap and so successful identification of UN within an unknown sample typically relies on preparing xanthidrol based derivatives with characteristic signatures that can be detected with modified separation methods (116, 117). This is particularly challenging within post-blast residues as contamination and interfering compounds can obstruct a positive identification.

## **1.5 Application of chemometrics in explosives analysis**

Many forensic disciplines use a multitude of analytical instrumentation to chemically characterise a range of evidence types, often generating large and complex datasets (118-120). Interpretation of this data and visual comparison methods is laborious and requires highly expert personnel which can still lead to false positives or be affected by cognitive biases (118, 120). For these reasons, a substantial amount of research investigating the applicability of multivariate statistical methods has been conducted, with the aim of developing more objective and reliable approaches to evidence interpretation (119). Chemometric analysis is one approach that has seen increasing use within forensic processes, being combined with analytical techniques for characterisation and discrimination purposes (118, 119). Chemometric methods allow for the timely and accurate interpretation of evidence compared to visual inspections and can be used with data obtained from a range of instrumentation including spectroscopy, chromatography and X-ray based techniques (120, 121). The literature has highlighted the use of chemometrics in many forensic applications including drug profiling and document examination, as well as the discrimination and source determination of many evidence types including biological fluids, glass, paint, fire debris, fibres and soil (118).

Several studies have examined the use of chemometrics with an assortment of analytical techniques for the identification and discrimination of trace residues recovered from high and low explosives, however few studies have investigated nitrate based HMEs (119). Within the chemometric investigations of low order explosives, a significant portion of work involves the analysis of gunshot residues (GSRs) and propellants (122-127). High explosives that are often investigated include those used for military or commercial purposes (128-130). Previous work on the discrimination

and source attribution of inorganic based HMEs, as well as the chemometric techniques used within this study is described below.

### 1.5.1 Chemometric techniques

Chemometric analysis encompasses a broad range of statistical methods that are used to analyse and model chemical information. In addition to improving the objectivity of data analysis, these techniques are often used to identify relationships and reveal underlying trends within complex datasets to enhance sample discrimination (119, 131). Methods used throughout this study are categorised as pattern recognition techniques, which aim to extract the latent information from a dataset in order to classify, discriminate and explain the relationships between variables. This information may be critical to establish connections and gather intelligence within an investigation and complements the data obtained from instrumental analysis.

#### 1.5.1.1 Principal component analysis

Principal component analysis (PCA) is classified as an unsupervised pattern recognition technique and is used to visualise trends within a dataset without establishing prior groupings or labels and therefore minimises the amount of human bias and subjectivity. This provides a more reliable and objective analysis approach as no previous assumptions about the dataset are made. PCA reduces the dimensionality of large and complex datasets by extracting orthogonal sources of variation referred to as principal components (PCs) (24, 119). Each PC represents a different combination of variation identified within the original variables. Each successive PC is calculated to describe the maximum proportion of remaining variance within the dataset and so majority of the variation observed is within the first few PCs (24, 119). Samples are then projected into a space where each axis is described by a different PC, therefore generating a plot that visualises the distribution of samples across selected PCs as well as any established groupings. The position of each sample across a particular PC can also be attributed to specific areas of variation within the dataset by examining the loadings, which is useful for identifying the basis of any discrimination observed or explaining the relationships between samples.

### 1.5.1.2 Linear discriminant analysis

Discriminant analysis (DA) is a supervised pattern recognition technique that is often carried out after preliminary data reduction as the number of samples must exceed the number of descriptors. DA involves constructing a discriminant function by classifying samples into pre-defined classes with the aim of maximising the ratio of between-group to within-group variance and thus establishes maximum discrimination between classes (24, 119). If it is further assumed that the discriminant function separating samples is linear, then the method is referred to as linear discriminant analysis (LDA) (24, 119). The two main processes involved in LDA include construction and validation of the discriminant function which is used to describe trends in complex datasets and classify future samples. A discriminant function is constructed by establishing a set of pre-defined classes which the model then classifies samples from a training set into the known classes, outputting a confusion matrix that provides a summary of the classifications (24, 119). This matrix details the predicted classes of each sample and thus is used to determine the discrimination accuracy of the model and highlights samples that were misclassified or not effectively separated from neighbouring classes.

The predictive accuracy of the model can then be assessed by several validation approaches, two of which were used throughout this study. The first cross-validation procedure is referred to as the leave-one-out method which involves removing a single sample from the training set from which the discriminant function was constructed and then classifying the sample with the resultant model. This process is repeated for every sample within the training set. Although more reliable validation methods can be used, this method provides an indication of the model's predictive efficacy and is useful within limited datasets or when building an independent test set is not possible. A more reliable approach is to validate the model with a test set containing samples that are completely independent from the training set. This method results in a more accurate assessment of the model's prediction capabilities and should be the preferred method when performing LDA.

### 1.5.2 Discrimination and source attribution of HMEs involving chemometrics

As nitrate based HMEs are prepared from commercially available ingredients, the use of chemometric techniques can potentially support the identification of the explosive and infer the source of the precursors and products used. Chemometric techniques have previously been used subsequent to a number of analytical techniques to provide additional source information. Most studies use these techniques in conjunction with more advanced non-routine instrumentation such as isotope ratio mass spectrometry (IRMS) and inductively coupled plasma mass spectrometry (ICPMS), however alternative techniques such as infrared and Raman hyperspectral imaging have also been reported (132, 133).

Suppajariyawat *et al.* used a combination of PCA-LDA with GCMS and FTIR methods to discriminate between ANFO mixtures prepared with eight different diesel oil brands (134). It was shown that the variation in trace components across diesel products allowed for the visualisation of discrete sample groups and discrimination of brands. The predictive accuracy of the LDA model was then assessed using a leave-one-out cross validation approach. Using spectral and GCMS data, respectively, 90 and 98% of removed samples were correctly classified, highlighting the effectiveness of using chemometrics to discriminate between precursor brands.

The source attribution of AN as an explosive precursor has been further investigated by discriminating between AN fertilisers. Brust *et al.* used a combination of IRMS and ICPMS to discriminate between fertiliser samples from 19 different manufacturers (73). Isotopic and elemental profiles were combined with PCA-LDA to assess the discrimination between brands and within batches originating from the same manufacturer. It was found that combining profiles from both techniques afforded high discriminatory power between manufacturers, however discriminating between individual batches was more challenging.

Fraga *et al.* explored the discrimination of calcium ammonium nitrate (CAN) fertiliser which is also frequently used to make HMEs (135). ICPMS and partial least squares discriminant analysis (PLSDA) was used on 125 samples from 11 CAN fertiliser stocks that originated from 6 different factories. Additionally, the source determination of samples mixed with powdered sugar and aluminium powder was



assessed to simulate potential HME mixtures. The use of elemental profiling and chemometrics permitted the prediction of 73% and 100% respectively of pristine samples and mixtures prepared with sugar. Poor source predication was achieved with samples mixed with aluminium due to a number of interfering compounds.

Lastly, PCA performed with FTIR data has also been used to show the variation between post-blast residues recovered from consumer fireworks when collected with different swab types and across different surfaces (103). Aside from using PCA to discriminate between HME precursors, this investigation highlighted its use within recovery protocols which is a crucial aspect within the investigation of HMEs.

## **1.6 Forensic intelligence of HMEs**

The implementation of forensic intelligence models within law enforcement systems and investigative procedures is an ongoing effort within forensic science (136, 137). Forensic intelligence has previously been defined as the accurate, timely and useful product of logically processing forensic case data and aims to contribute to decision making and inform the law enforcement system prior to an event taking place, through to prosecution within the courts (138, 139). If used properly, forensic intelligence can significantly contribute to all stages of the investigative process by supporting strategic decisions, police operations, and the interpretation and dissemination of data (138, 140). Furthermore, in addition to supporting single case procedures, forensic intelligence aims to assist across multiple cases in order to generate leads and contribute to crime disruption and prevention (137, 139).

Within the context of explosive investigations, forensic intelligence has previously proven to play an important role in countering IEDs and disrupting networks that employ these devices (141). Many countries including Australia and US have implemented programs that utilise the forensic intelligence of IEDs to report technical information, inform analytical and counter measure procedures and predict future IED activity (141, 142). Although this shows the role of forensic intelligence within a broad military context, it highlights its potential use and importance within law enforcement and forensic case procedures.

Within the chemical analysis and potential source attribution of HMEs, a substantial amount of the analytical protocol relies on previously established intelligence and knowledge surrounding how they are prepared and what chemical signatures are required to report a positive identification (1, 14). As HMEs can be prepared from a vast range of commercially available products and precursors, any explosive sample resulting from a HME could potentially be unique. Therefore, for any given HME, knowledge of the precursors required, synthetic routes, products used, and the chemical information obtained from different analytical techniques is essential for establishing an effective analysis procedure. Furthermore, this knowledge is crucial for providing additional source information beyond a positive identification, in order to link explosive samples to specific products, brands and retail sources.

To achieve this within the context of nitrate based HMEs, knowledge of the relevant products and synthetic procedures that can be carried out to prepare explosives such as AN and UN is required. The sources of precursors will vary between countries and jurisdictions based on imposed restrictions; however, many will be accessible everywhere. Investigations into the capacity to repurpose commercial products for the preparation of a HME would largely contribute to forensic intelligence and assist law enforcement and forensic chemists to establish links between explosive samples, precursor products and potentially provide additional source information. Knowledge such as where precursors can be purchased, what quantities can be covertly obtained, their physical state (e.g., solid pellets, aqueous solution), if extraction is required (e.g., precursor contained within mixture) and their affordability.

Improving and developing methods for the analysis of HMEs from alternatively sourced products is also required, which will reveal the amount of information produced from select techniques and whether it can be used for discrimination and source attribution purposes. This would reduce the uncertainty surrounding HME identification and simplify forensic analysis protocols.

## **1.7 Summary and aims**

This work was a direct response to the local and international forensic need to better the understanding and improve the forensic characterisation capabilities of nitrate based HMEs. The investigative, analytical and statistical procedures demonstrated

were used to explore the complete identification, characterisation and source attribution of three nitrate based HMEs including party sparklers, AN and UN. NU is also explored as a potential successor to UN as it can also be made with readily available commercial products. The analytical framework outlined can further be repurposed to improve the knowledge of any HME that is currently in frequent use or yet to emerge.

To summarise, there are three main aims that are consistent throughout each chapter and within the investigation of each HME.

- Perform a market study and identify the commercial products, brands and readily available precursors that can be used to source or prepare the HME being explored. For AN and UN, the capacity to prepare large amounts of explosive material from each product was also assessed. This information contributes to HME intelligence and the disruption of HME manufacture.
- Characterise the set of products collected for each HME with a number of routine and non-routine analytical techniques and assess whether the information obtained can be used for discrimination purposes. The characteristic data would assist in identifying sample features such as mixture composition, preparation history, possible precursors used, retail source, purity and capacity to function as an explosive.
- Perform chemometric analysis with select data to evaluate the source determination capabilities and demonstrate the ability to link explosive material back to the precursors used or individual product brands collected. Techniques used with chemometrics including ATR-FTIR, XRD and ICPMS were also directly compared to demonstrate the effectiveness of using different types of data as well as routine and non-routine explosive analysis techniques. This part of the investigation aims to improve the forensic analysis and evidential value of HMEs by further demonstrating the ability to identify precursor sources and product brands using chemometric methods.

As this work involves the synthesis and ignition of highly energetic materials, Chapter 2 begins with a discussion of the experimental considerations for preparing, handling and conducting research on explosive materials. An overview of the synthetic

procedures and instrumental and statistical methods that are used consistently throughout subsequent chapters is also detailed.

Chapter 3 details the characterisation and source attribution of nitrate-based party sparklers, which are frequently used to prepare HMEs and make up the majority of explosive related casework in Western Australia (WA). Nineteen Australian sourced sparklers were collected and analysed using multiple techniques, reporting the characteristic and discriminatory information that can be obtained with different analytical methods. This provided a substantial amount of information that may be used to improve the evidential value of seized party sparkler samples within a forensic investigation. Chemometric analysis was subsequently performed with spectral and elemental data, demonstrating the source determination capabilities of unburnt and burnt residues before the attribution of post-blast sparkler residues is explored in Chapter 6. The work presented in this chapter could further be modified and applied to consumer fireworks, which are heavily used to prepare HMEs in countries such as the US.

Chapters 4 and 5 follow a similar investigative procedure in that a number of commercial products were first purchased and used to synthesise homemade AN and UN, also comparing the capability of preparing bulk amounts from each product. A suite of routine techniques was used to analyse each product, identifying the characteristic chemical signatures produced and assessing whether they can be used to achieve product and brand discrimination. This was further assessed with the use of chemometric methods, demonstrating the source determination capabilities of alternatively sourced fertiliser based HMEs with ATR-FTIR, ICPMS and XRD.

In addition to the forensic characterisation of pre-blast explosive residues, Chapter 6 applies the methodologies established in previous chapters to demonstrate the forensic characterisation and source determination capabilities of post-blast residues recovered from party sparkler and UN based IEDs. The preparation, ignition, and challenges of conducting post-blast experiments was discussed. Furthermore, the recovery and analysis procedures adopted were directly compared between experiments involving low order (sparkler bombs) and high-order (UN based devices) explosives. This information will significantly contribute to the forensic intelligence literature on

pyrotechnic and fertiliser based IEDs and assist future research involving post-blast attribution.

Lastly, Chapter 7 presents a conclusive summary of the work presented in this thesis and future work is detailed. Application of the investigative strategy established in this thesis for the investigation of other inorganic based HMEs, such as chlorate or perchlorate-based explosives is discussed. The additional work required to improve validation procedures and application of source attribution methods within forensic casework is also considered.

## Chapter 2. Experimental methods and instrumentation

Portions of the experimental and synthetic methods detailed in this chapter have been published as follows:

Joshua A. D’Uva, David DeTata, Christopher D. May, Simon W. Lewis. Investigations into the source attribution of party sparklers using trace elemental analysis and chemometrics. *Analytical methods* **2020** 12, 4939-4948 DOI:

Joshua A. D’Uva, David DeTata, Ryan Fillingham, Robert Dunsmore, Simon W. Lewis. Synthesis and characterisation of homemade urea nitrate explosive from commercial sources of urea. *Forensic Chemistry* **2021** 26, 1-9 DOI: <https://doi.org/10.1016/j.forc.2021.100369>

Joshua A. D’Uva, David DeTata, Simon W. Lewis. Source determination of homemade ammonium nitrate using ATR-FTIR spectroscopy, trace elemental analysis and chemometrics. *Forensic Chemistry* **2022** 28, 1-11 DOI: <https://doi.org/10.1016/j.forc.2022.100411>

## 2.1 Introduction

This chapter focuses on the preparation and analysis of explosive compounds used throughout this study. The section begins with a discussion of the experimental considerations required to work with pyrotechnic and explosive samples, including information on risk management, storage and disposal, and multi-agency collaboration. Synthetic procedures and alternative preparation methods of explosive samples are described. The generic instrumentation used across subsequent chapters is outlined, with any adaptations to the methods, setup conditions or sample preparation specified within relevant chapters. Chemometric and data analysis methods are also described. Details regarding the preparation and ignition of improvised explosive devices (IEDs) are detailed in Chapter 6.

## 2.2 Experimental considerations

The research of pyrotechnic and explosive compounds is inherently challenging due to the potential hazards and risks present throughout all stages of the investigative process. Thus, this research was conducted with ongoing collaboration and input from experts currently active in explosive investigations, as well as access to facilities that allow for the preparation and analysis of explosive compounds and IEDs.

This chapter details the synthesis of ammonium nitrate (AN) and urea nitrate (UN) from alternative sources. All compounds were prepared within ChemCentre facilities under the supervision and guidance of ChemCentre personnel and with direct input from the Western Australia Bomb Response Unit (WABRU). If a variation to the procedure needed to be made based on the precursor source, a minimal amount (< 1g) was initially prepared before being scaled up to amounts required for post-blast investigations. For characterisation purposes, a minimal amount was prepared and then disposed of once completely characterised. If large quantities were required (to prepare IEDs), batches of 100g were prepared and immediately transported and stored in appropriate facilities by the WABRU. Large amounts of explosive material was handled solely by WABRU personnel.

Analysis of explosives prepared by various techniques also required preliminary planning and discussion. There is no reported literature regarding sample preparation

and analysis of alternatively sourced AN and UN or party sparkler material using many of the techniques detailed in this study. Although both AN and UN are relatively stable, they are still highly energetic compounds that have been prepared using unconventional commercial ingredients. Therefore, preliminary experiments were conducted on small amounts of sample to establish appropriate preparation and analysis procedures that proved to be both low risk and effective. Burn tests were also conducted to assess the compounds sensitivity and to make informed comparisons with known energetic materials regarding sensitivity.

Post-blast experiments involving the preparation and initiation of IEDs are inherently complex and presented many additional challenges and limitations. These, along with all experimental considerations made, are detailed in Chapter 6.

## **2.3 Preparation of homemade explosives**

Synthetic procedures for the preparation of homemade explosives (HMEs) used throughout this study are described. Precursor, product, and average yield information is detailed within relevant chapters.

### **2.3.1 Ammonium nitrate**

#### **2.3.1.1 Synthesis from commercial sulfate of ammonia fertiliser and laboratory reagents**

This procedure outlines the preparation of AN from calcium nitrate and ammonium sulfate. The source and brand of the reagents were unique to each AN product; however, the synthesis was consistent throughout.

Calcium nitrate (5g, 0.031 mol) was added to water (50 mL) and heated until dissolved. Ammonium sulfate (4g, 0.030 mol) was added to water (50 mL) and heated until dissolved. Solutions were combined and the calcium sulfate precipitate was removed by vacuum filtration. The solution was heated until all of the water had evaporated, which yielded ammonium nitrate (~ 2.5 – 4g).



### 2.3.1.2 Synthesis from Black Marvel and African Violet Food

This procedure outlines the preparation of AN from an alternative fertiliser mixture. This procedure could also be used with other fertiliser mixtures containing  $\text{NH}_4$ , however the expected yield would differ depending on the percentage amount of  $\text{NH}_4$  compared to other components within the mixture.

Calcium nitrate (5g, 0.031 mol) was added to water (50 mL) and heated until dissolved. Black Marvel Food (7g) or African Violet Food (8g) was added to 100 mL of water and heated for 30 minutes with stirring. The solution was filtered by vacuum filtration before being added to the aqueous calcium nitrate. Calcium sulfate precipitate was removed by vacuum filtration and the remaining solution was heated until all of the water had evaporated, which yielded ammonium nitrate (~3 – 4g).

### 2.3.2 Urea nitrate

UN was synthesised by the reaction of nitric acid and urea, following the method reported by Oxley *et al.* (68). The method was adapted depending on the source of urea used as detailed below.

#### 2.3.2.1 Synthesis using chemical grade urea and urea fertiliser

Urea (5 g, 0.083 mol) was dissolved in water (12 mL) with stirring. Excess nitric acid (15.9 M, 6 mL, 0.0954 mol) was added dropwise with stirring. The solution was cooled using an ice bath during the addition of acid and the temperature was monitored to ensure it did not exceed 40 °C. The solution was allowed to stir for an additional 15 minutes and then vacuum filtered. The white solid was dried in an oven (40 °C) overnight to yield urea nitrate.

#### 2.3.2.2 Synthesis using urea based cold packs

The cold pack was cut open and the urea prills were removed without disrupting the water bag contained within the packet. The method described above in section 4.2.2.1 was then performed to yield urea nitrate.

### 2.3.2.3 Synthesis using diesel exhaust fluid

Excess nitric acid (15.9 M, 6 mL, 0.0954 mol) was added dropwise to diesel exhaust fluid (DEF) (15.4 g) with stirring. The solution was cooled using an ice bath during the addition of acid and the temperature was monitored to ensure it did not exceed 40 °C. The solution was allowed to stir for an additional 15 minutes and then vacuum filtered. The white solid was dried in an oven (40 °C) overnight to yield urea nitrate.

### 2.3.2.4 Synthesis using alternative fertiliser mixtures

Osmocote prills (15g) or Green boost prills (13.4 g) were ground to form a fine powder. Water (12 mL) was added and the mixture was allowed to stir for 30 minutes. The mixture was vacuum filtered to remove undissolved solids. Excess nitric acid (15.9 M, 6 mL, 0.0954 mol) was added drop-wise with stirring. The solution was cooled using an ice bath during the addition of acid and the temperature was monitored to ensure the solution did not exceed 40 °C. The solution was allowed to stir for an additional 15 minutes and then vacuum filtered. The white solid was dried in an oven (40 °C) overnight to yield urea nitrate.

## 2.4 Instrumentation

### 2.4.1 Infrared spectroscopy

Infrared (IR) spectra were obtained using a Nicolet iS50 Fourier transform infrared (FTIR) spectrophotometer with a single-bounce attenuated total reflectance (ATR) diamond crystal and KBr beam splitter (Thermo Fisher Scientific, USA). Spectra were acquired over the 4000 – 400  $\text{cm}^{-1}$  spectral range using 16 co-added scans and a spectral resolution of 4  $\text{cm}^{-1}$  in absorbance mode. An ATR correction was applied to each spectrum using the in-built software (Omic 9, Thermo Fisher Scientific). Spectral analysis was performed on a small sample taken from the bulk product material using the pressure arm to maintain a consistent contact pressure. The diamond was then cleaned with ethanol and a new sub-sample was analysed. This method applies to all samples analysed throughout this study, differing only in a number of replicates obtained, which is detailed in appropriate sections.

## 2.4.2 Raman spectroscopy

Raman spectra were obtained with a Renishaw inVia confocal Raman microscope (Galactic Scientific, AUS). Spectra were acquired over the 1800 – 100  $\text{cm}^{-1}$  range using three accumulations and a ten second exposure time. Samples were viewed with a 20x objective and excited at 795 nm. A baseline correction was performed on each spectrum after collection. This method applies to all samples analysed throughout this thesis with the exception of laser power, which varied depending on the purity of the product and is detailed in appropriate sections.

## 2.4.3 Ion chromatography

A Dionex ICS-6000 (Thermo Fisher Scientific, USA) reagent free Ion Chromatography (IC) Eluent Generation system, composed of an autosampler, gradient pump module, eluent generator and conductivity detector, was used for IC determination in this study. Data was processed using Chromeleon 7.2.7 software.

Cation separation was obtained using a Dionex IonPac CS-12A ( $3 \times 250$  mm) column attached to a Dionex IonPac CG12A ( $4 \times 50$  mm) guard column maintained at 30 °C. A flow rate of 0.7 mL/min was utilised with eluent generated by an EGC 500 methanesulfonic acid (MSA) cartridge. The eluent flow rate was 10 mM MSA from 0-5 minutes, followed by a step change to 30 mM MSA from 5-30 minutes, followed by a second step change to 10 mM from 30-33 minutes, followed by the maintenance of 10 mM to the end of the run at 45 minutes.

Anion analysis was obtained using a Dionex IonPac AS20 ( $2 \times 250$  mm) column attached to a Dionex IonPac AG20 ( $2 \times 50$  mm) guard column maintained at 30 °C. A flow rate of 0.250 mL/min was utilised with eluent generated by an EGC 500 potassium hydroxide cartridge. The eluent flow rate was 5 mM potassium hydroxide from 0-5 minutes, followed by a step change to 30 mM potassium hydroxide from 5-15 minutes, followed by a second step change to 55 mM from 15-30 minutes, followed by a third step change to 5 mM potassium hydroxide from 30-30.1 minutes, followed by the maintenance of 5 mM potassium hydroxide to the end of the run at 40 minutes.

MilliQ water, generated by a MilliQ IQ 7000 system (Merck Millipore, USA) was used for sample preparation and blanks. Cation and anions were quantified using a 5-

point calibration curve using standards at 5, 10, 20, 50 and 100 ppm (Inorganic Ventures, VA, USA). The cations were lithium, sodium, ammonium, potassium, magnesium, calcium, strontium and barium. Anions were chloride, chlorite, nitrite, chlorate, nitrate, sulfate, thiosulfate and perchlorate. Sample preparation is detailed in appropriate chapters.

#### 2.4.4 Scanning electron microscopy

Sample analysis was performed using a Tescan Mira field emission scanning electron microscope (FESEM) equipped with two Oxford Ultim Max (100 mm<sup>2</sup>) energy dispersive x-ray spectroscopy (EDS) detectors. The Tescan Essence™ and Oxford Aztec EDS software was used for chemical imaging, elemental composition analysis and interpretation of data. Analysis was performed with an accelerating voltage of 25 keV, beam current of 3nA and a working distance of 15 mm. Bulk analysis was done initially on a select flat region of the sample and then subsequent analysis on key spots was performed if necessary.

#### 2.4.5 Gas chromatography mass spectrometry

Gas chromatography mass spectrometry (GCMS) was carried out on an Agilent (Santa Clara, CA, USA) 7890B gas chromatograph fitted with an Agilent J&W DB-1701 column (30 m × 0.25 mm ID capillary column chemically bonded with 14% Cyanopropylphenyl / 86% Dimethyl polysiloxane at 0.25 μm film thickness) coupled to an Agilent 5977B mass spectrometer used in electron ionisation mode. GCMS data was processed using Agilent MassHunter Version 10.

The injection port temperature was set to 250 °C using splitless mode, with the inlet set to purge to the split vent at 0.5 minutes after injection; helium was used as the carrier gas; and an injection volume of 1 μL was used. Column temperature was initially held at 45 °C for 5 minutes and then increased to 280 °C at a rate of 15 °C/min, then held for 16 minutes, giving a total run time of 36.67 minutes. The MS was operated in positive full scan mode for a mass range of m/z 40–500 amu with the ion source set to 70 eV and current emission of 34.6 μA.

Sparkler material was stripped off the wire with gloves and ground to a fine powder using a mortar and pestle. Samples were prepared by dissolving sparkler material (100

mg) in dichloromethane (DCM) (5 mL). Samples were sonicated for 10 minutes before being filtered using a 25 mm Acrodisc® (0.45 µm hydrophilic polyethersulfone membrane) syringe filter attached to a 10 mL terumo hypodermic syringe. Blanks of the solvent and sample procedure were also prepared.

#### 2.4.6 X-ray diffraction

Samples were analysed using a Malvern PANalytical EMPYREAN III Diffractometer system equipped with a dCore-fitted Pixcel3D detector, 240 mm radius theta-theta goniometer, a Reflection-transmission spinner 3.0 sample stage, and an iCore-fitted Co generator with K- $\alpha_1$  1.78901 Å, K- $\alpha_2$  1.79290 Å and K- $\beta$  nickel filter. The samples were collected at an operating current of 30 mA and tension of 40 keV at a range 4 – 80 2-theta, 0.026 step size and approximately 299 seconds per step, with an incident beam mask of 14mm and automatic divergence slits. The data was K- $\alpha_2$  stripped before interpretation. Within both AN and UN studies, all samples were prepared and analysed in duplicate approximately one month apart.

#### 2.4.7 Inductively coupled plasma mass spectrometry

Elemental analysis was performed using an Agilent 7900 inductively coupled plasma mass spectrometer (ICPMS) (Santa Clara, CA, USA) with ISIS-3 discrete sampling introduction, coupled to an ASX-560 autosampler (Teledyne CETAC technologies, Omaha, NE, USA). The concentration of 58 elements were determined by 6-point calibration in the range of 0.2 – 50 ppb prepared from 100 ppm 68 multi-elemental standards A, B, C and Hg (Choice Analytical, NSW, AUS).  $^{103}\text{Rh}$  and  $^{193}\text{Ir}$  were used as internal standards and analysed under no gas, hydrogen and helium modes. The 10 ppb 68 multi-elemental standards A, B and C, as well as a drift solution, were analysed multiple times within a given run to assess quantitative drift. Dilution was performed using a Hamilton MicroLab 600 series auto-dilutor using 1% distilled nitric acid prepared from an OmniPure acid still. Sample preparation is detailed in appropriate chapters.

## 2.4.8 Chemometric methods

### 2.4.8.1 Chemometric analysis using spectral data from ATR-FTIR spectroscopy

Spectral data was processed using the Unscrambler X 11.0 software (Camo Analytics, Oslo, Norway). The 2340-1880  $\text{cm}^{-1}$  region was first removed from all spectra as it contains interference from absorbance of the diamond crystal. Spectra were then baseline corrected and range normalised, which is a function performed by the Unscrambler X software that involves scaling all samples in the range between 0 and 1, thus accounting for the variability in the ATR contact pressure. Principal component analysis (PCA) was performed using the non-linear iterative partial least squares (NIPALS) algorithm on the normalised dataset, calculating up to the first seven PCs. Discrimination of products was assessed by evaluating the distribution of samples and factor loading plots.

Linear discriminant analysis (LDA) was subsequently carried out using the linear distance and up to the first six principal components (PCs) with equal probabilities assumed. Products were either treated as individual classes or grouped based on the clusters formed after PCA. A stepwise classification approach was performed with select datasets, as described in appropriate chapters. Discriminant models generated from LDA were used to predict the sources of an independent data set. The predicted and actual sources were compared in order to evaluate the accuracy of the model. Discriminant values (DVs) were also analysed to assess the degree of separation between classes.

### 2.4.8.2 Chemometric analysis using X-ray diffraction patterns

X-ray diffraction (XRD) data was processed with the Unscrambler X 11.0 software. The data was baseline corrected and range normalised before PCA was performed using the NIPALS algorithm on the normalised dataset, calculating up to the first seven PCs. Discrimination of products was assessed by evaluating the distribution of samples and factor loading plots. Chemometric analysis coupled with XRD was only performed on AN and UN samples. LDA was not performed due to a limited sample set.

#### 2.4.8.3 Chemometric analysis using elemental concentration data from ICP-MS

Elemental data was processed with the Unscrambler X 11.0 software. From the 58 elements analysed, those present due to contamination, as well as trace elements that were detected at concentrations below the calibration range, were removed. Elements retained for analysis are described in relevant chapters. The data was mean centred and standardised to ensure the same quantitative scale was used across each PC. PCA was performed using the NIPALS algorithm on the standardised dataset, calculating up to the first seven PCs. Discrimination of products was assessed by evaluating the distribution of samples and factor loading plots.

LDA was subsequently carried out using the linear distance and up to the first four PCs with equal probabilities assumed. Products were either treated as individual classes or grouped based on clusters formed after PCA. A stepwise classification approach was performed with select datasets, as described in appropriate chapters. Discriminant models were generated using a randomised leave-one-out approach. This involved randomly removing one sample from the classification set to be used for validation. To further improve reliability of this approach, LDA was repeated a total of 20 times, each with a different randomised classification and validation set. The predicted and actual sources were compared to evaluate the accuracy of the model. Source determination capabilities of generated discriminant models were also assessed with independent datasets containing burnt and post-blast samples, which is detailed in appropriate chapters.

#### 2.4.8.4 ANOVA based feature selection

Analysis of variance (ANOVA) based feature selection was performed on the elemental data obtained from ICPMS analysis of unburnt, burnt, and post-blast party sparkler material prior to classification by PCA. This process reduces the number of classifiers in large datasets to identify elements that significantly contribute to the separation of classes. F-ratios were calculated for each element in Microsoft Excel using the ANOVA class-to-class and within-class variance equations (Figure 2.1) (143, 144).

$$(1) \quad \sigma_{cl}^2 = \frac{\sum(\bar{x}_i - \bar{x})^2 n_i}{(k - 1)}$$

$$(2) \quad \sigma_{err}^2 = \frac{((\sum \sum (x_{ij} - \bar{x})^2) - (\sum (\bar{x}_i - \bar{x})^2 n_i))}{(N - k)}$$

$$(3) \quad f \text{ ratio} = \frac{\sigma_{cl}^2}{\sigma_{err}^2}$$

**Figure 2.1:** Equations used to calculate f-ratios. The between class variance (1) is divided by the within class variance (2) to give the f-ratio for a selected element (3).

As the magnitude of the f-ratio indicates the amount of class separation, elements with the highest f-ratios will have a large contribution to the separation of samples. F-ratios were ranked in ascending order and a series of scores plots were generated with an increasing f-ratio threshold. The distribution and separation of samples was assessed to determine which elements did not contribute to separation and which elements were necessary for discrimination. The refined elemental profiles are described within relevant sections.



## **Chapter 3. Multi-technique analysis of homemade explosives containing commercial party sparklers**

A portion of this chapter has been published as followed:

**Joshua A. D’Uva**, David DeTata, Christopher D. May, Simon W. Lewis. Investigations into the source attribution of party sparklers using trace elemental analysis and chemometrics. *Analytical methods* **2020** 12, 4939-4948

### 3.1 Introduction

Improvised explosive devices (IEDs) typically contain inorganic explosives due to ease of availability and low cost. In Western Australia (WA), 'sparkler bombs' or other devices primarily comprised of party sparkler residue make up the majority of the IEDs seized by police. Sparklers and sparkler residue can be used to prepare an endless number of unique explosive devices but regardless of the design, all have the potential to initiate fires as well as cause major damage to people and property (1, 145). There is a high forensic interest in analysing pre- and post-blast residues from incidents involving party sparklers to establish a link between the residue and a specific commercial product or source (88, 99). Defining these links provides forensic investigators with information regarding where and how the sparklers were obtained, which may lead to the person/s involved. Drug profiling highlights the importance and amount of information that can be gained from source attribution methods within a forensic investigation and so further advancements in the profiling of explosive residues is needed (120, 146, 147). Developing an analytical approach capable of identifying the origin of sparkler material and discriminate between different sparkler brands would enhance source determination capabilities and improve the evidential value of sparkler residues within forensic casework. To achieve this, analysis of unburnt and burnt residues is first required to determine whether party sparklers themselves can be classified based on their chemical composition.

Party sparklers are primarily used for festivities or celebrations and are readily purchased through local retail or online stores (148, 149). They are inexpensive, can be purchased in bulk quantities and have a long shelf life. A sparkler typically consists of a metal rod coated in an energetic mixture that burns when ignited, producing colourful sparks (89, 150-152). The chemical composition between brands varies slightly but will contain four major components which include an oxidising material, a fuel, a combustible binder and a metallic component (88, 89, 150, 152). Common oxidising agents include barium, potassium or strontium nitrate, as well as potassium chlorate or perchlorate (83, 150). Aluminium, iron and titanium metal powders or flakes are added to act as an accelerant or retardant. Different metals are also added to produce different colour or sparkler effects. Binders such as dextrin, nitrocellulose and sugars serve a dual function in that they bind together the ingredients within the

mixture and act as a fuel to promote burning (150). The varying formulations used between brands may provide a unique chemical profile that could be used to differentiate between sources.

The inorganic and organic components within explosives are readily analysed using routine instrumental techniques. Ion chromatography (IC) and capillary electrophoresis (CE) produce the greatest sensitivity and selectivity for the analysis of cations and anions, as well as having the advantage of being field deployable (96-98, 113, 115, 153). Other chromatographic methods such as gas chromatography (GC) and liquid chromatography (LC) are routinely applied to the analysis of organic explosives and can be used to characterise binders incorporated in pyrotechnic compositions (113, 154-157), whilst less expensive methods such as infrared (IR) and Raman spectroscopy have also been used to analyse both inorganic and organic components (95, 105-107, 158). Alternative techniques including scanning electron microscopy (SEM) (10, 87, 107, 108, 159) and ion mobility spectrometry (IMS) can be used to detect a range of explosive mixtures but cannot provide quantitative results (160). Party sparklers primarily consist of an inorganic salt and a metal fuel, but also contain organic binders and resins. Therefore, multiple techniques may be used to analyse sparkler material and the analytical sequence would depend on what chemical information is desired.

Multiple studies have previously reported using the techniques above to identify the primary oxidising agent and other components within pyrotechnic mixtures which are routinely utilised in forensic casework (97, 115, 161-163). X-ray techniques such as X-ray fluorescence (XRF) and X-ray diffraction (XRD) are also suitable to determine the intact chemical composition of pyrotechnic mixtures (105, 109, 110). Spectroscopic techniques and electron microscopy have a large presence in literature within the analysis of consumer fireworks with an increasing use of spectrometric techniques in more recent years, including the use of attenuated total reflectance Fourier transform infrared (ATR-FTIR) spectroscopy to characterise post-blast residues from exploded fireworks by Alberca *et al.* (88, 103). However currently, while the active components within pyrotechnic mixtures can be successfully detected and identified, these techniques often do not provide enough characteristic information to distinguish between sources of the same substance. Furthermore, limited research

has been conducted on the analysis and source attribution of party sparklers, which has a large presence in explosive casework within Australia.

The aims of this chapter are to analyse an assortment of commercially sourced party sparklers with an array of routine and non-routine techniques before exploring the source attribution capabilities of unburnt and burnt sparkler material when select techniques are coupled with chemometrics. Sparklers primarily contain a nitrate salt among a wide range of additional components; therefore, the trace chemical information obtained can potentially be exploited to discriminate between different brands. The characterisation and successful discrimination of different party sparkler brands largely contributes to the forensic intelligence of party sparklers as inorganic explosives. This information could subsequently be used to improve the analysis and evidential value of sparkler residues within a forensic investigation and may assist with generating leads and establishing links between seized material and a suspect. The experimental methods and analysis outlined in this investigation can additionally be applied to post-blast sparkler residues or other pyrotechnic products.

## **3.2 Experimental**

### **3.2.1 Party sparkler collection**

Packets of sparklers were purchased from a variety of local and online Australian retail stores. Multiple packets from eight different brands were purchased and analysed throughout this study. Multiple colour types within Artwrap and Korbond brands were also obtained. It was found that all were manufactured in China by different companies, however information on the specific location of each factory within China could not be obtained. Sparkler samples were separated into two groups as detailed in Tables 3.1 and 3.2. The full sample set contains 19 different sparkler types and includes sparklers from the Artwrap and Korbond brand that were coated in different coloured resins (See Figure A.1). The refined sample set includes sparklers from eight unique brands, all without coloured coatings or additional distinguishing features. All sparklers within the refined sample set are also included in the full sample set. Source and sample information are also detailed in Tables 3.1 and 3.2.

**Table 3.1:** Full sample set that includes 19 different sparklers purchased from a variety of local and online Australian retail stores. Sparklers were collected from eight different brands with additional coloured sparklers collected from within the Artwrap and Korbond brand. Throughout this study, specific sparklers are referred to by the sample name listed. Brand, distributor and main distinguishing feature is also detailed.

\* These sparklers came from a multi-coloured pack of 12, containing only three of each colour

^ These sparklers came from a multi-coloured pack of 16, containing only four of each colour

<b>Key</b>	<b>Sample name</b>	<b>Brand name</b>	<b>Colour/feature</b>	<b>Dimensions (cm) (Full/material only)</b>	<b>Mass (g) (Full/material only)</b>	<b>Quantity per packet/cost of packet</b>	<b>Distributor/supplier</b>
<b>1</b>	WLP	We love 2 Party	No coat	40 / 20.5	9.1 / 3.8	8 / \$3	A.Royale & Co
<b>2</b>	AGold	Artwrap	Gold coat	21 / 11	2.7 / 1.7	3 / \$2 *	IG Design Group Australia
<b>3</b>	ASilver	Artwrap	Silver coat	20.5 / 10.5	2.1 / 1.1	3 / \$2 *	IG Design Group Australia
<b>4</b>	APurple	Artwrap	Purple coat	20.5 / 10	2.5 / 1.5	3 / \$2 *	IG Design Group Australia
<b>5</b>	APink	Artwrap	Pink coat	20.3 / 10.5	2.0 / 1.1	3 / \$2 *	IG Design Group Australia
<b>6</b>	AGreen	Artwrap	Green coat	20.5 / 11.5	2.2 / 1.2	3 / \$2 *	IG Design Group Australia
<b>7</b>	Artwrap	Artwrap	No coat	20.5 / 11	2.1 / 1.0	20 / \$1	IG Design Group Australia
<b>8</b>	T2P	Time 2 Party	No coat	24 / 12	2.3 / 1.0	10 / \$2	IG Design Group Australia
<b>9</b>	Wizard	Wizard	No coat	70 / 40	20.6 / 6.9	6 / \$6	IG Design Group Australia

<b>10</b>	FF	Firefox	No coat	23.5 / 11.5	2.3 / 1.1	8 / \$2	IG Design Group Australia
<b>11</b>	PC	Party central	No coat	25 / 13.5	3.4 / 1.4	10 / \$2	PJ SAS Trading Pty Ltd
<b>12</b>	FC	Fun and creative	No coat	24 / 13	2.95 / 1.5	15 / \$2.35	KD Trading PTY LTD
<b>13</b>	KSilver	Korbond	Silver coat	24 / 10.5	2.3 / 1.1	4 / \$3 ^	Korbond
<b>14</b>	KGold	Korbond	Gold coat	24 / 10.5	2.3 / 1.1	4 / \$3 ^	Korbond
<b>15</b>	KGreen	Korbond	Green coat	24 / 11	2.2 / 1.0	4 / \$3 ^	Korbond
<b>16</b>	KBlue	Korbond	Blue coat	24 / 11	2.1 / 1.0	4 / \$3 ^	Korbond
<b>17</b>	KPink	Korbond	Pink coat	24 / 11	2.4 / 1.1	4 / \$3 ^	Korbond
<b>18</b>	KPurple	Korbond	Purple coat	24 / 11	2.4 / 1.2	4 / \$3 ^	Korbond
<b>19</b>	Korbond	Korbond	No coat	24 / 13.5	2.7 / 1.0	24 / \$2	Korbond

**Table 3.2:** Refined sample set that includes sparklers collected from eight different brands. All samples within the refined set have no distinguishing features or additional coatings and only differ by their manufacturer/brand. Throughout this study, specific sparklers are referred to by the sample name listed. Place of purchase is also detailed.

<b>Sample name</b>	<b>Brand name</b>	<b>Place of purchase</b>	<b>Distributor/supplier</b>
<b>WLP</b>	We love 2 party	Big W	A.Royale & Co
<b>Artwrap</b>	Artwrap	Big W	IG Design Group Australia
<b>T2P</b>	Time 2 party	Big W	IG Design Group Australia
<b>Korbond</b>	Korbond	Woolworths	Korbond
<b>PC</b>	Party central	Red Dot	PJ SAS Trading Pty Ltd
<b>FC</b>	Fun and creative	Ebay Australia	KD Trading PTY LTD
<b>FF</b>	Firefox	Ebay Australia	IG Design Group Australia
<b>Wizard</b>	Wizard	Discount party warehouse online	IG Design Group Australia

### 3.2.2 Infrared spectroscopy

Spectral analysis of the party sparkler samples was performed using the method outlined in Chapter 2, section 2.4.1. Sparkler material was stripped off the wire with gloves and ground to a fine powder using a mortar and pestle. Ten spectra were collected from each sparkler sample from the full sample set. The same method was repeated with another five spectra from each product being collected, totalling 15 spectra for each sparkler sample.

### 3.2.3 Gas chromatography mass spectrometry

Gas chromatography mass spectrometry (GCMS) analysis was performed using the instrument and method outlined in Chapter 2, section 2.4.5. Eight samples were

prepared from three different brands including a silver WLP sparkler, an uncoated T2P, an uncoated Artwrap sparkler, and five coloured Artwrap sparkler variants.

### 3.2.4 Ion chromatography

IC was performed using the instrument and method outlined in Chapter 2, section 2.4.3. Sparkler material was stripped off the wire with gloves and ground to a fine powder using a mortar and pestle. Samples were prepared by dissolving sparkler material (100 mg) in MilliQ water (5 mL). Samples were sonicated for 10 minutes before being filtered using a 25 mm Acrodisc® (0.45 µm hydrophilic polyethersulfone membrane) syringe filter attached to a 10 mL terumo hypodermic syringe. Samples were diluted 100-fold and MilliQ water and procedural controls were also prepared. The same method was used to prepare burnt sparkler material samples.

For studies comparing ground and unground residue, samples were prepared from ASilver (sparkler 3 from full sample set). Eight ground samples were prepared as detailed above and eight additional samples were prepared without grounding down the sparkler material. Across all IC analysis, a single sparkler was used to prepare exactly one sample, therefore every sample was prepared from a different sparkler.

### 3.2.5 Scanning electron microscopy

Scanning electron microscopy electron dispersive spectroscopy (SEM-EDS) was performed using the instrument and method outlined in Chapter 2, section 2.4.4. Eight samples were prepared from three different brands including a silver WLP sparkler, and uncoated T2P, an uncoated Artwrap sparkler, and five coloured Artwrap sparkler variants. Sparkler material was stripped of the wire with gloves and ground to a fine powder using a mortar and pestle. Elemental analysis was performed on select points across the samples as well as a bulk analysis of the entire area. For studies comparing ground and unground residue, samples were prepared from the ASilver brand. Eight unground and eight ground samples were prepared. A single sparkler was used to prepare exactly one sample, therefore every sample was prepared from a different sparkler.



### 3.2.6 Inductively coupled plasma mass spectrometry

Inductively coupled plasma mass spectrometry (ICPMS) was performed using the instrument and method outlined in Chapter 2, section 2.4.7. Sparkler material was stripped off the wire with gloves and ground to a fine powder using a mortar and pestle. 10 mL of 10% nitric acid was added to 100 mg of sparkler material in a glass test tube that had been soaked in a 10% nitric acid solution for 2 hours. The sample was sonicated for 10 minutes, capped, and left undisturbed for 24 hours. The sample was filtered into another acid washed test tube using a 25 mm Acrodisc® (0.45 µm hydrophilic polyethersulfone membrane) syringe filter attached to a 10 mL terumo hypodermic syringe. Samples were diluted 10 and 100-fold and controls of the MilliQ water, procedure, diluter and nitric acid were also prepared. Six samples were prepared from each brand totalling 48 samples. The same method was used to prepare burnt sparkler material samples.

### 3.2.7 Chemometrics and feature selection

#### 3.2.7.1 Chemometric analysis using spectral data from infrared spectroscopy

Principal component analysis (PCA) and linear discriminant analysis (LDA) was performed using the method described in Chapter 2, section 2.4.8.1. The classification set used to construct the discriminant model contained ten replicate IR spectra collected from each party sparkler within the full sample set (see Table 3.1). An independent dataset used to validate the models generated by LDA contained five replicate spectra from each party sparkler within the full sample set.

#### 3.2.7.2 Feature selection and element reduction

Elemental data obtained from ICPMS analysis was refined before PCA-LDA was performed. After initial examination of the data, elements present due to contamination or detected at concentrations below the calibration were removed. Elements which presented a low number of counts (<1000) were also removed. Analysis of variance (ANOVA) based feature selection was performed on the remaining elements, which has previously proven to be an effective approach at reducing the number of classifiers in order to give greater separation between samples (143, 144). F-ratios were calculated using the method described in Chapter 2 section

2.4.8.4. Elements were then ranked in increasing order and multiple scores plots were generated to assess the sample distribution with an increasing f-ratio threshold. This process was performed on the unburnt and burnt sparkler samples. The refined elemental profiles and subsequent analysis is detailed in the relevant section below.

### 3.2.7.3 Chemometric analysis using elemental concentration data from ICPMS

PCA-LDA was performed using the method described in Chapter 2, section 2.4.8.3. From the analysis of unburnt and burnt sparkler material, 22 elements were retained for chemometric analysis after element reduction processes. Classification sets contained five samples from each brand from the refined sample set. Discrimination models for source prediction were generated using a randomised leave-one-out approach as described in Chapter 2, section 2.4.8.3. Additional source prediction was performed using the burnt sparkler samples, to determine whether they could be linked to the unburnt samples of the same brand.

## **3.3 Results and Discussion**

### 3.3.1 Physical analysis

Party sparklers are easily identified against other commercial pyrotechnics due to their characteristic build. They can be found as different shapes, colours, lengths, and textures, however, the most affordable and easy to source form is the straight (~20 cm), uncoated sparkler, which is represented in the refined sample set. Physical analysis of these types found that there are no distinguishing features across varying brands. Approximately 1 g of residue can be stripped off the wire and packets of 20 can often be purchased for \$1 (AUD), therefore, a large amount of material can be isolated with minimal cost.

### 3.3.2 Preliminary investigations

Preliminary experiments were performed to assess the homogeneity and reproducibility of sparkler material within and between sparklers. Analysis of unground and ground material was also compared by IC and SEM-EDS. Firstly, ATR-FTIR spectra was collected of five two cm sections of a single PC sparkler (Figure A.2a). Spectra of five individual PC sparklers taken from the same packet were also

collected (Figure A.2b). Overlaid spectra showed no observable difference between sections or individual sparklers within a packet. In a separate experiment, eight samples from sparkler 3 (ASilver) were analysed by IC and compared against another eight samples that had been ground to a fine powder (Table B.1). Elemental analysis of eight ground and unground samples was also performed by SEM-EDS. Comparison revealed that although the same elements and ionic species were detected, they were present in notably larger amounts within the ground material. Approximately twice the amount of the primary components barium and nitrate was detected by IC and also showed increased signals from SEM analysis. IC results showed a lower standard deviation between ground samples indicating that the inorganic components are more evenly distributed throughout the material thus resulting in more consistent quantitative data. From these results, all subsequent analysis of party sparklers was conducted so that a sample was prepared from ground material taken from a single sparkler.

### 3.3.3 Chemical characterisation of party sparklers

#### 3.3.3.1 Infrared spectroscopy

Characteristic spectra of each sparkler from the full sample set were collected by ATR-FTIR spectroscopy. All spectra contain the characteristic nitrate ion peaks with minor signals throughout the fingerprint region. Library search using the SensIRtx library provided a 75- 90% match against barium nitrate across the different sparkler brands. Some trace differences in peak heights were observed across the different samples but no notable absence or presence of additional peaks was observed that may distinguish between brands. Figure 3.1a shows spectra of all samples from the Artwrap brand, revealing little variability within a brand regardless of the sparklers having different coloured coatings. Figure 3.1b shows an overlay of the refined set of samples, containing uncoated sparklers from eight different brands. Again, visualisation of the spectra revealed no notable differences apart from the FF sparkler, which has a very minor signal at  $1674\text{ cm}^{-1}$ .

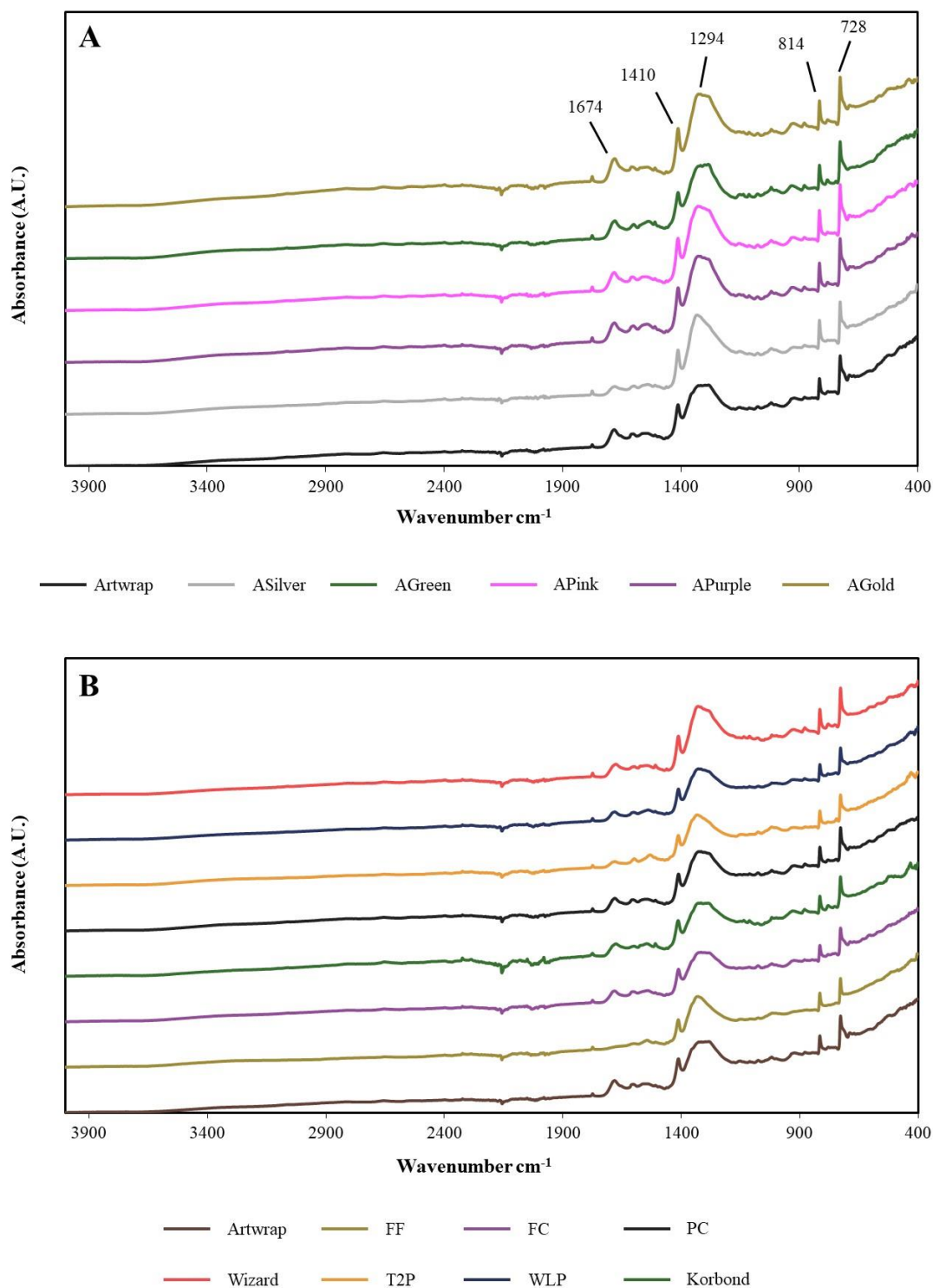


**Figure 3.1:** ATR-FTIR spectra of party sparkler samples from full and refined sample set. Six sparklers of varying colours from the Artwrap brand (a) and eight uncoated sparklers from different brands purchased from online and local Australian retail stores (b). No discernible difference was observed between or within brands. Spectra has been offset for better visualisation of individual samples.

Burnt sparkler material from a PC sparkler was also analysed which displayed none of the characteristic nitrate peaks present in the unburnt spectra, suggesting that the primary oxidising agent is completely consumed when burnt (Figure 3.2). Spectra of burnt material revealed little information about the sample but is easily distinguishable from an unburnt sample. These results suggest that IR analysis of sparkler residue could infer the primary oxidising agent and can discern between unburnt and burnt material but cannot provide any additional discriminatory information. However, as trace differences can be observed, subsequent chemometric analysis may be capable of discriminating between brands.

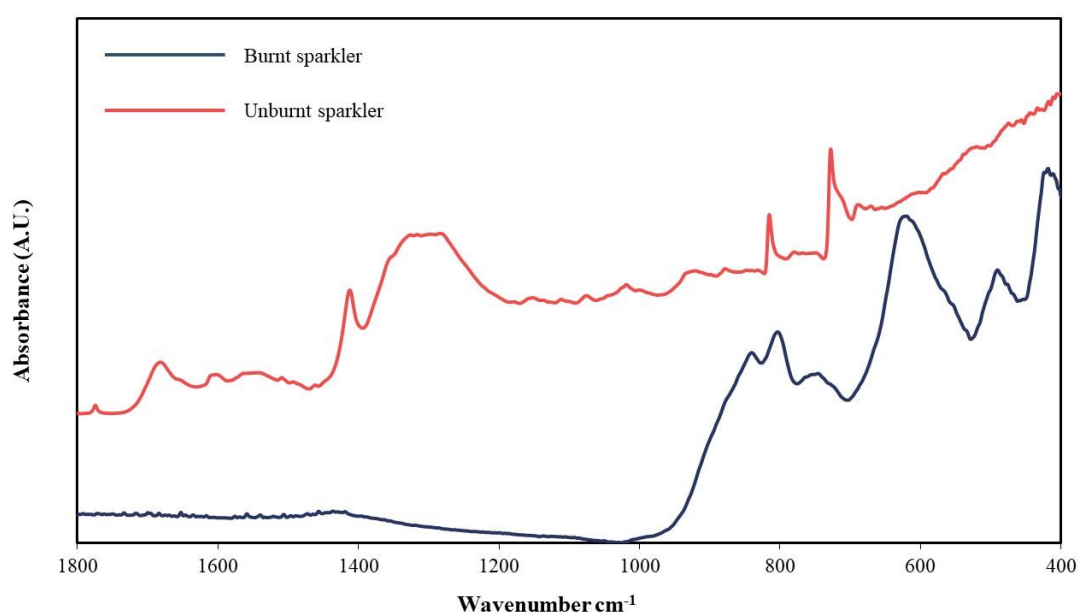


**Figure 3.2:** ATR-FTIR spectra of sparkler material from an unburnt and burnt PC sparkler. Spectra of burnt material can be discerned from an unburnt sparkler based on the absence of nitrate (3900 – 1800 cm<sup>-1</sup> region removed as no information was present as seen in Figure 3.1).

### 3.3.3.2 Gas chromatography mass spectrometry

The analysis of inorganic pyrotechnics by GCMS is not routine in casework as identifying the primary oxidising salt is typically the main objective, which is achieved with alternative techniques. However, as many of the sparkler samples had coloured coatings as well as contain organic binding compounds, GCMS was performed to determine whether coloured sparklers of the same brand could be differentiated from each other and from regular uncoated sparklers. Eight sparklers were analysed including a silver WLP, an uncoated T2P and six coloured Artwrap sparklers (Figure

3.3). An additional peak was detected at 25.1 minutes within the purple, pink, green and blue sparklers which was identified as terephthalic acid (PTA) (Figure A3). This compound is often used to prepare polyester resins and is applied to generic metal coatings (164). A minor peak at 7.6 minutes was observed within the gold sparkler, which was attributed to paraxylene, a precursor to PTA, however PTA itself was not detected (Figure A4). The silver sparkler showed a minor signal likely attributed to 2-bornanone at 12.1 minutes, which is used as a plasticiser in the preparation of fireworks and explosive compositions (Figure A5). The uncoated sparkler did not contain any additional peaks. Mass spectra of identified peaks are shown in Appendix A.

These results indicated that GCMS can identify some organic compounds within the sparkler coatings but cannot be used for discrimination purposes. The chromatograms were not consistent across all coloured sparklers and the silver WLP sparkler displayed an identical profile to the uncoated T2P sparkler. Therefore, detection of the PTA or p-xylene peak could deduce whether the sample originated from a coated or uncoated sparkler, but no further characteristic information can be obtained. To further discriminate between different coloured sparklers, LCMS methods could be used to potentially separate and identify the trace components responsible for the coloured coatings. If a synthetic organic pigment or dye has been used it is likely to contain compounds such as cyanines or phthalate esters, which could be separated by and identified by chromatography. X-ray methods could also be used to detect trace metal oxides if inorganic pigments are used within the coloured coatings. The ability to identify these components would contribute to the complete chemical characterisation of party sparkler material and potentially provide additional source information by discriminating between different coloured sparklers within a single brand.

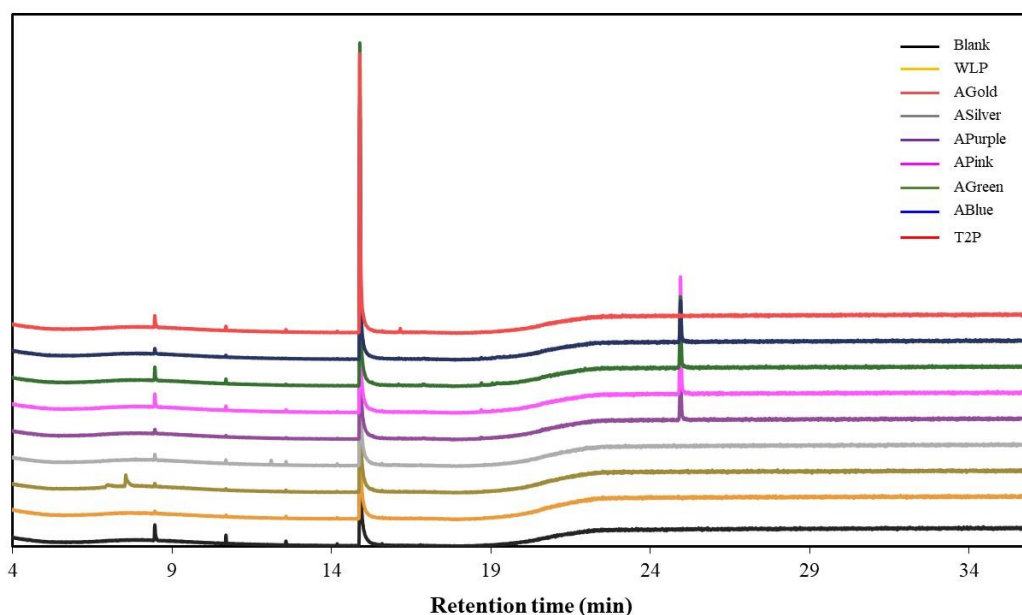


**Figure 3.3:** Chromatograms from GCMS analysis of eight different party sparklers including a silver WLP, an uncoated T2P and six coloured Artwrap sparklers (offset for better visualisation of peaks).

### 3.3.3.3 Ion chromatography

IC can determine the primary oxidising agent and other trace ions within inorganic explosives. The full sample set of unburnt and burnt party sparklers was analysed by IC for a range of cations and anions. Although the sample set contained eight different brands sourced from different locations, all contained barium nitrate as the primary oxidising agent as shown by the high concentrations displayed in Table 3.3. No other ions were detected within the unburnt material aside from trace amounts of calcium. Although minor differences were observed within the concentration of barium and nitrate, additional data would be required to distinguish between brands.

Analysis of the burnt material revealed numerous ions that were not detected in the unburnt samples. Barium was still detected in notably lower amounts however nitrate was not, which is in agreement with the IR spectrum of a burnt sparkler that showed the absence of the characteristic nitrate peak. In the absence of nitrate, ammonium was found to be present in all samples with some also containing strontium. Samples that contained strontium appear to correlate with those that also showed increased levels of barium, suggesting that strontium may be present in all brands but at levels below the detection limit. Calcium, chloride and chlorate were also present in trace amounts within all burnt samples.

The process of burning a sparkler appears to have two main effects on the ionic profile. Firstly, as the sparkler burns, barium nitrate decomposes forming BaO, O<sub>2</sub> and nitrogen oxides (NO and NO<sub>2</sub>) (83). Most of these products are lost resulting in only trace amounts of barium remaining in the burnt material. Secondly, additional decomposition products such as ammonium, chloride and chlorate are formed from the burning of additional fuels and binding components, which explains their presence across burnt samples. Analysis of party sparklers prepared with other nitrate salts are likely to yield similar results. Other oxidisers including chlorate and perchlorate salts that have been used to prepare party sparklers decompose to form O<sub>2</sub> and a chloride salt, therefore it would be expected to see increased levels of chloride and chlorate within burnt samples compared to a nitrate based sparkler (83).

These results indicate that IC can effectively identify the primary oxidising agent within sparkler material and is capable of identifying additional trace species. However, the ionic profiles displayed in Table 3.3 cannot be used to reveal any additional source information.



**Table 3.3:** Concentration of cations and anions (ppm) in 100 mg of unburnt and burnt sparkler material from different brands. Species that are reported < 5 ppm were present within the sample at concentrations below the lower limit of the calibration range. (ions not detected in samples are labelled as n.d).

<b>Ionic species</b>											
<b>Unburnt samples</b>	Ba <sup>2+</sup>	Ca <sup>2+</sup>	NO <sub>3</sub> <sup>-</sup>		<b>Burnt samples</b>	Ba <sup>2+</sup>	Sr <sup>2+</sup>	Ca <sup>2+</sup>	NH <sub>4</sub> <sup>+</sup>	Cl <sup>-</sup>	ClO <sub>3</sub> <sup>-</sup>
<b>WLP</b>	70.0	< 5	59.7		<b>WLP</b>	11.0	< 5	< 5	< 5	< 5	< 5
<b>AGold</b>	77.5	< 5	66.5		<b>AGold</b>	< 5	n.d	< 5	< 5	< 5	< 5
<b>ASilver</b>	83.6	< 5	72.9		<b>ASilver</b>	< 5	n.d	< 5	< 5	< 5	< 5
<b>APurple</b>	68.8	< 5	59.2		<b>APurple</b>	6.2	n.d	< 5	< 5	< 5	< 5
<b>APink</b>	77.3	< 5	66.8		<b>APink</b>	6.0	n.d	< 5	< 5	< 5	< 5
<b>AGreen</b>	57.9	< 5	50.4		<b>AGreen</b>	< 5	n.d	< 5	< 5	< 5	< 5
<b>Artwrap</b>	61.9	< 5	53.6		<b>Artwrap</b>	< 5	n.d	< 5	< 5	< 5	< 5
<b>T2P</b>	61.9	< 5	53.3		<b>T2P</b>	< 5	n.d	< 5	< 5	< 5	< 5
<b>Wizard</b>	66.8	< 5	59.0		<b>Wizard</b>	< 5	n.d	< 5	< 5	< 5	< 5
<b>FF</b>	56.9	< 5	50.8		<b>FF</b>	14.3	< 5	< 5	< 5	< 5	< 5
<b>PC</b>	70.9	< 5	62.8		<b>PC</b>	< 5	n.d	< 5	< 5	< 5	< 5
<b>FC</b>	63.3	< 5	56.2		<b>FC</b>	< 5	n.d	< 5	< 5	< 5	< 5

<b>KSilver</b>	60.8	< 5	53.8		<b>KSilver</b>	52.8	< 5	< 5	< 5	< 5	< 5
<b>KGold</b>	62.9	< 5	55.9		<b>KGold</b>	7.9	n.d	< 5	< 5	< 5	< 5
<b>KGreen</b>	59.2	< 5	52.7		<b>KGreen</b>	< 5	n.d	< 5	< 5	< 5	< 5
<b>KBlue</b>	80.1	< 5	71.8		<b>KBlue</b>	< 5	n.d	< 5	< 5	< 5	< 5
<b>KPink</b>	62.8	< 5	56.5		<b>KPink</b>	< 5	n.d	< 5	< 5	< 5	< 5
<b>KPurple</b>	67.0	< 5	59.7		<b>KPurple</b>	< 5	n.d	< 5	< 5	< 5	< 5
<b>Korbond</b>	55.7	< 5	51.3		<b>Korbond</b>	< 5	n.d	< 5	< 5	< 5	< 5

#### 3.3.3.4 Scanning electron microscopy

Eight sparklers were analysed by SEM-EDS to visualise the particles and identify any bulk or trace metals throughout the samples. Results revealed little chemical information beyond the elevated presence of barium and iron, suggesting that all sparkler samples collected contained iron as the metal fuel component. This suggests that all sparkler samples collected contained iron as the metal fuel component. This was later confirmed by contacting one of the distributors which detailed their product containing 50% and 33% of barium and iron respectively by weight. Minor signals from titanium, strontium and copper were also present across all samples. These results align with IC and ICPMS described in the next section, which found all three elements to be present in increased amounts compared to other species. This data indicates that when coupled with IC, the two major components being the oxidising salt and metal fuel can be identified. Although additional elements were detected, SEM cannot be used to reveal additional source information or to distinguish between brands and sparkler types.

#### 3.3.3.5 Inductively coupled plasma mass spectrometry

The analysis of party sparkler material by ICPMS has not previously been reported and so preliminary experiments were performed to establish an appropriate sample preparation and analysis procedure. The impact of the solvent, solvent strength, dilution factor and extraction time was explored using a sparkler from the PC brand. Samples were extracted using MilliQ water, 1% nitric acid and a 1% nitric/hydrochloric acid (1:1) solution and then analysed after dilution by a factor of 1, 10 and 100. Subsequent experiments analysed samples extracted in 1, 5 and 10% nitric acid and samples extracted in 10% nitric acid for 1, 2, 4 and 24 hours. Results from these experiments found that extraction in 10% nitric acid for 24 hours with a dilution factor of 10 and 100 prior to analysis gave optimal results, therefore, this methodology was used for all subsequent ICPMS analysis.

The concentration of 58 elements within party sparklers from the refined sample set was determined by ICPMS analysis. Many elements were found to be present in bulk and trace amounts within the sparkler material (Table B.2). Additionally, the concentration of most elements varied greatly across brands. While the residue

consisted mostly of barium, other elements such as cobalt, strontium, manganese, copper and chromium were also present in elevated amounts. Previous investigations found that ~88% of the Artwrap sparklers is attributed to barium and iron, whilst also containing ~9% aluminium by weight (contributed by the wire). These additional metals likely originate from impurities contained within the bulk raw materials, explaining their elevated presence compared to other trace elements detected. Interestingly, many trace elements (< 1 ppm) such as tungsten, lead, arsenic, tin, molybdenum and antimony were also found. Again, the presence of these elements may be a result of impurities from the other inorganic and organic components, or contamination during the manufacturing process and location. This highlights that although all sparklers were manufactured in China, the variability of precursors used within the manufacturing process has resulted in each brand displaying a highly varied elemental profile. Analysis also found that there were no brands containing certain elements that were not present in the others, therefore none of the brands could be immediately discriminated based on the presence or absence of a certain element.

Analysis of burnt material produced similar results in that several elements were detected in highly varied amounts across brands. Comparable to IC, some species were present in increased amounts within the burnt samples as highlighted in Figure 3.4, which compares the unburnt and burnt elemental profile from the Party Central samples. This appears to be more prominent in the elements present at higher concentrations (Figure 3.4a) such as titanium, chromium, manganese and zinc. In the process of burning the sparklers, these elements may have reacted to form compounds with a higher solubility within the solvent used and so appeared at higher concentrations within burnt residues. Although concentrations differ between residue types, the relative proportions of elements are highly similar, which is displayed in Figure 3.4. This highlights the persistence of the inorganic components within burnt residues and suggests that the similar proportions observed could be exploited with chemometric methods to link burnt residues to unburnt sparkler material of the same brand.

Results from ICPMS shows elemental concentrations are highly variable across brands. Although no immediate discrimination can be made based on visual examination of the profiles, subsequent chemometric analysis could allow for brand

discrimination and successful source prediction based on the unique elemental profiles observed.

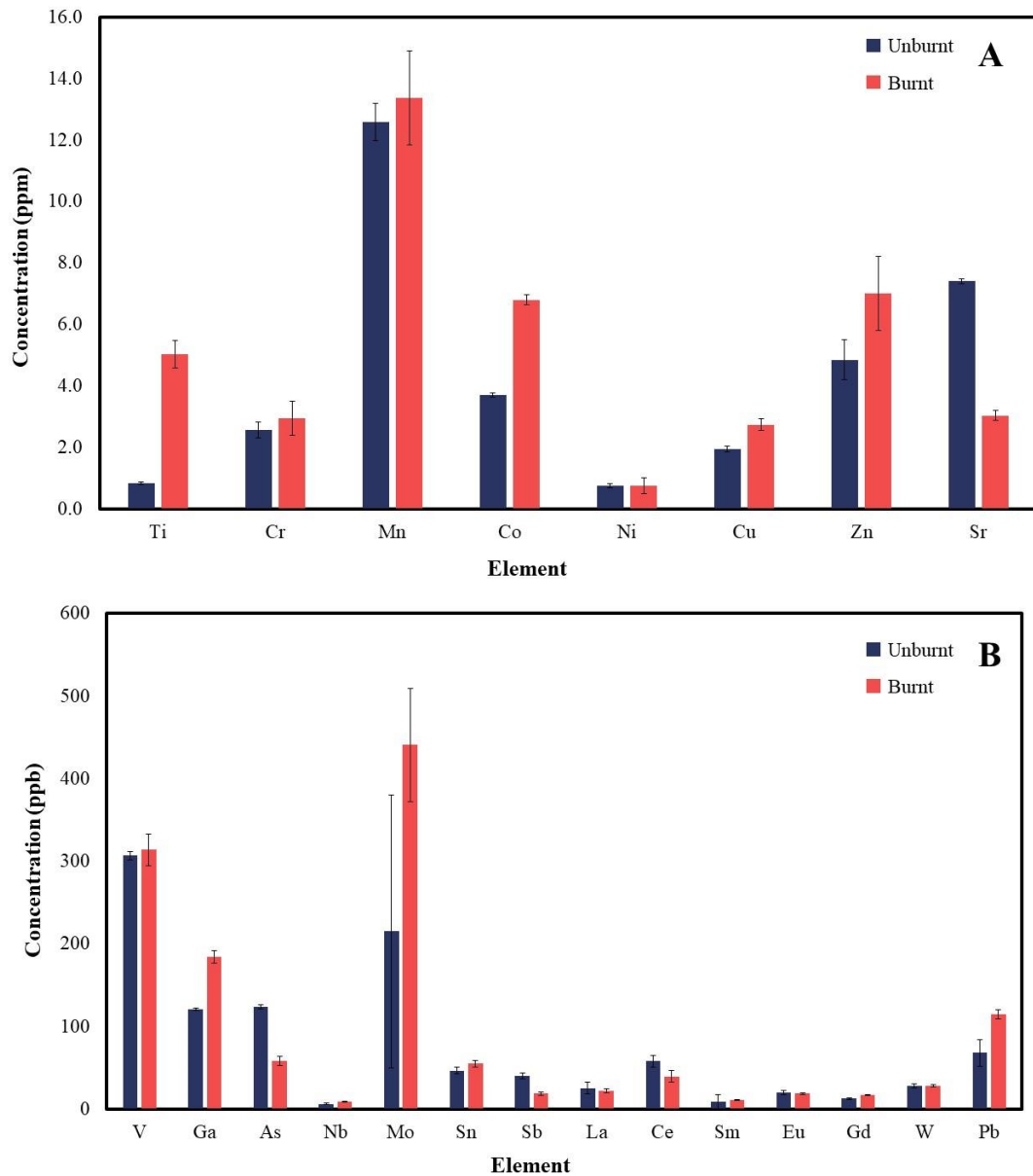


**Figure 3.4:** Average concentration of elements within unburnt and burnt samples. Elements that were present at concentrations > 1 ppm (a) and < 1 ppm (b).

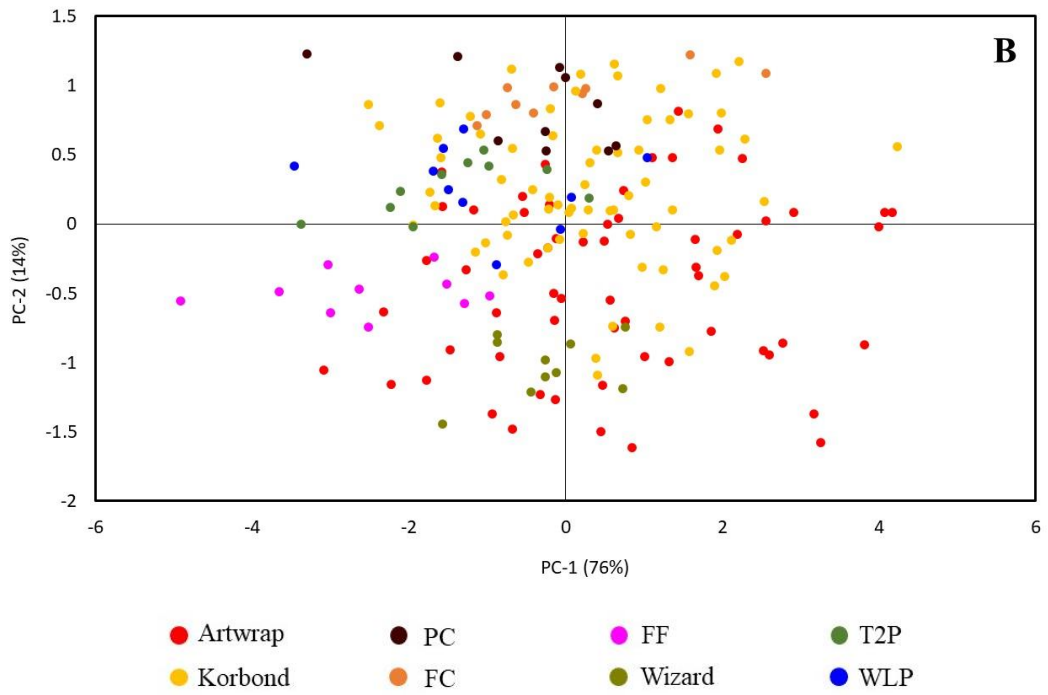
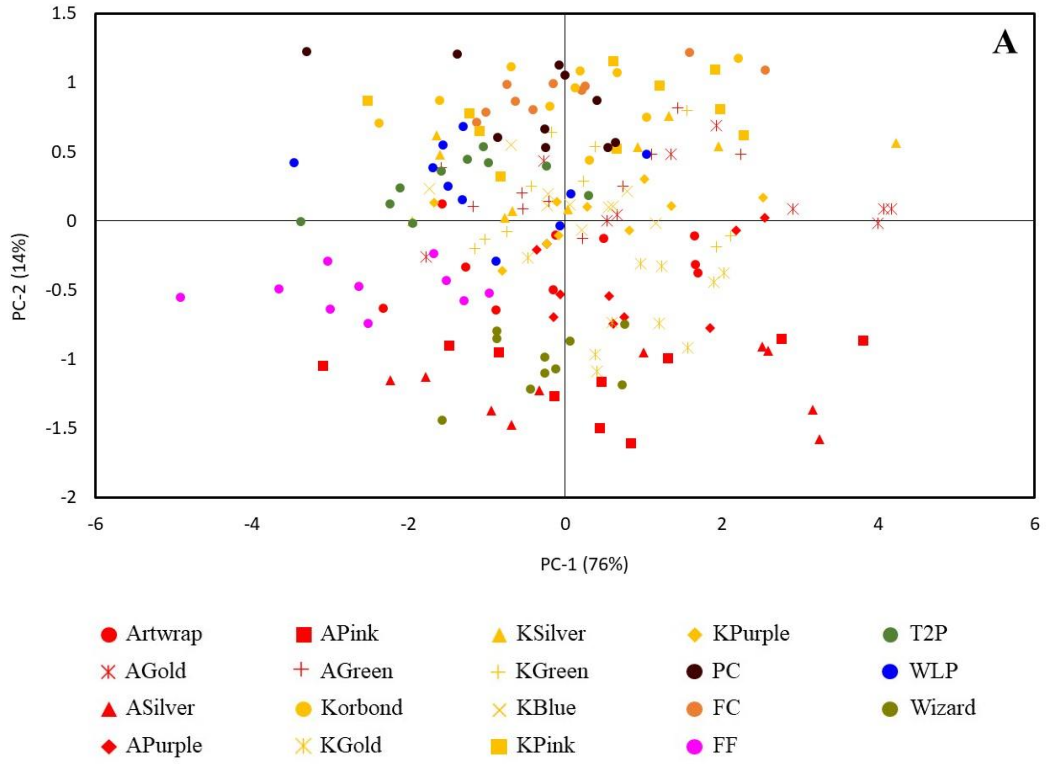
### 3.3.4 Source attribution of party sparklers with chemometrics

#### 3.3.4.1 Discrimination of party sparklers by ATR-FTIR spectroscopy

IR analysis of the full sparkler sample set revealed only trace differences between samples and so no discrimination could be achieved within or between brands based on visual interpretation. However, the trace differences in peak height and position could provide additional source information with subsequent chemometric analysis. Spectral data of ten samples from each party sparkler from the full sample set was used for chemometric analysis. For every sample, a small amount of ground material was taken from the bulk sparkler and analysed once, giving ten individual samples.

PCA was conducted using only the fingerprint region ( $1800 - 400 \text{ cm}^{-1}$ ) as no chemical information or peaks were present outside of this range for any sample. Four 2-D scores plots were generated to evaluate whether spectral data can be used to discriminate between sparkler brands. Firstly, PCA was performed on the full set of samples with each brand and colour classified as an individual class, resulting in 19 classes (Figure 3.5a). PCA was repeated with the coloured sparklers grouped as one brand (Figure 3.5b) and with the refined sample set, resulting in eight classes for both (Figure 3.5c). Lastly, a scores plot was generated with only the Korbond samples to determine whether any discrimination could be achieved within a single brand (Figure 3.5d).

When each brand was treated as an individual class, no clear groupings were observed nor was any useful discrimination, suggesting that the trace differences within spectra is not significant enough to discern between or within brands. Figures 3.5b and 3.5c shows similar results as neither display any separation between brands. The final scores plot includes only the samples from the Korbond brand and again, no distinct sample groupings were observed which further suggests that PCA combined with spectral data cannot be used to discriminate within a single brand.



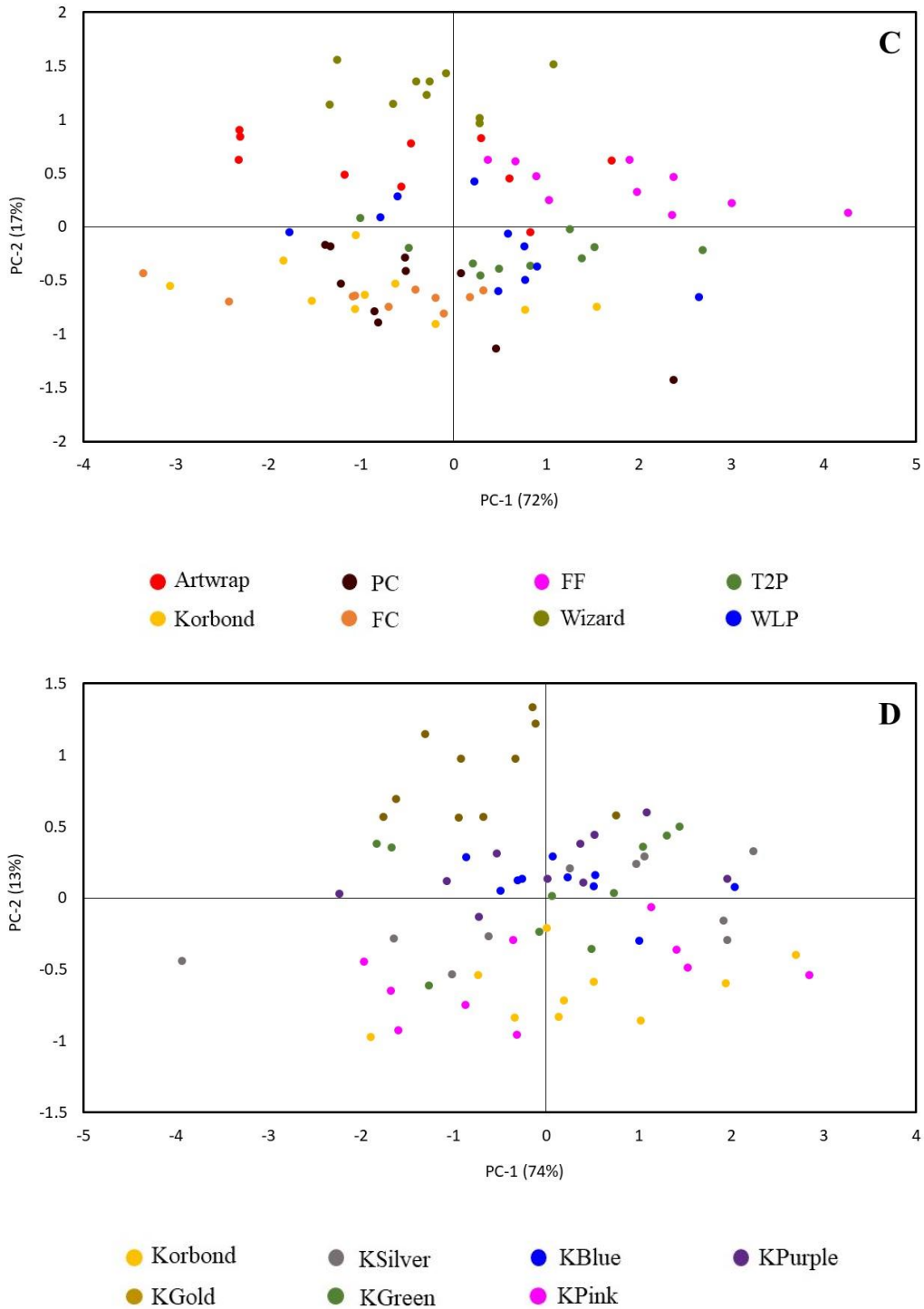


**Figure 3.5:** 2-D scores plots generated from PCA performed on party sparklers from full and refined sample sets. The classification of samples and number of classes differs in each scores plot: (a) was generated using the full sparkler sample set with each sparkler classified as an individual brand (19 classes, 190 samples), (b) was generated using the full sparkler sample set with coloured variants of the same brand grouped into a single class (eight classes, 190 samples), (c) was generated using the refined sample set with each sparkler classified as an individual brand (eight classes, 80 samples), (d) was generated using samples from within the Korbond brand (seven classes, 70 samples).



To further evaluate the source prediction capabilities of using spectral data with chemometrics, LDA was performed on the full and refined samples set. Both models were generated using the linear distance and first six PCs with equal probabilities assumed. The first discriminant model was generated using 10 samples from 19 classes of sparklers which was subsequently used to predict the source of 95 samples (five from each class) from an independent dataset. Classification and validation results are shown in Table 3.4 which details an initial calibration accuracy of 82.6%. Although no distinct classes were observed within the scores plot, inclusion of additional PCs allowed for nine out of the 19 classes to return a 100% calibration rate. All remaining classes contained samples that were incorrectly defined to their respective brand. Consequently, the model was not capable of consistently predicting the source of samples as the overall prediction rate was 46.3%. Only four classes returned a 100% prediction accuracy which align with the few classes that displayed a 100% classification accuracy.

LDA performed on the refined samples set generated a discriminant model with a high classification accuracy of 95%, with only two samples within the FC brand classified as a PC sparkler. Although no distinct classes were observed within the scores plot, inclusion of the additional PCs has resulted in a high classification rate across the eight uncoated sparkler brands. Using the model to predict the source of 40 sparklers from the same independent dataset used previously returned a successful prediction rate of 67.5% (Table 3.5). Although notably higher than previously analysis, 50% of the classes contained incorrect predictions, indicating that the model cannot consistently predict the source of a sparkler sample that is from one of the eight brands within the dataset.

Interpretation of the discriminant values (DVs) generated from validation of the model constructed with the refined sample set can indicate how well separated the predicted samples are from adjacent classes (Table 3.6). Overall, the source of 27 out of 40 samples were correctly predicted however 20 of these samples are attributed to four classes with the rest scattered amongst remaining classes. The samples correctly predicted within the four classes that returned a 100% prediction rate displayed strong separation against other classes based on the large differences observed in the DVs. The remaining seven samples were correctly assigned to their brands however the DVs

indicate extremely poor separation against neighbouring classes, suggesting that the prediction rate produced from these classes may not be an accurate representation of the model's predictive power.

A thorough analysis of the full and refined sample set using PCA-LDA in combination with spectral data revealed that this technique has minimal source determination capabilities regarding unburnt party sparkler samples. Investigations into the separation of samples within and between brands shows no distinct groupings and subsequent LDA generated discriminant models with a low predictive power. Therefore, FTIR analysis can infer the primary oxidising agent within a party sparkler sample but cannot be used to provide any additional source information.

**Table 3.4:** Classification and validation results from LDA on the full sparkler sample set using the first six PCs with equal probabilities assumed. Discriminant model was generated with ten samples from 19 classes and validated using an independent dataset that contained five samples from each class (95 samples total). Number of correct vs incorrect classifications is shown.

Class #	Brand	Correct		Incorrect		% Correct	
		Classification	Validation	Classification	Validation	Classification	Validation
1	WLP	10	4	0	1	100	80
2	AGold	5	3	5	2	50	60
3	ASilver	10	5	0	0	100	100
4	APurple	7	4	3	1	70	80
5	APink	10	5	0	0	100	100
6	AGreen	10	0	0	5	100	0
7	Artwrap	10	3	0	2	100	60
8	T2P	10	5	0	0	100	100
9	Wizard	10	2	0	3	100	40
10	FF	10	4	0	1	100	80
11	PC	6	0	4	5	60	0

<b>12</b>	FC	4	1	6	4	40	20
<b>13</b>	KSilver	9	2	1	3	90	40
<b>14</b>	KGold	9	5	1	0	90	100
<b>15</b>	KGreen	5	1	5	4	50	20
<b>16</b>	KBlue	7	0	3	5	70	0
<b>17</b>	KPink	9	0	1	5	90	0
<b>18</b>	KPurple	6	0	4	5	60	0
<b>19</b>	Korbond	10	0	0	5	100	0
	Total					82.6	46.3

**Table 3.5:** Classification and validation results from LDA on the refined sparkler sample set using the first six PCs with equal probabilities assumed. Discriminant model was generated with 10 samples from eight classes and validated using an independent dataset that contained five samples from each class (40 samples total). Number of correct vs incorrect classifications is shown.

Class #	Brand	Correct		Incorrect		% Correct	
		Classification	Validation	Classification	Validation	Classification	Validation
1	WLP	10	3	10	2	100	60
2	Artwrap	10	5	10	0	100	100
3	T2P	10	5	10	0	100	100
4	Korbond	10	0	10	5	100	0
5	PC	10	2	10	3	100	40
6	FC	8	2	2	3	80	40
7	FF	10	5	10	0	100	100
8	Wizard	10	5	10	0	100	100
	Total					95	67.5

**Table 3.6:** Discriminant values of samples within the independent data set used for validation. Discriminant values and predictions represent the samples within Table 3.5. Shaded cells indicate correct (green) and incorrect (red) predictions.

Correct class / Sample number	Discriminant values for each class								Predicted class
	1	2	3	4	5	6	7	8	
1.1	-6.3	-85.1	-90.2	-47.0	-21.9	-32.4	-67.0	-18.7	1
1.2	-6.5	-76.7	-95.3	-32.2	-13.1	-21.7	-72.9	-21.6	1
1.3	-15.3	-43.6	-125.8	-34.6	-7.2	-9.1	-119.9	-28.7	5
1.4	-5.4	-92.4	-58.2	-72.1	-26.9	-31.5	-78.8	-40.6	1
1.5	-17.7	-79.9	-88.5	-70.8	-42.5	-52.7	-67.2	-10.1	8
2.1	-119.0	-10.4	-313.6	-107.1	-73.0	-63.6	-307.8	-88.0	2
2.2	-215.9	-39.2	-462.5	-161.7	-142.1	-128.5	-438.3	-157.9	2
2.3	-338.3	-110.7	-649.1	-230.2	-226.1	-206.5	-610.8	-277.8	2
2.4	-180.5	-31.7	-327.0	-210.5	-131.6	-105.9	-421.1	-185.9	2
2.5	-219.6	-40.6	-403.8	-221.0	-151.8	-124.1	-484.0	-216.7	2

3.1	-101.0	-306.2	-8.0	-267.3	-183.7	-190.9	-97.5	-192.4	3
3.2	-111.6	-331.5	-10.1	-274.3	-194.9	-203.0	-99.5	-210.0	3
3.3	-142.6	-390.7	-28.6	-295.3	-225.8	-235.2	-114.1	-253.6	3
3.4	-83.4	-290.6	-17.7	-197.7	-147.3	-157.8	-67.4	-168.4	3
3.5	-74.7	-265.1	-9.6	-198.7	-142.1	-151.7	-62.1	-148.6	3
4.1	-63.1	-60.6	-209.1	-50.4	-54.2	-66.7	-129.3	-21.1	8
4.1	-54.0	-56.2	-204.8	-37.2	-41.0	-51.4	-128.8	-19.4	8
4.3	-36.8	-30.5	-157.7	-49.4	-29.4	-34.0	-129.7	-18.9	8
4.4	-96.4	-46.1	-294.4	-49.3	-60.2	-66.7	-209.0	-44.4	8
4.5	-75.0	-47.3	-247.0	-39.9	-48.9	-56.7	-169.6	-30.5	8
5.1	-46.3	-57.2	-210.6	-16.8	-10.2	-12.7	-174.9	-60.7	5
5.2	-49.4	-42.9	-216.3	-18.2	-13.9	-16.3	-175.4	-48.2	5
5.3	-95.5	-52.3	-293.5	-33.3	-35.4	-32.5	-254.8	-97.1	6
5.4	-230.1	-84.1	-473.5	-126.5	-134.2	-122.5	-436.4	-210.5	2
5.5	-149.7	-52.6	-369.7	-70.1	-75.3	-69.3	-325.1	-133.5	2

6.1	-144.9	-27.9	-367.4	-110.6	-86.5	-75.4	-347.5	-109.6	2
6.2	-32.7	-42.8	-176.0	-21.7	-5.5	-6.3	-156.8	-46.7	5
6.3	-44.8	-52.8	-190.8	-30.8	-9.1	-5.4	-190.1	-75.5	6
6.4	-51.8	-31.6	-210.7	-34.1	-16.3	-13.1	-193.9	-56.0	6
6.5	-82.6	-23.3	-268.2	-61.9	-36.3	-28.4	-259.3	-77.8	2
7.1	-65.7	-247.3	-106.1	-100.1	-114.8	-146.4	-9.1	-66.4	7
7.2	-82.8	-268.7	-123.9	-107.5	-131.7	-165.7	-14.1	-77.6	7
7.3	-83.3	-265.8	-134.9	-95.5	-125.6	-159.0	-18.9	-78.3	7
7.4	-111.6	-288.7	-189.2	-91.5	-141.5	-177.2	-44.1	-97.4	7
7.5	-157.3	-322.9	-235.3	-138.1	-196.8	-237.9	-63.3	-111.6	7
8.1	-43.1	-80.6	-178.0	-41.1	-45.8	-61.7	-93.6	-7.5	8
8.2	-47.4	-60.2	-186.8	-44.5	-44.2	-56.6	-115.1	-8.5	8
8.3	-61.9	-66.9	-198.7	-72.0	-66.2	-77.9	-128.4	-9.4	8
8.4	-116.0	-65.1	-312.6	-88.7	-95.0	-103.9	-217.1	-39.7	8
8.5	-43.6	-45.4	-171.8	-68.3	-46.2	-52.7	-133.0	-9.6	8



#### 3.3.4.2 Discrimination of party sparklers using trace elemental data

All previous analysis of sparkler material has not provided enough discriminatory chemical information to link party sparkler samples to their original brand. Initial results from ICPMS found that the elemental profiles contained a large amount of highly variable data. Chemometric analysis was performed to determine whether the variation observed within the elemental data could be used to discriminate between the party sparklers from the refined sample set.

Table B.2 details the elements remaining after those present due to contamination or detected at concentration below the calibration range were removed. PCA was performed using contributions from these 22 elements to observe the distribution of samples before feature selection was applied to the data (Figure 3.6). The scores plot shows three distinct classes including T2P, FC and FF, however all classes have a high spread across PC-1.

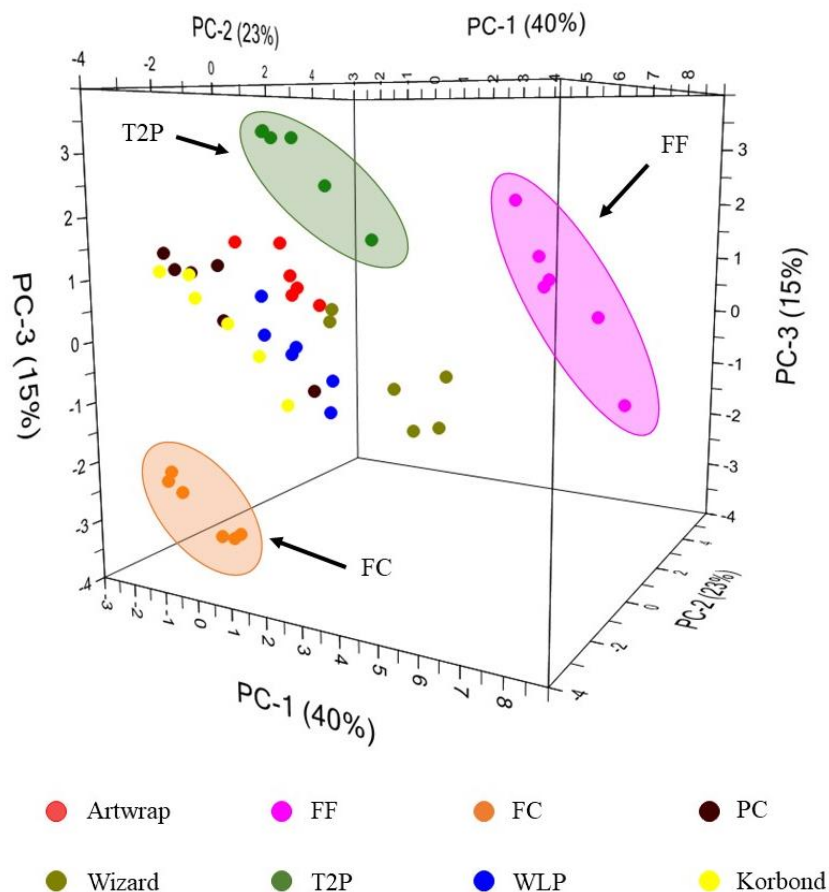


**Figure 3.6:** 3-D scores plot from PCA of the refined sparkler sample set using the trace concentration data from 22 elements. Distribution of sample data shows three distinct classes including the T2P, FC and FF samples.

In an attempt to improve the separation between samples, ANOVA based feature selection was performed on the remaining list of elements. F-ratios were calculated for each remaining element, therefore ranking them based on their contribution to the separation of samples (Table 3.7). By raising the f-ratio threshold, elements with the lowest contribution are removed from the data and PCA can be performed using the newly refined elemental profile to visualise the distribution of samples, ultimately determining whether the eight sparkler brands can be discriminated based on their elemental composition.

Removing elements below a threshold of 150 did not appear to have a notable impact on sample distribution as scores plots generated displayed similar clustering to that shown in Figure 3.6. A notable change was observed once the f-ratio threshold was increased to 200 and manganese was removed from the dataset (Figure 3.7). The 2-D

scores plot shows another two distinct classes containing the Artwrap and WLP samples. The FF, FC and T2P classes remain separated but display a notably smaller spread compared to the groupings in Figure 3.6, indicating that contributions from removed elements had a negative impact on separation within the original dataset.

**Table 3.7:** F-ratio values calculated for each element and ranked in ascending order. Elements with a high f-ratio contribute most to the separation of classes.

	<b>Eu</b>	<b>Sm</b>	<b>Gd</b>	<b>La</b>	<b>Mo</b>	<b>Nb</b>	<b>Pb</b>
<b>F ratio</b>	3	3	4	39	41	65	99
	<b>Cr</b>	<b>Ga</b>	<b>Ce</b>	<b>Mn</b>	<b>Cu</b>	<b>Zn</b>	<b>Ti</b>
<b>F ratio</b>	114	117	131	180	221	267	289
	<b>Ni</b>	<b>Sb</b>	<b>V</b>	<b>Co</b>	<b>Sn</b>	<b>W</b>	<b>Sr</b>
<b>F ratio</b>	367	386	393	865	1393	2963	4109

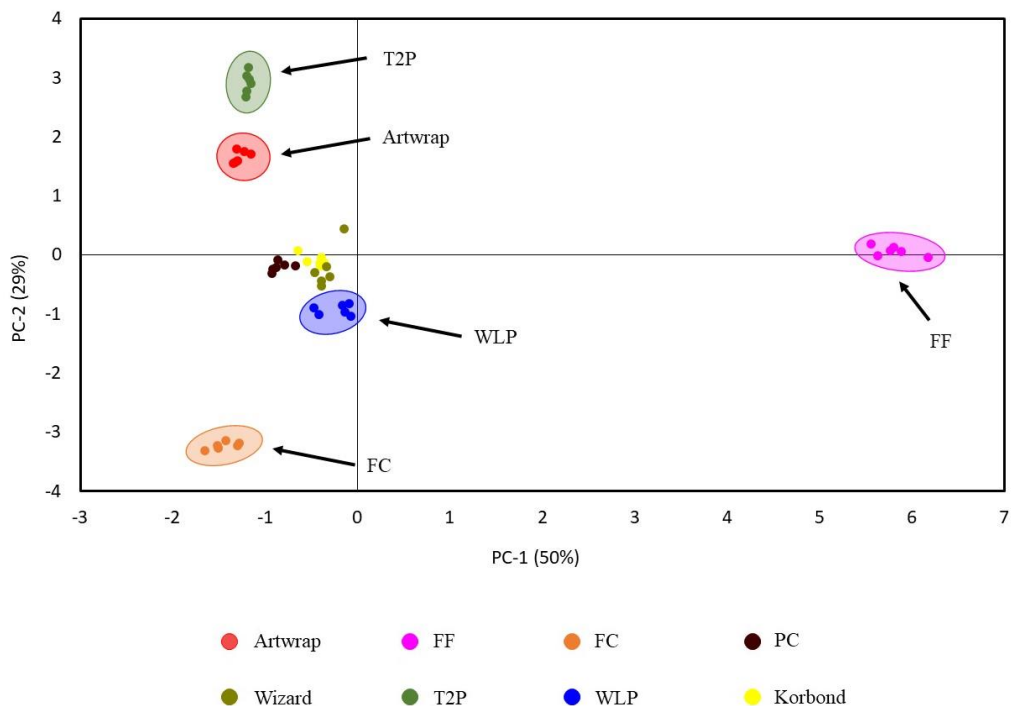


**Figure 3.7:** 2-D scores plot from PCA of the refined sparkler sample set after elements with a f-ratio < 200 were removed. Distribution of sample data shows five distinct classes including the T2P, FC, FF, Artwrap and WLP samples.

This process was repeated until no improvement in separation could be observed which occurred at an f-ratio threshold of 300, resulting in a discriminatory 7-element profile. PCA was performed using elemental contributions from Sr, W, Sn, Co, V, Sb and Ni, generating a 3-D scores plot where all brands formed distinguishable tightly clustered groups as shown in Figure 3.8a. Three of the classes appear to have little separation between them but repeated PCA on the cluster shows the classes can be easily discerned (Figure 3.8b). Results from PCA coupled with ANOVA based feature selection reveal that full discrimination between the eight sparkler brands can be achieved using trace elemental data from a refined 7-elemental profile, thus suggesting this method could be used to provide additional source information regarding a seized party sparkler sample.

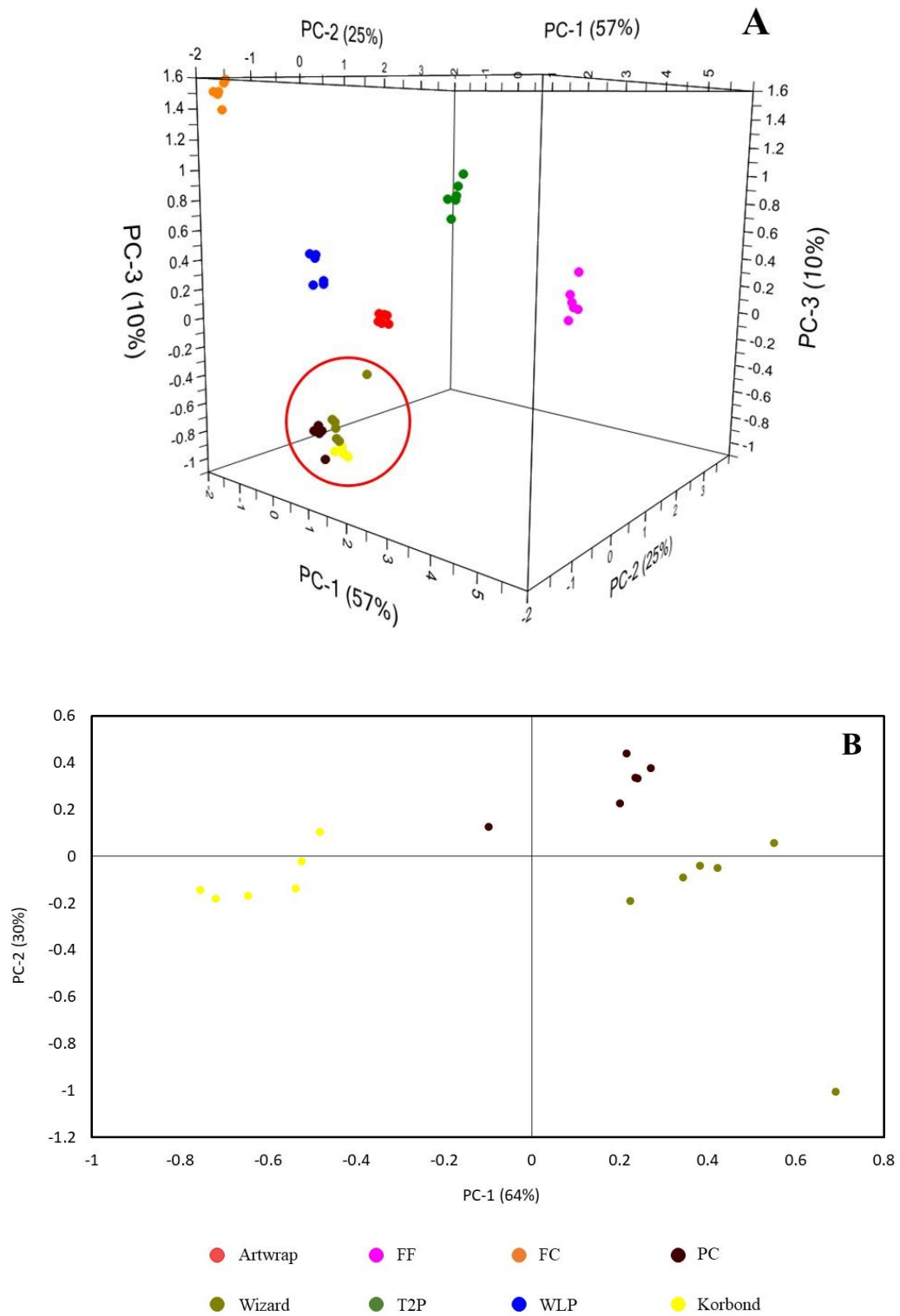


**Figure 3.8:** 3-D scores plot from PCA of the refined sparkler sample set using a refined 7-element profile that shows five distinct classes and three with minimal separation (a), repeated PCA on the highlighted cluster reveals full discrimination between the three classes across the first two PCs (b).

Analysis of the factor loadings associated with Figure 3.8a highlights the elemental contributions within each PC. The FF brand is largely separated across PC1 which is contributed to the large presence of Sn, Sb and W, which can be observed in Table B.2. The minor variation between these elements also contribute to the separation of the three classes across PC-1 within the highlighted cluster. Separation across PC2, responsible for the discrimination of the T2P and Artwrap brands was attributed to the highly variable concentration of Ni and Sr. Variation across PC3 is primarily attributed to Co and V, which explains the distribution of FC samples at the extreme positive end of PC3 as they contained approximately twice the amount of cobalt compared to other brands. The variation observed between elements is likely attributed to the range of impurities present within the party sparkler ingredients as well as contamination from the manufacturing process and location. Overall, contributions from all seven elements are required to achieve brand discrimination, additional elements can be added to the profile but may negatively impact separation as shown previously.

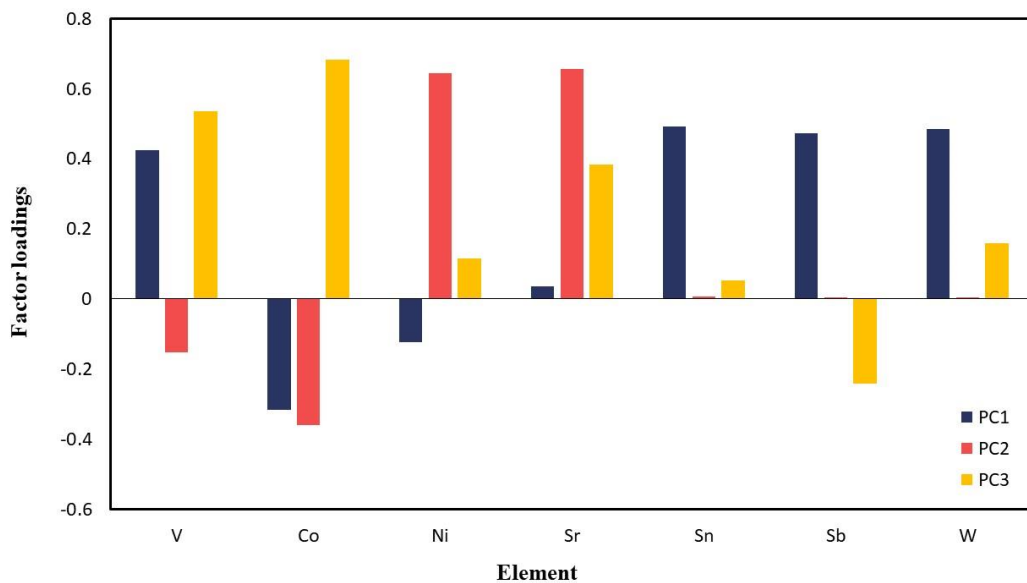


**Figure 3.9:** 3-PC factor loadings plot for elemental data acquired from PCA performed on refined sparkler sample set using a 7-element profile.

Given the effective discrimination observed within PC scores plots, source determination capabilities were further assessed by LDA, which was conducted using the linear distance and first four PCs with equal probabilities assumed. LDA was performed with each brand treated as an individual class to generate a discriminant

model that was used to predict the source of samples from an independent dataset. As a separate dataset could not be obtained from the limited number of samples, an alternative 'leave-one-out' approach was adopted that randomly assigned one sample from each brand for prediction purposes. As the model could only be validated with a small sample set, this approach can only give an approximate assessment of the model's predictive accuracy. To further improve reliability, this process was repeated 20 times, each with a different randomised validation set. Results from each analysis returned a 100% classification accuracy. Furthermore, the models correctly predicted the source of every sample across each iteration. Even though three brands were poorly separated within the PC scores plot, repeated source prediction showed that trace elemental coupled with PCA-LDA is extremely effective at discriminating and predicting the brand of party sparklers.

Source determination capabilities of this technique was further assessed by applying it to burnt residues. An identical procedure was conducted in that six burnt samples from each sparkler brand was analysed by ICPMS with ANOVA based feature selection being performed prior chemometric analysis. Repeated PCA was conducted with an increasing f-ratio threshold to remove elements that had a strong negative contribution to the separation of samples. This process afforded a 6-element profile that was used to produce the 3-D scores plot shown in Figure 3.10. Comparable to the distribution of unburnt samples, full discrimination can be achieved with all brands forming distinct classes across the first three PCs. The main difference observed is the refined elemental profile required to achieve discrimination, as only six elements including V, Co, As, Sr, Sn and W were used. This indicates that different sparkler brands can be distinguished regardless of whether a seized sample is burnt or unburnt.

The effectiveness of the unburnt model to predict the source of an unknown sample was further assessed with the burnt dataset. Two discriminant models were generated by LDA; the first included elemental contributions from the refined 7-element profile used to discriminate between unburnt samples and the other used an elemental profile that combined the discriminatory elements from both unburnt and burnt analysis. Each were then used to predict the source of 48 burnt samples, a summary of the results is displayed in Table 3.8. Little difference was observed between the two models as using the combined elemental profile resulted in one additional successful prediction.

Although the overall prediction rate was relatively high, both could not effectively discern between the Artwrap, Korbond and T2P brands which lowered the prediction capabilities of both models. These results indicate that discrimination and source determination can be achieved with individual unburnt and burnt sample models, however the unburnt model cannot be used to consistently determine the original brand of burnt samples.

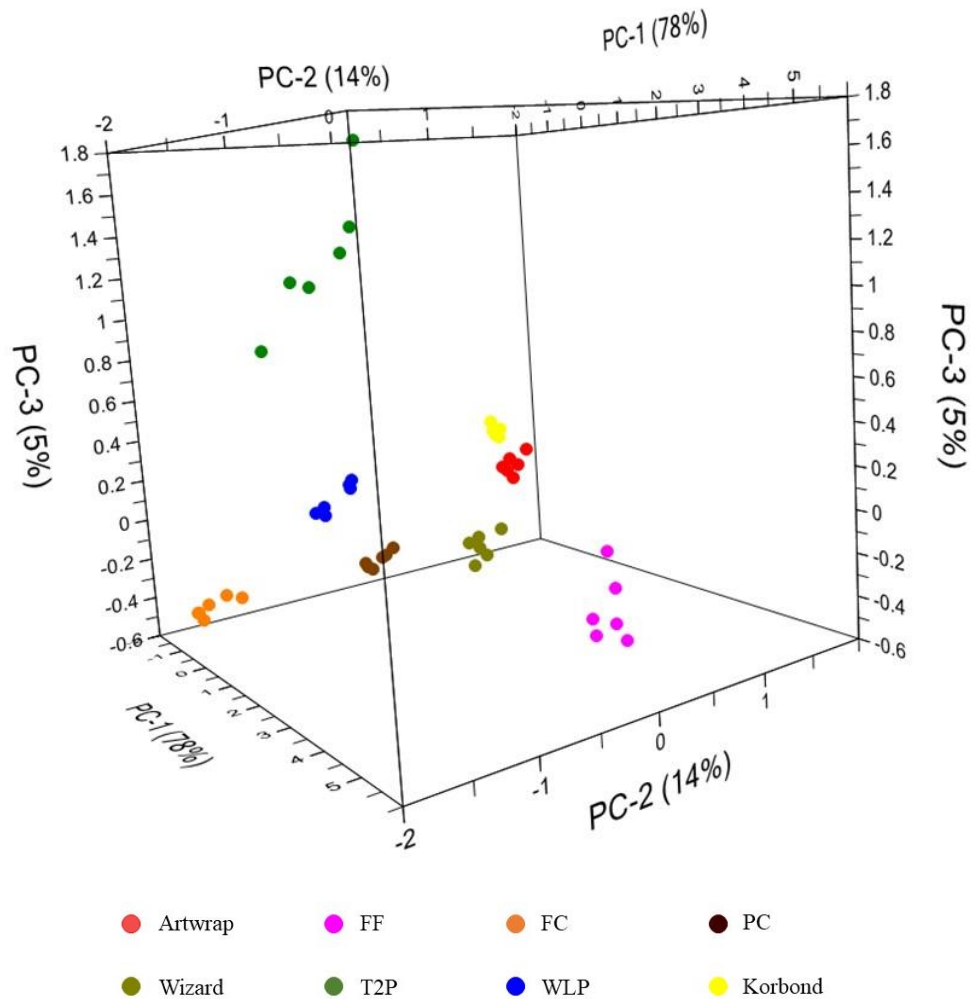


**Figure 3.10:** 3-D scores plot from PCA using a 6-element profile showing the distribution of burnt sparkler samples that shows full discrimination between the eight classes.



**Table 3.8:** Number of correct vs incorrect classifications from validation of a four PC LDA model. Discriminant model was constructed using trace concentration data from the refined 7-element profile or using a combined profile that included elements within the refined burnt profile.

<b>LDA performed using elements from unburnt profile</b>				
<b>Class #</b>	<b>Brand</b>	<b>Correct</b>	<b>Incorrect</b>	<b>% Correct</b>
<b>1</b>	WLP	6	0	100
<b>2</b>	Artwrap	0	6 (Predicted as class 4)	0
<b>3</b>	T2P	1	5 (Predicted as class 2)	17
<b>4</b>	Korbond	6	0	100
<b>5</b>	PC	5	1 (Predicted as class 2)	83
<b>6</b>	FC	6	0	100
<b>7</b>	FF	6	0	100
<b>8</b>	Wizard	5	1 (Predicted as class 2)	83
	Total			73
<b>LDA performed using elements from combined unburnt and burnt profile</b>				
<b>1</b>	WLP	6	0	100
<b>2</b>	Artwrap	0	6 (Predicted as class 4)	0
<b>3</b>	T2P	1	5 (Predicted as class 2)	17
<b>4</b>	Korbond	6	0	100
<b>5</b>	PC	5	1 (Predicted as class 2)	83
<b>6</b>	FC	6	0	100
<b>7</b>	FF	6	0	100
<b>8</b>	Wizard	6	0	100
	Total			75

### 3.4 Conclusions

Party sparklers are an inexpensive and easily accessible low order pyrotechnic that can be used to prepare homemade explosive mixtures and IEDs that could potentially cause damage to people, animals or property. Within a forensic investigation of seized sparkler material, analytical procedures focus on identifying the primary components and any additional explosive material it is mixed with. This chapter significantly improves the evidential value of sparkler material by providing characteristic information from a range of techniques and exploring the source determination capabilities of unburnt and burnt residues.

Infrared spectroscopy can effectively distinguish party sparkler residues from other low order inorganic explosives such as black powder, however, can only provide a preliminary identification of the oxidising agent. IC and SEM can easily identify the primary components within sparklers with IC also capable of identifying additional trace metals within burnt samples. GCMS can also be used to infer whether the sampler originated from a colour coated sparkler based on the presence of resin or binding compounds. However, it was found that none of these techniques can provide enough discriminatory information that could be used to distinguish between brands and link sparkler material to its source.

ICPMS coupled with PCA-LDA showed the greatest potential for source attribution of unburnt and burnt residues. ANOVA based feature selection produced a refined elemental profile that contained elements with high discriminatory power. Subsequent PCA-LDA showed that eight brands of party sparklers could be discriminated and generated models with a high predictive accuracy. Analysis of burnt samples showed comparable results, however when projected onto the unburnt model, source prediction was inconsistent. These findings indicate that chemometrics combined with trace elemental data is a potentially effective approach to providing additional source information from a seized party sparkler. This information could be used to generate investigative leads or establish connections within a forensic investigation

The experimental methods and characteristic data presented in this chapter greatly contributes to the forensic intelligence of party sparklers as a low order pyrotechnic and explosive precursor. To further improve source determination capabilities, a larger

dataset with more brands and sparkler types is required to increase the diversity of the model. This method could also be applied to other firework or pyrotechnic products which is relevant in jurisdictions where party sparklers may not be as commonly used. However, to continue improving the proficiency and consistency of source attribution techniques with explosives and pyrotechnics, ongoing studies characterising more brands, products and mixtures are required.

## **Chapter 4. Preparation, characterisation, and source attribution of homemade ammonium nitrate as an explosive precursor**

A portion of this chapter has been published as followed:

Joshua A. D’Uva, David DeTata, Simon W. Lewis. Source determination of homemade ammonium nitrate using ATR-FTIR spectroscopy, trace elemental analysis and chemometrics. *Forensic Chemistry* 2022 28, 1-11 DOI: <https://doi.org/10.1016/j.forc.2022.100411>

## 4.1 Introduction

Ammonium nitrate (AN) is a nitrogen-rich, white crystalline solid that has many applications in industry globally. It is manufactured in a number of forms including chemical, fertiliser and explosive grade, each having varying characteristics and legitimate uses (165-167). Fertiliser grade AN, one of the most widely used products within agriculture, is produced as highly dense, low porosity pellets which are less sensitive to detonation and easily transportable (67, 134, 168). Explosive grade AN is a lower density and high porosity product, which is mixed with fuel oil to prepare ammonium nitrate fuel oil (ANFO), a powerful high explosive used within the mining industry (134, 169-171). In Australia, approximately 2 million tonnes of AN is manufactured annually and approximately 90% is used to prepare ANFO (63, 64). Commercial AN is primarily prepared by the reaction between ammonia and nitric acid, but can also be made by mixing calcium nitrate and ammonium carbonate in solution to form solid AN once evaporated (67, 165, 172). Although many forms of AN can be prepared, all are highly stable, have a low sensitivity to friction and shock, and are mass produced in many countries (73, 169, 173). These properties, combined with its accessibility, low cost and ease of preparation, has made it one of the most widely used explosive precursors by terrorist and extremist groups throughout history (73, 134, 172). Consequently, AN is frequently encountered in forensic casework and so its detection, identification and source attribution is crucial for gathering evidence and generating investigate leads within an investigation (73).

AN is classified as a tertiary high explosive, requiring a booster for reliable detonation (134). AN is often mixed with fuels such as aluminium powder, sugar, fuel oil, inorganic salts or nitromethane, forming emulsions or slurries to improve its effectiveness as a homemade explosive (HME) (2, 174-181). Improvised explosive devices (IEDs) prepared using different AN mixtures can have detonation velocities ranging from 1400 – 1600 ms<sup>-1</sup> and a TNT equivalence of 25 – 100% (2, 182). Preparing ANFO by the simple addition of fuel oil can result in IEDs with a detonation velocity of up to 4750 ms<sup>-1</sup> (134, 182, 183). AN based IEDs have been linked to bombings in Oklahoma City (USA, 1995) and Oslo (Norway, 2012) which involved the detonation of a 2300 kg ANFO based vehicle bomb and a 950 kg AN/aluminium IED respectively (36, 184). Multiple attacks have also occurred across Northern

Ireland and the United Kingdom (UK) in the 1990s, and it has also been recorded that calcium ammonium nitrate (CAN) based explosives were once used as the primary explosive in over 85% of IEDs used against coalition forces in Afghanistan (135, 184, 185). Furthermore, with improper storage or transport practices, AN can be susceptible to a rapid exothermic decomposition process that may result in accidental explosions (186-192). This has occurred on numerous occasions and most recently was the cause of the devastating explosion that occurred in Lebanon (2020), highlighting its potential for mass destruction (193-198).

As a result of its widespread use, extensive regulations across multiple countries have been mandated in an attempt to restrict the illicit purchase, preparation and use of AN. Attacks in the UK imposed restrictions on the sale of high purity AN throughout Ireland and replaced it with CAN, which aimed to reduce its use as an explosive precursor (34). The United States also acted to desensitise commercial AN and limit its accessibility (34, 74). The European Commission took a stricter approach and introduced regulations that prohibited the distribution of AN fertilisers containing a nitrogen percentage of over 16% (72, 73). In Western Australia (WA), where this research was conducted, it is illegal to purchase, sell, store or transport security sensitive AN (SSAN), which refers to AN or AN mixtures that contain greater than 45% AN (66, 90). However, AN can still be sourced from alternative products, such as instant cold packs, and easily prepared from commercial ingredients and mixtures. Therefore, studies investigating how AN can be commercially sourced and prepared are vital, as well as research into the development of new analytical approaches that can identify the origin of AN and its precursors.

The forensic profiling of explosives for source determination purposes has previously been reported using a range of analytical techniques including infrared and Raman spectroscopy (95, 103, 199, 200), microscopy (201, 202) and chromatographic methods (203-205). In particular, attenuated total reflectance Fourier transform infrared (ATR-FTIR) spectroscopy is routine in the analysis of bulk explosives, as it is a fast and easy to perform technique available in many forensic laboratories (12, 106). The discrimination of various forms of AN and its precursors has also been investigated, primarily using techniques such as isotope ratio mass spectrometry (IRMS) and inductively coupled plasma mass spectrometry (ICPMS) to generate

characteristic isotopic and elemental profiles (73, 135, 165, 172, 206). ICPMS is not routine in explosive analysis; however, it allows for trace characterisation and has been shown to effectively discriminate between pure AN sources (135). Additionally, forensic profiling of explosives has been combined with chemometric techniques such as principal component analysis (PCA) and linear discriminant analysis (LDA), improving source determination capabilities (119, 130, 207, 208).

Benson *et al.* used a combination of oxygen, hydrogen and nitrogen isotope values to differentiate between AN fertiliser from three Australian manufacturers, as well as samples from five different overseas sources (165). However, limited discrimination was achieved between the Australian and overseas pellets. Another study used a combination of ICPMS and chemometrics to discriminate between 125 CAN samples taken from six different factories (135). The authors were able to classify samples into five factory groups, with one containing two from the same manufacturing company, and subsequently predict the source of CAN samples with varying degrees of success. Effective prediction was dependent on whether CAN samples were pristine or reprocessed with adulterants. Brust *et al.* used a combination of isotopic and elemental profiles with chemometrics to discriminate between samples from 19 AN fertiliser manufacturers (73). The authors concluded that combining the characteristic profiles resulted in effective discrimination between manufacturers, sample types and individual batches.

Although there are several studies relating to the source determination of AN, all have focussed on the discrimination of pure AN or AN fertilisers. As discussed previously, increasing restrictions around the purchasing of commercial AN will inevitably result in AN being sourced and prepared from alternative sources. When AN is manufactured in different forms, various coating and modifying agents as well as other additives and trace elements may be added to achieve particular properties (165). The variation in these trace components may be used to discriminate between sources and show that alternative AN samples can be linked to their origin. Further studies investigating the source determination of alternative AN are therefore critical.

The aim of this chapter was to: (1) identify accessible commercial products that contain or can be used to prepare AN, (2) characterise AN products using a suite of routine and non-routine analytical techniques, and (3) evaluate the source

determination capabilities of using chemometrics coupled with select techniques. Knowing what products can be used to prepare AN, the practicality of preparing large amounts, and what information can be gained from different techniques would substantially benefit the forensic intelligence of AN as a HME and aid in many stages throughout a forensic investigation and court of law.

## **4.2 Methodology**

### **4.2.1 Sources of ammonium nitrate and precursors**

Nine AN products were sourced and prepared within this study. For comparison purposes, three of the products are termed as ‘pure form’ as they were collected in their original form and did not require any further extraction or synthesis. These include chemical grade AN, explosive grade AN and AN obtained from cold packs. Explosive grade AN is in the form of small white prills which are used to prepare ANFO for the mining industry (Figure 4.1a). In Australia, it cannot be sold, purchased, transported or stored without a government issued license. Chemical grade AN is a highly pure form of AN that appears as a translucent crystalline solid. This can be purchased from multiple chemical suppliers but is subject to the same regulations as explosive grade AN or SSAN as it has a purity > 45%. The AN contained within cold packs has been processed to form white pellets which are slightly larger in size than explosive grade pellets. Cold packs can be purchased legally at retail stores and contain approximately 100 g of AN within a single packet, along with a bladder of water that is punctured to create an endothermic AN solution (Figure 4.1b).

The remaining six products investigated are termed ‘homemade’ as they were synthesised from commercial ingredients. One of the homemade products was prepared from laboratory reagents, and the remaining five were prepared using commercial products purchased from various hardware and garden stores. Three of the products were prepared from commercial calcium nitrate and varying brands of ammonium sulfate, an example of which is shown in Figure 4.1c. Commercial calcium nitrate can be purchased in hydroponic nutrient products (Figure 4.1d). The remaining two products were prepared from alternative fertiliser mixtures including Black Marvel Fruit and Citrus Food (11.7% w/w NH<sub>4</sub>) and African Violet Food (10.5% w/w NH<sub>4</sub>) (Figure 4.1e and Figure 4.1f).





**Figure 4.1:** Sources and precursors used to prepare AN: (a) explosive grade AN, (b) AN based cold packs, (c) commercial ammonium sulfate fertiliser, (d) hydroponic nutrient product containing calcium nitrate, (e) Black Marvel fertiliser containing 11.7% w/w  $\text{NH}_4$  and (f) African Violet Food containing 10.5% w/w  $\text{NH}_4$ .

#### 4.2.2 Preparation of ammonium nitrate products

AN synthesis from different products is described in Chapter 2, section 2.3.1. The precursor sources and average yield information is summarised in Table 4.1 below.

**Table 4.1:** Source and average yield information of AN products and their precursors. Products are separated into ‘pure form’ and ‘homemade’ groups based on how they were prepared or obtained.

<b>Pure form AN</b>	<b>Source</b>		<b>Yield</b>
<b>Chemical grade</b>	Merck, AUS		-
<b>Explosive grade</b>	Western Australian Bomb Response Unit (Western Australian Police) (WAPOL)		-
<b>Cold pack</b>	Office supplies retailer		100g per packet
<b>Homemade AN</b>	Calcium nitrate source	Ammonium sulfate source	Approx. Yield (%)
<b>Chemical grade</b>	Ajax Finechem, AUS	Merck, AUS	66
<b>Baileys</b>	Hydroponic nutrient (Manutec, AUS)	Sulfate of ammonia (Baileys fertiliser, AUS)	53
<b>Richgro</b>	Hydroponic nutrient (Manutec, AUS)	Sulfate of ammonia (Richgro, AUS)	82
<b>SREDA</b>	Hydroponic nutrient (Manutec, AUS)	Sulfate of ammonia (SREDA garden products, AUS)	66
<b>Black Marvel</b>	Hydroponic nutrient (Manutec, AUS)	Black Marvel Fruit and Citrus Food (Richgro, AUS)	67
<b>African Violet</b>	Hydroponic nutrient (Manutec, AUS)	African Violet Food (Manutec, AUS)	81

#### 4.2.3 Infrared spectroscopy

Spectral analysis of the AN products was performed using the instrument and method outlined in Chapter 2, section 2.4.1. Ten spectra were collected from each AN product. The same method was repeated one week later with another five spectra from each product being collected, which was used for validation purposes within chemometric analysis.

#### 4.2.4 Raman spectroscopy

Raman spectroscopy was performed using the instrument and method outlined in Chapter 2, section 2.4.2. Raman spectra was collected for each AN product using the same parameters throughout, with the exception of laser power. It was found that due to the varying levels of purity across the products, a minor adjustment in the strength of the laser was required. A laser power of 0.5% (chemical grade AN), 1% (explosive and cold pack grade AN), and 5% (all remaining 'homemade' AN) was used depending on the product.

#### 4.2.5 Ion chromatography

Ion chromatography (IC) was performed using the instrument and method outlined in Chapter 2, section 2.4.3. Samples were prepared by dissolving AN (10 mg) in MilliQ water (10 mL) and diluted to a final concentration of 100 ppm.

#### 4.2.6 Scanning electron microscopy

Scanning electron microscopy (SEM) was performed using the instrument and method outlined in Chapter 2, section 2.4.4. Before mounting onto a sample stub (carbon tab on 12 mm aluminium pin mount) samples were dried in an oven at 40°C overnight to ensure no moisture was present. Elemental analysis was performed on select points across the samples as well as a bulk analysis of the entire area. Back scattered electron (BSE) images were collected of each product.

#### 4.2.7 X-ray diffraction

X-ray diffraction (XRD) was performed using the instrument and method outlined in Chapter 2, section 2.4.6. Before mounting onto a silicon zero background plate (ZBP), samples were dried in an oven at 40°C overnight to ensure no moisture was present. Each AN product was prepared and analysed in duplicate approximately one month apart using the same instrument and method.

#### 4.2.8 Inductively coupled plasma mass spectrometry

ICPMS was performed using the instrument and method outlined in Chapter 2, section 2.4.7. Sample preparation for AN samples was adapted from the procedure outlined in

Brust *et al.*; AN (200 mg) was dissolved in 70% nitric acid (3 mL) in a 20 mL polypropylene tube (73). The sample was heated in an oven (90 °C) for 2 hours. MilliQ water was added to a total volume of 10 mL. Samples were diluted 10 and 100-fold and blanks of the MilliQ water, diluter, nitric acid and sample procedure were also prepared.

#### 4.2.9 Chemometrics

##### 4.2.9.1 Chemometric analysis using spectral data from infrared spectroscopy

PCA-LDA was performed using the method described in Chapter 2, section 2.4.8.1. The classification set contained ten replicate spectra from each AN product. An independent dataset used to validate the models generated by LDA contained five replicate spectra from each AN product. A single model and stepwise classification approach was evaluated using the same data sets, which is detailed in section 4.3.3.1.

##### 4.2.9.2 Chemometric analysis using X-ray diffraction patterns

PCA was performed using the method described in Chapter 2, section 2.4.8.2. The dataset contained two samples from each AN product.

##### 4.2.9.3 Chemometric analysis using elemental concentration data from ICPMS

PCA-LDA was performed using the method described in Chapter 2, section 2.4.8.3. From the 58 elements analysed, ten were retained for chemometric analysis including B, Ti, Mn, Ni, Cu, Se, Rb, Sr, Ba and U. The classification set contained five samples from each UN product. Discriminant models for source prediction were generated using a randomised leave-one-out approach as described in Chapter 2, section 2.4.8.3.

### **4.3 Results and Discussion**

#### 4.3.1 Preliminary assessment of ammonium nitrate products

The aim of this chapter was to first identify the several ways AN can be sourced and prepared, which greatly contributes to forensic intelligence of AN as an explosive precursor. As the sale and purchase of AN is heavily regulated in Australia, the preparation of a large scale AN based explosive device would require the sourcing of

commercial products. The AN products collected were characterised with a range of spectroscopic and analytical techniques before investigating whether they can be linked to their source using chemometrics. Therefore, initial investigations were performed to identify how AN can be commercially sourced and prepared. Furthermore, the capability of an individual with minimal knowledge of chemical synthesis preparing large amounts of AN was also assessed in order to understand the practicality of preparing AN based IEDs using homemade AN.

Large quantities of highly pure AN were shown to be easily sourced from products such as cold packs, and can also be prepared from commercially available calcium nitrate, a hydroponic nutrient, and ammonium sulfate fertiliser. This highlights that although AN cannot be purchased, there is no limit to how much can be prepared and so there is no 'maximum charge size'. The reaction between calcium nitrate and ammonium sulfate is a simple double displacement reaction that requires the mixing of two aqueous solutions. A vacuum filtration system may not be readily available to a regular civilian; however, this can be substituted with other filtration methods so the procedure can still be easily performed.

This method was found to consistently produce AN in relatively high yields (> 50%) and given that these products can generally be purchased in 1 – 10 kg amounts, large quantities of AN can potentially be prepared in a short amount of time. AN could also be prepared from alternative fertiliser mixtures containing varying amounts of ammonium. The purity and yield of AN prepared from these mixtures is highly variable as it depends on the percentage of ammonium compared to the other bulk and trace chemicals present.

A total of nine AN products were investigated within this study and for ease of comparison, three of the products were grouped as being pure form products and the remaining six were grouped as being homemade. All AN products were visually identical and appeared as white crystalline powders besides the one prepared from African Violet Food. This product appeared as a vibrant purple colour and had a characteristic ATR-FTIR spectrum containing several peaks that were absent from the others (Figure A.6). It was found that although this product contained AN, it also contained a variety of salts and impurities that persisted throughout the synthesis from the precursor material. The safety data sheet (SDS) and packaging of the product

specifies containing ammonium sulfate, potassium nitrate, mono ammonium phosphate, urea and a range of trace metals (209). Because of its highly characteristic colour and spectrum, physical examination and interpretation of its spectra could easily discriminate it from the other products and so was omitted from subsequent characterisation and chemometric analysis.

#### 4.3.2 Chemical characterisation of ammonium nitrate products

##### 4.3.2.1 Infrared and Raman spectroscopy

Characteristic spectra of each AN product were collected by ATR-FTIR spectroscopy (Figure A.7). Initial examination revealed that the spectra of the pure form products were near identical and showed only minor differences in peak height. All were representative of the pure chemical grade AN, despite the explosive grade and cold pack AN undergoing a prilling process. Spectra from the homemade AN products were also near identical, but noticeably different from the pure form products as they contained additional peaks. Figure 4.2 shows an example of one of the pure form and homemade products.

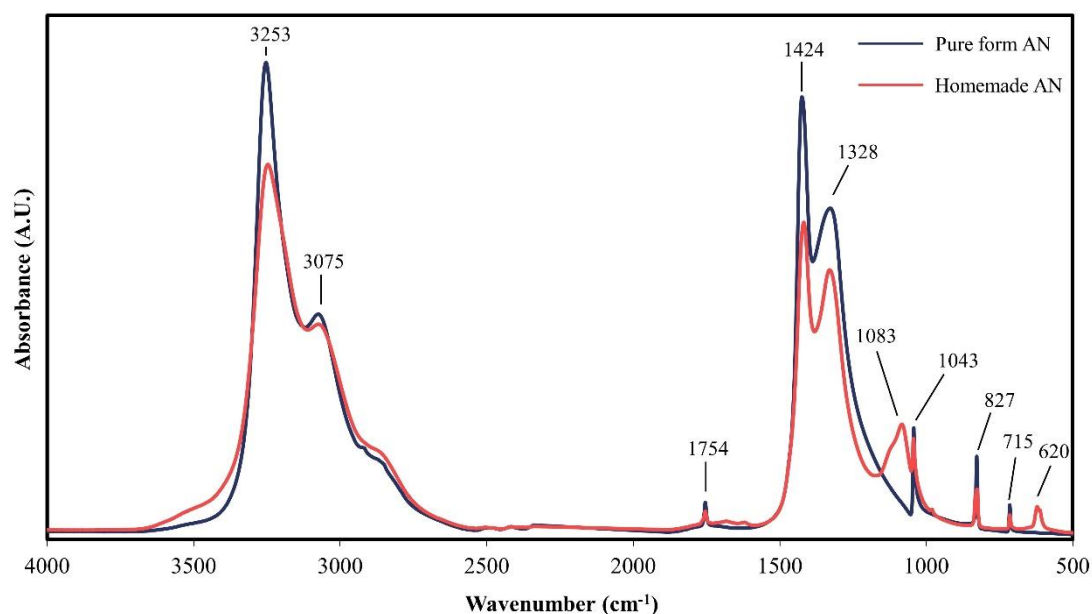


**Figure 4.2:** ATR-FTIR spectra of a typical pure form AN product (explosive grade AN) and homemade AN product (synthesised from Richgro sulfate of ammonia and commercial calcium nitrate). Identifiable peaks are labelled across both spectra.

All spectra contained characteristic peaks of AN, which included the two strong absorption bands in the region  $3300 - 3000 \text{ cm}^{-1}$  and  $1450 - 1300 \text{ cm}^{-1}$ . The peaks at  $3253 \text{ cm}^{-1}$  and  $3075 \text{ cm}^{-1}$  corresponded to the anti-symmetric stretch and deformation vibration modes of the ammonium ion (134, 210). The peaks at  $1424 \text{ cm}^{-1}$  and  $1328 \text{ cm}^{-1}$  were characteristic of the ammonium and nitrate ion respectively. It is suggested that these peaks were attributed to the triple degenerated ammonium cation deformation and double degenerated stretching vibration of the nitrate anions (102, 210). Other notable peaks that appeared across all products include those at  $1043$ ,  $827$  and  $715 \text{ cm}^{-1}$ , which were attributed to symmetric stretching vibration, out-of-plane and in-plane deformation of the nitrate ion respectively (102, 210).

The main differences between the pure form and homemade products could be seen within the fingerprint region, where broad peaks at  $1083$  and  $620 \text{ cm}^{-1}$  were evident in those that were synthesised. This was likely attributed to the sulfate anion, which comes from unreacted ammonium sulfate or other sulfate salts formed throughout the synthesis, such as calcium sulfate (211, 212). Additionally, a spectrum of the sulfate of ammonia fertiliser (Richgro brand) was collected and showed peaks at  $1078$  and  $613 \text{ cm}^{-1}$ , which aligned closely with those observed in the homemade AN products, providing strong evidence for the presence of sulfate (Figure A.8).

Each AN product was also characterised using Raman spectroscopy (Figure A.9). Similar results to IR analysis were obtained, as the pure form and homemade products could be distinguished by a number of distinct bands, however, the spectra of products within each class were near identical. Figure 4.3 highlights the typical spectra obtained from a pure form and homemade product. All spectra contained the characteristic AN bands located at  $715$  and  $1045 \text{ cm}^{-1}$ , which correspond to the  $\text{NO}_3^-$  ion in-plane deformation and symmetric stretch respectively (213-216). A number of additional bands were present within the homemade products, again being attributed to the sulfate ion, which was in agreement with what was observed within the IR spectra (Figure A.9). The most notable band related to the sulfate ion was seen at  $980 \text{ cm}^{-1}$ , which is the symmetric stretching mode (217). Other bands located at  $450$  and  $620 \text{ cm}^{-1}$  were attributed to the symmetric bending and anti-symmetric stretching modes of the sulfate anion (Figure 4.3b) (217). Closer inspection of the main band at  $1045 \text{ cm}^{-1}$  revealed the sulfate anti-symmetric bend, which was also present across the homemade

products at approximately  $1050\text{ cm}^{-1}$ , highlighted in Figure 4.3c (217). This band was poorly resolved due to it being closely positioned to the major nitrate band; however, it could still be identified within the homemade products. Resolution of this band could potentially be improved with optimisation of instrument parameters such as the diffraction grating, laser excitation and slit size. Although, if this band cannot be resolved, it has been shown that due to the presence of several other distinct bands, homemade and pure form products can still be discerned using this method.

Results from spectroscopic analysis suggested that an AN sample of unknown origin could be identified as being either from a pure or homemade source, as the presence of a number of distinct peaks and bands attributed to the sulfate ion indicated it was likely synthesised from an ammonium sulfate product or alternative fertiliser mixture. ATR-FTIR instrumentation would also be commonplace in most laboratories and could provide a simple, fast and cost-effective means of gaining some source information before additional analysis is performed, with portable units also being available.

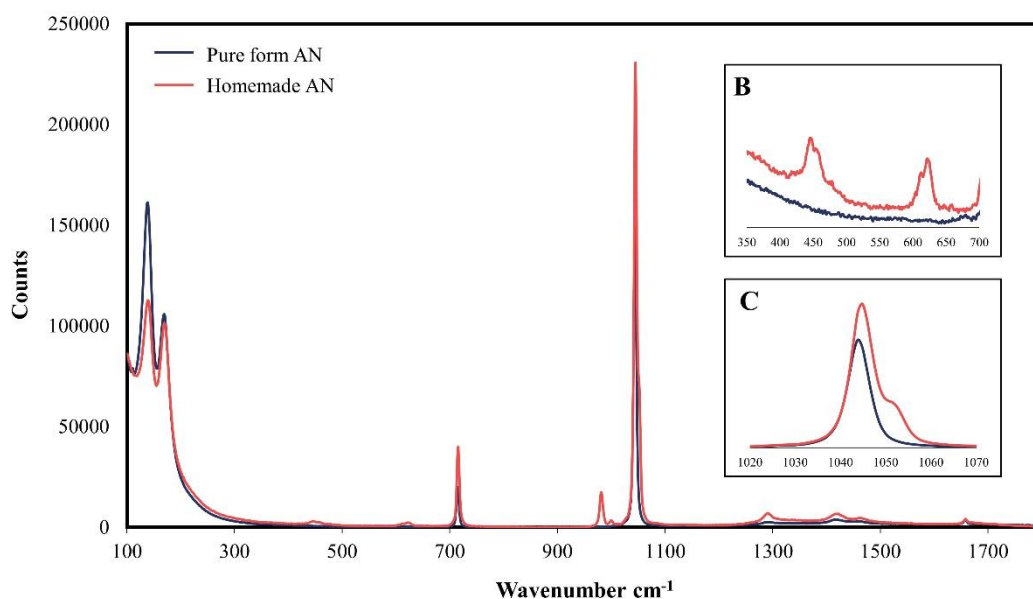


**Figure 4.3:** Raman spectra of a typical pure form AN product (chemical grade AN) and homemade AN product (synthesised from Baileys sulfate of ammonia and commercial calcium sulfate). Close-up view of  $350 - 700\text{ cm}^{-1}$  region (b) and  $1020 - 1070\text{ cm}^{-1}$  region (c) highlights bands associated with the sulfate ion present in the homemade AN products.



#### 4.3.2.2 Ion chromatography

Ion chromatography was used to determine the concentration of a range of cations and anions within the AN products. The cations that were analysed included  $\text{Li}^+$ ,  $\text{Na}^+$ ,  $\text{NH}_4^+$ ,  $\text{K}^+$ ,  $\text{Mg}^{2+}$ ,  $\text{Ca}^{2+}$ ,  $\text{Sr}^{2+}$  and  $\text{Ba}^{2+}$ . The anions that were analysed included  $\text{Cl}^-$ ,  $\text{ClO}_2^-$ ,  $\text{NO}_2^-$ ,  $\text{ClO}_3^-$ ,  $\text{NO}_3^-$ ,  $\text{SO}_4^{2-}$ ,  $\text{S}_2\text{O}_3^{2-}$  and  $\text{ClO}_4^-$ . Similar to previous analysis using spectroscopic techniques, IC could also be used to distinguish between pure form and homemade products. Table 4.2 reports the concentration of analytes found within the samples and as shown, all homemade products contained a large amount of sulfate whereas the pure form products did not. These results were in agreement with observations made from ATR-FTIR and Raman spectra, which indicated the presence of sulfate within the homemade products. The product synthesised from Black Marvel Food was also identifiable by the presence of potassium and chloride.

No other analytes were detected, indicating that if the AN products did contain additional trace metals or ions, they were likely present at concentrations of less than five parts per million (ppm). These results suggested that IC is capable of providing strong evidence that an unknown AN product has been synthesised from commercial ingredients or sourced in its pure form, and can further support the data obtained from ATR-FTIR and Raman analysis.

**Table 4.2:** Concentration of cations and anions (ppm) in 10 mg of AN from different sources (ions not detected in samples are labelled as n.d).

	<b>Ionic species</b>				
	Na <sup>+</sup>	K <sup>+</sup>	Cl <sup>-</sup>	NO <sub>3</sub> <sup>-</sup>	SO <sub>4</sub> <sup>2-</sup>
<b>Pure form AN</b>	Na <sup>+</sup>	K <sup>+</sup>	Cl <sup>-</sup>	NO <sub>3</sub> <sup>-</sup>	SO <sub>4</sub> <sup>2-</sup>
<b>Chemical grade</b>	25.3	n.d	n.d	83.9	n.d
<b>Explosive grade</b>	27.4	n.d	n.d	90.7	n.d
<b>Cold pack</b>	20.8	n.d	n.d	69.0	n.d
<b>Homemade AN</b>	Na <sup>+</sup>	K <sup>+</sup>	Cl <sup>-</sup>	NO <sub>3</sub> <sup>-</sup>	SO <sub>4</sub> <sup>2-</sup>
<b>Chemical grade</b>	22.4	n.d	n.d	55.6	15.2
<b>Baileys</b>	32.2	n.d	n.d	82.5	20.2
<b>Richgro</b>	21.2	n.d	n.d	57.3	10.9
<b>SREDA</b>	28.7	n.d	n.d	74.0	17.9
<b>Black marvel</b>	25.5	9.2	8.0	72.8	13.0

#### 4.3.2.3 Scanning electron microscopy

AN products were analysed using SEM-EDS to examine particle morphology and identify any metals in the sample. Notable differences in morphology between the pure form and homemade products can be seen in Figure 4.4. The homemade products appeared to be a heterogeneous mixture of AN and small rectangular particles scattered throughout the bulk material (Figure 4.4d-h). The explosive grade sample contained notably smaller particle sizes (Figure 4.4b). The smaller particle size was consistent with its intended use as a precursor for ANFO, as this would lead to a more effective explosive. The product made from Black Marvel Food was distinctive and showed large crystals with bright spots scattered throughout the bulk material (Figure 4.4h). This was indicative of various salts and metals that originated from the initial fertiliser mixture, as it was shown with previous chemical analysis techniques that this product contains trace amounts of sulfate, potassium and chloride.

Elemental analysis of the bright spots within the homemade products revealed high levels of sulfur and calcium, indicating that these may be calcium salt deposits, such as calcium sulfate, a by-product of the synthesis. The Black Marvel product contained many trace metals including manganese, chlorine, potassium, magnesium, zinc and copper, which was in agreement with results obtained from IC. Elemental analysis was also performed on the pure form products, however, trace elements that were observed within the homemade products could not be detected and so no additional chemical information could be obtained. It is possible that these products do contain trace materials, however, they would have to be present at low concentrations. These results were consistent with previous chemical analysis techniques, exhibiting the ability to distinguish between pure form and homemade products based on the presence of sulfur, calcium and bright salt deposits that can be visualised throughout the bulk material. Although SEM did not provide enough discriminatory information to differentiate products within each class, it can be used to infer the type of starting materials used, which could be useful in generating investigative leads within an investigation.

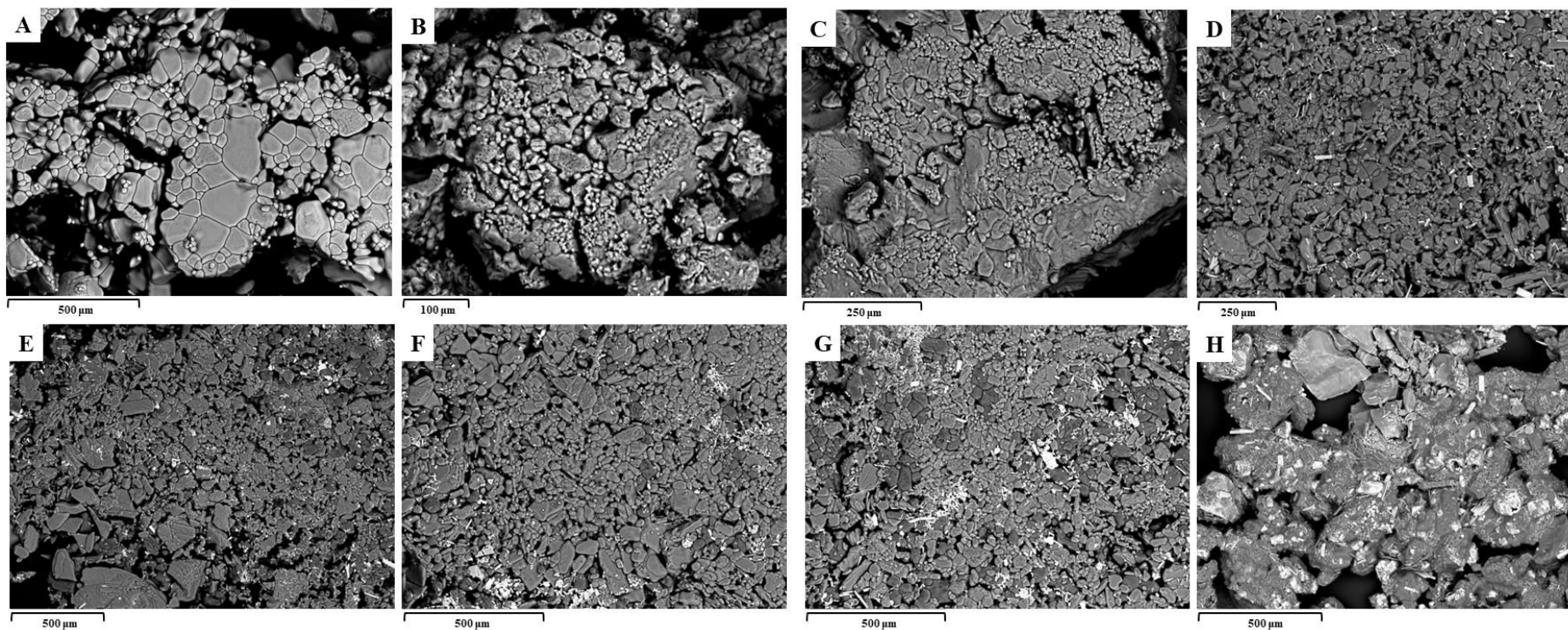


**Figure 4.4:** Scanning electron microscopy back-scattered electron image of AN products: chemical grade (a), explosive grade (b), cold pack (c), synthesised from chemical reagents (d), synthesised from Richgro ammonium sulfate (e), synthesised from Baileys ammonium sulfate (f), synthesised from SREDA ammonium sulfate (g) and synthesised from Black Marvel Food (h).

#### 4.3.2.4 X-ray diffraction

Interpretation of collected diffraction patterns showed that the pure form and homemade products were noticeably different, but identical within each class. The product made from Black Marvel fertiliser was an exception, as it had a distinctive diffraction pattern compared to other homemade products. Diffraction patterns for all pure form products are shown in Figure A.10. Comparison against reference patterns found that the pure form products matched the typical diffraction pattern obtained from synthetic gwihabaite (ammonium nitrate), confirming the sample as crystalline AN (Figure 4.5).

Diffraction patterns from homemade products also aligned with this reference pattern, indicating AN was present in the same crystalline form, however, there appeared to be a number of additional reflections (Figure 4.6). These were likely caused by sulfate salt crystals, the presence of which was previously confirmed by other techniques. Thorough analysis of the patterns revealed an additional reflection present in the Richgro and SREDA products at  $17.5^\circ$  and  $28.8^\circ 2\theta$  respectively. Furthermore, the Black Marvel product had a visually different diffraction pattern and did not contain many of the reflections associated with AN. Considering results from previous analysis, this suggested that AN was still present within the sample, but not in crystalline form, so does not appear in the diffraction pattern. The pattern was dominated by other crystalline material, most likely being potassium, sulfate or chloride salts.

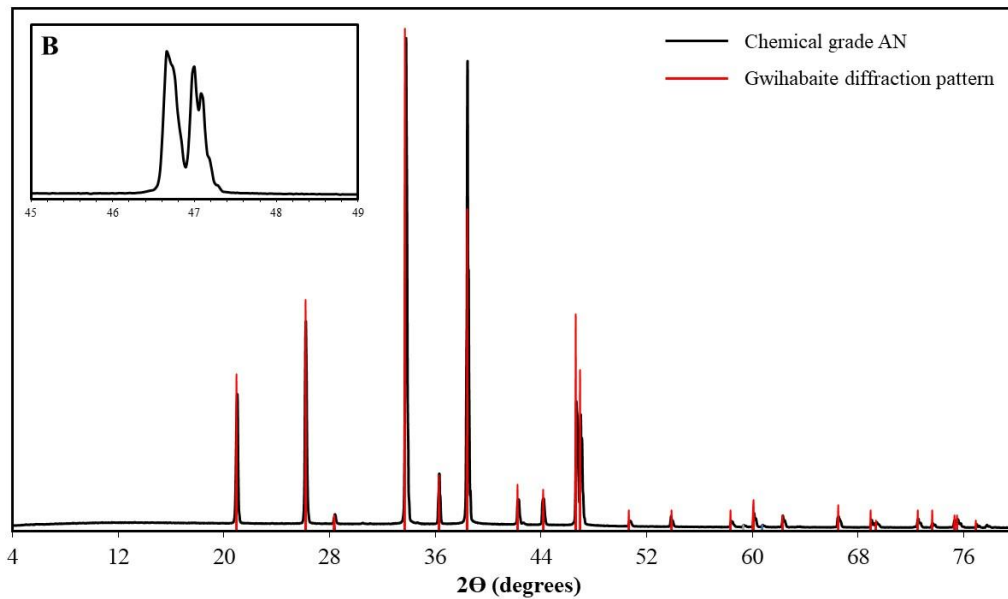


**Figure 4.5:** X-ray diffraction pattern of chemical grade AN. Overlaid is the typical diffraction pattern associated with synthetic gwihabaite (ammonium nitrate). Close-up view of the 45-49°  $2\theta$  region (b) is also displayed.

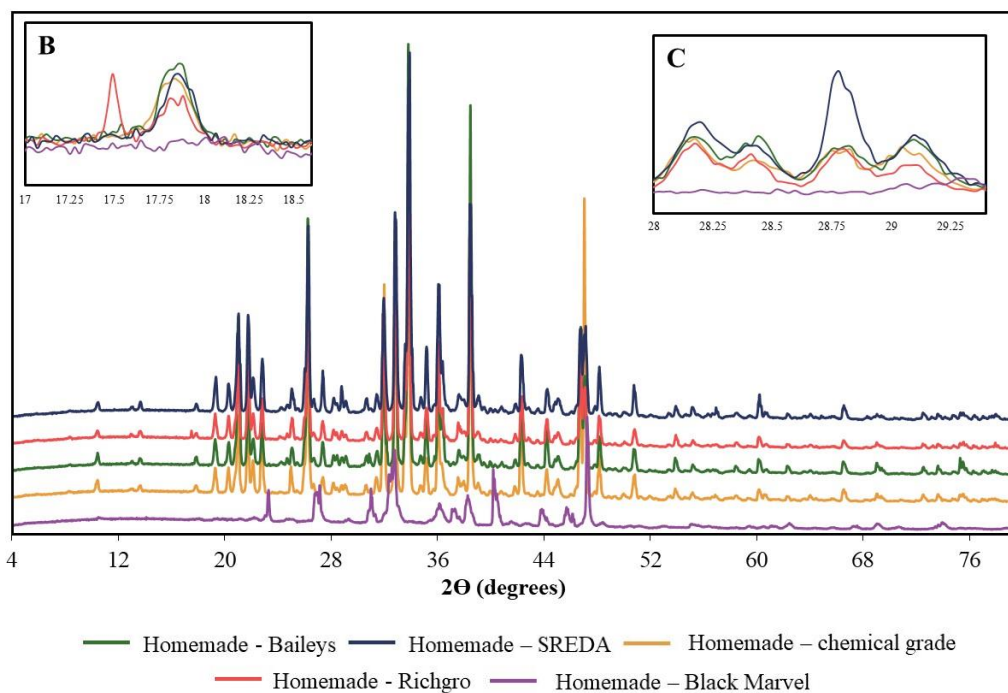


**Figure 4.6:** X-ray diffraction pattern of homemade AN products (baseline has been offset for better visualisation). Close-up view of the 17-18.5°  $2\theta$  region that shows an additional reflection in the Richgro product (b), and a close-up view of the 28-29.2°  $2\theta$  region that shows an additional reflection in the SREDA product (c).

#### 4.3.2.5 Inductively coupled plasma mass spectrometry

The concentrations of 58 elements within the AN products were determined by ICPMS. After initial examination of the data and removal of elements detected at concentrations below the calibration range or present due to contamination, 10 elements were retained for further analysis. Isotope selection was also performed to minimise potential interferences and to assist in data reduction. Table 4.3 summarises the average concentration of elements found by analysing five samples from each product. Initial observations showed that there was a notable difference between the samples, as trace amounts of only half of the retained elements were consistently detected throughout the pure form products. The concentration of elements was extremely varied between the homemade products, with some being present in very large amounts, such as nickel, manganese and copper. The increased concentration seen in the Black Marvel product was to be expected, as this fertiliser mixture is designed to provide an abundance of trace nutrients. The three products made from varying brands of commercial ammonium sulfate fertiliser were also highly characteristic, which may be attributed to the quality and purity of the products or contamination during the manufacturing process. The differences seen between the pure form products were likely caused by the process in which they were prilled. AN used within the mining industry would be processed differently to AN used within cold packs and so varying levels of trace contaminants would be expected.

**Table 4.3.** Average concentration (ppb) of elements within 200 mg of each AN product. (elements not detected in samples are labelled as n.d).

	<b>Elements</b>				
<b>Pure form AN</b>	B	Ti	Mn	Ni	Cu
<b>Chemical grade</b>	n.d	0.39 ± 39%	1.28 ± 2%	1.46 ± 12%	< 0.2
<b>Explosive grade</b>	n.d	0.95 ± 37%	1.73 ± 12%	7.32 ± 13%	< 0.2
<b>Cold pack</b>	n.d	3.14 ± 6%	2.07 ± 7%	6.08 ± 3%	< 0.2
	Se	Rb	Sr	Ba	U
<b>Chemical grade</b>	n.d	< 0.2	0.3 ± 7%	0.29 ± 43%	n.d
<b>Explosive grade</b>	n.d	< 0.2	1.19 ± 27%	1.83 ± 9%	n.d
<b>Cold pack</b>	n.d	0.61 ± 3%	2.88 ± 2%	1.28 ± 21%	n.d
<b>Homemade AN</b>	B	Ti	Mn	Ni	Cu
<b>Chemical grade</b>	6.88 ± 22%	221 ± 6%	106 ± 10%	28 ± 34%	6.14 ± 39%
<b>Richgro</b>	181 ± 7%	174 ± 6%	26.1 ± 6%	859 ± 12%	26.3 ± 7%



<b>Baileys</b>	114 ± 8%	204 ± 5%	262 ± 6%	2.05x10 <sup>3</sup> ± 10%	106 ± 10%
<b>SREDA</b>	250 ± 2%	156 ± 6%	14.3 ± 8%	7.66 ± 23%	10.8 ± 21%
<b>Black marvel</b>	355 ± 1%	304 ± 3%	8.34x10 <sup>4</sup> ± 3%	1.44x10 <sup>3</sup> ± 7%	2.54x10 <sup>4</sup> ± 5%
	Se	Rb	Sr	Ba	U
<b>Chemical grade</b>	n.d	0.82 ± 7%	146 ± 8%	39.7 ± 2%	n.d
<b>Richgro</b>	15.5 ± 6%	9.12 ± 4%	212 ± 8%	405 ± 3%	n.d
<b>Baileys</b>	24.9 ± 3%	9.97 ± 1%	229 ± 4%	372 ± 1%	0.32 ± 4%
<b>SREDA</b>	10.3 ± 5%	8.45 ± 3%	177 ± 2%	246 ± 4%	n.d
<b>Black marvel</b>	102 ± 6%	152 ± 3%	293 ± 3%	373 ± 2%	3.57 ± 2%

### 4.3.3 Source attribution of ammonium nitrate with chemometrics

It has been shown that a range of analytical techniques can provide some source information without additional interpretation or analysis. All techniques previously discussed were capable of identifying whether an unknown AN product was from a pure or homemade source, which is useful information that could be used within a forensic investigation. Furthermore, techniques such as SEM-EDS and IC could also identify a product prepared from an alternative fertiliser mixture, based on the presence of additional trace metals. However, further investigation is warranted to determine whether the source of each individual product can be identified. Three different techniques, ATR-FTIR, XRD and ICPMS, were subsequently used in combination with chemometrics to determine whether full discrimination of samples could be achieved. ICPMS showed the greatest potential for source attribution as the elemental profiles were highly characteristic. ATR-FTIR and XRD displayed less potential for source discrimination but are routinely used to analyse explosive residues, unlike ICPMS.

#### 4.3.3.1 Discrimination of ammonium nitrate by ATR-FTIR spectroscopy

Initial interpretation of the ATR-FTIR spectra indicated an observable difference between the pure form and homemade products. Even though products within each class could not be distinguished, subtle differences in peak height and position could be used in combination with chemometric techniques to provide further discrimination.

Spectral data of ten samples from each AN product was used for chemometric analysis. For each sample, a small amount of material was taken from the bulk product and analysed once, allowing for ten individual samples to be analysed. PCA was first performed on the data and 2-D scores plots were generated using the entire spectral region, followed by just the fingerprint region ( $1800 - 400 \text{ cm}^{-1}$ ). It was found that when the fingerprint region was used, the two classes that were formed were tightly clustered and appeared to be better separated across the principal component (PC) 1 axis (Figure 4.7). This was expected, as most of the variation appeared to be in this region when examining the individual spectra. Therefore, all further chemometric analysis was performed using only the  $1800 - 400 \text{ cm}^{-1}$  region.

As shown in Figure 4.7, the scores plot generated shows the distribution of sample data across the first two PCs, accounting for 89% of the total variation. Two distinct classes were observed; one containing the pure form products, and the other containing those that were homemade. These two classes were primarily separated on PC1 which accounts for 75% of the total variance, with no additional discrimination achieved across PC2. PCA was repeated on each class to see whether the individual brands and sources could be further discriminated, however, only a minor improvement in separation was seen (Figure 4.8). Within the pure form class, three sample clusters could be seen spread across PC2, causing some explosive and chemical grade samples to overlap with cold pack samples. A similar trend could be seen within the homemade class where two clusters containing Black Marvel and SREDA samples formed, however, most of the remaining clusters had a number of overlapping samples.

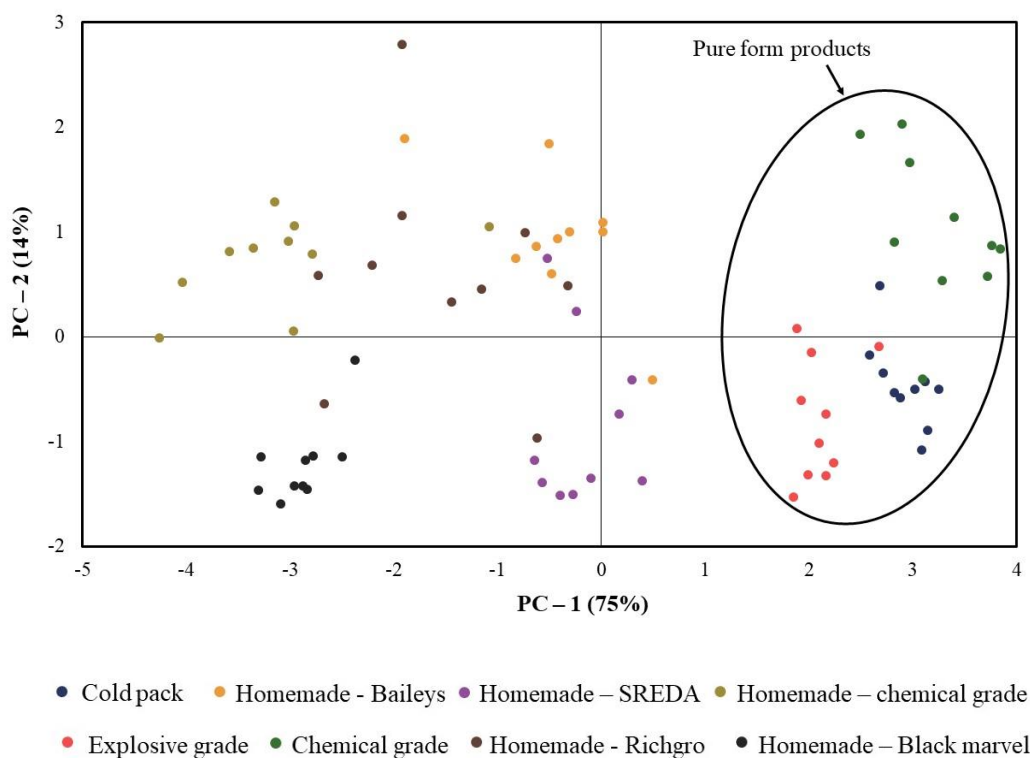


**Figure 4.7:** 2-D scores plot from PCA showing the distribution of samples using ATR-FTIR spectral data. The circled group contains all pure form products including the chemical grade, explosive grade and cold pack samples.

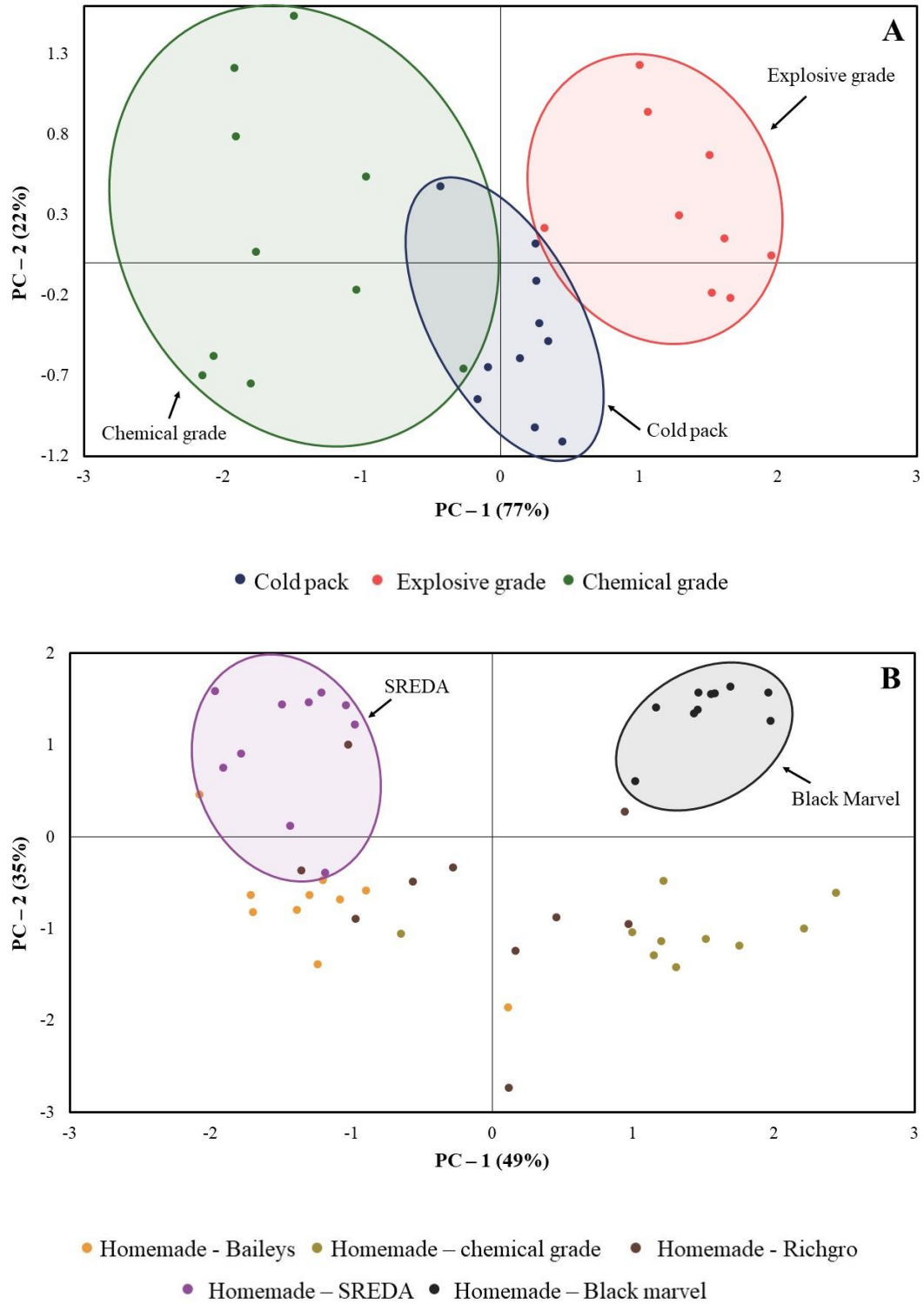


**Figure 4.8:** 2-D scores plot from PCA performed on the samples included in the pure form (a) and homemade (b) classes. Some sample clusters have been highlighted in each plot to show class discrimination.

Analysis of the factor loadings plot associated with PCA performed on the entire sample set highlighted which regions of the spectra contributed most to the separation across the different PCs (Figure 4.9). Most of the variation across PC1, which explains how the pure form and homemade products were separated, was attributed to the sulfate peaks present at 1083 and 620  $\text{cm}^{-1}$  within the homemade products. The plot displayed these peaks as having a strong negative correlation with PC1, which explains why all the pure form products were clustered together in the positive direction of PC1, due to the absence of these peaks.

Within each class, the samples were mostly dispersed across PC2 as a result of the minor variations in peak heights in the 1450 – 1300  $\text{cm}^{-1}$  region, which contains the characteristic ammonium and nitrate peaks. The minor spread observed could suggest that within each class, the products were of a similar purity. The variation on PC2 being attributed to the sample purity was supported by the opposing placement of the chemical grade and Black Marvel samples, which represented the highest and lowest purity forms of AN across the different products. The Black Marvel samples had a strong negative correlation to the characteristic peaks at 1328 and 1424  $\text{cm}^{-1}$ , indicating the samples were lower in purity, and therefore they clustered together in the negative direction of PC2.

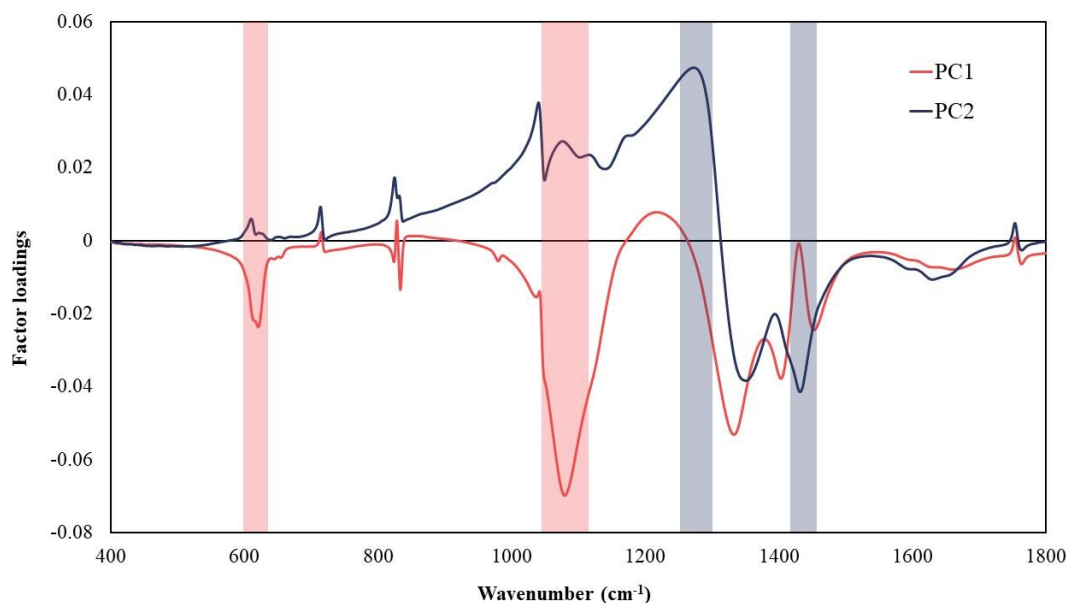


**Figure 4.9:** PC factor loadings plot for ATR-FTIR spectra acquired from the PCA performed on all AN products. Shaded areas indicate the regions which have strong contribution to the separation of samples across PC1 (red) and PC2 (blue).

To further evaluate the effectiveness of using spectral data to discriminate AN products, LDA was performed. Two approaches were taken to evaluate the predictive accuracy of the LDA model, but within both, LDA was conducted using the linear distance and first five PCs with equal probabilities assumed. Although no improvement in separation was seen within PCA when using additional PCs, it was found that using up to five PCs with LDA, which accounted for 99.4% of variation, resulted in additional discrimination between the homemade products (Figure A.11).

For the first approach, LDA was performed using each AN product as an individual class, thus generating a single discriminant function that was used to predict the source of samples from an independent dataset. This discriminant model returned a calibration accuracy of 92.5%. Only three of the samples within both the pure form and homemade classes were misidentified, which was in agreement with the overlapping of samples observed within the scores plot. These samples included two chemical grade and one explosive grade sample, which were all misidentified as being from a cold pack, and three Richgro samples, which were misidentified as being synthesised from chemical grade reagents or SREDA ammonium sulfate.

The model was then used to predict the source of 40 samples from an independent dataset, five from each AN product. It was found that 85% of samples had their source correctly predicted (Table 4.4). As expected, most incorrect classifications were obtained against the homemade class but were mostly attributed to the Richgro product. As seen in Figure 4.8b, the Richgro samples were clustered in the middle of the population density with a number of overlapping samples, resulting in a higher number of incorrect classifications.

The second method of analysis performed involved a stepwise approach. Firstly, a discriminant function was generated that predicted whether the sample was a pure form or homemade product. Repeated LDA was then used to predict the source of the AN product within each class. The effectiveness of this approach was then compared to the first method by predicting the source of the same 40 samples. It was found that this method of classification was very effective at predicting whether a sample was a pure form or homemade product, as all samples from the validation set were correctly assigned to either the pure form or homemade class.

When the specific origin of the samples was then predicted, the individual pure form and homemade models were able to correctly predict the source of 100% and 80% of the samples respectively (Table 4.5). The combined weighted average of this classification approach was 87.5%, which was a marginal improvement compared to classifying the samples with a single discriminant function. Although this approach was only moderately effective at predicting the brand of fertiliser used, the source of the pure form products could be identified. This could potentially be an important distinction within a forensic investigation, as sourcing and storing chemical or explosive grade AN may be illegal without the proper licenses, whereas possession of AN based cold packs is not.

**Table 4.4.** Number of correct vs incorrect classifications from the validation set using a five-PC LDA model with each AN product treated as an individual class.

<b>Class #</b>	<b>Pure form AN</b>	<b>Correct</b>	<b>Incorrect</b>	<b>% Correct</b>
<b>1</b>	Cold pack	4	1 (Predicted as class 3)	80
<b>2</b>	Explosive grade	5	0	100
<b>3</b>	Chemical grade	5	0	100
	Homemade AN			
<b>4</b>	Chemical grade	4	1 (Predicted as class 8)	80
<b>5</b>	Baileys	4	1 (Predicted as class 7)	80
<b>6</b>	Black marvel	5	0	100
<b>7</b>	SREDA	5	0	100
<b>8</b>	Richgro	2	3 (Predicted as class 4/5/7)	40
	Total			85



**Table 4.5.** Number of correct vs incorrect classifications from validation set using a stepwise five-PC model with each AN samples classified as either a pure form or homemade product before its source is predicted.

<b>Class #</b>	<b>Pure form AN</b>	<b>Correct</b>	<b>Incorrect</b>	<b>% Correct</b>
<b>1</b>	Cold pack	5	0	100
<b>2</b>	Explosive grade	5	0	100
<b>3</b>	Chemical grade	5	0	100
	Total			100
	Homemade AN			
<b>4</b>	Chemical grade	4	1 (Predicted as class 5)	80
<b>5</b>	Baileys	4	1 (Predicted as class 7)	80
<b>6</b>	Black marvel	5	0	100
<b>7</b>	SREDA	5	0	100
<b>8</b>	Richgro	2	3 (Predicted as class 7)	40
	Total			80
	Total average			87.5

Discriminant values (DVs) assigned to samples used for validation from the step-wise LDA approach are shown in Table 5.6. These values represent the distance measured between a given sample and the centroid of the group, indicating how well-separated a sample is from the classes it was not predicted as. All pure form samples were correctly predicted which was supported by the large differences observed in the discriminant values between classes. One Baileys sample was misclassified to class 7 (SREDA), however samples 5.3, 5.4 and 5.5 were not well-separated from the rest and were close to being classified within class 7 as well. Again, the Richgro class had the highest number of incorrect classifications, however, the samples were consistently misclassified as SREDA samples as opposed to the first validation approach where the misclassified samples were from three different classes.

The higher classification rate and more consistent separation observed within the discriminant values indicated that for this dataset, a stepwise LDA approach was more effective overall. However, if an unknown sample simply needed to be classified as being either pure or homemade, a single model approach could be used to achieve the same result.

**Table 4.6.** Discriminant values of samples within the independent data set used for validation. Discriminant values and predictions represent the products within Table 4.5. Shaded cells indicate correct (green) and incorrect (red) predictions.

Pure form products				
Correct class / Sample number	Discriminant values for each class			Predicted class
	1	2	3	
1.1	-2.6	-8.7	-19.9	1
1.2	-2.3	-7.7	-24.0	1
1.3	-4.0	-7.4	-29.4	1
1.4	-1.9	-9.4	-20.8	1
1.5	-4.6	-19.4	-11.2	1
2.1	-10.5	-2.3	-42.7	2
2.2	-12.3	-2.5	-46.4	2
2.3	-7.0	-6.7	-28.5	2
2.4	-13.5	-2.2	-47.6	2
2.5	-10.3	-2.5	-44.3	2

3.1	-22.3	-64.3	-8.3	3		
3.2	-10.2	-37.5	-4.0	3		
3.3	-81.8	-133.4	-32.2	3		
3.4	-47.3	-86.2	-14.6	3		
3.5	-17.4	-55.0	-2.7	3		
Homemade products						
Correct class / Sample number	Discriminant values for each class					Predicted class
	4	5	6	7	8	
4.1	-3.8	-14.5	-642.0	-30.0	-8.6	4
4.2	-9.9	-27.8	-701.0	-43.9	-23.8	4
4.3	-11.1	-10.5	-612.1	-19.5	-14.1	5
4.4	-5.2	-8.2	-633.6	-23.9	-5.8	4
4.5	-4.4	-12.2	-638.7	-26.0	-5.7	4

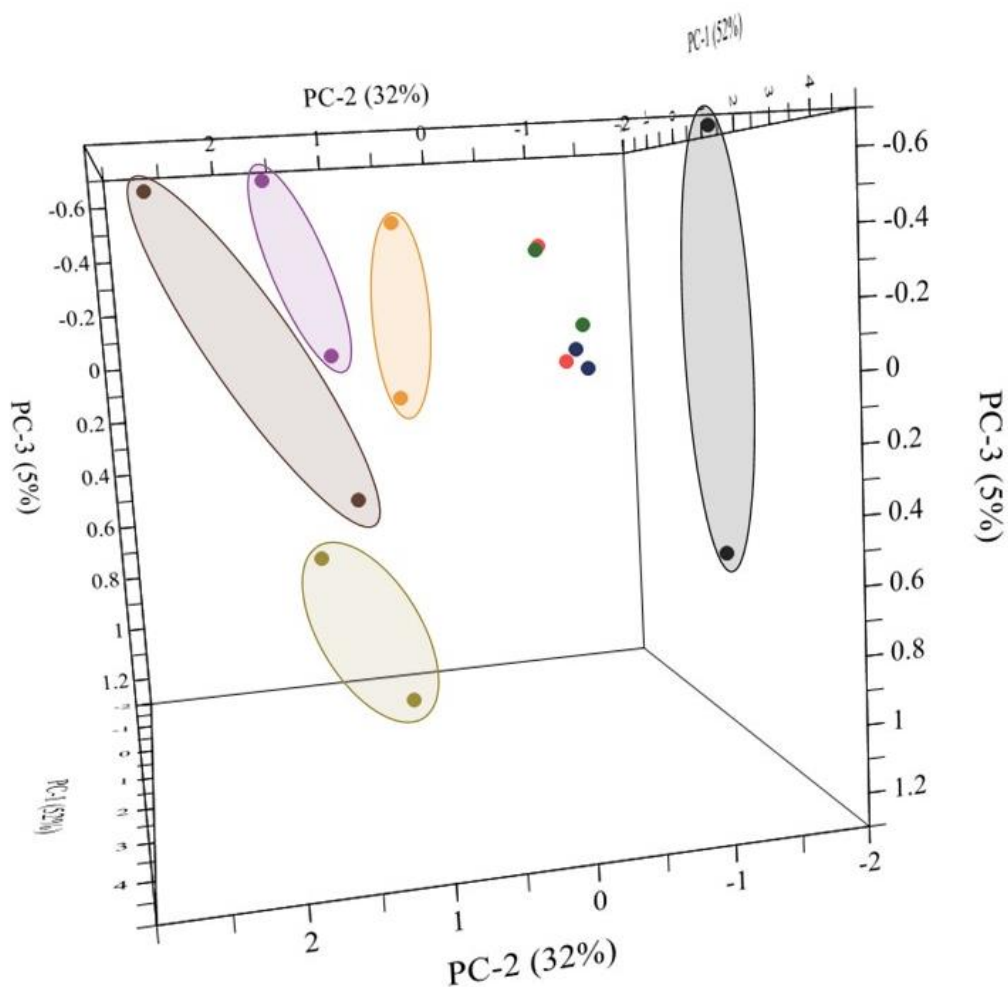
5.1	-100.0	-79.6	-508.6	-62.3	-98.6	7
5.2	-21.7	-4.5	-545.3	-6.4	-11.3	5
5.3	-27.0	-13.2	-533.7	-13.9	-25.3	5
5.4	-31.0	-17.8	-515.6	-18.5	-30.7	5
5.5	-17.6	-3.9	-575.2	-5.1	-10.0	5
6.1	-465.9	-417.8	-18.4	-382.6	-447.2	6
6.2	-465.8	-414.2	-17.9	-379.1	-443.3	6
6.3	-440.1	-386.7	-30.2	-354.9	-409.1	6
6.4	-460.8	-409.9	-18.9	-376.6	-435.2	6
6.5	-534.4	-477.4	-17.8	-435.7	-512.9	6

7.1	-28.0	-11.4	-544.7	-6.5	-19.9	7
7.2	-32.5	-13.6	-590.0	-8.8	-21.6	7
7.3	-34.6	-28.2	-591.9	-20.2	-34.6	7
7.4	-27.9	-16.6	-574.0	-8.0	-20.7	7
7.5	-19.8	-7.0	-597.3	-4.8	-11.3	7
8.1	-18.1	-23.0	-551.5	-12.6	-15.3	7
8.2	-14.6	-14.3	-547.8	-7.0	-10.6	7
8.3	-16.9	-5.4	-608.4	-4.4	-9.3	7
8.4	-10.3	-7.2	-589.8	-6.5	-3.6	8
8.5	-12.2	-4.1	-610.1	-5.4	-3.9	8

#### 4.3.3.2 Discrimination of ammonium nitrate using X-ray diffraction

Diffraction patterns collected from each AN product revealed notable differences between pure form and homemade products, but showed a high level of similarity within each class. This emphasises the advantage of performing subsequent chemometric analysis, as the minor variation between diffraction patterns could be utilised to provide additional discrimination. PCA was performed using the full X-ray diffraction patterns of two samples from each AN product. The pure form products appeared to form a tight cluster, whilst the homemade products were spread across the three PCs. As highlighted in Figure 4.10, each homemade product was grouped and appeared to be discriminated, however, there was a high spread between duplicate samples so the groups were not well defined. As XRD relies on the preparation of a flat, dry, homogenous sample of crystalline particles, minor variations in sample preparation that occurred one month apart may have introduced inconsistencies within the analysed sample, thus resulting in a high spread of data.

Interpretation of the diffraction patterns indicated that due to additional reflections present in the Richgro and SREDA products, these would likely be differentiated, however, this was not observed within the scores plot. Looking at the diffraction patterns of both Richgro samples, it was found that the extra reflection at  $17.5^\circ 2\theta$  was only present in one of the samples. This suggests that the amount of crystalline material responsible for the additional reflection may not be consistent across samples, which resulted in the high spread observed in the scores plot. Repeated PCA on the pure form products did not provide any additional discrimination, as the samples were highly spread out across the first two PCs (Figure 4.11). Similar to using spectral data in combination with PCA, XRD was capable of discriminating between the pure and homemade classes of products, however, could not differentiate samples within each class.



- Cold pack    ● Homemade - Baileys    ● Homemade – SREDA    ● Homemade – chemical grade
- Explosive grade    ● Chemical grade    ● Homemade - Richgro    ● Homemade – Black marvel

**Figure 4.10:** 3-D scores plot from PCA showing the distribution of pure form and homemade AN samples using X-ray diffraction patterns. Distribution of sample data shows distinct groupings of all homemade products while all pure form products are positioned in a single tight cluster.



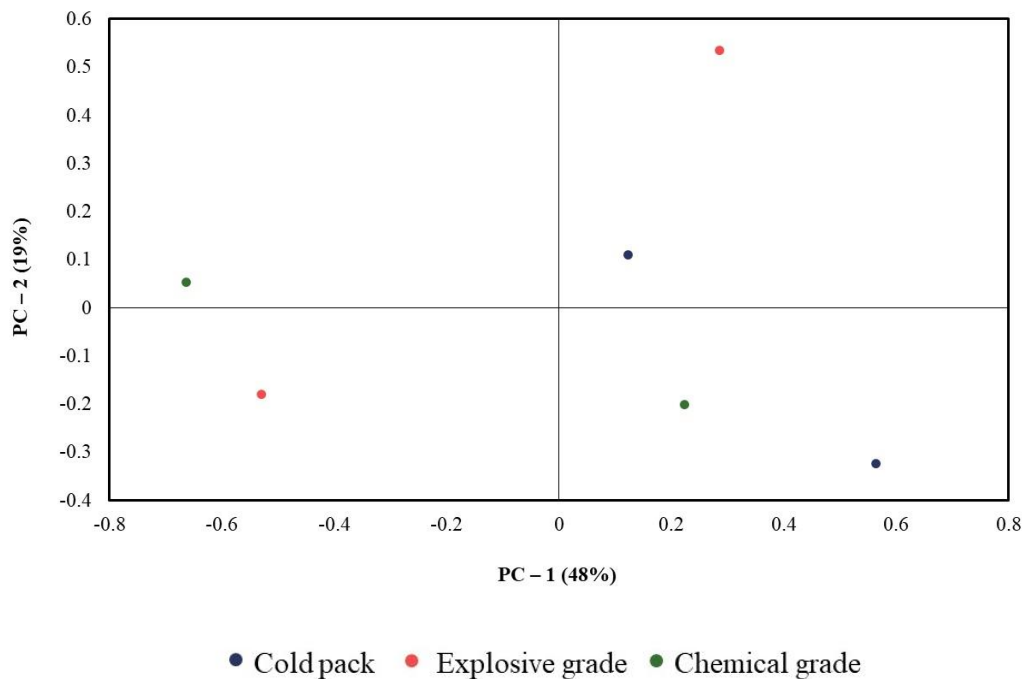


**Figure 4.11:** 2-D scores plot from PCA performed on the cluster of pure form AN samples. No additional discrimination was achieved with repeated PCA.

Interpretation of the 3-D scores plot and analysis of the factor loadings showed that separation of the pure form products was attributed primarily to  $31 - 35^\circ 2\theta$  (Figure 4.12). This region contained a large number of intense reflections in the homemade samples, whereas the pure form patterns contained only one. Within the 3-D scores plot, the pure form samples were located at the extreme negative regions of both PC1 and PC2. This aligns with the factor loadings plot, which shows the pure form samples negatively correlated with the highest intensity reflection across PC1, and positively correlated with the additional reflections observed within the homemade products. This suggests that if analysis was repeated, the two classes could potentially be separated using just this small region of the diffraction pattern.

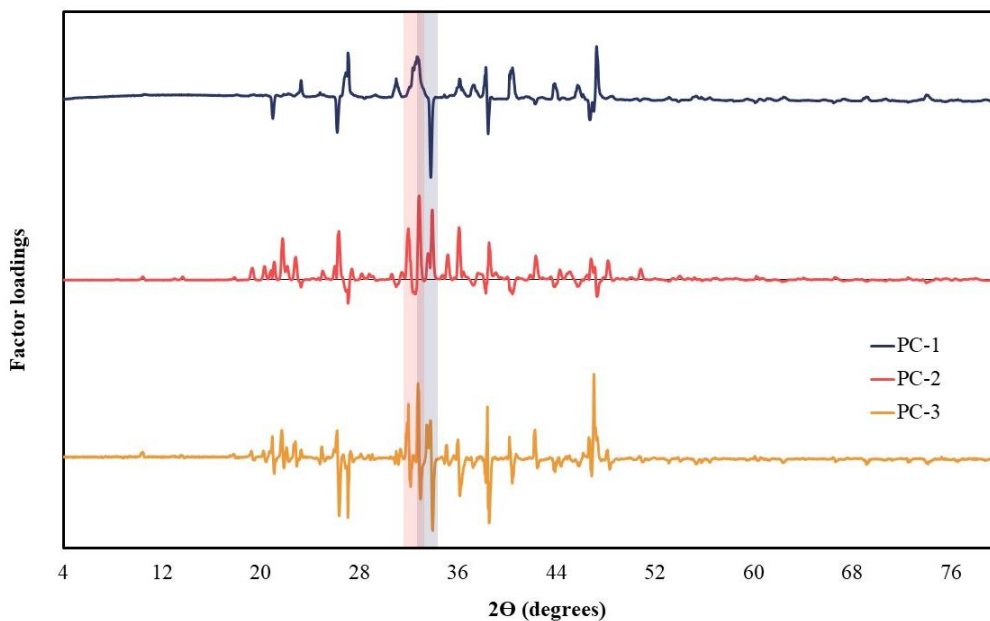


**Figure 4.12:** PC factor loadings plot for X-ray diffraction patterns acquired from PCA performed on all AN products. Shaded areas indicate the regions which have strong contribution to the separation of samples across PC1 (red) and PC2 (blue).

#### 4.3.3.3 Discrimination of ammonium nitrate using trace elemental data

Techniques such as ATR-FTIR and XRD are routine in explosive analysis due to their accessibility, simplicity and ability to effectively identify a range of explosive compounds. Although characterisation using these techniques revealed some source information of an unknown AN product, varying fertiliser brands and pure form sources could not be discriminated using spectral data or diffraction patterns. Therefore, to improve the source determination capabilities of AN as an explosive precursor, a technique is required that can detect the ultra-trace components within the fertiliser mixtures.

Chemometric analysis was performed to determine whether the variation observed within the elemental data obtained from ICPMS analysis could be used to discriminate between the AN products. PCA was performed using trace elemental data and the distribution of samples across three PCs is shown in Figure 4.13. PC1 accounted for 75% of the variation extracted from the samples, with a total variance of 97% across the first three PCs. A number of distinct sample groupings with extremely tight clustering were observed. Full separation was seen between the five homemade

products and the remaining three pure form products were grouped together in a single cluster as highlighted in Figure 4.13. This shows that while ATR-FTIR spectra and XRD patterns were not characteristic enough to discriminate between the homemade products, elemental data has the potential to discriminate between AN that was prepared from laboratory reagents, commercial products or even alternative fertiliser mixtures.

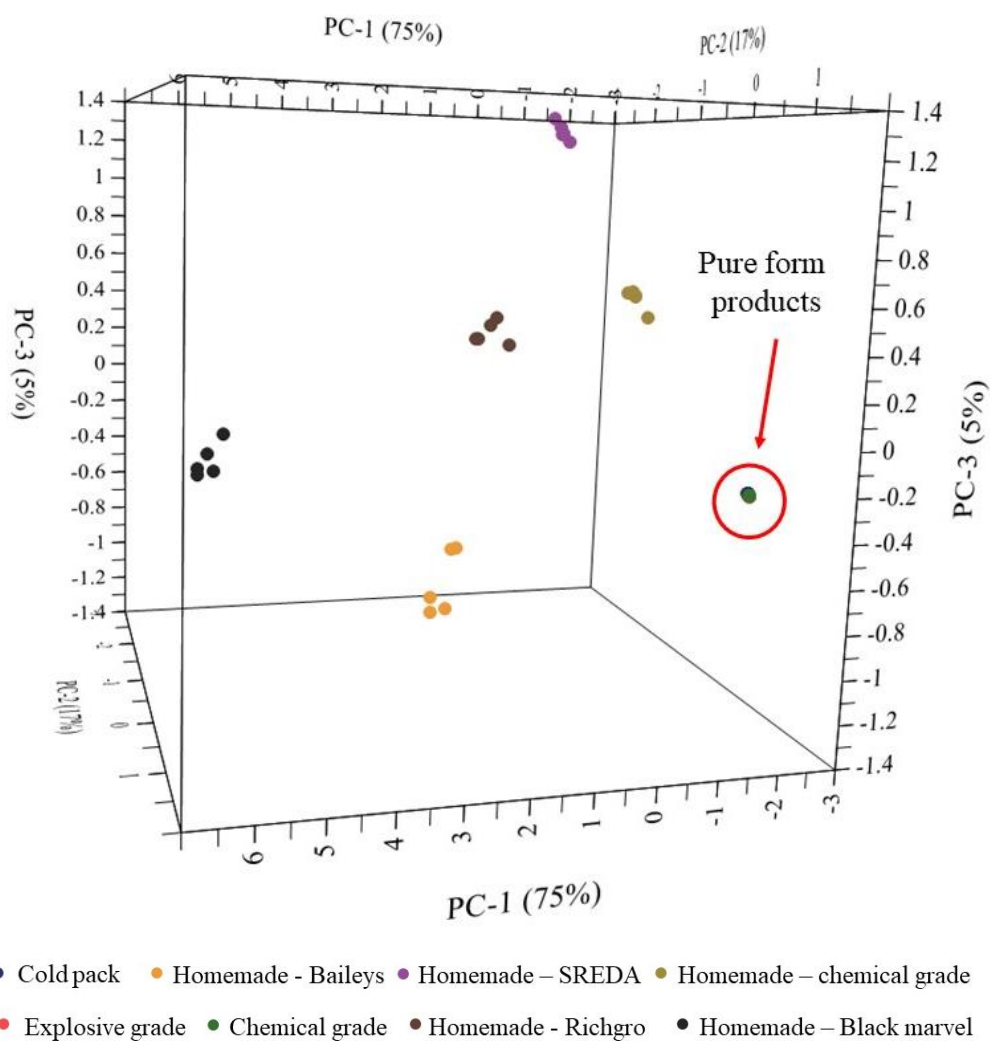


**Figure 4.13:** 3-D scores plot from PCA showing the distribution of pure form and homemade AN samples using trace elemental data. Distribution of sample data shows full discrimination of all homemade products and all pure form samples grouped together in a single tight cluster.

PCA was repeated on the cluster of pure form samples to observe how they were distributed across two PCs (Figure 4.14). Again, full separation was achieved between the pure form products using data from only five of the ten elements. Sample groups

were mostly separated across PC1, which accounts for 76% of the total variation. The explosive grade samples were spread across PC2; however, this was primarily caused by one of the five samples. Ultimately, the scores plot revealed that the pure form products could be discriminated using the variation extracted on PC1, with PC2 only appearing to have a strong contribution to separation due to the lone explosive grade sample.

Analysis of the factor loadings associated with the 3-D scores plot containing the entire data set revealed that all elements contributed almost equally to the separation of the homemade products, with the exception of nickel, which had a particularly large contribution to PC3 (Figure 4.15). The concentration of nickel was extremely varied between the homemade products, particularly between the three brands of ammonium sulfate. As displayed in Table 4.3, the SREDA samples contained trace amounts of nickel compared to the Richgro samples which contained approximately 300 times more.

Data from only five elements was used to achieve full discrimination between the pure form samples. Observation of the factor loadings showed that titanium, rubidium, and strontium contributed the most to the separation of the pure form samples. Rubidium was not detected in the chemical grade and explosive grade samples, and the concentration of titanium was notably higher in the cold pack samples. This variation allowed for the source attribution of each pure form product. These elements are likely attributed to contamination during manufacture, or variation within the finishing process, which involves prilling and granulation to convert the AN into a form suitable for storage and transport. Granulation determines the overall water content in the final product and prilling involves the addition of anti-caking agents, suggesting both processes could introduce the trace elements observed within the data. Barium appeared to have a strong contribution on the variation across PC2, however, this was caused by the lone explosive grade sample, as discussed earlier. This sample had five times the amount of barium compared to the other four explosive grade samples, which resulted in the increased spread observed across PC2.

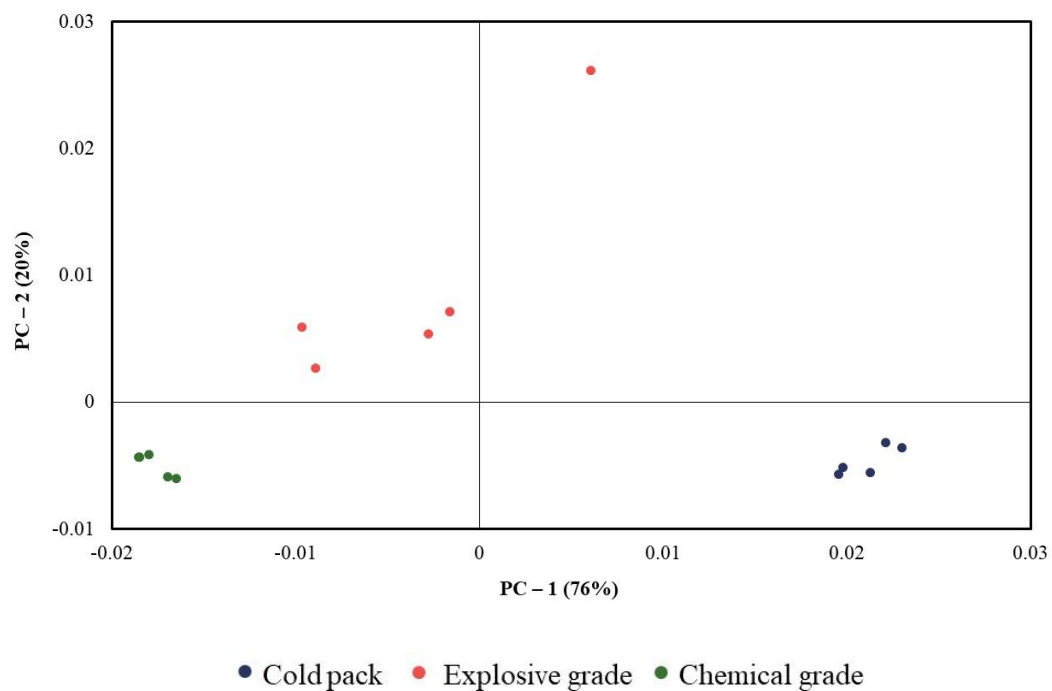


**Figure 4.14:** 2-D scores plot from PCA performed on the highlighted cluster of pure form AN samples in Figure 4.13. Repeated PCA allowed for the full discrimination of the pure form samples across 2 PCs.

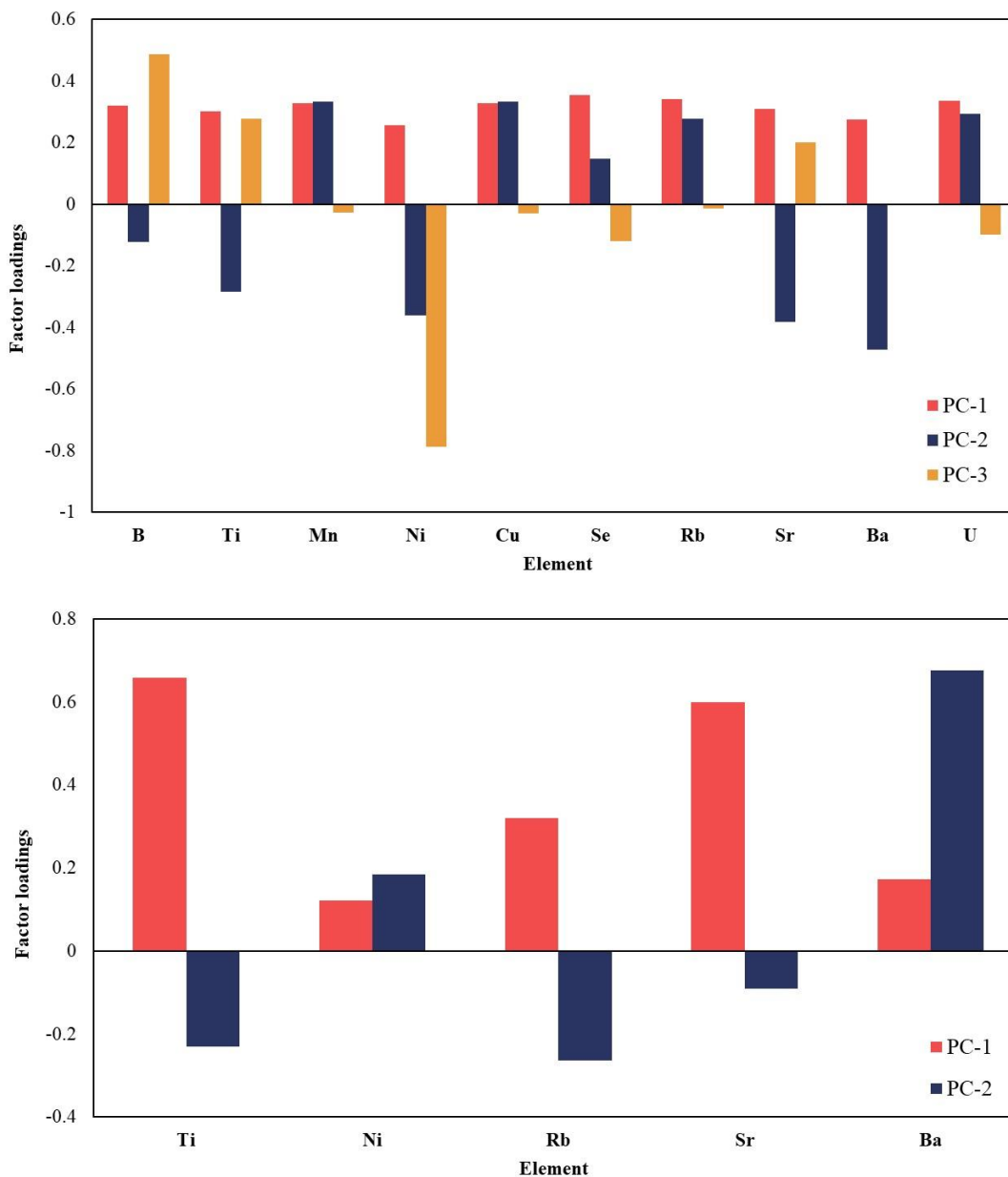


**Figure 4.15:** PC factor loadings plots for elemental data acquired from PCA performed on all AN products (top) and the pure form cluster (bottom).

LDA was subsequently used to determine if trace elemental data could be used to predict the source of an unknown AN product. LDA was conducted using the linear distance and first four PCs with equal probabilities assumed. As described in section 4.3.3.1, a similar stepwise approach was performed. As the pure form products could only be discriminated within their own class, LDA was performed where each homemade product was treated as an individual class and the pure form products were grouped together. This resulted in the model first predicting the specific source of the

sample if it was a homemade product, otherwise it was classified as a generic pure form product. LDA was then repeated on those in the pure form class, thus determining whether a sample was either chemical or explosive grade or from a cold pack. Due to the limited number of samples, an independent dataset could not be obtained to evaluate the model. Alternatively, a randomised ‘leave one out’ approach was adopted. This was not ideal as it could overestimate the model’s performance, however, it may provide an approximate assessment of the model’s predictive accuracy.

Results showed every model from the 20 iterations performed returned a 100% classification accuracy. Furthermore, the model correctly predicted the source of every sample across each iteration. Although the dataset used for validation was limited, results from PCA and LDA indicate that trace elemental data is extremely effective at discriminating AN products.

Comparable to using chemometrics with ATR-FTIR and XRD data, ICPMS can be used to distinguish between the pure form and homemade products. However, ICPMS can subsequently be used to identify whether an AN product is of chemical or explosive grade or from a cold pack, and can also specify the brand or mixture used in synthesis. Differentiating between these forms of AN is an important distinction within a forensic investigation and would provide additional evidence that could link seizures of AN.

#### **4.4 Conclusions**

This chapter provided a thorough investigation into the preparation, characterisation and source attribution of AN as an explosive precursor. Nine products were sourced and prepared from a range of commercial ingredients. It was found that although the purchase of highly pure AN is restricted in Australia, large amounts could either be obtained or prepared from commercially available products, such as cold packs and ammonium sulfate fertiliser.

Characteristic spectra, diffraction patterns and elemental profiles have been reported using a range of techniques. It was revealed that all were capable of distinguishing between pure and homemade AN. Therefore, given an unknown sample, some source information could quickly be determined using the methods described in this chapter.

Most techniques could also identify the sample prepared from alternative fertiliser mixtures, based on the presence of additional trace metals.

Source determination capabilities of ATR-FTIR, XRD and ICPMS coupled with chemometrics was also compared. PCA-LDA performed using spectral data was able to correctly predict the source of 100% of the pure form samples, but only 80% of those that were homemade, resulting in a total prediction rate of 87.5%. As ATR-FTIR spectroscopy is routine in explosives analysis and common in most laboratories, this work highlights its potential for providing additional source information beyond identifying a seized sample as AN. PCA performed with XRD data was also able to differentiate between pure and homemade products.

PCA-LDA performed with trace elemental data was able to fully discriminate all AN products across two models, using the concentrations from ten elements. Substantial variation between elements such as nickel, manganese and copper were used to discriminate between the homemade products, while the trace differences observed in Ti, Ni, Rb, Sr and Ba were used to differentiate between the pure form products. Although a limited dataset was used, repeated LDA resulted in a 100% source prediction rate. These results illustrate that different grades of AN as well as varying brands of fertiliser can be differentiated based on elemental profiles.

As this research was conducted in Australia, products, brands and sources of AN will differ internationally. However, the methodologies, characteristic data and chemometric findings presented in this chapter provides an understanding of how to analyse alternatively sourced AN, as well as the amount and type of source information that can be obtained using a range of techniques. This research also bring attention to how easy it can be for an individual to prepare a large amount of AN, and highlights the potential products that may be used. This is not only beneficial to the current forensic intelligence of AN as an explosive, but will also aid future forensic investigations of seized AN of unknown origin.



## **Chapter 5. Investigations into the preparation and source attribution of homemade urea nitrate and nitrourea explosive**

A portion of this chapter has been published as followed:

Joshua A. D'Uva, David DeTata, Ryan Fillingham, Robert Dunsmore, Simon W. Lewis. Synthesis and characterisation of homemade urea nitrate explosive from commercial sources of urea. *Forensic Chemistry* **2021** 26, 1-9 DOI: <https://doi.org/10.1016/j.forc.2021.100369>

## 5.1 Introduction

The white crystalline salt urea nitrate (UN) is an energetic salt composed of the uronium cation and nitrate anion that has comparable chemical properties to ammonium nitrate (AN) (218-220). It is insensitive to friction, impact, and shock whilst being relatively safe and easy to prepare compared to other organic or peroxide-based explosives (1). It can also easily be prepared in ‘back-yard’ or clandestine laboratories with minimal training and knowledge of chemical synthesis. These characteristics explain its ongoing preparation and use by criminal and terrorist groups in a global context (221). UN has been linked to numerous explosive attacks, most notably the 1993 World Trade Centre bombings, and is a commonly used explosive throughout Israel and Palestine (34, 221). UN can further react with commercially available sulfuric acid to form the explosive compound nitrourea (NU); a precursor to several high energy density materials (HEDMs) that exhibit high detonation capabilities (1, 76-79).

UN is like AN as both are fertiliser-based explosives that can be prepared from commercial products (2, 184, 222). It can be synthesised in large quantities by the simple addition of nitric acid (prepared from commercial ingredients) to urea, a common garden fertiliser. As discussed in Chapter 4, imposed restrictions have limited commercial access to high purity forms of AN, including AN fertilisers. In contrast, urea fertiliser is unregulated and is sold in a wide variety of retail stores. Other products containing urea such as instant cold packs or diesel exhaust fluid (DEF), are also readily available and can be used to prepare homemade UN. This increases the potential of UN to become the preferred choice as a homemade explosive (HME).

Most published studies of UN have focussed on improving and developing detection methods, as identifying UN in pre- and post-blast residues can be difficult and complex (116, 117). Numerous studies have investigated the colorimetric and fluorescence detection of trace UN with p-dimethylaminocinnamaldehyde (p-DMAC) to improve the rapid detection of UN on-site (221, 223-225). Recent work has further modified the technique by using hydrogels (226, 227). Pre-blast UN has been characterised by analytical techniques including X-ray diffraction (XRD) and infrared and Raman spectroscopy (220, 228-230). Liquid chromatography (LC) (116), gas chromatography (GC) (117) and mass spectrometry (MS) have also been used for the

identification of UN (231-235). However, these detection methods do not necessarily provide information about the urea source. As commercial urea products continue to be sold without restrictions, the characterisation and identification of different urea sources warrants immediate attention.

Oxley *et al.* reported a comprehensive study on the characterisation and discrimination of UN from NU (75). UN was analysed using spectroscopic and chromatographic methods, reporting distinct spectra, physical properties, and fragmentation patterns. The chemical characterisation of UN significantly contributes to the forensic intelligence of UN as a HME and improves the capacity of personnel to successfully recover and identify seized UN to generate investigative leads and establish connections within a criminal investigation. However, only UN that had been prepared from chemical grade urea was investigated. Aranda *et al.* explored the source determination of UN synthesised from urea fertiliser, using isotopic ratio mass spectrometry (IRMS) to link synthesised UN to the batch of urea fertiliser used based on the carbon and nitrogen isotope compositions (236). The study indicated that IRMS could be used to link synthesised UN to urea or nitric acid reactants, warranting subsequent investigations into the source attribution of UN from alternative urea sources not yet explored.

Although characteristic information from some forms of UN has been reported, initial stages of this research discovered that little is known about the sources and synthesis of homemade UN. A review of the literature and discussions with several laboratories and forensic agencies within the Forensic International Network for Explosive Investigations (FINEX) revealed that there is a fundamental lack of knowledge and awareness surrounding UN as an explosive. Knowledge of how UN can be commercially sourced and synthesised and determining whether UN prepared from different products can be linked back to its urea precursor could provide significant aid to criminal and terrorist investigations. Therefore, the research presented in this chapter was a direct response to the forensic need to gain a better understanding of UN.

This research began with conducting a thorough investigation into how UN can be sourced and prepared from commercial products available within Western Australia (WA). The practicality of preparing large amounts of explosive grade UN from

different sources was also explored. Additional aims involved characterising UN products using a range of analytical techniques and determining whether they can be traced back to the initial precursors used. The characterisation and source attribution of NU from alternatively prepared UN was also explored. This information provides a major contribution to the forensic intelligence of explosives and lays the groundwork for the methodologies and procedures adopted within future forensic investigations involving UN and NU.

## 5.2 Experimental

### 5.2.1 Sources of urea

Eight unique sources of urea were used within this study to prepare UN. These included chemical grade urea, three different urea fertiliser brands, urea cold packs, DEF and two alternative fertiliser mixtures. Apart from chemical grade urea, all urea products were sourced and purchased from a variety of local Australian retail stores (Figure 5.1).

Chemical grade urea was purchased from a chemical supplier in the form of white translucent crystalline shards (Figure 5.1a). Three urea fertilisers were purchased in bulk 1 – 10 kg bags from various commercial hardware and garden stores. These fertilisers contained urea in pellet form and only differed by their manufacturer, an example of which is shown in Figure 5.1b. Each urea fertiliser contained a minimum of 98.5% urea with the addition of various trace impurities according to the manufacturer's details. Urea cold packs were purchased from a pharmacy, each containing approximately 100 g of urea pellets (Figure 5.1c). No information could be found on the purity of these pellets. Penrite AdBlue DEF (1L) was purchased from an automotive parts store. AdBlue consists of a clear colourless aqueous urea solution (32.5% w/w) (Figure 5.1d) and can typically be purchased in 1 – 10 L containers. No information could be found on the type or purity of the urea used to prepare the solution.

Many other fertiliser products contain urea nitrogen and have the potential to be used to prepare UN. Two alternative fertiliser mixtures were chosen for this study; Total All-Purpose Osmocote and Green Boost Soluble Fertiliser (Figure 5.1e-f). These were

chosen as they contained a high percentage of urea nitrogen compared to other products, with Osmocote and Green Boost containing 15.2% and 17.4% urea nitrogen respectively. The safety data sheet (SDS) for the Osmocote mixture lists a 30-60% urea content as well as potassium sulfate, AN, mono ammonium phosphate, sulfur and an assortment of sulfate salts (237). Other components of Green Boost fertiliser include potassium nitrate, potassium sulfate, mono ammonium phosphate and a range of trace metals (238).



**Figure 5.1:** Urea products used to prepare UN: (a) chemical grade urea, (b) fertiliser urea, (c) cold pack urea, (d) DEF, (e) Osmocote fertiliser mixture, (f) Green Boost fertiliser mixture.

### 5.2.2 Preparation of urea nitrate products

Urea nitrate synthesis from different sources is described in Chapter 2, section 2.3.2. The precursor sources and average yield information is summarised in Table 5.1 below.

**Table 5.1:** Source and yield information of UN samples used throughout this study.

<b>Source of urea</b>	<b>Supplier/brand</b>	<b>Yield (%)</b>
<b>Chemical grade</b>	Chem Supply, USA	92
<b>Fertiliser – Richgro</b>	Richgro, AUS	90
<b>Fertiliser – Baileys</b>	Baileys fertiliser, AUS	95
<b>Fertiliser – SREDA</b>	SREDA garden products, AUS	94
<b>Urea cold pack</b>	Medi-Ice Pak, AUS	85
<b>Diesel Exhaust Fluid</b>	Penrite AdBlue, AUS	83
<b>Osmocote fertiliser</b>	Scotts, AUS	~50
<b>Green Boost fertiliser</b>	Manutec, AUS	~50

### 5.2.3 Infrared spectroscopy

Spectral analysis of the UN products was performed using the method outlined in Chapter 2, section 2.4.1. Analysis was repeated until ten spectra were collected from each UN product. The same method was repeated one week later with another five spectra from each product being collected, which was used for validation purposes within chemometric analysis.

### 5.2.4 Raman spectroscopy

Raman spectroscopy was performed using the method outlined in Chapter 2, section 2.4.2. Samples were viewed with a 20x objective and excited at 785 nm with 10% laser power. Spectra were collected for each UN product using the same scan parameters.

### 5.2.5 Ion chromatography

Ion chromatography (IC) was performed using the instrument and method outlined in Chapter 2, section 2.4.3. Samples were prepared by dissolving UN (10 mg) in MilliQ water (10 mL) and diluted to a final concentration of 100 ppm.

## 5.2.6 Scanning electron microscopy

Scanning electron microscopy (SEM) was performed using the instrument and method outlined in Chapter 2, section 2.4.4. Before mounting onto a sample stub (carbon tab on 12mm aluminium pin mount) the UN samples were dried in an oven at 40 °C overnight to ensure no moisture was present. Back scattered electron (BSE) images were collected, and elemental analysis was performed on selected areas across the samples as well as a bulk analysis of the entire sample area.

## 5.2.7 X-ray diffraction

XRD was performed using the instrument and method outlined in Chapter 2, section 2.4.6. Before mounting onto a silicon zero background plate (ZBP) the UN samples were dried in an oven at 40 °C overnight to ensure no moisture was present. Each UN product was prepared and analysed in duplicate approximately one month apart to account for synthesis and instrument variability.

## 5.2.8 Inductively coupled plasma mass spectrometry

Inductively coupled plasma mass spectrometry (ICPMS) was performed using the instrument and method outlined in Chapter 2, section 2.4.7. Samples were prepared for analysis by adaptation of the procedure outlined by Brust *et al.*, which details the preparation of AN for elemental analysis (73). UN (200 mg) was dissolved in 70% nitric acid (3 mL) in a 20 mL polypropylene tube. The sample was heated in an oven at 90 °C for 2 hours. MilliQ water was added to a total volume of 10 mL. Prior to analysis, samples were diluted 10 and 100-fold and blanks of the MilliQ water, nitric acid, diluter, and sample procedure were also prepared.

## 5.2.9 Chemometrics

### 5.2.9.1 Chemometric analysis using spectral data from infrared spectroscopy

Principal component analysis (PCA) and linear discriminant analysis (LDA) was performed using the method described in Chapter 2, section 2.4.8.1. The classification set contained ten replicate spectra from each UN product. An independent dataset used to validate the models generated by LDA contained five replicate spectra from each

UN product. A single model and stepwise classification approach was evaluated using the same data sets, as detailed in section 5.3.3.1.

#### 5.2.9.2 Chemometric analysis using X-ray diffraction patterns

PCA was performed using the method described in Chapter 2, section 2.4.8.2. The dataset contained two samples from each UN product.

#### 5.2.9.3 Chemometric analysis using elemental concentration data from ICPMS

PCA-LDA was performed using the method described in Chapter 2, section 2.4.8.3. From the 58 elements analysed, six (Mn, Co, Ni, Rb, Sr and Ba) were retained for chemometric analysis. The classification set contained five samples from each UN product. Discriminant models for source prediction were generated using a randomised leave-one-out approach as described.

## 5.3 Results and discussion

### 5.3.1 Preliminary assessment of urea nitrate prepared from urea

Initial aims of this chapter were to identify how UN can be sourced and prepared. Although having similar explosive characteristics to AN, little research on UN as a HME has been reported. Unlike AN, UN cannot be sourced in its pure form, apart from purchasing small amounts from a chemical supplier. Therefore, if an individual or group wanted to prepare a UN based improvised device, they would need to prepare it from commercial ingredients. To aid future forensic investigations and personnel involved in explosive casework, it is crucial to know how UN can be commercially prepared and understand the practicality of an individual being able to covertly prepare large amounts of explosive grade UN.

The preparation of UN from different urea sources could be performed using the same procedure detailed in Chapter 2, section 2.3.2.1, apart from DEF and the alternative fertiliser mixtures. As DEF is comprised of urea pre-dissolved in water, the initial dissolution step could be avoided. The Osmocote and Green Boost fertiliser mixtures are comprised of an assortment of pellets containing a variety of compounds and so the solution is filtered prior to nitration to remove any undissolved solids. Preparing UN from chemical grade and fertiliser grade urea resulted in the greatest yields, which



was to be expected due to the increased purity of the starting material. Preparation from DEF was the most efficient method but resulted in a slightly lower yield. This is due to the concentration of the initial solution, as typically a ~46% urea solution is formed before nitration, yet DEF contains 32.5% urea by weight. As nitric acid can be directly added to a container of DEF without any prior steps, it could be labelled as a one-pot reaction, making it ideal for an individual with little knowledge of chemical synthesis. The yield could also be improved if a small amount of solution was evaporated prior to nitration. The percentage yield from the alternative fertiliser mixtures was low in comparison to other sources due to the lower percentage of urea and additional extraction process; therefore, more starting material and time would be required to prepare a comparable amount of UN when using other products such as fertiliser urea of cold packs.

No notable differences regarding the visual appearance of the UN products were observed, apart from the alternative fertiliser mixture samples. UN prepared from two separate batches of Osmocote purchased at different times resulted in a slight blue and yellow tint observed in the final products respectively (Figure 5.2). The Green Boost product also presented as bright green. The yellow and blue products were successfully prepared multiple times from their respective mixtures; however, it should be noted that later samples of UN prepared from Osmocote purchased post-November 2020 gave the distinctive blue product. From the date that the original Osmocote product was purchased, the manufacturer has potentially altered the formulation of the minor components, which has resulted in a different coloured product. This may be a response to the availability of additives or could be a permanent modification to the product.

The product formed from the Green Boost fertiliser was uniquely green and had a highly characteristic spectrum. As examination of its physical appearance and spectra could easily discriminate it from the other products, it was omitted from subsequent characterisation and chemometric analysis (Figure A.12). The yellow Osmocote product was initially characterised with several techniques and included in the post-blast experiments detailed in Chapter 6. However, as it could not be consistently reproduced using other Osmocote mixtures purchased post November 2020, it was omitted from subsequent chemometric analysis and nitrourea experiments.

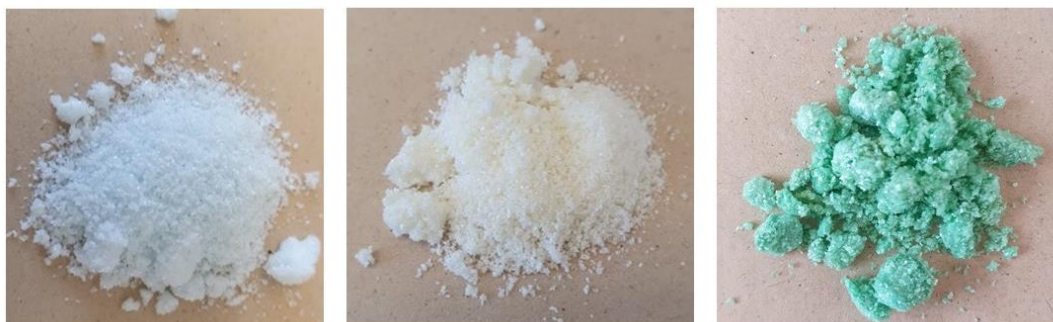


**Figure 5.2:** UN prepared from different fertilisers containing urea: from left to right, Osmocote purchased in May 2020, Osmocote purchased in November 2020 and Green Boost fertiliser.

### 5.3.2 Chemical characterisation of urea nitrate

Within a forensic investigation, multiple techniques may be employed to positively identify an unknown explosive sample as homemade UN. However, this can only be achieved if the analytical results can be compared to existing reference data that is characteristic to a specific type of UN. This section aims to provide a collection of characteristic data from homemade UN prepared from alternative urea sources, which will contribute to the analysis and identification of seized UN within casework.

#### 5.3.2.1 Infrared and Raman spectroscopy

Characteristic spectra of each UN product were collected by attenuated total reflectance Fourier transform infrared (ATR-FTIR) spectroscopy. Figure 5.3a highlights the spectrum of UN prepared from chemical grade urea, which contained peaks consistent with those observed in literature. The strong bands around  $3360 - 3407\text{ cm}^{-1}$  and  $3202 - 3250\text{ cm}^{-1}$  were assigned to  $\text{NH}_2$  antisymmetric and symmetric stretching respectively. It is suggested that the characteristic broad peak at  $2418\text{ cm}^{-1}$  was due to hydrogen bonding between the uronium cation and nitrate anion,  $\text{C}=\text{O}\cdots\text{H}\cdots\text{ONO}_2$  (75, 229). The remaining peaks were assigned as follows,  $1706\text{ cm}^{-1}$  ( $\text{C}=\text{O}$  symmetric stretch),  $1571\text{ cm}^{-1}$  (N-H angular deformation),  $1429\text{ cm}^{-1}$  (C-N),  $1313\text{ cm}^{-1}$  ( $\text{NO}_3^-$  asymmetric stretch) and  $894\text{ cm}^{-1}$  ( $\text{NO}_3^-$  out-of-plane deformation) (36, 229).

Spectra of the remaining samples were consistent with the chemical grade sample and showed little variation (Figure 5.3b). The most notable difference was seen in the

sample prepared from the Osmocote fertiliser (blue product), as there was a minor peak present at  $1150\text{ cm}^{-1}$ . This was most likely representative of a sulfoxide stretch (S=O) from several sulfate salts that were present in the starting material and persisted throughout the synthesis of the UN product.

The Osmocote mixture was investigated further to determine if the urea could be isolated. The mixture contained nine distinct pellet/rock types that differed by their size, colour, and texture (Figure 5.4a). Each type of pellet was analysed using ATR-FTIR spectroscopy and it was discovered that two were primarily urea (Figure 5.4b). Compared against chemical grade urea, spectra from the spotty and brown pellet are almost identical (Figure 5.4). This suggests that even though the Osmocote mixture contains various chemicals, urea can be isolated and used to prepare UN with a higher yield and purity as opposed to using the bulk mixture. This process would be more complex and requires additional knowledge than other methods discussed, however, it would be extremely challenging for forensic personnel to trace suspected UN to a specific urea product if prepared in this way.

Results show that infrared (IR) spectroscopy can effectively confirm the presence of UN regardless of the type of urea used. However, IR spectra do not provide enough chemical information that could be used to identify the precursor products used during synthesis. Nevertheless, presence of a sulfate peak could infer that a product was prepared from an alternative fertiliser mixture, which could be supported by subsequent confirmatory analysis.

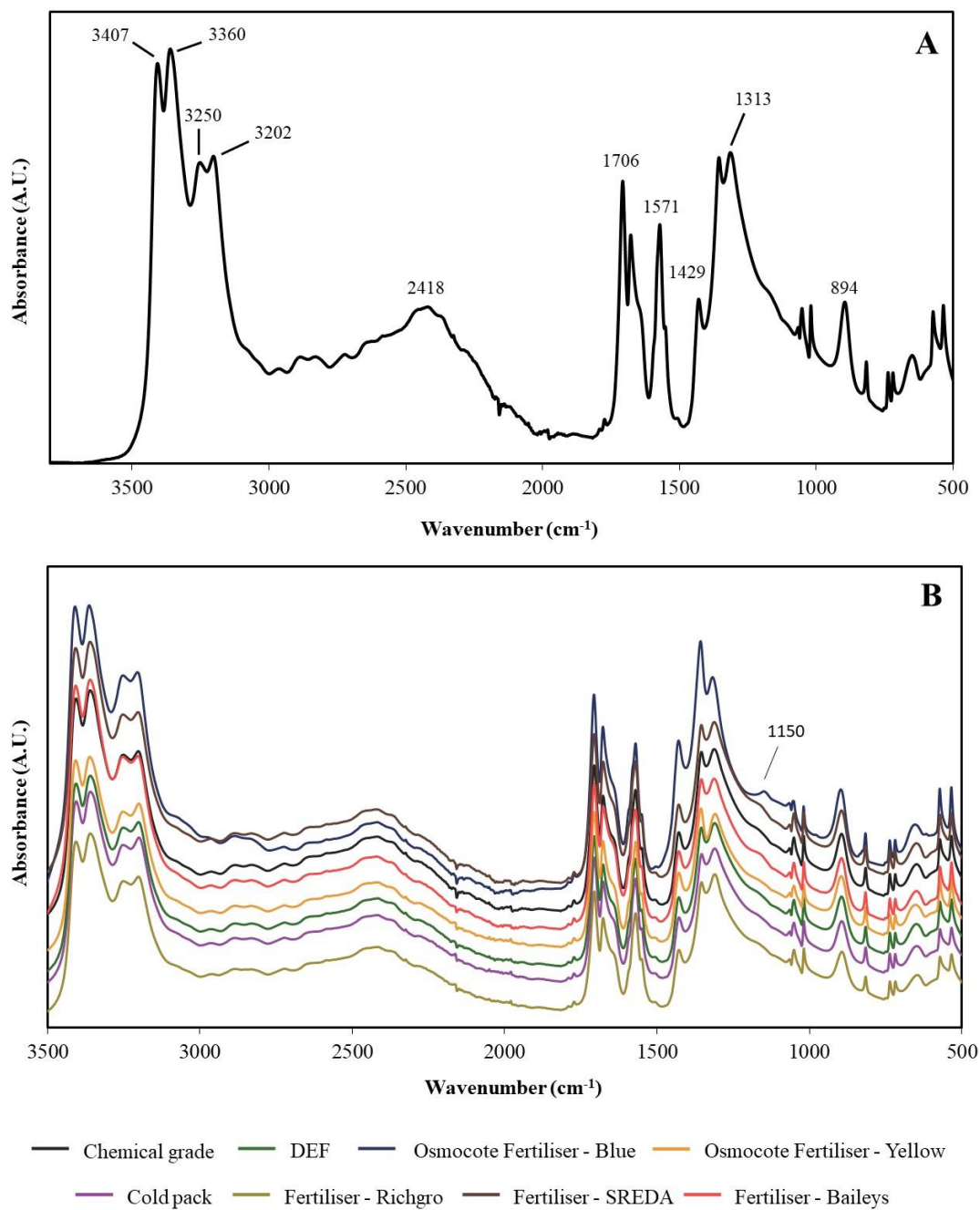


**Figure 5.3:** ATR-FTIR spectra of UN prepared from chemical grade urea (a) and overlay of all UN samples (b) (baseline has been offset for better visualisation of individual spectra). Labelled peak in (b) suggests presence of sulfate within product prepared from Osmocote fertiliser.

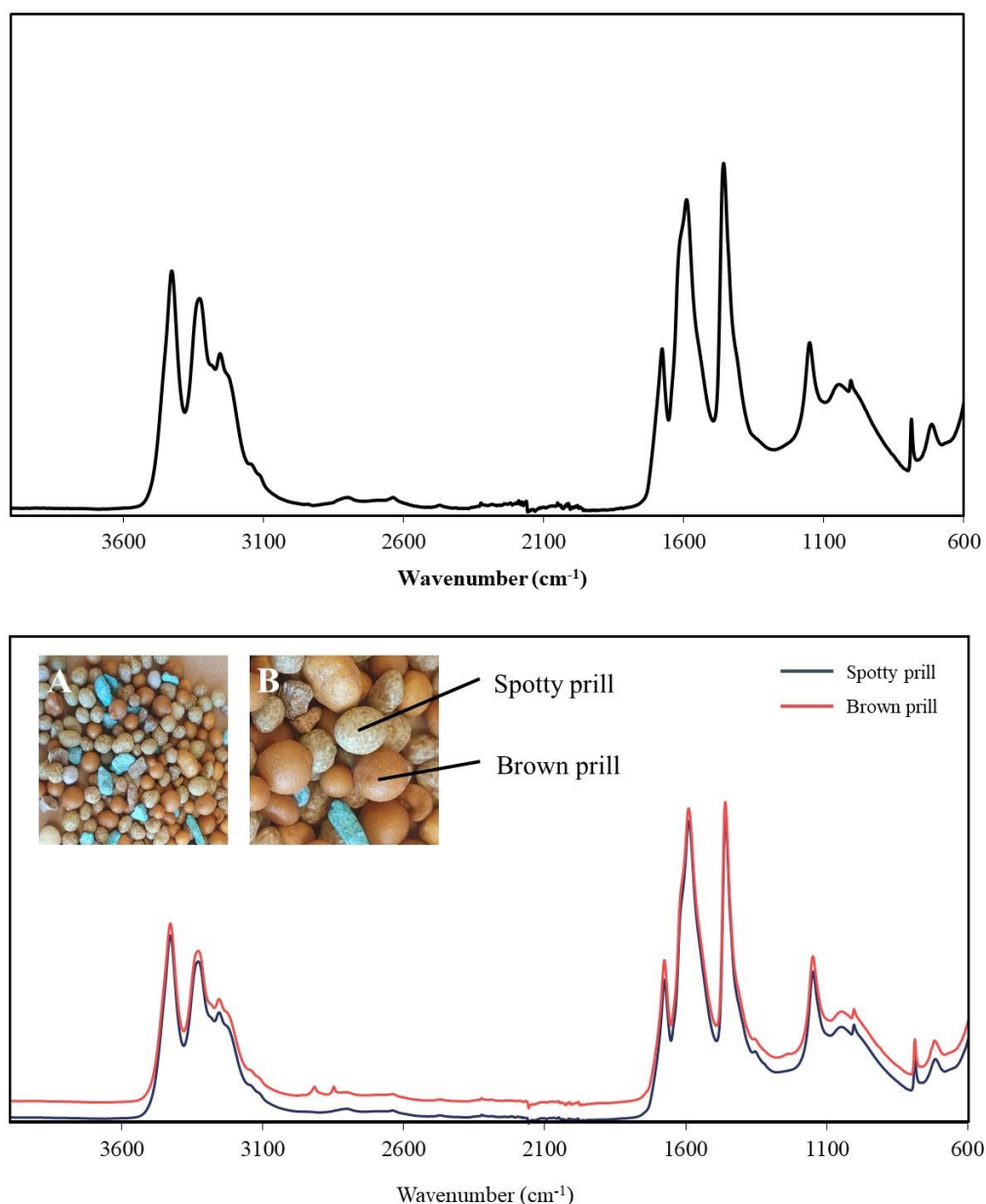


**Figure 5.4:** ATR-FTIR spectra of chemical grade urea (top) and select pellets from the Osmocote fertiliser mixture (bottom). A sample of the mixture (a) and the two pellets primarily composed of urea is shown (b).

UN products were analysed using Raman spectroscopy with spectra shown in Figure 5.5. Comparable to IR analysis, no notable difference was observed between spectra, all being representative of chemical grade UN (Figure 5.5a). The most prominent peaks at  $1020\text{ cm}^{-1}$  and  $1058\text{ cm}^{-1}$  are attributed to the urea and nitrate ions respectively. The peak at  $1020\text{ cm}^{-1}$  is also present in the Raman spectra for urea and has been assigned to the C-N symmetric stretch (75). The peak at  $1058\text{ cm}^{-1}$  is attributed to symmetrical stretching vibrations of the nitrate ion (75, 239). Other

notable peaks are those between 500 – 800  $\text{cm}^{-1}$ . Previously reported spectra have shown this region to contain three peaks (75), however, spectra collected in this study coincides with that reported by Li *et al.* (230). The peak at 534  $\text{cm}^{-1}$  was assigned to deformation of the C-N bond and the peaks at 573  $\text{cm}^{-1}$  and 722  $\text{cm}^{-1}$  are assigned to NCO deformations and in-plane bending of the nitrate ion respectively. All identifiable peaks were present throughout the samples; the only variation seen was within the intensity of the peaks at 1020  $\text{cm}^{-1}$  and 1058  $\text{cm}^{-1}$ . Raman spectroscopy could only confirm the presence of UN, and not provide further indication of potential precursors used in its synthesis.

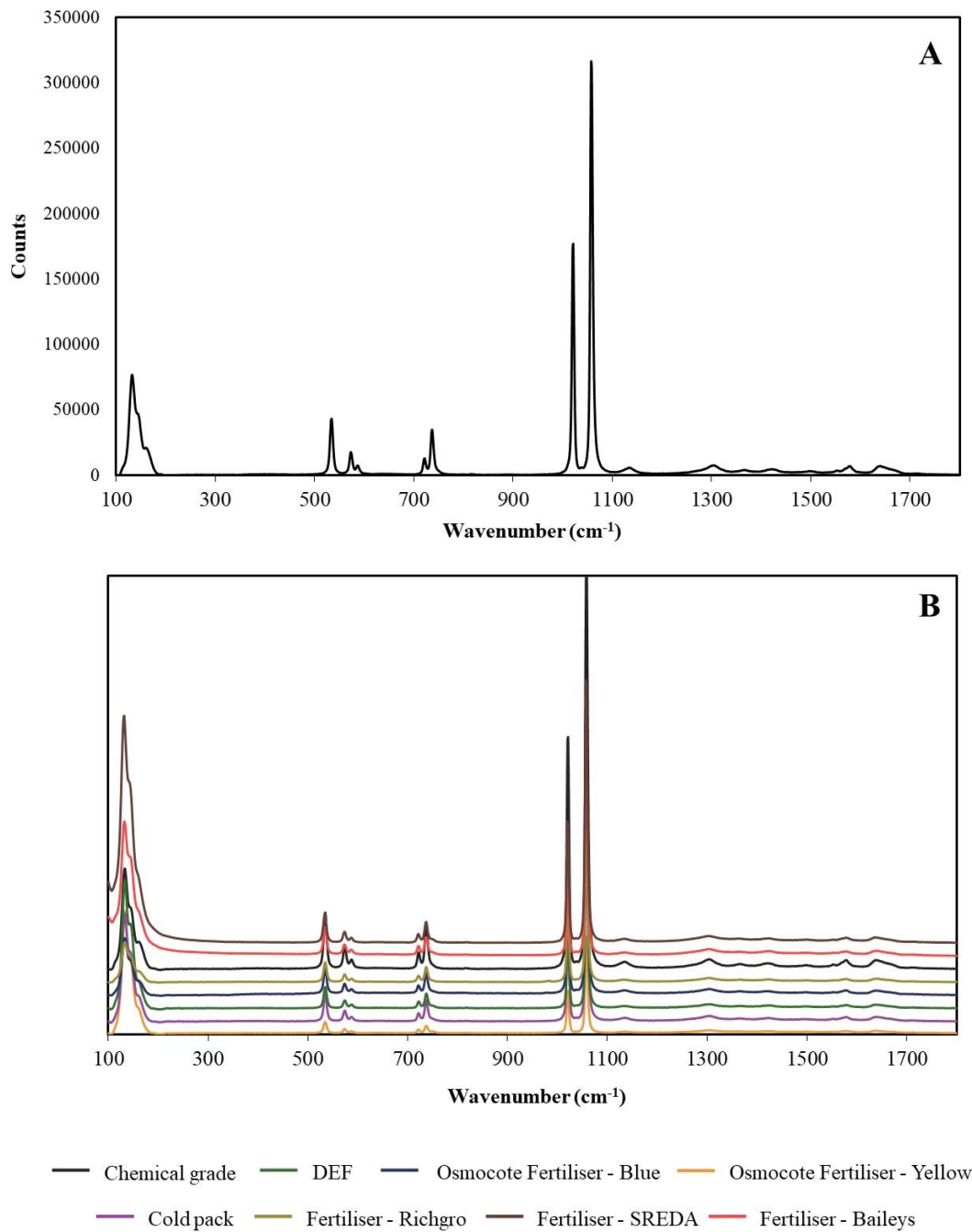


**Figure 5.5:** Raman spectra of UN prepared from chemical grade urea (a) and overlay of all UN products (b) (baseline has been offset for better visualisation of individual spectra).

### 5.3.2.2 Scanning electron microscopy

All UN samples were analysed by SEM energy dispersive X-ray spectroscopy (EDS) to provide bulk morphology, which could be used to distinguish between different precursor materials. The UN prepared from chemical grade, urea fertiliser, cold packs and DEF appeared consistent in their morphology and composition (Figure 5.6a-f). The only observable difference was in the samples prepared from Osmocote fertiliser. The BSE images of the Osmocote samples show the particle morphology as large flat sheets with bright spots scattered throughout the bulk material (Figure 5.6g and 5.6h). Bulk elemental analysis of these samples indicated the presence of iron, potassium, magnesium, sulfur, manganese, phosphorus, calcium, and sodium. This is indicative of various salt compounds that originate from the initial Osmocote fertiliser mixture. Elemental analysis of the individual bright spots revealed the same elements at much higher levels. This shows that UN prepared from Osmocote will contain an assortment of salts and metals that are distributed throughout the bulk material. Although SEM-EDS can be used to discriminate the Osmocote samples, subsequent elemental analysis is necessary to detect the trace impurities present that could be used to discriminate between the remaining samples.



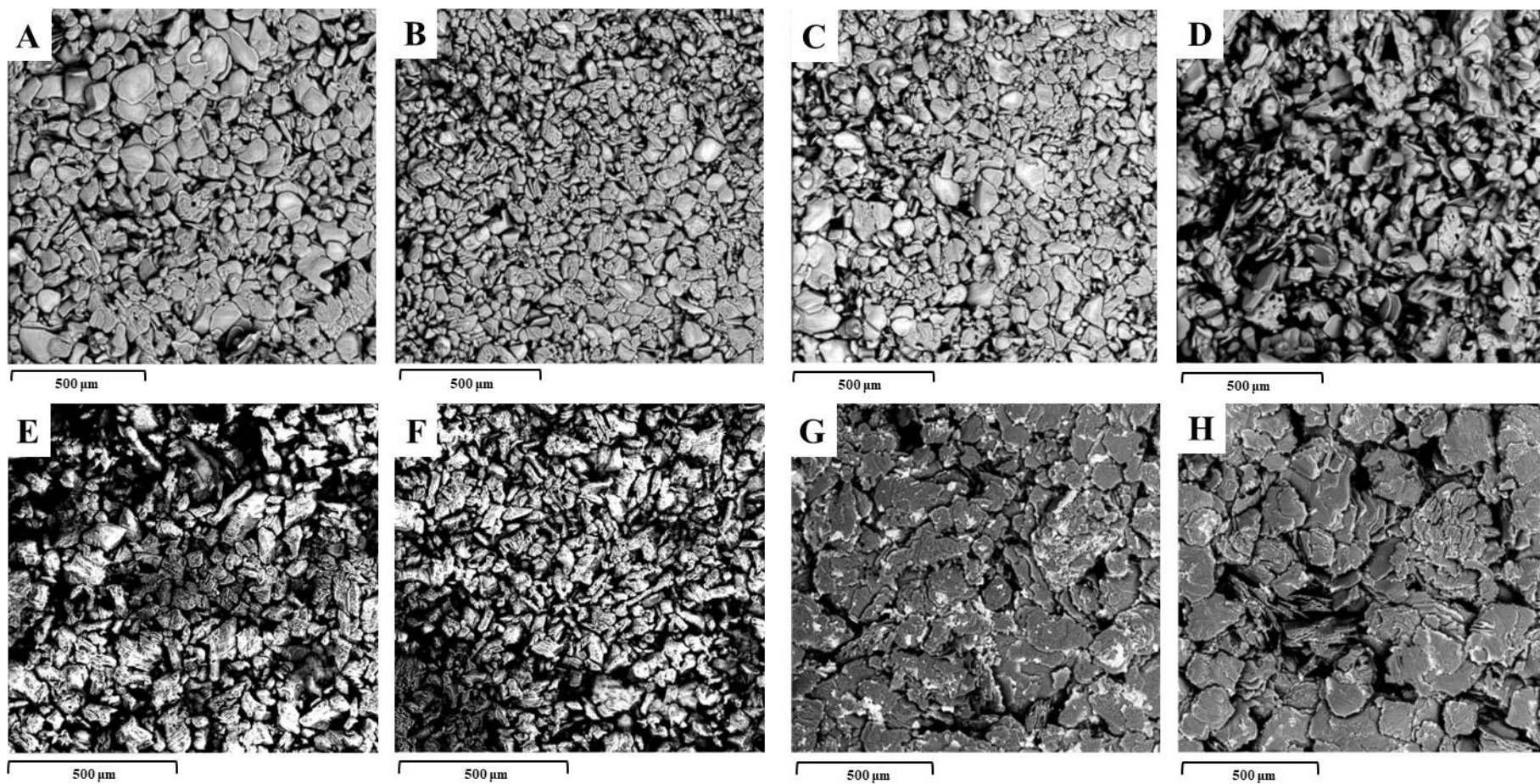


**Figure 5.6:** SEM BSE image of UN products: chemical grade (a), cold pack (b), DEF (c), Richgro fertiliser (d), SREDA fertiliser (e), Baileys fertiliser (f), Osmocote (blue product) (g), Osmocote (yellow product) (h).

### 5.3.2.3 X-ray diffraction

Characterisation of the UN products by XRD revealed no discernible difference between diffraction patterns (Figure 5.7). No reference patterns for homemade UN were found in literature, making this the first study to report characteristic diffraction patterns for pure and alternatively sourced UN. The intense reflection at  $33.5^\circ$   $2\theta$  was comparable to the highest intensity reflection in the diffraction pattern for ammonium nitrate reported in Chapter 4, section 4.3.2.4. This peak was likely attributed to the nitrate ion and may confirm the presence of crystalline UN. XRD was shown not to be useful in discriminating between UN products, however, the reported patterns can be used as a comparable reference to support the identification of an unknown explosive sample suspected to be UN.

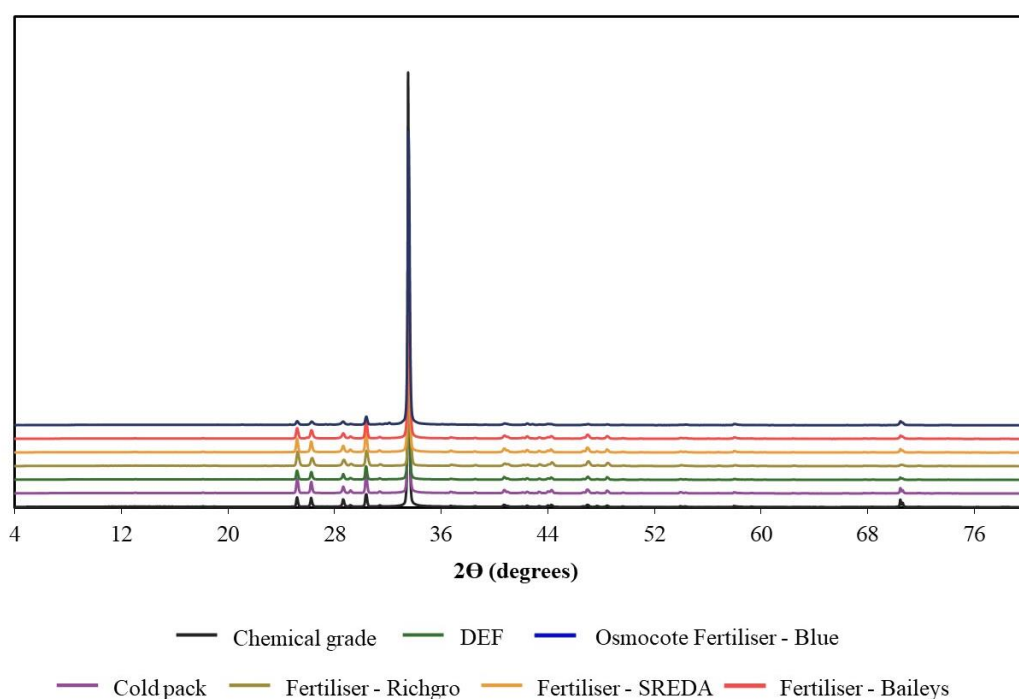


**Figure 5.7:** X-ray diffraction pattern of all UN products (baseline has been offset for better visualisation of individual patterns).

### 5.3.2.4 Ion chromatography

IC was used to determine the concentration of a range of cations and anions within the UN products. The cations that were analysed include  $\text{Li}^+$ ,  $\text{Na}^+$ ,  $\text{NH}_4^+$ ,  $\text{K}^+$ ,  $\text{Mg}^{2+}$ ,  $\text{Ca}^{2+}$ ,  $\text{Sr}^{2+}$  and  $\text{Ba}^{2+}$ . The anions that were analysed include  $\text{Cl}^-$ ,  $\text{ClO}_2^-$ ,  $\text{NO}_2^-$ ,  $\text{ClO}_3^-$ ,  $\text{NO}_3^-$ ,  $\text{SO}_4^{2-}$ ,  $\text{S}_2\text{O}_3^{2-}$  and  $\text{ClO}_4^-$ . Apart from the obvious presence of nitrate, all products contained small amounts of sodium, potassium, and calcium (Table 5.2). The Osmocote samples also contained a large amount of sulfate, which agrees with previous spectroscopic analysis and so could be discriminated from other samples. Although the blue product contained a notably higher amount of sulfate and potassium than the yellow product, more information would be required to accurately discern between them. These results are similar in comparison to the data presented from SEM-EDS analysis, as a sample prepared from an alternative fertiliser mixture can be identified. However, no additional discriminatory information can be obtained that would assist in identifying the remaining samples.

**Table 5.2:** Concentration of cations and anions (ppm) in 10 mg of UN prepared from different sources (ions not detected in samples are labelled as n.d).

Source of urea	Ionic species				
	$\text{Na}^+$	$\text{K}^+$	$\text{Ca}^{2+}$	$\text{Mg}^{2+}$	$\text{SO}_4^{2-}$
<b>Chemical grade</b>	3.6	< 5	< 2	n.d	n.d
<b>Fertiliser – Richgro</b>	5.2	< 5	< 2	n.d	n.d
<b>Fertiliser – Baileys</b>	1.9	< 5	< 2	n.d	n.d
<b>Fertiliser – SREDA</b>	1.8	< 5	< 2	n.d	n.d
<b>Urea cold pack</b>	4.5	< 5	< 2	n.d	n.d
<b>Diesel exhaust fluid</b>	3.6	< 5	< 2	n.d	n.d
<b>Osmocote – Blue</b>	3.9	12	< 2	< 2	27
<b>Osmocote – Yellow</b>	3.6	7.7	< 2	< 2	13

### 5.3.2.5 Inductively coupled plasma mass spectrometry

The concentrations of 58 elements in UN samples were determined by ICPMS. After initial analysis of the data, six elements were retained for further examination after those present due to contamination or detected at concentrations below the calibration range were removed. Isotope selection was also performed to minimise potential interferences and to assist in data reduction. Table 5.3 summarises the average concentration of elements found within five samples from each UN product. Analysis of the retained elements shows that like previous techniques, discrimination of the Osmocote samples is easily achievable. A large amount of manganese was detected in both Osmocote samples as well as trace levels of rubidium that were not detected in other products. UN prepared from DEF can also be identified by the large concentration of nickel present. It is possible that the water used to prepare the DEF contains trace amounts of nickel as nickel sulfate, or rather the urea used is of a lower quality than what is found in fertiliser urea, which could be a more refined product.

There is little variation between the chemical grade, cold pack, and fertiliser samples. The products prepared from Baileys and SREDA urea have a higher concentration of nickel compared to the Richgro product, however there is only minor variation within other elements. The observed differences across the products would primarily be a result of how the urea is commercially processed and the trace contaminations present within different manufacturing facilities and locations.

Similar to previous techniques, the Osmocote samples can be identified, however, ICPMS can additionally identify a UN sample that has been prepared from DEF. Furthermore, as minor variations can be observed across the products, subsequent statistical and chemometric analysis may lead to the discrimination and identification of the remaining products.

**Table 5.3:** Average concentration (ppb) of detected elements within 200 mg of UN products.

	<b>Elements</b>					
<b>Source of urea</b>	<b>Mn</b>	<b>Co</b>	<b>Ni</b>	<b>Rb</b>	<b>Sr</b>	<b>Ba</b>
<b>Chemical grade</b>	0.86 ± 7%	1.67 ± 5	7.95 ± 3%	< 0.2	0.58 ± 54%	4.95 ± 5%
<b>Fertiliser – Richgro</b>	0.92 ± 8%	0.17 ± 3%	8.65 ± 19%	< 0.2	0.50 ± 10%	0.50 ± 21%
<b>Fertiliser – Baileys</b>	2.84 ± 9%	0.41 ± 16%	47.2 ± 21%	< 0.2	0.56 ± 38%	1.64 ± 35%
<b>Fertiliser – SREDA</b>	2.33 ± 7%	0.28 ± 8%	80.1 ± 9%	< 0.2	0.74 ± 12%	2.24 ± 20%
<b>Urea cold pack</b>	1.47 ± 5%	0.14 ± 4%	18.1 ± 6%	< 0.2	0.65 ± 40%	1.86 ± 15%
<b>Diesel exhaust fluid</b>	1.41 ± 4%	0.16 ± 8%	316 ± 5%	< 0.2	0.55 ± 37%	19.3 ± 9%
<b>Osmocote – Blue</b>	8150 ± 5%	13.8 ± 4%	66.0 ± 5%	16.7 ± 5%	11.2 ± 4%	5.93 ± 37%
<b>Osmocote – Yellow</b>	9690 ± 6%	25.0 ± 7%	74.4 ± 12%	14.7 ± 6%	4.19 ± 14%	5.01 ± 5%

### 5.3.3 Source attribution of urea nitrate using chemometrics

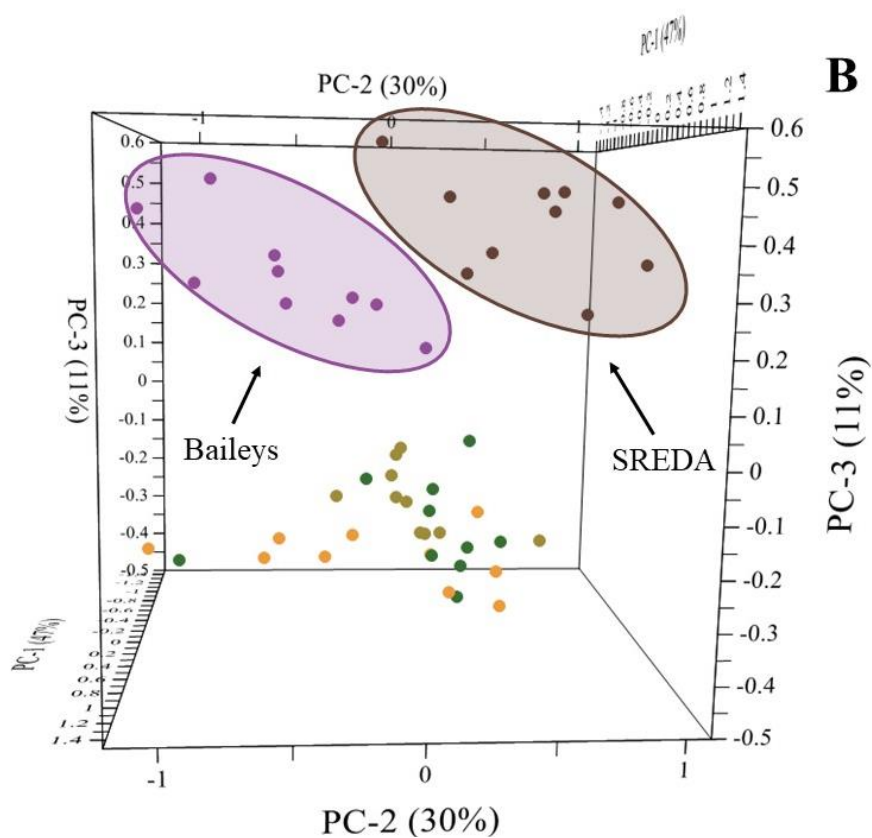
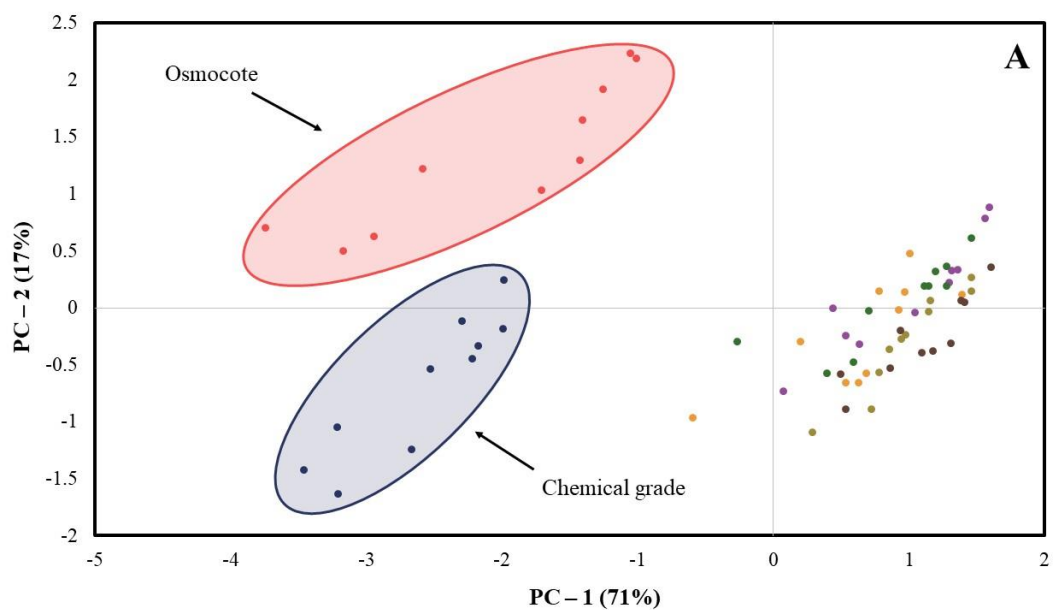
Although beneficial to the forensic intelligence of UN as an explosive, characterisation of the UN products with a range of techniques provided little discriminatory information in relation to the precursor source. The product prepared from Osmocote could be identified with most analyses performed, and the DEF product was discerned with elemental data; however, no further discrimination was achieved through visual assessment of the data. Chemometric analysis was therefore performed as the latent variation within the data may reveal additional source information. Chemometric analysis of the data from ATR-FTIR, XRD and ICPMS was performed to determine whether full discrimination of samples could be achieved. This also allowed a direct comparison between using characteristic data from ATR-FTIR and XRD, two routine techniques in explosive analysis, and ICPMS, which is not routinely used but showed the greatest potential for source attribution based on the highly diverse profiles observed.

#### 5.3.3.1 Discrimination of urea nitrate by ATR-FTIR spectroscopy

As outlined in section 5.3.2.1, ATR-FTIR spectra collected revealed no notable difference between UN samples upon visual interpretation apart from the sample prepared from Osmocote Plant Food. Although only one sample could be discriminated, subsequent analysis with PCA-LDA could provide additional discriminatory information based on the trace differences in the peak height and positions. Spectra from ten samples of each UN product were used for chemometric analysis. PCA was first performed using the entire spectral region and just the fingerprint region ( $1800 - 400 \text{ cm}^{-1}$ ). The 2-D scores plots generated revealed no differences in clustering or separation between these two approaches and so the entire spectral region was used for all further chemometric analysis.

The 2-D scores plot shows the distribution of samples across the first two principal components (PCs), accounting for 88% of the total variance (Figure 5.8a). Three clusters have formed, with the chemical grade and Osmocote samples discriminated from the remaining samples across PC1. These two classes are also separated from each other across PC2, highlighting that some discrimination is initially achieved. Repeated PCA on the large cluster containing five of the seven classes resulted in the

discrimination of another two classes, including the Baileys and SREDA fertiliser samples. These samples are separated primarily across PC2 and PC3. Discrimination of the Osmocote product was predictable due to the noticeable difference in the IR spectra, however, no observable difference could be seen across the remaining products. This additional discrimination achieved highlights the effectiveness of using chemometrics in combination with spectral data. As IR spectroscopy is routine in explosive analysis and commonplace in many laboratories, this method could be used as a rapid means of eliminating potential sources of seized UN, therefore narrowing down possible lines of inquiry before subsequent chemical analysis is performed.



- Chemical grade    ● Cold pack    ● Diesel exhaust fluid    ● Osmocote Plant Food
- Urea fertiliser - Richgro    ● Urea fertiliser - SREDA    ● Urea fertiliser - Baileys

**Figure 5.8:** Scores plot from PCA showing the distribution of UN samples using ATR-FTIR spectral data: 2-D scores plot with all UN samples (a) and 3-D scores plot of sample cluster (b). Highlighted groups in both plots show separated classes.



Analysis of the factor loadings across both score plots highlights which regions of the spectra contribute most to the separation of samples across PCs 1-3. Discrimination of the chemical grade and Osmocote samples across PC1 is mostly attributed to the peaks associated with the ammonium ion at 3400 and 1400  $\text{cm}^{-1}$  (Figure 5.9a). These two classes themselves are separated across PC2, which is primarily attributed to the characteristic nitrate ion peak at 1300  $\text{cm}^{-1}$ . As these samples are grouped based on the minor variation observed in this region, this implies that separation across PC2 is based on the relative purity of the sample. This is evident as these two classes likely represent the highest and lowest purity forms of UN within the sample set, which has resulted in them being distinguished from the remaining samples.

Figure 5.9b represents the factor loadings associated with the 3-D scores plot of the unresolved cluster (Figure 5.8b). The variance appears to mainly be distributed across PC1 and PC2, however the minor contributions from PC3 resulted in the discrimination of another two fertiliser brands/sources. The Baileys and SREDA fertiliser classes are separated across PC3, which is associated with the minor variation between the characteristic ammonium and nitrate peaks. Again, these peaks show a strong correlation across PC3, suggesting that the Baileys and SREDA product is of a higher purity than the Richgro fertiliser product. Different fertiliser manufacturers would have unique sources of contamination due to a combination of location, source of urea and prilling processes, which will result in a final product of varying purities. PCA was repeated once more on the three remaining classes, which include the DEF, cold pack and Richgro samples, however no additional discrimination was achieved.

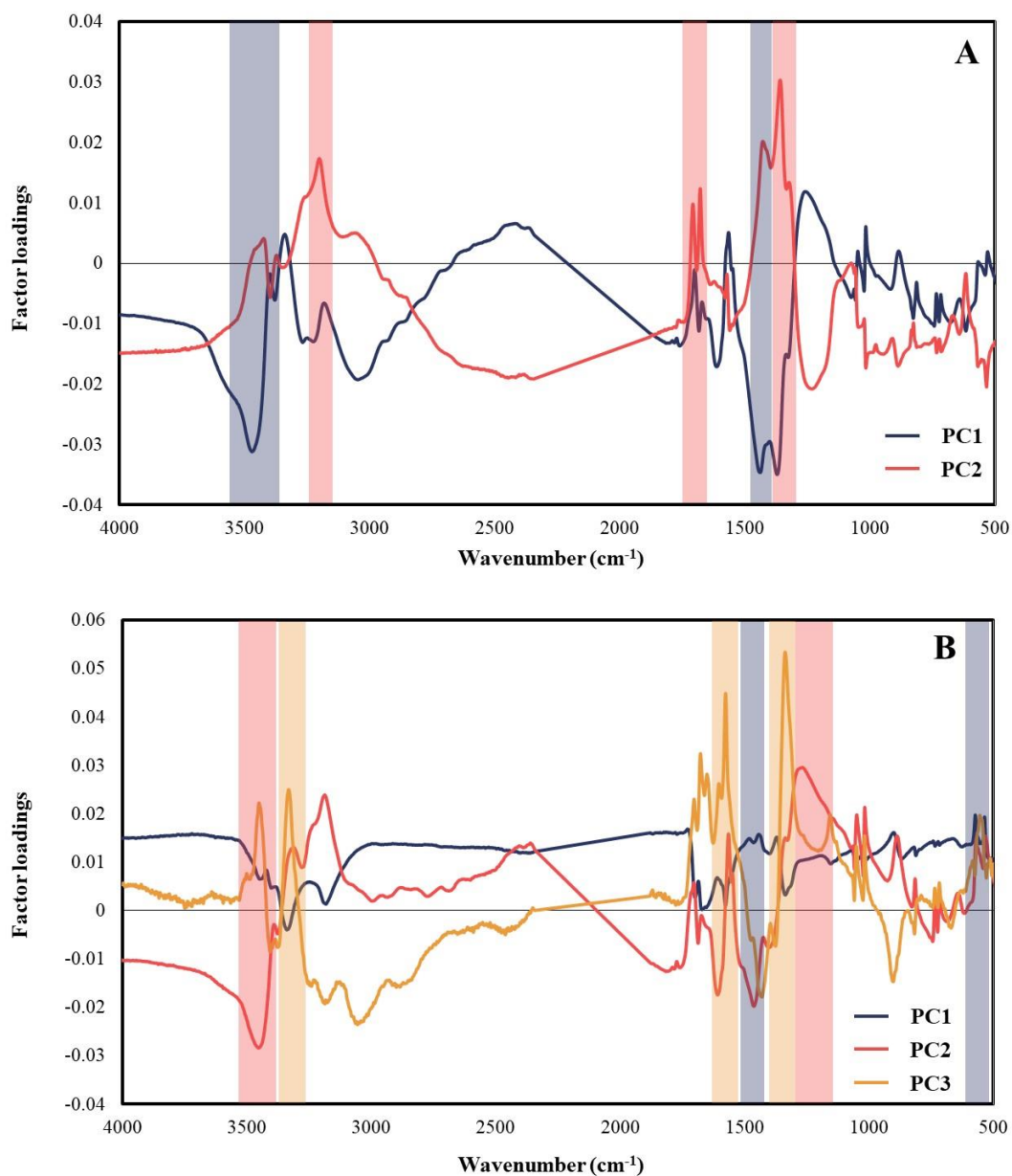


**Figure 5.9:** PC factor loadings plot for ATR-FTIR spectra acquired from PCA performed on all UN products (a) and highlighted cluster (b). Shaded areas indicate regions that have strong contribution to the separation of samples across PC1 (blue), PC2 (red) and PC3 (yellow).

LDA was subsequently performed to assess the effectiveness of using spectral data to predict the source of an unknown UN product. Two approaches were taken to evaluate the predictive accuracy of the model by LDA, but within both, LDA was conducted using the linear distance measure and first five PCs, with equal prior probabilities assumed. Although up to three PCs were used with PCA, it was found that the

additional PCs resulted in a higher classification accuracy and better discrimination (Figure A.13).

For the first approach, LDA was performed treating each UN product as an individual class, thus generating a single discriminant function that was used to predict the source of samples from an independent dataset. The discriminant model returned a calibration accuracy of 100% which was then used to predict the source of 35 samples from an independent dataset, five from each UN product. The model successfully predicted the source of 80% of the samples within the validation set (Table 5.4). All incorrect predictions came from the products within the observed overlapping cluster in Figure 5.8a. However, utilising the variation across additional PCs, the cold pack and SREDA samples in this cluster returned a 100% prediction accuracy. Most of the samples from the Baileys and Richgro product were misidentified as SREDA and cold pack samples respectively. Although the model displayed a high prediction rate across most products, it struggled to discern between two of the fertiliser brands and the cold pack samples.

The second approach taken was to perform a stepwise LDA which considered the groupings observed within the PC score plots. An initial LDA model was used to identify samples originating from chemical grade urea or from Osmocote, with the remaining samples classified as a generic UN product. LDA was repeated on the remaining samples, classifying them as either a Baileys, SREDA or generic UN product. A final LDA was performed to discern between the remaining three products (240). The first two models returned a calibration accuracy of 100% with the third only reaching 90%. It was found that this approach was very effective at predicting the source of an unknown UN sample, as only three of the 35 samples were misidentified (Table 5.5). Two cold packs samples were classified as being a DEF and Richgro product and one DEF sample was misclassified as a cold pack sample. Although resulting in a higher predictive accuracy, the stepwise approach would only be appropriate with the current dataset. If additional UN sources were added, the order in which classification is performed would likely change. Therefore, the first approach is more indicative of what type of source information could be obtained from an unknown UN product.

**Table 5.4:** Number of correct vs incorrect classifications from the validation set using a five-PC LDA model with each UN product treated as an individual class.

<b>Class #</b>	<b>UN type</b>	<b>Correct</b>	<b>Incorrect</b>	<b>% Correct</b>
<b>1</b>	Chemical grade	5	0	100
<b>2</b>	Cold pack	5	0	100
<b>3</b>	DEF	4	1 (Predicted as class 2)	80
<b>4</b>	Baileys	2	3 (Predicted as class 5)	40
<b>5</b>	SREDA	5	0	100
<b>6</b>	Richgro	2	3 (Predicted as class 2)	40
<b>7</b>	Osmocote	5	0	100
	Total			80

**Table 5.5:** Number of correct vs incorrect classifications from the validation set using a three part stepwise five –PCA-LDA model.

<b>Class #</b>	<b>UN type</b>	<b>Correct</b>	<b>Incorrect</b>	<b>% Correct</b>
<b>1</b>	Chemical grade	5	0	100
<b>2</b>	Cold pack	3	2 (Predicted as class 3+6)	60
<b>3</b>	DEF	4	1 (Predicted as class 2)	80
<b>4</b>	Baileys	5	0	100
<b>5</b>	SREDA	5	0	100
<b>6</b>	Richgro	5	0	100
<b>7</b>	Osmocote	5	0	100
	Total			91

Discriminant values (DVs) assigned to samples used for validation from the first LDA approach described are shown in Table 5.6. The chemical grade and Osmocote samples were correctly predicted, which is supported by the large differences observed in the DVs between classes. The cold pack samples were correctly classified however are not well separated from the DEF samples. Classes containing incorrect predictions including class 3, 4 and 6 displayed a similar trend as the few correctly classified samples aligned closely with neighbouring classes. These observations suggest that the model may not be capable of consistently predicting the source of samples that originate from these classes and so the overall prediction rate reported is not a true representation of the model's predictive power. Additional source prediction studies with a more extensive and diverse validation set are required to further assess the predictive power of using spectral data with chemometrics to link UN to its precursor products.

**Table 5.6:** Discriminant values of samples within the independent data set used for validation. Discriminant values and predictions represent the products within Table 5.4. Shaded cells indicate correct (green) and incorrect (red) predictions.

Sample number	Discriminant values for each class							Predicted class
	1	2	3	4	5	6	7	
1.1	-2	-812	-3926	-114795	-46354	-8649	-196	1
1.2	-12	-558	-3004	-91889	-34892	-6278	-243	1
1.3	-10	-619	-3272	-93664	-35616	-6576	-189	1
1.4	-22	-555	-2441	-80948	-28466	-4168	-193	1
1.5	-10	-708	-3232	-106515	-39044	-6354	-249	1
2.1	-2061	-24	-76	-12964	-2686	-63	-1390	2
2.2	-1345	-16	-37	-12047	-1553	-90	-1027	2
2.3	-981	-3	-80	-13811	-2621	-20	-854	2
2.4	-1133	-7	-33	-9483	-1125	-81	-930	2
2.5	-1341	-34	-202	-18959	-5568	-88	-1032	2

3.1	-1585	-35	-7	-5390	-354	-102	-1255	3
3.2	-1043	-40	-8	-5137	-287	-229	-990	3
3.3	-1195	-28	-6	-6461	-404	-193	-1074	3
3.4	-2382	-45	-88	-6477	-621	-311	-1485	2
3.5	-1267	-26	-6	-4958	-317	-447	-1052	3
4.1	-1487	-680	-365	-80	-41	-2453	-1387	5
4.2	-1825	-658	-332	-144	-67	-1848	-1535	5
4.3	-3185	-943	-625	-20	-42	-2300	-2168	4
4.4	-2500	-927	-560	-12	-55	-2402	-1876	4
4.5	-1341	-527	-205	-506	-86	-975	-1314	5
5.1	-2660	-487	-255	-143	-34	-846	-1940	5
5.2	-2967	-504	-295	-105	-10	-968	-2050	5
5.3	-2500	-366	-178	-502	-3	-584	-1830	5
5.4	-3505	-503	-340	-336	-11	-881	-2249	5

5.5	-3616	-584	-367	-120	-4	-827	-2355	5
6.1	-1373	-26	-64	-10350	-2033	-8	-1117	6
6.2	-1504	-11	-67	-12367	-2561	-4	-1130	6
6.3	-1992	-60	-87	-7497	-1056	-90	-1412	2
6.4	-2671	-80	-98	-9975	-2384	-92	-1696	2
6.5	-1365	-11	-65	-10943	-1931	-12	-1062	2
7.1	-529	-5118	-11565	-237272	-86113	-41191	-4	7
7.2	-479	-3928	-9321	-193171	-70851	-30198	-4	7
7.3	-523	-4893	-11546	-236978	-88566	-40049	-2	7
7.4	-605	-4357	-10388	-207804	-76875	-34043	-6	7
7.5	-497	-5911	-12729	-269452	-97685	-46932	-4	7



### 5.3.3.2 Discrimination of urea nitrate with X-ray diffraction

Visual assessment of XRD patterns revealed no discernible differences between the UN products. However, as shown previously, chemometric analysis may prove useful as the minor variation between diffraction patterns could provide additional discrimination. PCA was performed using the full XRD patterns of two samples from each UN product (Figure 5.10a). The sample distribution across the first two PCs revealed three separated clusters including the chemical grade, DEF and Osmocote classes. The remaining classes were highly spread and not well separated from the other groupings. This was expected as the diffraction patterns displayed a high level of similarity, exhibiting only minor variation in reflection heights. This suggests that any separation observed was attributed to the relative amount of crystalline material within the sample. This is inconsistent with the results, as the high purity chemical grade samples appear to be negatively correlated to the  $33.5^\circ$   $2\theta$  peak across PC1. Despite the observations made, it is difficult to draw conclusions about sample purity and amount of crystalline material based on extremely minor variation in reflection heights from a limited dataset. Repeated analysis with a larger dataset containing varying forms of UN is required to draw meaningful conclusions from this analysis. Nevertheless, results from initial experiments suggest that although some classes could be identified, XRD combined with chemometrics is not effective at providing additional source information for UN prepared from alternative sources.

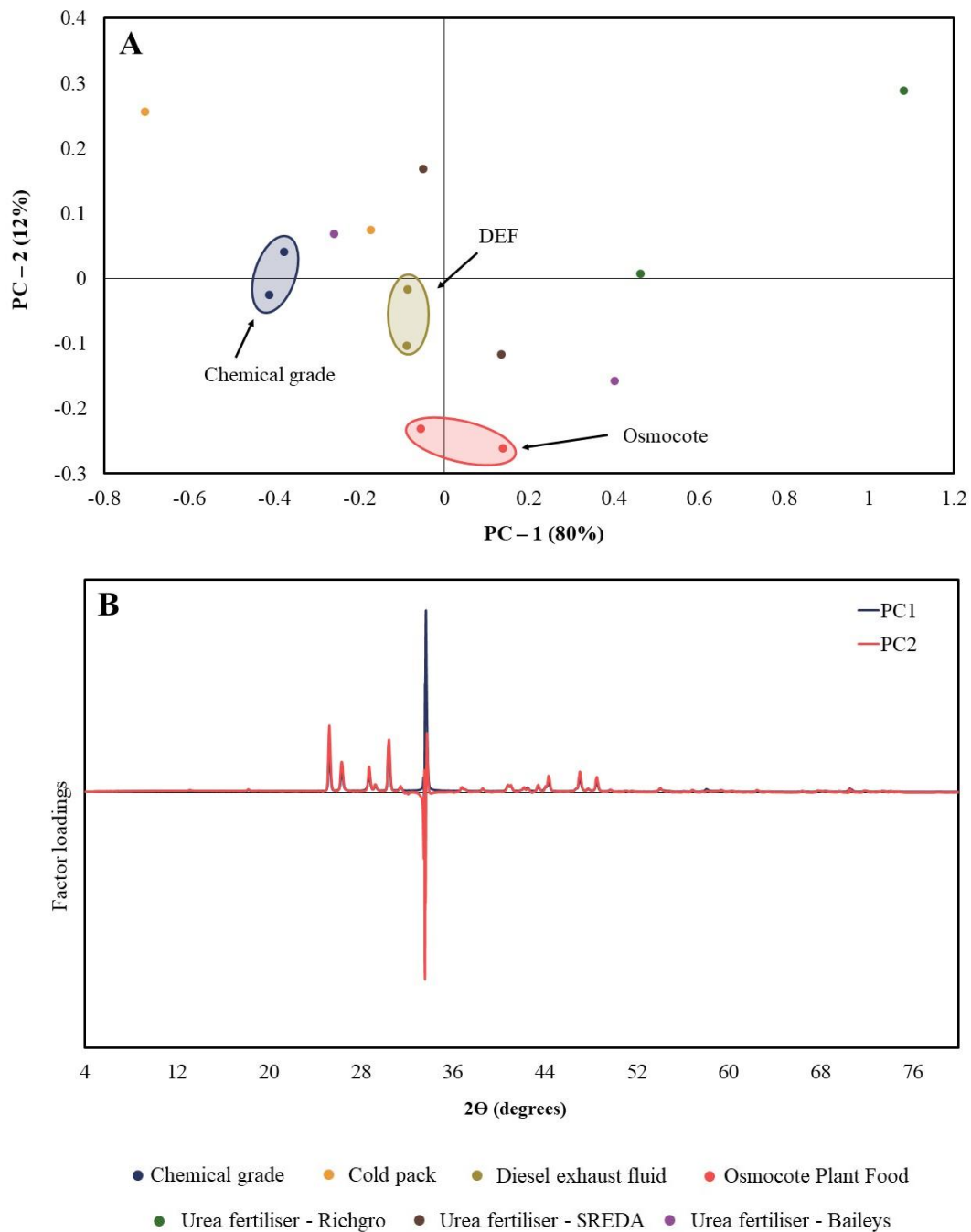


**Figure 5.10:** 2-D scores plot from PCA showing the distribution of UN samples using X-ray diffraction patterns (a) and PC factor loadings showing regions which have strong contribution to the separation of samples across PC1 and PC2 (b).

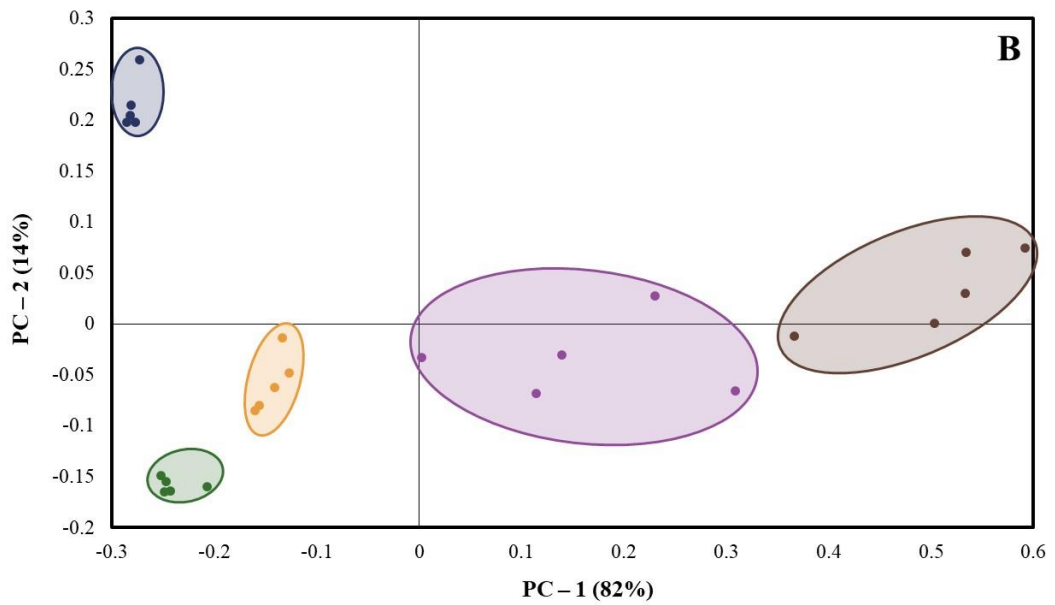
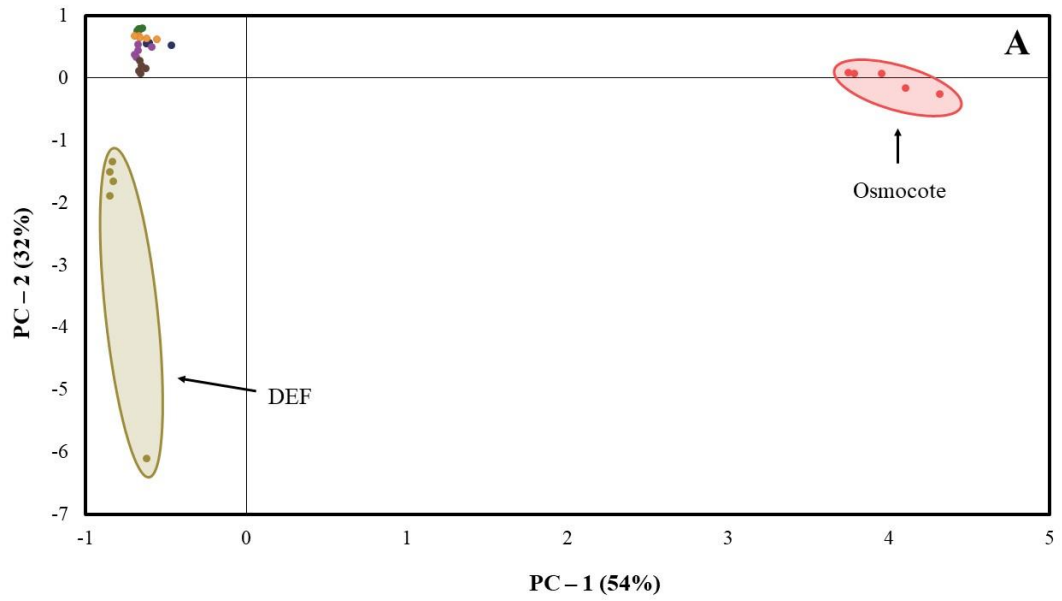
### 5.3.3.3 Discrimination of urea nitrate by ICPMS

Chemometrics coupled with ATR-FTIR and XRD revealed some additional source information regarding an unknown UN product, however, was not capable of discriminating between all classes. This is consistent with the findings of Chapter 4, as pure and homemade ammonium nitrate products could be differentiated, however full separation of samples was achieved only when trace elemental data was used. This highlights the effectiveness of performing source attribution with characteristic elemental profiles and so this method was performed to assess whether the sources of the UN products can also be determined.

PCA was performed using trace elemental data and the distribution of samples across the first two PCs is shown in Figure 5.11a. Two distinct sample groupings are observed, being the DEF and Osmocote samples, with the remaining samples forming a tight cluster at the extreme positive end of PC2. The discrimination of Osmocote was expected as a large amount of manganese, cobalt and strontium was detected within the samples, along with a quantifiable amount of rubidium which was absent from the other products. This aligns with elemental contributions detailed within the factor loadings plot, which shows a positive correlation towards these elements across PC1, where the Osmocote class is observed (Figure 5.12a). The separation of DEF samples is primarily attributed to the concentration of nickel, which was consistently present in large amounts across the five samples. Factor loadings also indicate a positive correlation to barium; however, a high concentration of barium was only observed in one sample and should not be considered a key contributor to the discrimination of this class (Figure 5.12a). This may have been caused by contamination during sample preparation or instrumental variability.

Repeated PCA on the remaining sample cluster is shown in Figure 5.11b. Removing the DEF and Osmocote classes allows minor contributions from select elements to be emphasised, enhancing discrimination of the remaining classes. Each class subsequently forms identifiable clusters across the first two PCs, with varying amounts of spread amongst samples. The greatest amount of spread was observed in samples prepared from SREDA and Baileys urea fertiliser. This could be attributed to the manufacturing process such that these products are less refined or processed, resulting in a less homogenous product compared to the Richgro fertiliser. Analysis of the factor

loadings highlights that separation was achieved with only four elements, as rubidium was not detected within these products and the concentration of manganese was consistent throughout. Most separation occurs across PC1, accounting for 82% of the total variance, and is primarily attributed to the concentration of nickel, which was highly variable across products. Chemical grade samples are positioned at the extreme positive end of PC2, which shows a positive correlation to cobalt and barium. These results indicate that using a select number of trace elements, a large amount of source information can be obtained from an unknown UN product. UN prepared from a cold pack, DEF or commercial fertiliser can be distinguished, as well as varying fertiliser brands. This information would be highly beneficial to a forensic investigation and court of law in establishing links between a precursor and the final explosive product.



- Chemical grade    ● Cold pack    ● Diesel exhaust fluid    ● Osmocote Plant Food
- Urea fertiliser - Richgro    ● Urea fertiliser - SREDA    ● Urea fertiliser - Baileys

**Figure 5.11:** Scores plot from PCA showing the distribution of UN samples using trace elemental data: 2-D scores plot with all UN samples (a) and 2-D scores plot of highlighted cluster (b). Highlighted groups show separated classes.

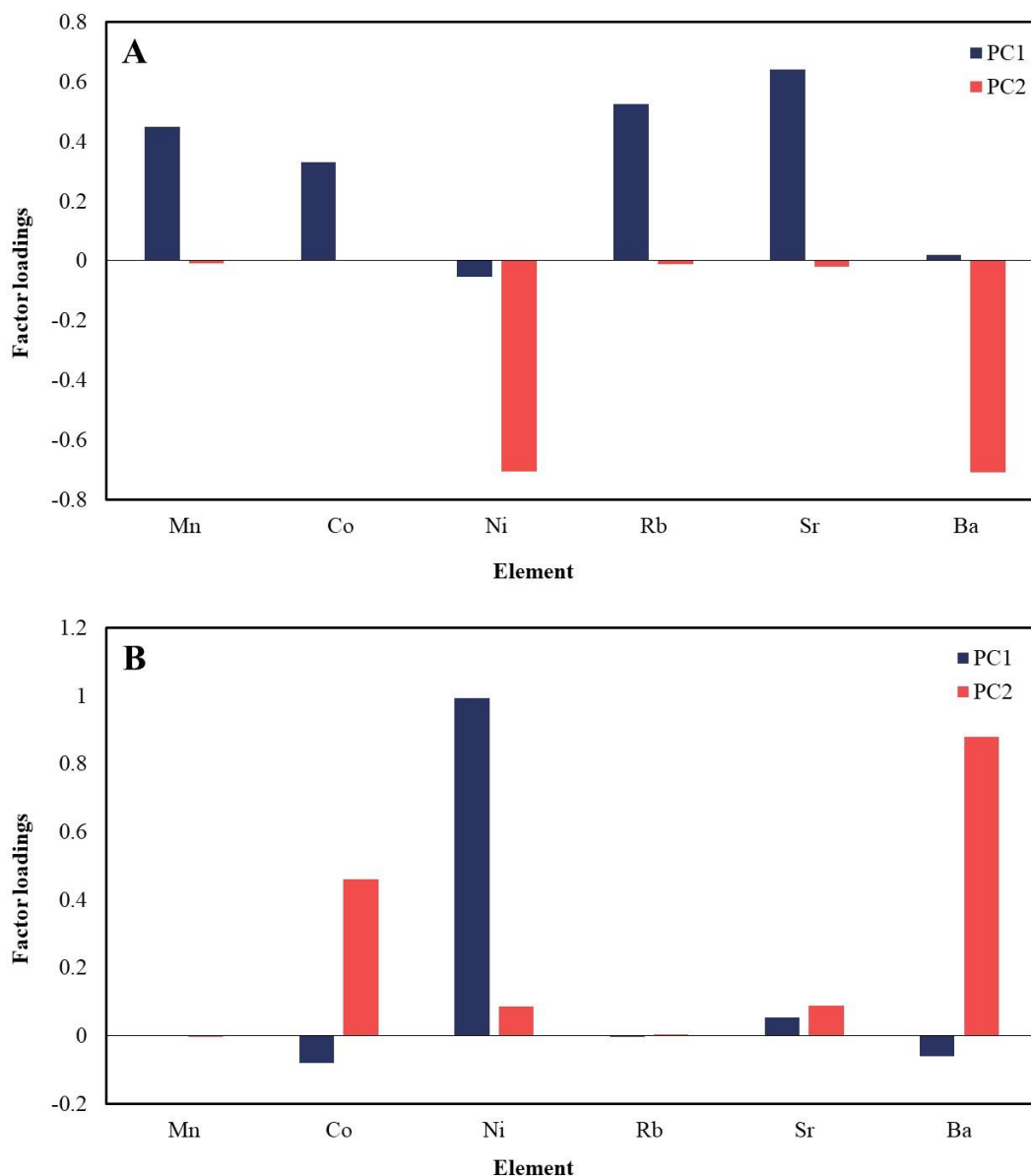


**Figure 5.12:** PC factor loadings plot for elemental data acquired from the PCA performed on all urea nitrate products (top) and sample cluster (bottom).

LDA was performed to determine the efficacy of predicting the source of an unknown UN product. The same stepwise approach detailed in section 5.3.3.1 was used, in that LDA was first performed to classify samples as being from DEF, Osmocote or as a generic UN product. LDA was repeated on those classified in the generic cluster, thus classifying samples into the remaining five sources. Due to the limited number of samples, a randomised ‘leave-one-out’ approach was adopted. Results showed each model returned a 100% classification accuracy for every analysis performed. Additionally, the model correctly predicted the source of every sample with the

stepwise classification approach. Although the validation set was limited, these results suggest that trace elemental data coupled with PCA-LDA is a highly effective source attribution technique.

## **5.4 Preparation and source attribution of homemade nitrourea**

NU is an explosive compound that can readily be produced using UN and shares similar explosive properties. Although the synthesis and characterisation using varying analytical techniques is described in literature, preparation from alternative sources has not been reported. The aim of this section was to first assess the practicality of preparing large amounts of NU from several UN products before characterising them and determining whether they can be traced back to the original urea precursors.

Two main synthetic methods have previously been reported (75). NU can be prepared by slowly adding UN to a heated mixture of acetic anhydride and acetic acid. The product is then collected by vacuum filtration, rinsed with benzene, and dried in an oven. The second method involves slowly adding UN to concentrated sulfuric acid that is cooled to  $-3\text{ }^{\circ}\text{C}$  via a salt/ice bath. The product is collected by vacuum filtration, rinsed with water, and dried under vacuum. Both methods require additional synthetic knowledge than what is required to prepare UN, with the second method more accessible as it requires only sulfuric acid, which can be obtained commercially. Therefore, a small amount of NU was prepared from the seven UN products discussed in section 5.3.1 using the sulfuric acid method

### **5.4.1 Synthesis of nitrourea using urea nitrate and sulfuric acid**

Sulfuric acid (7.54 g, 0.0769 mol) was cooled to  $-3.0\text{ }^{\circ}\text{C}$  in a salt/ice bath before UN (1.17 g, 0.0096 mol) was slowly added, ensuring the temperature was maintained between  $-3.0$  and  $0\text{ }^{\circ}\text{C}$ . The mixture was allowed to stir for 30 minutes, keeping the temperature below  $3\text{ }^{\circ}\text{C}$ . The mixture was poured over ice and the white precipitate was collected by vacuum filtration. The product was rinsed with two aliquots of cold water and dried under vacuum. NU was then dried in an oven at  $40\text{ }^{\circ}\text{C}$ . Yields from the varying types of UN is detailed in Table 5.7.

**Table 5.7:** Yield information of nitrourea samples prepared from different UN products.

Type of nitrourea	UN precursor	Yield (%)
Chemical grade	Chemical grade urea	16
Fertiliser – Richgro	Fertiliser urea	26
Fertiliser – Baileys	Fertiliser urea	15
Fertiliser – SREDA	Fertiliser urea	33
Cold pack	Urea based cold pack	18
Diesel Exhaust Fluid	Diesel Exhaust Fluid	12
Osmocote	Osmocote fertiliser	15

#### 5.4.2 Preliminary assessment of nitrourea products

The preparation of NU from UN requires additional equipment and knowledge of chemical synthesis however can still be easily prepared using commercially available ingredients and products. It was found that all UN products prepared from alternative urea sources could be used to prepare NU. The preparation from different UN products resulted in low but varying yields, indicating that it would be difficult to prepare large amounts of highly pure NU explosive compared to UN. Although some products resulted in greater yields, the differences observed is likely attributed to minor variations in temperature, stirring and drying times rather than some products being a more effective precursor.

Each NU product appeared as a white powder, with no notable distinguishing features. NU can be further recrystallised from acetic acid but was not undertaken as part of this study. Increasing the number of preparation steps would make discrimination harder to establish, and so investigating whether discrimination can first be achieved with crude products could infer whether it is possible with a highly pure form of NU. Due to the small amount of NU collected, products were characterised by ATR-FTIR and ICPMS as these techniques have previously shown to provide varying amounts of discriminatory information.



### 5.4.3 Infrared spectroscopy

Characteristic spectra of each NU product were collected. Figure 5.13 highlights the spectra of NU synthesised from the Richgro UN product, which is representative of the remaining NU samples aside from the one prepared from chemical grade UN. Whilst the typical NU signatures are displayed between  $3450 - 2750 \text{ cm}^{-1}$ , they appeared as low intensity broad peaks. The peak at  $1610 \text{ cm}^{-1}$  is also mostly absent and the sharp peak at  $1310 \text{ cm}^{-1}$  appears as two small broad peaks within the chemical grade NU spectra. This suggests that the sample contains unreacted UN and sulfuric acid that is contributing to the non-characteristic spectra. However, this highlights the variation that may be observed when analysing a poorly synthesised sample or a sample that contains a UN/NU mix.

The observed peaks within the Richgro NU product align closely with those reported in Oxley *et al.* (75). At least five peaks are resolved between the  $3430 - 2780 \text{ cm}^{-1}$  region, with characteristic peaks at  $1711$  and  $1310 \text{ cm}^{-1}$ , which correspond to CO and NO respectively. NU can clearly be distinguished from UN by additional peaks in the  $3500 - 3200 \text{ cm}^{-1}$  region, as well as the absence of the broad peak at  $2400 \text{ cm}^{-1}$ , which is also shown in Figure 5.13. This broad peak appears more prominently in the chemical grade NU sample, which supports the presence of unreacted UN. Comparable to IR analysis of the UN sample set, no notable differences were observed between the pure NU products aside from minor variation in peak heights. On that basis, IR can be used to identify a sample as NU or containing NU but does not provide any discriminatory or source information that could distinguish between precursors. The characteristic spectra reported from NU prepared from alternatively sourced UN products also significantly contributes to the forensic intelligence of NU as a homemade explosive.

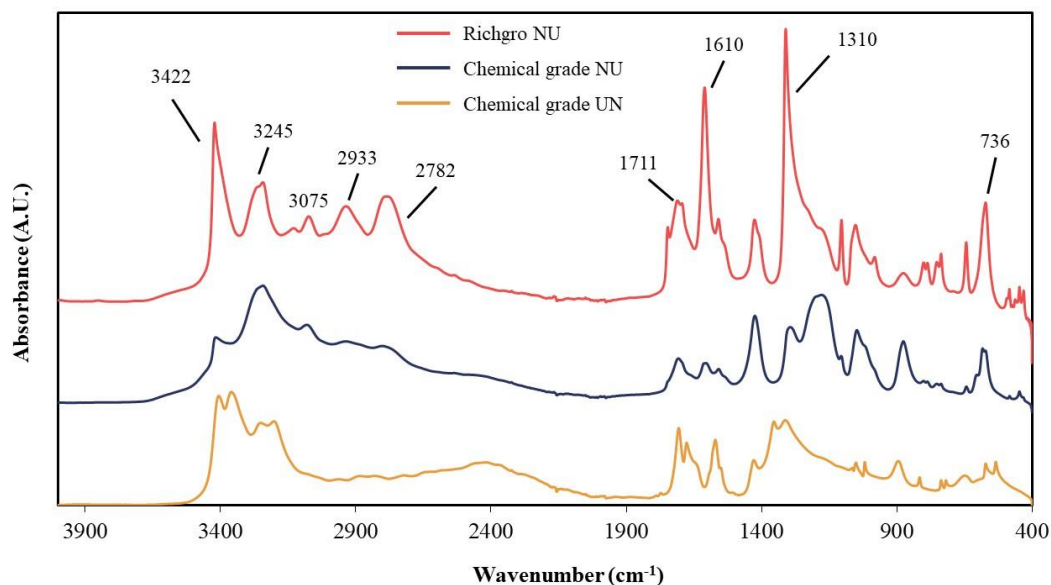


**Figure 5.13:** ATR-FTIR spectra of NU prepared from Richgro UN, chemical grade UN. Spectra of chemical grade UN is shown for comparison. Labelled peaks are aligned with those reported in Oxley *et al* (75).

#### 5.4.2 Inductively coupled plasma mass spectrometry

Two samples from each NU product were analysed by ICPMS using the instrument and method outlined in Chapter 2, section 2.4.7. NU (50 mg) was dissolved in 5% nitric acid (10 mL) in a 20 mL polypropylene tube. Prior to analysis, samples were diluted 10 and 100-fold using 1% nitric acid. Blanks of the MilliQ water, sulfuric acid, diluter, and sample procedure were also prepared. Analysis focussed on the elements detected within UN samples that were retained for further analysis; Mn, Co, Ni, Rb, Sr and Ba.

The conversion of UN to NU removed most of the trace elemental variation detected throughout the UN products. Cobalt was detected at amounts below the calibration range and so was removed from analysis. Barium was detected at increased concentrations within the NU products, which suggests that it may not be present in real amounts within the samples, instead being caused by external or instrumental factors. This supports the discussion in section 5.3.3.3, regarding the DEF sample that contained an unusually large amount of barium. Therefore, it is recommended that barium be removed from the characteristic profile and subsequent chemometric analysis of both UN and NU. This would not have a notable impact on the

discrimination of the DEF and chemical grade UN samples as seen in previous sections, as contributions from cobalt and nickel can be used to achieve separation. As shown previously, UN prepared from DEF and Osmocote samples could be identified by the increased concentration of nickel and manganese respectively. This trend persists within the NU products, as the concentration of nickel and manganese is notably higher in DEF and Osmocote samples, suggesting that NU prepared from these sources could be traced back to the precursors used.

Subsequent chemometric analysis was performed using the concentration data from Mn, Ni, Rb and Sr. The data was mean centred and standardised to ensure the same quantitative scale was used across each PC. PCA was performed using the non-linear iterative partial least squares (NIPALS) algorithm on the standardised dataset, which contained two samples from each NU product, calculating up to the first four PCs (Figure 5.14). The scores plot shows most of the NU products are well separated with tight clustering. The DEF and Baileys samples are highly spread across PC1, which is attributed to the varied nickel concentration between the samples. Similar to UN analysis, discrimination of Osmocote samples along PC2 is attributed to the large presence of manganese. Although a limited dataset is used, these results further highlight the source determination capabilities of chemometrics coupled with trace elemental data and further suggest that even with contributions from only four elements, discrimination of samples can be achieved.

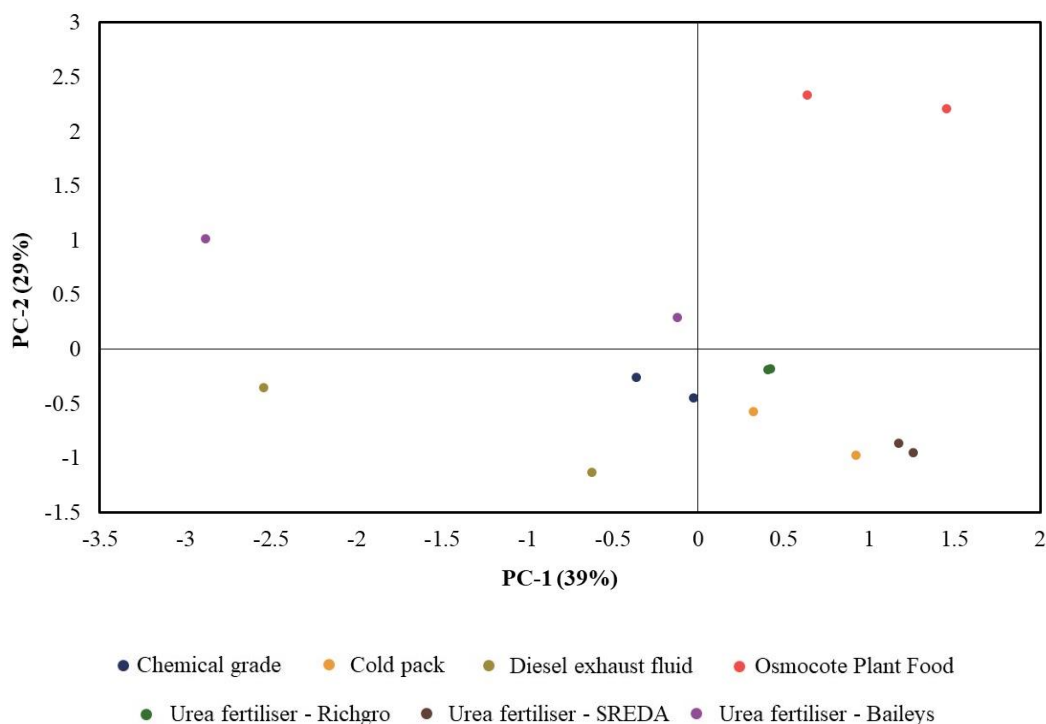


**Figure 5.14:** 2-D scores plot from PCA showing the distribution of NU samples using trace elemental data. No separation of classes was observed.

To assess whether the source of UN used to prepare each NU product could be determined, samples were projected onto the UN scores plot that was recreated using the four elements described above (Figure 5.15). Firstly, the exclusion of barium and cobalt did not impact the separation of urea nitrate samples, as the same clustering was observed when compared to Figure 5.11a. Repeated analysis on the sample cluster also revealed similar separation to that observed in Figure 5.11b, suggesting that UN can be fully discriminated with only four key elements. Projected NU samples did not adopt a similar spread, nor did they cluster near their respective source. The DEF samples are an exception, as the NU samples did appear grouped with the UN made from DEF, which is attributed to the persisting high nickel content as discussed earlier. The Osmocote NU samples appear to be positioned across the positive end of PC1, aligning with the Osmocote UN class, however, no other connections are observed with the remaining samples. Repeated analysis on the large cluster resulted in similar findings as the NU samples were spread across both PCs and showed no relation to the UN groupings. These results indicate that source determination of NU samples can

be achieved with a NU specific model, however, cannot be identified when projected alongside the UN samples.

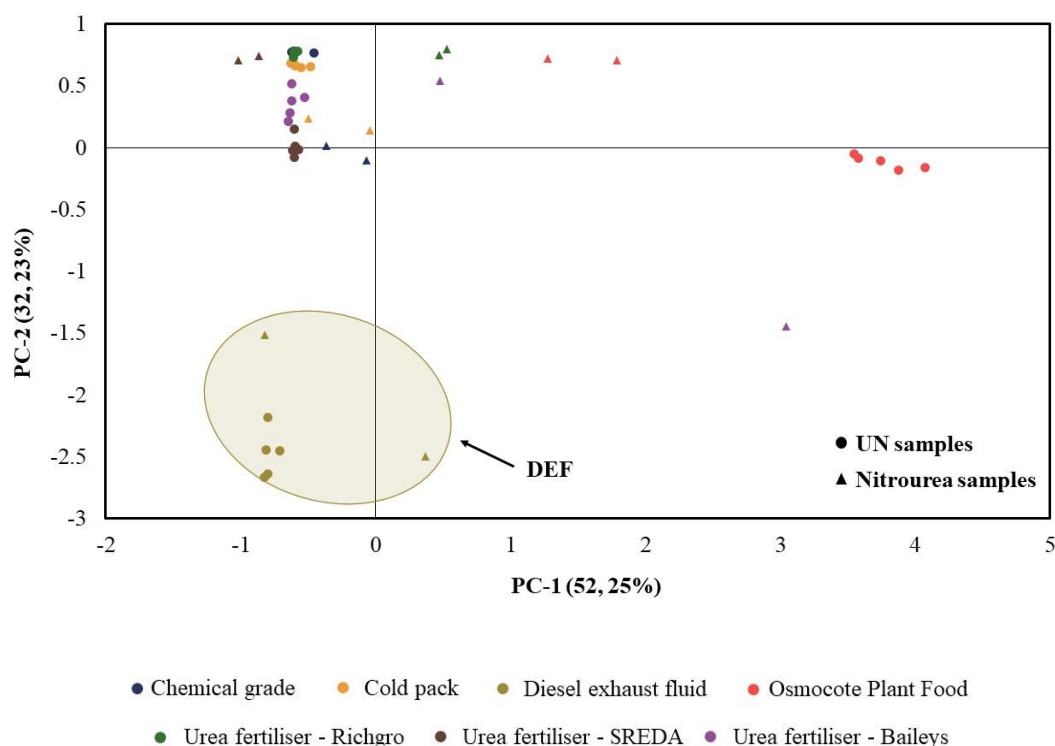


**Figure 5.15:** 2-D scores plot showing the distribution of NU samples projected on the UN scores plot with refined elemental profile. Highlighted group shows one separated class containing UN and NU samples prepared from the same urea source.

## 5.5 Conclusions

This chapter provided an extensive investigation into UN as a homemade explosive. The preparation, characterisation, and source attribution of UN from alternative sources was explored. It was found that several readily available products can be used to make large amounts of highly pure UN with little knowledge of chemical synthesis, including urea from fertilisers, cold packs or DEF. Characteristic spectra, diffraction patterns and profiles were reported, but none could discern between most products as all were of a similar purity. DEF and Osmocote samples could be identified using trace elemental data, however subsequent chemometric analysis was required to discriminate between products more accurately.

Source determination capabilities of ATR-FTIR, XRD and ICPMS coupled with PCA-LDA was compared. Using spectral data, approximately 80% of samples could be

correctly identified based on minor variation observed within peak heights. PCA-LDA performed with XRD data did not provide additional discriminatory information beyond what was achieved using spectral data. Utilising trace elemental data, all UN products could be identified across two models, using the concentrations from four elements. Substantial variation between elements such as nickel and manganese were used to discriminate and correctly predict the source of 100% of samples within the validation set.

The preparation and source attribution of NU prepared from UN was also explored. Although NU can be made from commercial ingredients, it is unlikely that large amounts of explosive grade NU would be prepared given the method is more complex and results in low yields. Nevertheless, characteristic spectra and trace elemental profiles for NU made from alternative UN has been reported. It was also found that NU samples could be discriminated using PCA with trace elemental data, however, did not correlate to the respective UN precursor when projected onto the UN model.

Research and discussions of homemade UN have little presence within literature. The methodologies, characteristic data and source attribution presented in this chapter are the first reported systematic study to provide an understanding of how different precursor sources can be used to prepare UN and what source information can subsequently be obtained. This research also highlights the feasibility of an individual with unlawful intentions to prepare large amounts of highly pure UN and what products may be used. This research is extremely beneficial to the forensic intelligence of UN as an explosive and will also contribute to the analytical procedures adopted when UN is seized within a forensic investigation.

**Chapter 6. Recovery and source attribution of post-blast residues from party sparkler and UN-based improvised explosive devices**

## 6.1 Introduction

Chapters 3 and 5 describe the chemical characterisation and source attribution of party sparklers and homemade urea nitrate (UN). Although the information presented is of high value within a forensic context, these studies focus on pre-blast samples. To further assess the identification and source determination capabilities of homemade explosives (HMEs), subsequent post-blast experiments with sparkler and UN-based improvised explosive devices (IEDs) were performed, applying the analytical and statistical methodologies established in previous chapters to samples representative of residues that may be found at a post-blast scene.

The forensic chemical analysis of debris from a post-explosion incident is a challenging process that requires collaboration of skilled personnel from a range of highly specialised disciplines to recover and identify the explosives present and reconstruct any devices used (6, 8-10). While low order devices may leave a large amount of unconsumed material, high order explosives detonate leaving minimal residue which is dispersed over a large area (1, 8, 9). The post-blast residues remaining from any device also often reside in complex matrices and are subject to many potential sources of contamination (60). This presents increased analytical challenges that could subsequently impact source determination capabilities. This highlights the importance of investigating the performance of identification and source attribution methods on real post-blast residues, to determine if the amount of chemical and discriminatory information obtained is comparable to that obtained from pre-blast samples.

Many of the challenges described as being present within the forensic investigation of a post-blast incident also contribute to the difficulties of performing post-blast research experiments. Few studies can be found on the chemical analysis or source determination of post-blast debris produced from HMEs, which is partly due to the increased risk, insufficient funding and the need for effective collaboration with law enforcement agencies (15). Furthermore, studies that do report the analysis of post-blast residues typically focus on identifying the explosives present with no further attempt to identify how it was prepared or the source of the precursors used. There is a large amount of evidentiary value that can be gained from the complete characterisation and source attribution of an explosive sample and so there is a need



for ongoing post-blast investigations focussing on improving source determination capabilities of post-blast residues (10, 15, 103).

Low order nuisance devices often contain inorganic explosive mixtures prepared from pyrotechnic products such as consumer fireworks or party sparklers and are commonly used in crimes involving the destruction of property, street violence and arson (88, 101, 104, 241, 242). Numerous studies have reported methods capable of identifying the primary oxidising agent along with other components commonly found in pyrotechnic mixtures (99, 102, 148, 150, 243-245). Capillary electrophoresis (CE) and ion chromatography (IC) methods have also proven effective at characterising pre- and post-blast residues from consumer fireworks and inorganic explosive mixtures (96, 97, 99-103, 246). However, few studies have characterised post-blast residues from actual IEDs containing pyrotechnic mixtures. Martin-Alberca *et al.* used ATR-FTIR to characterise post-blast residues from exploded fireworks and found that they can be traced back to their original pyrotechnic composition (103). A study reported by the Australian Federal Police (AFP) also found that 18 anions and 12 cations could be detected within post-blast residues from a controlled firing of a homemade explosive device, however, the explosive mixture was not specified (97).

Although methods to analyse inorganic post-blast residues are well established, previous studies have primarily used these methods on consumer fireworks, with the purpose of identifying the oxidising agent. No further attempt has been made to distinguish between brands or sources, which could aid in establishing connections or generate investigative leads within a forensic investigation. Furthermore, in Australia, the majority of consumer fireworks are illegal, leaving party sparklers the most common and easily accessible pyrotechnic on the market (90, 247, 248). As discussed in Chapter 3, trace elemental data coupled with chemometrics was used to discriminate between party sparkler brands. Applying this methodology to samples collected from real sparkler based IEDs to determine whether additional source information can be obtained would be extremely useful within a forensic investigation and contributes to the forensic intelligence of party sparkler based IEDs.

UN undergoes a rapid exothermic decomposition when detonated, releasing a massive amount of heat and energy into the surroundings. The decomposition mechanism of UN is extremely complex as a large number of products can be formed, depending on

the temperature and pressure conditions. Early studies reported UN decomposition begins at 125°C and completely volatilises at 275°C with no visible residue remaining beyond 325°C (249). Initial decomposition products include ammonium nitrate (AN) and isocyanic acid (HNCO), which later decomposes forming a number of gaseous products including N<sub>2</sub>O and H<sub>2</sub>O (249). Subsequent studies agree that there are two main decomposition pathways observed at low and high temperatures (36, 229, 250-252). At low temperatures around 100°C, UN dissociates into nitric acid and urea, which then decomposes to form gaseous ammonia and isocyanic acid. The urea reacts with isocyanic acid to form biuret, and the ammonia reacts with nitric acid to form AN in its condensed phase (36, 68, 229). At temperatures above 250°C, the formed urea and biuret totally decompose and small quantities of a number of condensed phase species can form, including nitrourea, nitrobiuret, cyanuric acid, ammelide, ammeline and melamine (36, 68, 75, 250, 253). As temperatures reach 360°C, all materials decompose to form carbon dioxide, water, ammonia and nitrous oxide as gaseous products (36, 250). The theoretical and experimental decomposition pathways not only explain why UN is used to prepare powerful IEDs, but also outline what products may be detected when analysing post-blast residues.

Many products have been identified to form during the decomposition of UN, however, the recovery and detection of these compounds and UN itself is extremely difficult. Urea and nitrate can be present at low levels within the environment and may lead to false positives (116). A UN charge could also be mistaken for AN, as ammonium and nitrate ions may be detected in post-blast debris. Therefore, within a post-blast investigation involving a UN-based device, identification of the intact ammonium nitrate ion pair is essential to confirm the presence of UN within the initial charge (116, 117, 234). Previous studies have successfully characterised the UN molecule using high performance liquid chromatography mass spectrometry (HPLCMS) with electrospray ionisation (ESI) and atmospheric pressure chemical ionisation (APCI) (232), which was also used to detect the presence of UN from a metal fragment collected from a fired rocket (233). However, it was found that UN may be formed during the analytical process and so detection of the characteristic adduct does not necessarily confirm the presence of UN. Ammonium nitrate has also been extracted from mixtures to form adducts using crown ethers, which are then characterised using spectroscopic techniques, elemental analysis or EI-MS (222, 234).

McCord and de Perre adapted a technique used to determine the presence of urea in wine and urine to detect trace levels of UN explosive by LC-UV/fluorescence (116, 254). This method could differentiate between UN and urea and showed no interference from AN mixtures. Alternative methods such as voltametric measurements (255) and infusion based EI-MS have been used to detect the intact UN molecule (235), however, most of the studies described did not collect post-blast residues.

Tamiri *et al.* describes the recovery and analysis of post-blast residues collected from firing three UN charges of various sizes (234). Residues were collected on an array of witness materials such as aluminium and wooden boards, cement blocks and cloth. They reported the detection of UN by LCMS in one out of 28 samples collected. Almog *et al.* adapted the technique described by McCord and de Perre by reacting the xanthidrol derivative with alcohol to form xanthylurethane, which can be detected by gas chromatography mass spectrometry (GCMS) (117). The authors provide details of a number of controlled firings including a 300 and 600g UN charge which were boosted with RDX (10% of UN weight), and collected residues on steel witness plates, cement blocks and within sand. The technique described could confirm the presence of the uronium cation in 25% of samples, which is the highest success rate reported across post-blast UN studies. Lastly, Phillips *et al.* described the firing of a 545kg UN charge with the intention to collect residues from a variety of witness plates including road signs, vehicles, wooden boards, and cloth (184). Although this study primarily reported the physical effects of the explosions upon certain objects, the information presented is useful for groups performing post-blast experiments.

Previous studies highlight that the recovery and analysis of organic post-blast residues is highly complex, and subsequent identification of the explosive used is difficult due to the trace quantities remaining and various sources of contamination or interference. Previous chapters outline the capability of identifying, discriminating and providing source information using inductively coupled plasma mass spectrometry (ICPMS) coupled with chemometrics. This method relies on the trace inorganic material, which may have a greater persistence on witness materials than the organic residues typically targeted. Although this method proved effective on pre-blast material, it should be assessed with real samples collected from controlled firings to determine whether the

trace components detected within post-blast debris can be traced back to the original source of precursors used. Identification and discrimination of the explosive used in an IED is essential to provide investigative leads and establish connections between the device and potential suspects.

As the number of post-blast experiments that could be performed was limited, investigations focussed on low order inorganic sparkler-based nuisance devices and high order organic UN-based IEDs. This allowed for a direct comparison of the experimental design, analytical procedures, and data analysis between two different types of explosive devices. The aims of these experiments were to collect and analyse post-blast residues from several party sparkler based and UN-based IEDs that have been prepared from precursors of varying sources, in order to explore whether any discriminatory or source information can be obtained using the methods outlined in previous chapters. Furthermore, these experiments provide an opportunity to assess the functionality of homemade IEDs and provide an outline of the challenges associated with performing post-blast experiments, which will aid future research involving the source attribution of post-blast residues.

## **6.2 Experimental**

### 6.2.1 Party sparkler experiments

#### 6.2.1.1 Materials

Packets of party sparklers were purchased from a variety of local and online Australian retail stores. Four out of the eight brands investigated in Chapter 3 were used to prepare IEDs, including the brands Artwrap, Firefox (FF), Party Central (PC) and Fun + Creative (FC). Materials used to construct the sparkler based IEDs were supplied by the Western Australian Bomb Response Unit (WABRU), including aluminium foil, duct tape and plastic plumbing (20 × 100 mm) and galvanised metal pipes (20 × 100 mm). Other materials required to conduct experiments were also supplied by the WABRU, including wire, remote and electric detonators, wood, 11.1 L handy-pail buckets, bricks and personal protective equipment (PPE).

### 6.2.1.2 Preparation of party sparkler based IEDs

Homemade party sparkler devices were constructed to replicate devices often encountered in Western Australian (WA) casework, an example of which is displayed in Figure 6.1. Party sparklers from four distinct market brands were used to prepare eight devices such that two identical devices were prepared using sparklers from each brand (each device contained sparkler material from a single source). An additional two devices were constructed using the Artwrap branded sparklers but using a small ( $7 \times 2$  cm) and large ( $10 \times 3$  cm) version of the CO<sub>2</sub> canister. All canisters were sourced from different locations. All tasks relating to the construction and initiation of the devices were performed by the WABRU.

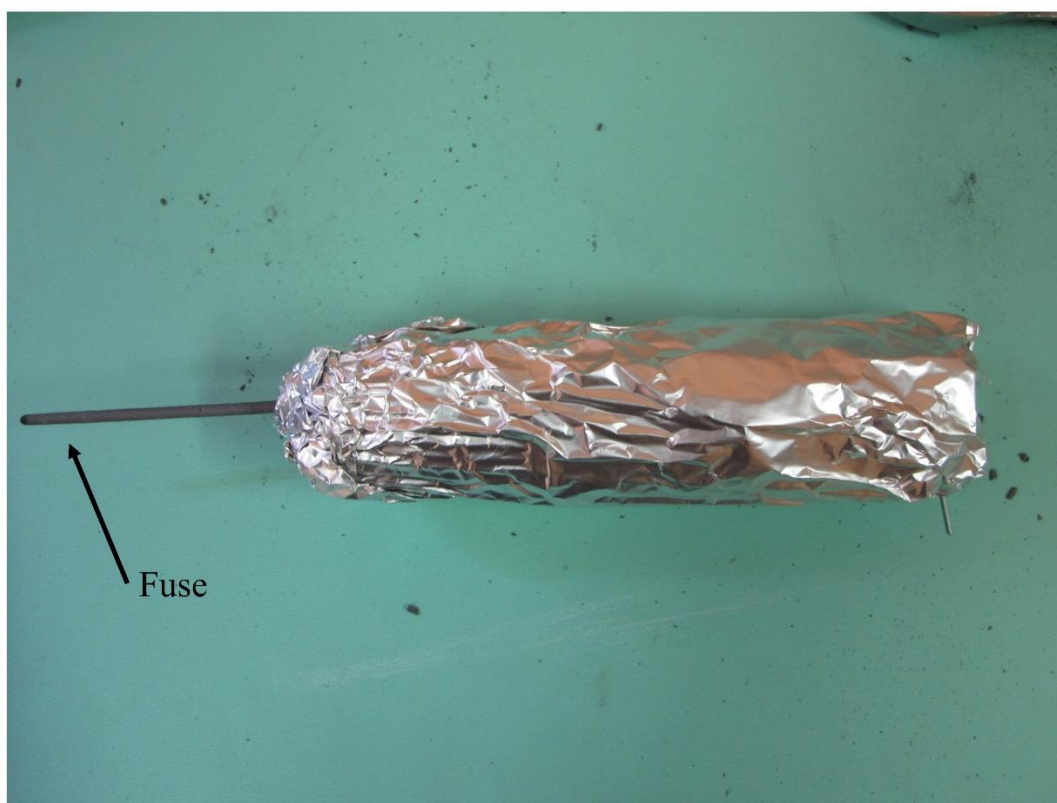


**Figure 6.1:** Example of party sparkler device prepared and used within post-blast experiments. A single sparkler was placed at the top of the device to act as the fuse, which was ignited using a gas lighter. The design and construction were modelled after devices typically seized within WA casework.

Each device was placed on a wooden block that was half protruding out of a 11.1L collection bucket. A large wooden box was built around the detonation area to ensure minimal damage to surroundings (Figure 6.2). The device was ignited by a member of

the WABRU, and the area was evacuated. Once the device had functioned and the area was rendered safe, the bucket was removed and immediately placed in a cryovac plastic bag (Sealed Air, USA), the area was swept of debris and another device was set up. This process was repeated until all devices had been functioned and collected. Recovered samples and residues were transported to the laboratory and remained untouched until further analysis was performed.

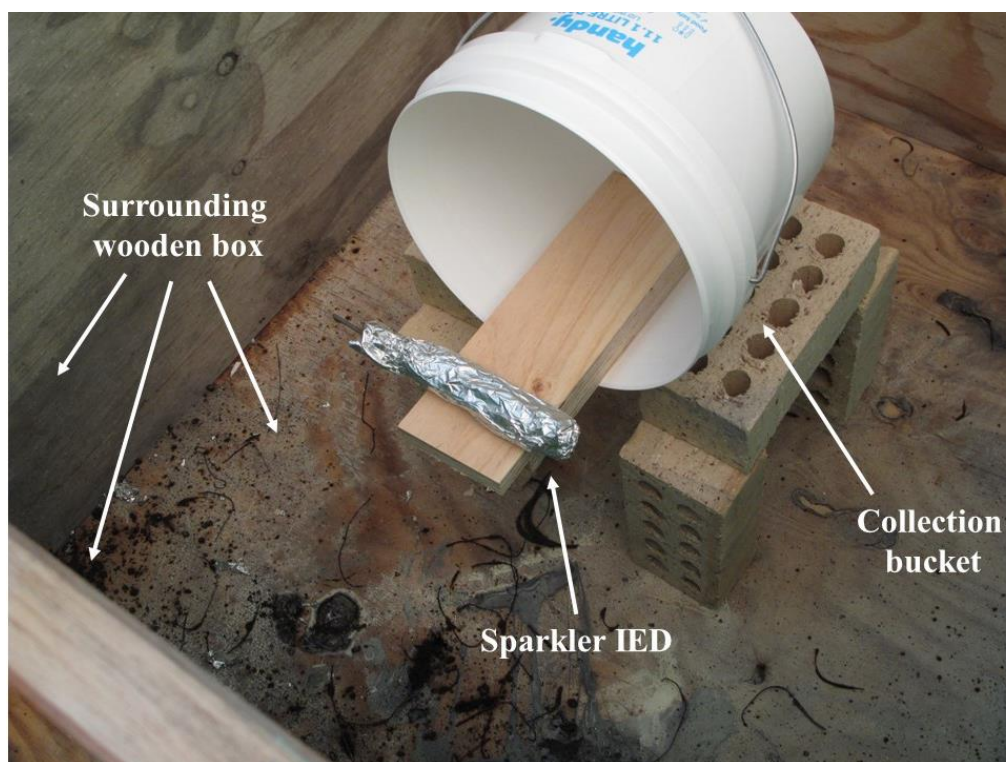


**Figure 6.2:** Experimental set up for functioning and collecting residues from party sparkler based IEDs. Sparkler device was positioned on a wooden plank which protruded from a collection bucket. A wooden box surrounded the scene to contain the explosion and minimise damage done to surroundings.

### 6.2.1.3 Preparation of party-sparkler based pipe bombs

Metal and plastic party sparkler based pipe-bombs were also prepared using approximately 125 g of party sparkler material in each device. The devices were placed on two wooden slats that were suspended over a bucket of water with one of the slats tied to a long rope that could be pulled. The set-up was surrounded by a wooden box to ensure minimal damage to surroundings (Figure 6.3). The pipe was ignited by a member of the WABRU, and the area was evacuated. If functioned as intended, the device was immediately placed in a cryovac plastic bag and transported

to the laboratory for further analysis. If a misfire occurred (failed detonation), the pipe was dropped into the bucket of water by pulling the wooden slat. The scene was rendered safe by the WABRU before any subsequent experiments were performed.

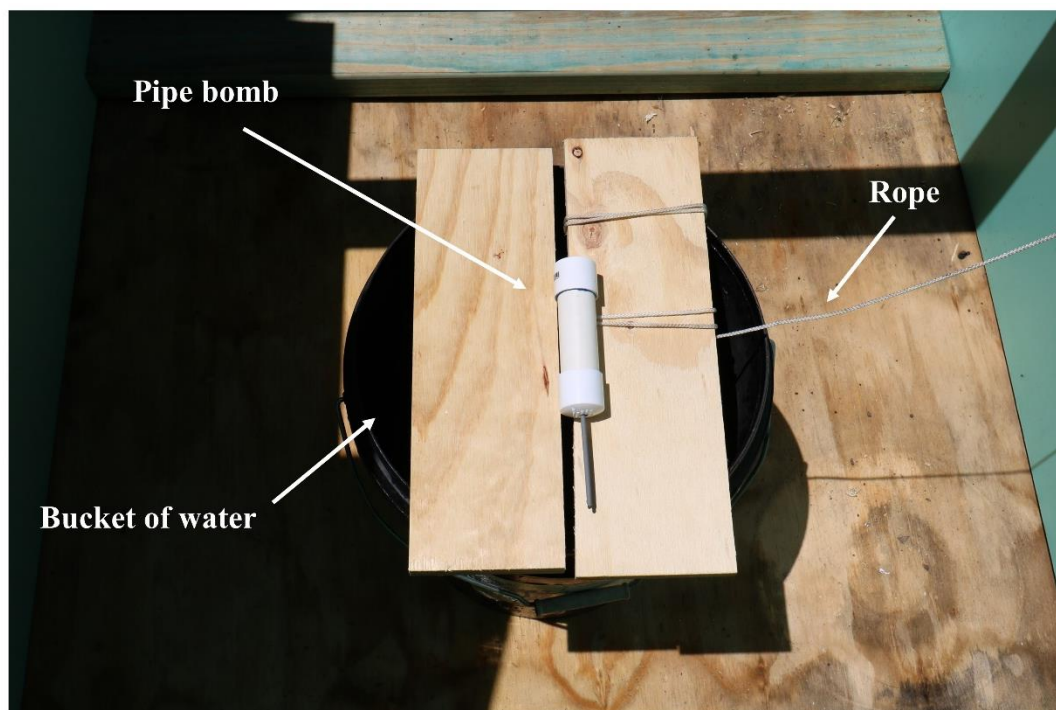


**Figure 6.3:** Example of the experimental set-up for functioning party sparkler based pipe bombs. A single sparkler was placed at the top of the device to act as the fuse, which was ignited using a gas lighter. Devices were placed over a bucket of water so that it could be dropped and rendered safe if a misfire occurred.

#### 6.2.1.4 Sample processing and analysis

The collected material from the sparkler devices was a mixture of intact post-blast particles, wood, aluminium, plastic, and sparkler material that was either unburnt or partially burnt. The post-blast material was isolated using a pair of plastic tweezers. Sample preparation was performed using the method outlined in Chapter 3, section 3.2.6 and then analysed by ICPMS using the method and instrumentation outlined in Chapter 2, section 2.4.7. Samples were diluted 10 and 100-fold and blanks of the MilliQ water, diluter, nitric acid and sample procedure were also prepared.



#### 6.2.1.5 Chemometric analysis

Principal component analysis (PCA) was performed using the method described in Chapter 2, section 2.4.8.3. From the 58 elements analysed, seven were retained for chemometric analysis including Co, As, Sr, Mo, Sn, Sb and W. A discriminatory profile was established using analysis of variance (ANOVA) based feature selection as described in Chapter 2, section 2.4.8.4. Additional PCA was performed to explore impact of the type of canister used within the IED and to compare against party sparkler discrimination described in Chapter 3, which is detailed in the relevant sections below.

Linear discriminant analysis (LDA) was performed using the linear distance and first five principal components (PCs) with equal probabilities assumed. A discriminant model was generated using the unburnt sparkler samples with each brand treated as an individual class. This model was used to predict the sources of 40 post-blast samples within an independent data set. The predicted and actual sources were compared to evaluate the accuracy of the model.

### 6.2.2 Urea nitrate experiments

#### 6.2.2.1 Materials

UN was synthesised from five different urea sources using methods outlined in Chapter 2, section 2.3.2 and stored in sealed containers that were collected by the WABRU prior to the experimental range days. Wooden and metal witness plates were purchased from a hardware store and corflute plates were purchased from an office supplies store. Plastic drinking bottles (600 mL) used to prepare the explosive devices were purchased from a grocery store, emptied, and cleaned of their contents. Other materials such as tape, string, glue, wire, remote and electric detonators and booster sheets were supplied by the WABRU.

#### 6.2.2.2 Experimental design

A total of five 200 g charges were prepared using five different UN products, including UN prepared from chemical grade urea, urea fertiliser (Richgro brand), diesel exhaust fluid (DEF), urea based cold packs and Osmocote fertiliser. A commercial No. 8



electric detonator (base charge containing pentaerythritol tetranitrate (PETN)) was used to function each device. The charge was suspended by wires approximately 1.5 m from the ground. One of each type of witness plate (wood, metal and corflute) were positioned upright perpendicular to the charge approximately 1.5 m away. One of each type of witness plate was also placed directly below the charge, therefore six plates were used to collect residues from each charge. All witness plates were 30cm × 30cm in size and cleaned with 1% nitric acid and MilliQ water and stored in a sealed cryovac plastic bag prior to being used in the experiment. These types of substrates were used to collect residues as they represent common materials that may be found at a post-blast scene. Once the charge had been placed, witness plates were taken out of their bags using gloves and placed in appropriate locations. All attempts to avoid contamination of the plates and the scene were made. Figure 6.4 shows a schematic of the experimental set-up.

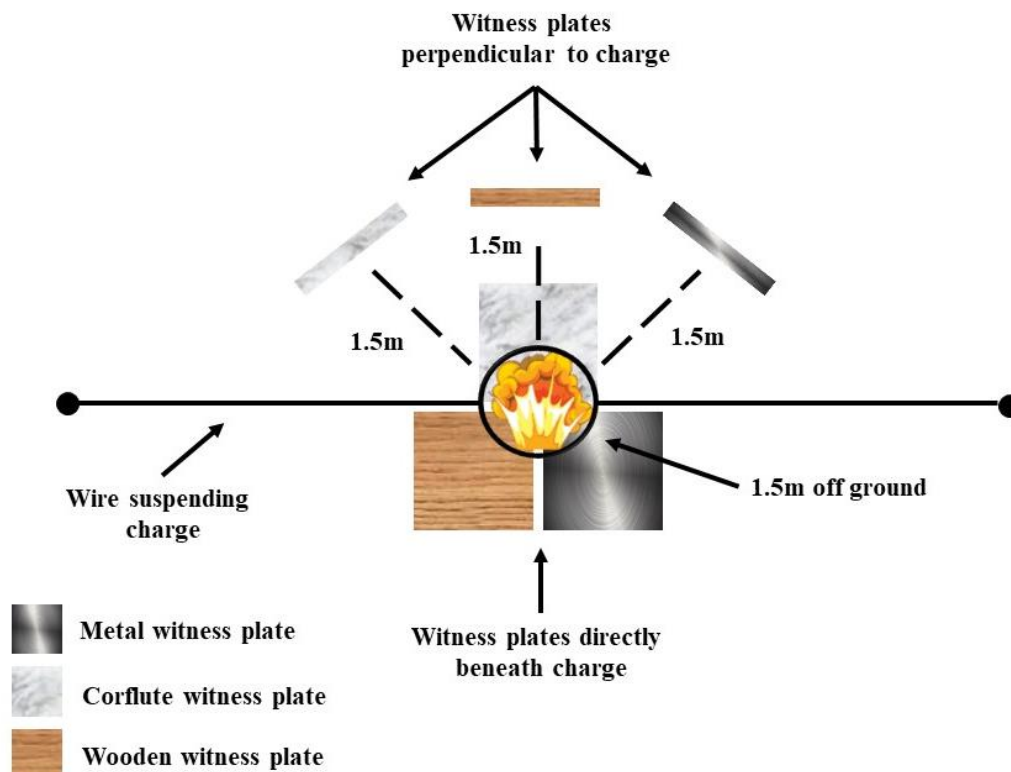


**Figure 6.4:** Example of the sample grid for post-blast UN experiments with witness plates of varying materials placed both perpendicular and beneath the charge. The charge was suspended on a wire approximately 1.5m from the ground and detonated using an electric detonator.

### 6.2.2.3 Recovery and storage of post-blast residues

Once a device had functioned and the area was secured by the WABRU, all plates were collected and placed in individually sealed cryovac plastic bags and returned to the laboratory for analysis. All physical debris was removed from the scene before the next charge and set of witness plates were prepared. This process was repeated until all devices had been functioned.

#### 6.2.2.4 Collection and analysis of post-blast residues

Witness plates were first examined for any noticeable areas where there would likely be a higher concentration of post-blast residues. This includes any holes or exit points, discolouration or debris. These areas were targeted to maximise the amount of residue collected. Each witness plate was rinsed with 10 mL MilliQ water which was run off into a test tube. A blank rinsing of each witness plate was also collected prior to being used in the experiments and after being washed and cleaned as described above. Collected samples were then analysed by ICPMS using the method and instrument outlined in Chapter 2, section 2.4.7.

#### 6.2.2.5 Chemometric analysis

PCA was performed using the method described in Chapter 2, section 2.4.8.3. From the 58 elements analysed, three were retained for chemometric analysis including manganese, nickel and strontium. Distribution of samples were visualised by generating a 2-D scores plot. LDA was not performed due to the small sample set.

### **6.3 Results and discussion**

#### 6.3.1 Preliminary considerations when performing post-blast experiments

Post-blast experiments were performed on three separate occasions, two of which focussed on UN based devices, and the other on sparkler-based nuisance devices. Each set of experiments presented a unique set of challenges, complications and limitations that needed to be considered when collecting, analysing and interpreting the collected data, which is detailed in the relevant sections below. The information presented in this chapter not only contributes to the forensic intelligence of HMEs and IEDs, but is also beneficial to any agency, laboratory or research group that intend to perform post-blast experiments.

### 6.3.2 Party sparkler experiments

Homemade explosive devices are inherently unpredictable due to the nature of their construction. Nuisance type devices containing party sparkler residue are known to be extremely varied as often they are constructed by an individual with little knowledge of how explosives or pyrotechnics function. A large range of uniquely prepared sparkler based IEDs have previously been seized within WA and are often filled with sparkler residue, black powder or a mixture of both. Although IEDs seized are often unique, some materials are much more common than others.

The aim of the party sparkler experiments was to first explore how these nuisance-type devices are sourced, prepared and functioned. The recovery, analysis and source attribution of post-blast residues were then investigated to determine whether any discriminatory source information can be obtained after a device has been functioned. To increase the operational relevance of this work, the devices used within experiments aimed to be representative of what has previously been encountered in WA instances. After reviewing the recent history of devices found and seized by the WABRU, it was found that devices containing sparkler residue surrounding a CO<sub>2</sub> canister appeared most frequently. Furthermore, metal and PVC pipe bombs were also found to be commonly seized. Party sparkler-based devices are more of a concern within Australia because the vast majority of pyrotechnic products and materials are restricted and difficult to obtain. Although the actual devices prepared may not be as common outside of Australia, details regarding the experimental design, recovery and analysis of post-blast residues and interpretation of the data is extremely beneficial to anyone undertaking post-blast experiments.

#### 6.3.2.1 Functionality of sparkler based IEDs

Initial attempts at constructing a functional sparkler based IED was unsuccessful as the first few devices that were made simply burned without generating sufficient heat to rupture the CO<sub>2</sub> canister, causing most of the device to melt (Figure 6.5a). This was due to the lack of party sparklers used as well as poor confinement of the CO<sub>2</sub> canister which did not reach a sufficient temperature to rupture. Subsequent attempts utilised a larger number of sparklers and tighter wrapping along with numerous layers of aluminium foil. Additional residue that was ground was also added to promote burning

down the canister. The modifications resulted in all remaining devices functioning as intended.

The IEDs took approximately 40 seconds to explode which is mostly dependent on the length and size of the sparklers and fuse. The sparklers used were around 30 cm in length and gave a large amount of time for the scene to be evacuated after ignition. The relatively small device produced a sizable amount of damage. The CO<sub>2</sub> canister acted as a sharp projectile as it ruptured and was launched in a random direction, often getting stuck in nearby surfaces (Figure 6.5b-c). The sparkler material was dispersed over a large area and holes were often found on collection buckets, with sparkler material melting onto the plastic (Figure 6.5d). This highlights the type of debris to be expected and the potential damage a small sparkler device can cause, particularly when contained in a small space such as a letter box or vehicle.



**Figure 6.5:** Examples of the damage caused, and debris produced from a functioned sparkler based IEDs: initial attempts where devices melted instead of rupturing (a), CO<sub>2</sub> canister recovered after rupturing (b), CO<sub>2</sub> canister embedded into wooden box surrounding the initial device (c), damaged bucket after device was functioned (d).

Post-blast experiments involving the construction and function of party sparkler based pipe bombs were unsuccessful as none functioned as intended. All devices misfired and so were submerged in water and rendered safe which did not allow for any post-blast residue to be collected and analysed. There was no further opportunities to repeat pipe bomb experiments during the course of this project.

#### 6.3.2.2 Analysis of post-blast residues by ICPMS

Post-blast material was collected from 10 devices constructed with four different brands of sparklers and three different types of canisters. Two devices were constructed using the Artwrap branded sparklers with a small and large CO<sub>2</sub> canister. The remaining eight devices were prepared using a medium sized canister with four different sparkler brands, two duplicate devices per brand. All were constructed by a single member of the WABRU using the same method and number of materials. The concentration of 58 elements within post-blast samples were determined by ICPMS. Five individual samples were analysed from each device resulting in ten samples per brand and an additional ten samples from the devices constructed with the small and large canister.

Comparable to ICPMS analysis of sparklers presented in Chapter 3, residues collected from homemade devices contained an abundance of elements, but data analysis focussed on those originally present within unburnt and burnt residues. Previous party sparkler analysis found that many elements were present at higher concentrations within burnt residues. It was suggested that the process of burning resulted in elements reacting to form species more easily extractable in solution and so were detected at higher concentrations. This was also observed between unburnt and post-blast residues as shown in Figure 6.6, which compares the average concentration of some of the elements present at relatively high (Figure 6.6a) and low (Figure 6.6b) concentrations from the Party Central brand.

Bulk elements such as manganese, cobalt, titanium, chromium, zinc and copper are present at higher concentrations within post-blast samples. This trend is also observed amongst many of the trace elements; however, the differences appear to be smaller. Although concentrations differ between residue types, the relative proportions of elements are near identical which is displayed in Figure 6.6. This highlights the

persistence of the inorganic components within post-blast residues as well as the importance of their recovery and analysis to provide identifying and potential source information within a forensic investigation.

Elements such as titanium and strontium appear to defy this underlying trend which could be attributed to several sources of potential contamination present within the experiments. The homemade device itself contained a large amount of aluminium foil and a metal CO<sub>2</sub> canister, therefore it is expected that samples are contaminated with metals originating from these materials. Furthermore, even though an effort was made to clean the scene between charges, the explosion would have mobilised additional material and residue from previous charges, which may have contributed to the increased elemental concentrations observed.

It should be further noted that the similarity of the two sample types suggests that the post-blast sample itself is comparable to unburnt material. It was previously noted that the material remaining after each explosion was a diverse mixture of intact post-blast particles, wood, aluminium, plastic, and sparkler material that was either unburnt or partially burnt. An effort was made to identify and isolate post-blast material; however, it is likely that the sample contained a notable amount of unreacted material as well, which is to be expected with post-blast samples from low order devices. Construction of the device involved adding a large amount of ground sparkler material on top of the canister to promote burning throughout the device. It is likely that a portion of this material did not burn and was dispersed amongst the remaining residue, which has resulted in the 'post-blast' sample collected and analysed being similar in nature to an unburnt sample. This is supported by comparing the IR spectra of an unburnt, burnt and post-blast sample, which shows the post-blast sample having features of both unburnt and burnt material (Figure 6.7). Therefore, the results presented in this section may not be a true representation of post-blast sparkler residue and more indicative of a complex pre/post-blast mixture. If experiments were to be repeated, primary fragments that were in close contact with the explosive mixture should be collected and analysed as the residues may be more representative of a true post-blast sample.

Although additional experiments are required to profile post-blast sparkler residues, these results highlight the complexities surrounding post-blast investigations. The

information presented also provides an understanding of the types of residues that may be encountered, as well as the collection and analytical procedures that can be performed to gain additional information about the sample that may assist in a forensic investigation.

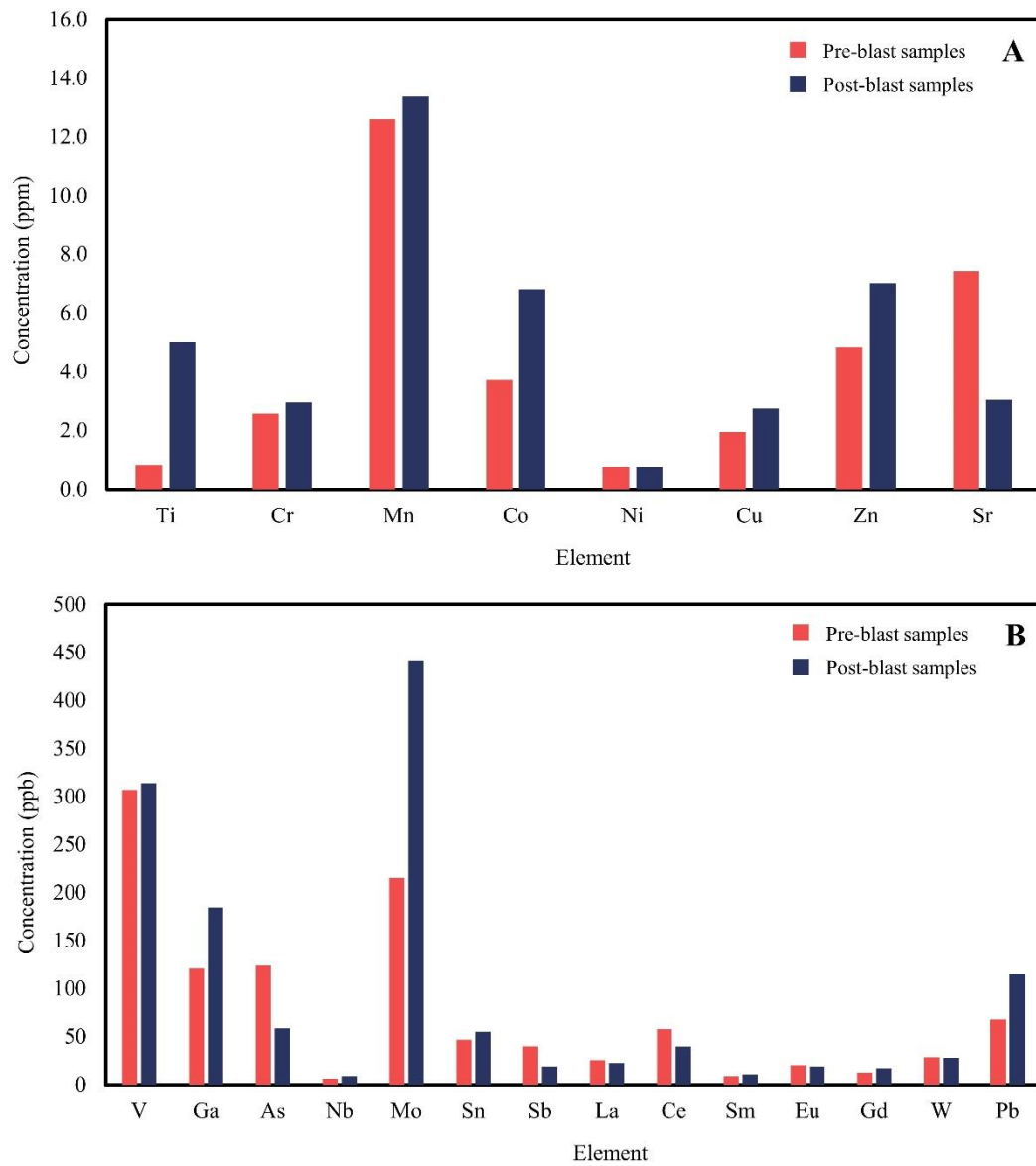


**Figure 6.6:** Comparison of average concentration of elements detected in post-blast samples from devices constructed using Party Central branded sparklers against unburnt samples from the same brand. Figure separated based on elements present at concentrations > 1ppm (a) and < 1 ppm (b).

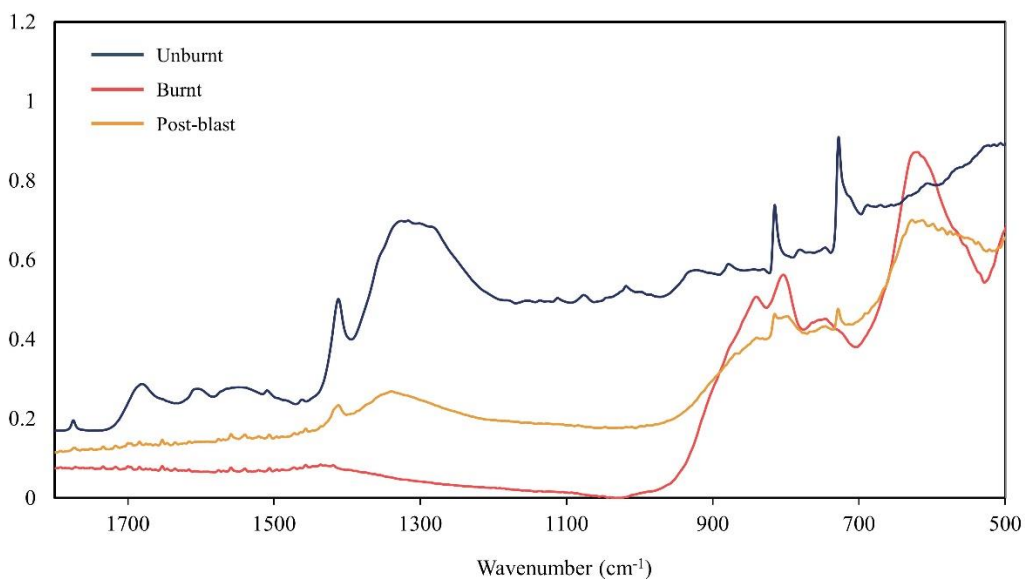


**Figure 6.7:** ATR-FTIR spectra of unburnt, burnt and post-blast party sparkler material from the Party Central brand.

### 6.3.2.3 Discrimination of party sparklers using trace elemental data

The sparkler material collected from a functioning homemade IED was shown to contain a large number of bulk and trace elements that were highly variable between brands. Subsequent chemometric analysis was performed to assess the source determination capabilities of using trace elemental data coupled with PCA-LDA, utilising the previous results and discriminatory elemental profiles established in Chapter 3.

Comparable to previous chemometric analysis detailed in Chapter 3, section 3.3.4.2, ANOVA based feature selection was first performed on the detected elements to reduce the number of classifiers and give greater separation between samples. PCA was carried out using the elements with the highest f-ratios, including Co, As, Sr, Mo, Sn, Sb and W. The distribution of samples across the first three PCs is shown in Figure 6.8.



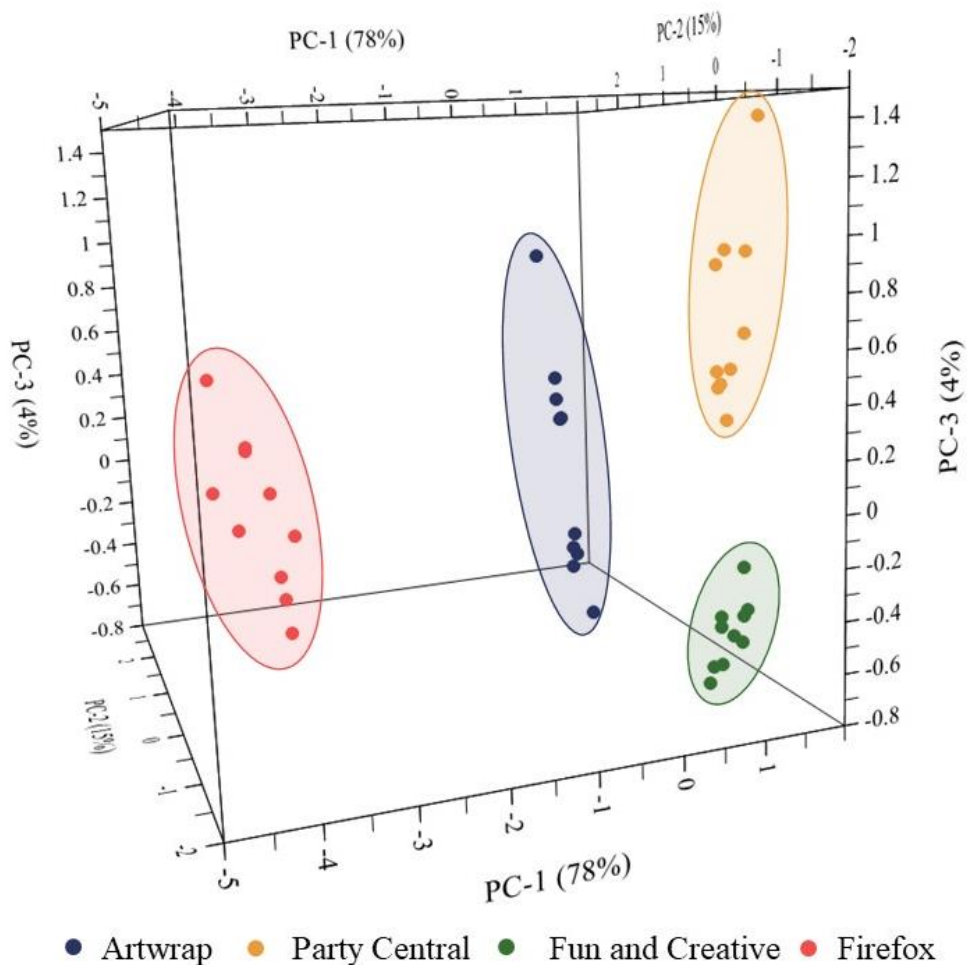


**Figure 6.8:** 3-D scores plot from PCA performed on the post-blast samples collected from devices prepared using four different party sparkler brands. Distribution of samples reveals four distinct groups indicating complete separation of brands.

Samples from each brand of sparkler used to prepare IEDs formed distinct groupings within the scores plot. This suggests that the elemental variability observed between sparkler brands persists within the post-blast material. Additionally, considering samples were taken from two separate devices made up of each brand, the sample spread within the groups is relatively small. Compared to the source attribution of unburnt and burnt residues, the elemental profile required to fully discriminate between post-blast samples includes arsenic and molybdenum but does not require nickel or vanadium.

Most of the variation is observed across PC1, which accounts for 78% of the total variation. The factor loadings shows that separation across PC1 is spread evenly across all elements, indicating that all elements are required for full discrimination to be

achieved. To distinguish between the FC and PC samples across PC3, the concentration of cobalt and molybdenum are the main contributors, which highlights the need for molybdenum in this model (Figure 6.9). This is further supported by performing PCA on the samples using the elemental profile used to discriminate between unburnt samples (Figure 6.10). As shown, the Artwrap and FF brands are easily separated, but the party central and fun and creative samples cannot be discerned.

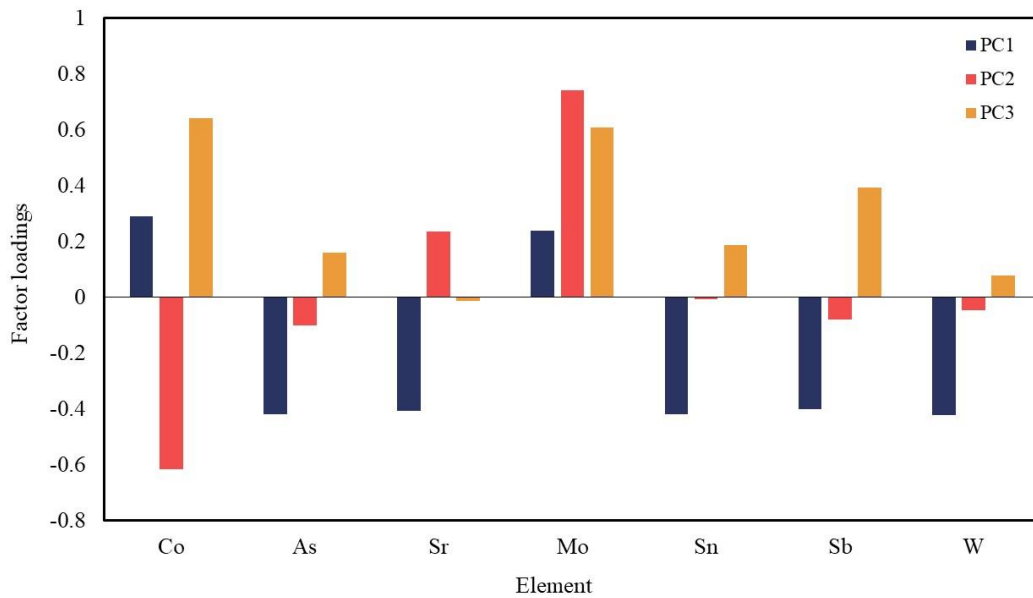


**Figure 6.9:** PC factor loadings plot for elemental data acquire from the PCA performed on post-blast samples, highlighting elemental contributions across the first three PCs.

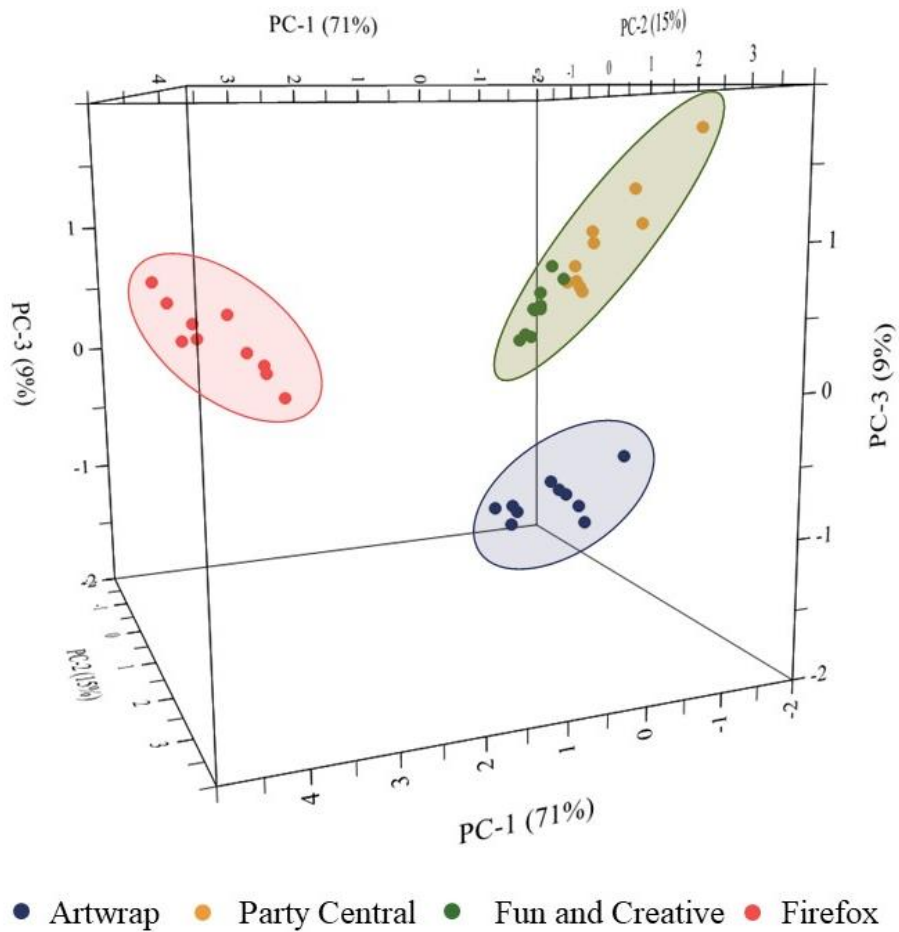


**Figure 6.10:** 3-D scores plot from PCA performed on the post-blast samples using the elemental profile that distinguished between unburnt samples. Distribution of samples reveals two distinct groups with the remaining samples overlapping.

To explore whether contributions from the canister had a notable impact on the elemental profile, and therefore discrimination against other samples, an additional ten samples were taken from two devices prepared with different canister types. Figure 6.11 displays a 2-D scores plot from PCA performed on the post-blast samples with the additional samples from IEDs constructed with different CO<sub>2</sub> canisters. Results suggest that PCA continues to be effective at discriminating between sparkler brands when the homemade device has been constructed with different materials. Samples from the large and small canister are closely aligned with the original Artwrap samples compared to other brands. Although the differing canisters have had some impact on the overall elemental profile, the Artwrap branded samples can still be distinguished from other brands. Despite this result, it does not conclusively prove that canisters

used within IEDs will not impact the elemental profile of the explosive residue. The size of the charge, type of HME mixture and amount of contact between the canister and explosive are all factors that could affect the amount in which the residues are contaminated with trace elements within the canister. Therefore, within a forensic investigation, recovery and analysis of both the explosive residue and canister would be necessary to show the true origin of the trace elements found.

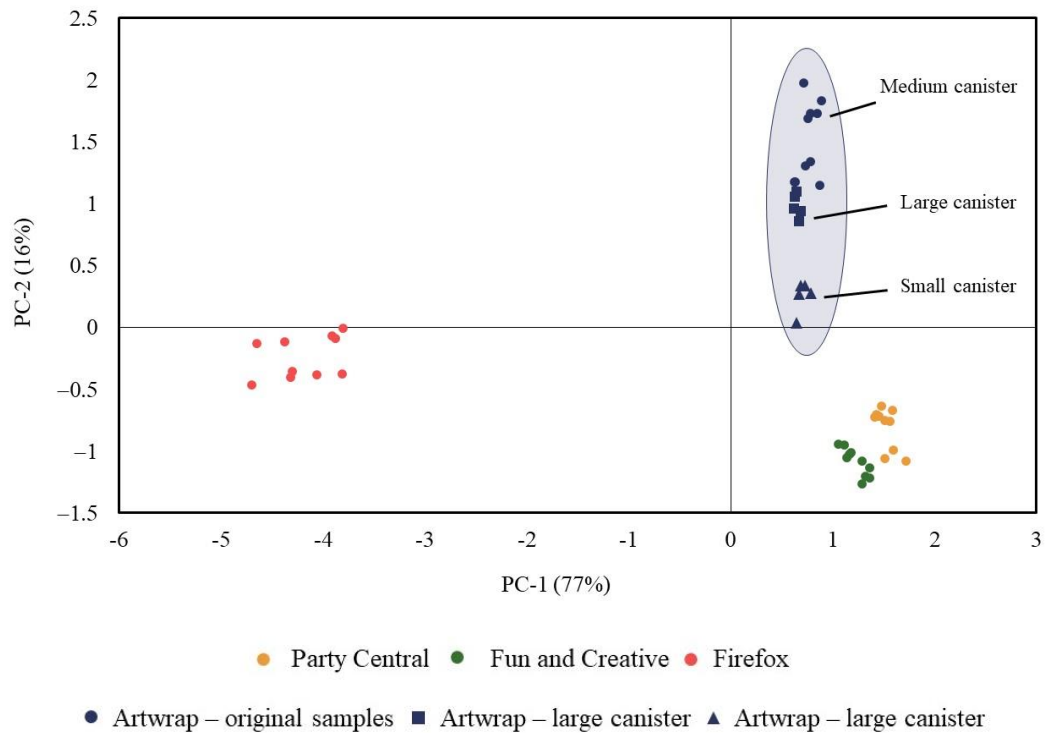


**Figure 6.11:** 2-D scores plot from PCA performed on the post-blast samples collected from all ten devices. Distribution of samples reveals four distinct groups with samples from different canister types grouped together with remaining Artwrap samples.

LDA was subsequently performed to evaluate the effectiveness of the original unburnt model to predict the brand of sparklers used to construct homemade IEDs. This involved using the unburnt samples (classification set) to build a discriminant function which would be used to predict the source of the 40 post-blast samples (validation set). As explained previously, full discrimination of post-blast samples was achieved when elemental data from seven elements were used, which differed from the elements used in the unburnt model. Therefore, data from nine elements were used for LDA, including V, Co, Ni, As, Sr, Mo, Sn, Sn, W, which combines the discriminatory profiles used for unburnt and post-blast samples. LDA was conducted using the linear

distance and the first five PCs with equal probabilities assumed. The discriminant model returned a calibration accuracy of 97.92%, with only one sample from the Party Central brand misidentified as a Wizard sample.

The model was used to predict the source of 40 samples from an independent dataset that included all post-blast samples from four sparkler brands. It was found that only 55% of samples had their source correctly predicted (Table 6.1). The model could only consistently identify the source of the Firefox samples, with all other groups containing misidentified samples. The misidentified Artwrap and FC samples were linked to brands that were not included in the post-blast model. All Party Central samples were incorrectly predicted as being from FC, which was its nearest group when visualised in the PC scores plot. These results indicate that although discrimination within the post-blast model was achieved, when projected onto the unburnt model for source determination purposes, samples cannot be consistently identified as being from a specific brand. Nonetheless, the ability to exclude some brands when attempting to identify the source of a post-blast sample would still assist an investigation.

**Table 6.1:** Number of correct vs incorrect classifications from validation set using a five-PCA model constructed with combined unburnt and post-blast elemental profile.

<b>Class #</b>	<b>Brand</b>	<b>Correct</b>	<b>Incorrect</b>	<b>% Correct</b>
<b>1</b>	Artwrap	3	7 (Predicted as Korbond)	30
<b>2</b>	Firefox	10	0	100
<b>3</b>	PC	0	10 (Predicted as FC)	0
<b>4</b>	FC	9	1 (Predicted as WLP)	90
	Total			55

### 6.3.3 Urea nitrate experiments

Collection and analysis of post-blast UN presented increased challenges compared to the sparkler investigations. As a fertiliser based high explosive, when functioned there is no visible residue and minimal debris unlike the sparkler devices where intact

particles could be clearly identified and collected. Experiments had to be performed outside with minimal containment due to the increased power of the explosive, which made collecting residues difficult. The additional materials used, and processes required to perform the experiment, as well as the minimal amount of residue collected also increases the potential for contamination. The difficulties faced were compounded due to the minimal literature and methodologies regarding the functionality, collection and analysis of inorganic residues from UN-based IEDs. This section provides information on the functionality, recovery, and analysis of homemade UN charges as well as the challenges and limitations encountered performing post-blast experiments which will aid future research and experiments involving the source attribution of post-blast residues.

#### 6.3.3.1 Preliminary trials

Post-blast UN experiments occurred over two separate range days, the first providing an opportunity to explore the proposed methodology and experimental parameters before a more thorough series of experiments were performed. Factors such as the size of the explosive charge, position and number of witness plates, type of detonator used, and amount of booster required were explored as well as the collection and analysis of witness plates.

A total of five devices were prepared consisting of  $2 \times 100$  g,  $2 \times 200$  g and a 300 g charge. All were prepared using the same type of UN (prepared from Richgro urea – Chapter 2, section 2.3.2.1). A commercial No. 8 remote detonator was used to function each device. A charge was boosted with 5 g of PETN sheet booster if required. The charge was suspended from a wire approximately 1.5m from the ground surrounded by one of each type of witness plate (Wood, metal and corflute), which were positioned upright perpendicular to the charge approximately 2m away. One of each type was also placed directly below the charge, therefore six plates were used to collect residues. All witness plates were 30cm  $\times$  30cm in size and cleaned with 1% nitric acid and MilliQ water before stored in a cryovac plastic bag prior to being used in the experiment.

The first two charges (100 g and 200 g + booster) failed to detonate as intended. It was found that the specific type of detonator used was not performing as intended. This

was swapped for an electric detonator and used with all subsequent charges. The next two charges included a 100 g and 200 g charge without a booster, which successfully detonated. This demonstrates that a homemade UN based charge is capable of functioning without the need of a booster, which is vital information that contributes to the forensic intelligence of UN explosives. It is still unknown as to why the remote detonator used consistently resulted in failed detonations. A 300g charge was also functioned but was found to cause significant damage to the witness plates and knocked them off their posts.

The witness plates collected were analysed using the method in section 6.2.2.4. Comparison between plates and charges was difficult due to the inconsistent detonations, however, results suggested that some elements related to UN were detected in quantifiable amounts across the different witness plates. Cobalt was present in small amounts compared to the blanks within the corflute samples (8.5 – 11.5 ppb) and consistent between the plates that were both perpendicular and beneath the charge. Strontium was also present in small amounts amongst all materials (8.0 – 43.0 ppb) but varied between duplicate plates. Metals such as titanium and lead were present amongst all samples in large amounts (14.5 – 91.5 ppb and 50.0 – 2125 ppb respectively) but likely to be a result of contamination based on the range location being a gun training facility.

After exploring results from initial trials, it was decided that additional experiments were necessary to determine if the trace elemental data within collected residues could provide any discriminatory information regarding the source of the UN used within homemade devices. Observations regarding the position of witness plates, size of charges, type of detonators used, and sample analysis were taken into consideration when conducting subsequent experiments.

#### 6.3.3.2 Functionality of urea nitrate IEDs

On the second range day, five 200 g charges were prepared and functioned, each containing UN prepared from a different source of urea. All charges functioned as intended without the need for a booster. Based on visual observations, no charge performed ‘better’ than others as the damage caused to the witness plates was

consistent across devices. Figure 6.12 highlights some of the damage caused to the witness plates positioned both perpendicular and beneath the charge.

Minimal physical debris from the device remained, with only small pieces of plastic and tape from the container being recovered. The number and size of fragments recovered confirms that the UN explosive charge high ordered and is therefore detonator sensitive. In comparison, an AN based charge requires a commercial booster to detonate. This ultimately means that it is easier to prepare and detonate a UN based charge as an additional booster, which is typically much more difficult to source, is not required. This is also the first conclusive report of UN being detonator sensitive, as various literature studies regarding UN devices either do not report the materials used or report using RDX as a booster (117, 184, 234). This information significantly contributes to the forensic intelligence of UN as a homemade explosive, as knowing it has the capacity to detonate without a secondary booster greatly increases its destructive potential. This information also provides important context for forensic officers that should be considered within forensic investigations involving the suspected firing of a UN based device. Furthermore, this finding will aid future forensic investigations into post-blast UN, as the absence of boosting material may simplify the experimental process.



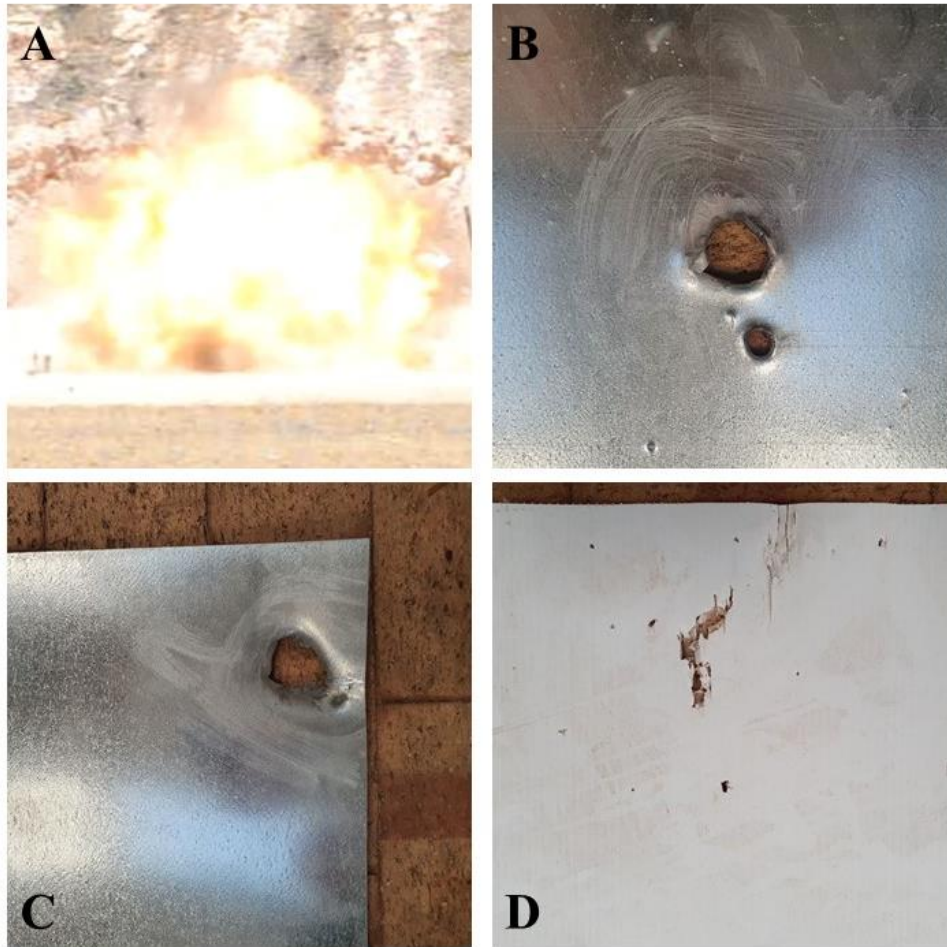


**Figure 6.12:** Images depicting the damage of UN based IEDs explosion and damage caused to surrounding witness plates. Explosion resulting from functioning the device (a), damaged metal witness plate placed perpendicular to the charge with visible holes (b), damaged metal witness plate placed beneath the charge (c), and damaged corflute witness plate placed perpendicular to the charge (d).

### 6.3.3.3 Characterisation of post-blast residues

Samples collected from witness plates were analysed by ICPMS, focussing on those elements present in previous trials and detected within pre-blast UN. Results showed that few elements out of the 58 analysed were detected in quantifiable amounts that were not present in blank samples. Furthermore, interpretation of the data discovered a large amount of contamination amongst most of these elements. Large levels of zinc, copper, tin, and lead were detected in highly varied amounts across witness plates. Comparison between witness plates placed directly beneath and perpendicular to the charge showed increased levels from the floor samples. This could be explained by the plates being directly below the charge as the detonators were placed ‘top-dead

centre', causing the explosive to detonate towards the ground, resulting in the floor plates receiving most of the residue. However, contamination from the environment surrounding the plates (sand, soil etc.) is likely to have contributed to the increased levels. To avoid uncertainty in future experiments, samples of the surrounding area should be collected and analysed prior to explosive trials to identify the primary sources of contamination.

Although the location these trials took place allowed for post-blast experiments to be conducted, the location is an active shooting range. As a result, there exists a high background of elements relating to firearm use, which has contributed to the high levels observed for some elements. An effort was made to reduce the amount of environmental impact, however as the explosion itself created a lot of sand, dust and debris to be mobilised, some level of contamination was inevitable. Ideally, these experiments would be performed in a sterile location with minimal environmental impact. Furthermore, a large tarp surrounding the blast area would be useful in minimising the amount of unwanted material affecting any residue collection media used. Table 6.2 highlights the differences observed between the perpendicular and floor samples.

**Table 6.2:** Average concentration (ppb) of some elements detected on witness plates positioned perpendicular of directly below the charge.

	<b>Witness plates perpendicular to charge</b>			
	Cu	Zn	Sn	Pb
Chemical grade	6.51	479	0.74	154
Fertiliser grade	6.00	124	0.81	118
Cold pack	14.3	137	1.84	346
DEF	91.0	520	19.7	2714
Osmocote	312	301	1.91	332
	<b>Witness plates directly below charge on floor</b>			
Chemical grade	825	1624	177	4.87x10 <sup>4</sup>
Fertiliser grade	2193	717	52.9	8.91x10 <sup>4</sup>
Cold pack	786	6814	56.0	3.00x10 <sup>4</sup>
DEF	727	941	99.8	4.18x10 <sup>4</sup>
Osmocote	672	655	90.5	4.43x10 <sup>4</sup>

Some elements including manganese, nickel and strontium were detected in quantifiable amounts within the calibration range that did not appear to be present from contamination. These elements were also highly discriminatory when differentiating between pre-blast UN samples described in Chapter 5, section 5.3.3.3. However, it is also likely that trace elements from the container, detonator and environment are contributing to these signals. A number of additional repeated experiments would need to be performed to explain whether these elements are being retained from the UN within the charge or from outside sources.

#### 6.3.3.4 Discrimination of urea nitrate using trace elemental data

Analysis of post-blast residues by ICPMS did not provide sufficient data for subsequent PCA-LDA, however, as some elements detected were consistent with those used to discriminate between pre-blast UN samples, a preliminary investigation

was performed to determine whether any information could be gained from PCA. As discussed, samples taken from witness plates directly below the charge were likely contaminated and so only those perpendicular to the charge were used. PCA was performed using trace elemental data from manganese, nickel and strontium with the distribution of samples across the first 3 PCs displayed in Figure 6.13.

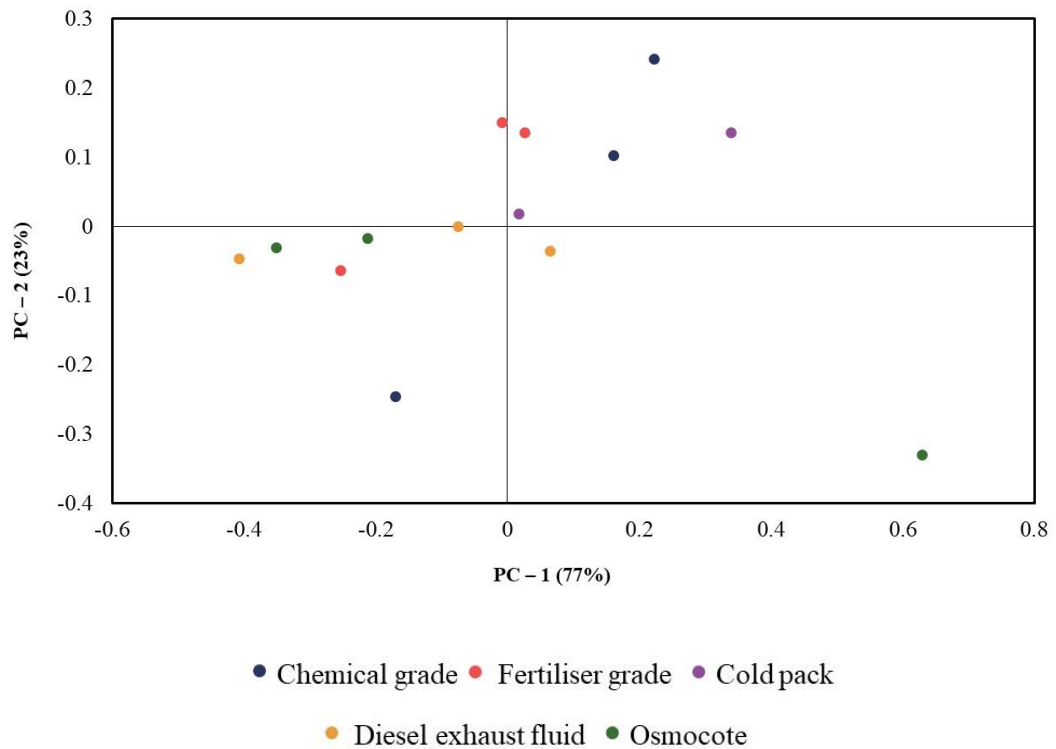


**Figure 6.13:** 2-D scores plot from PCA performed on the post-blast samples collected from various witness plates. Samples were collected from five devices that had been constructed with urea nitrate prepared from different source of urea.

The scores plot does not reveal any clear sample groupings with few samples located at the extreme ends of either PC. No discrimination was achieved which is due to the scores plot being formed using information from only three elements as well as there being little variation between classes but large variation within classes. These results, combined with previous discussions on sample contamination and experimental difficulties suggest that trace elemental analysis coupled with PCA, although proven

to be effective at discriminating between pre-blast UN, cannot be used to provide any source information from post-blast residues collected from homemade UN charges.

## **6.4 Conclusions and further work**

The experimental procedures and results presented in this chapter significantly contributes to the forensic intelligence of pyrotechnic mixtures, IEDs and homemade UN explosive. The source attribution of post-blast residues also provides further insight to the amount of source information that can be obtained from a post-blast scene.

The preparation and functionality of party sparkler and UN-based IEDs was reported. The devices constructed aimed to be representative of casework or similar to what likely could be prepared from homemade materials. Sparkler based IEDs were found to have the potential to cause large amounts of damage within a confined space. It was also confirmed that UN is detonator sensitive and does not require the need of a commercial booster or boosting material. This is the first time the sensitivity to detonation of UN has been reported as previous studies involving the firing of UN charges specify containing a commercial booster.

The source determination capabilities of using ICPMS coupled with chemometrics on post-blast residues was also explored. A 7-elemental profile was used to achieve full discrimination between the four brands used to construct devices, suggesting that different brands of sparklers can be identified from the analysis of post-blast debris. Furthermore, devices constructed with different canisters were grouped with the correct sparkler brand, indicating that the brand of sparkler could still be identified with alternative materials. LDA prediction of the samples using the unburnt model found only 55% of samples could be linked to the correct brand. However, analysis of the elemental data found that the post-blast material collected is likely to be a complex mixture of unburnt, partially burnt and post-blast debris, being more representative of unburnt material than a true post-blast sample. Therefore, to further assess this technique on post-blast residues, it is suggested that future experiments use alternative containers that produce fragmentation that can be collected and sampled, which would be more representative of post-blast material.

Controlled firings of UN-based IEDs were performed and a detailed description of the experimental design, sample collection and data analysis were reported. Samples collected from witness plates were analysed by ICPMS and it was found that only a few elements were present in quantifiable amounts that were not attributed to contamination or interference. Subsequent PCA did not reveal any discriminatory or source information and samples could not be linked to their original source of precursors used. Although the findings from UN experiments were mostly inconclusive, the experimental design and recovery and analysis protocols will aid future research regarding the source attribution of post-blast residues.

## **Chapter 7. Conclusions and future work**

## 7.1 Conclusions

The work presented in this thesis addressed a critical operational need for forensic laboratories to enhance their understanding of nitrate based homemade explosives (HMEs). As the access to precursors to manufacture HMEs has become increasingly monitored, the HME threat is constantly evolving with new compositions, synthetic methods and precursors continuing to emerge. Within a forensic investigation, the complete characterisation, identification, and source attribution of an explosive sample generates a significant amount of information that can be used to generate forensic intelligence and establish links based on previous evidence gathered. However, the forensic examination of pre- and post-blast residues is often left incomplete as analytical methodologies cease once the explosive has been identified. Therefore, this thesis aimed to improve investigative and analytical protocols by addressing fundamental knowledge gaps concerning how nitrate based HMEs are sourced and prepared as well as to determine the range of chemical and discriminatory information that can be gained from a combination of several analytical techniques.

The HMEs investigated within this work included ammonium nitrate (AN), urea nitrate (UN and nitrate-based party sparklers. Nitrourea (NU) was also explored as a potential HME that can be prepared from UN. AN and UN have a long history of use as HMEs and continue to be readily accessible within or can be prepared from commercial products. Nitrate-based party sparklers are also used to prepare HMEs and currently make up the majority of explosive-related casework in Western Australia (WA). To achieve the aims of this thesis, an investigative and analytical strategy was first devised that was then applied to each HME. This strategy aimed to explore the complete identification, characterisation and source attribution, as well as demonstrate how they can be sourced, prepared, and the capacity to prepare large amounts from accessible ingredients. This comprehensive approach was conducted in three main stages and was designed to produce a substantial amount of information that would apply to law enforcement and forensic case procedures, as well as forensic and military agencies that rely on gathered intelligence for recreating HME compositions and disrupting their commercial preparation. The stages of investigation for each HME are summarised below.



- A market study was first performed which identified the commercial products and available precursors that could be used to prepare the HME being explored. The capacity to prepare large amounts from alternatively sourced products was also investigated.
- The HME products were then characterised with a suite of analytical techniques to provide characteristic data and assess whether the information could be used for discrimination purposes. Techniques including Infrared (IR) and Raman spectroscopy, scanning electron microscopy (SEM), X-ray diffraction (XRD), gas chromatography mass spectrometry (GCMS) and ion chromatography (IC) were chosen as they are routinely used for identification of intact explosives and post-blast residues, and most would be commonplace within forensic laboratories. Although not routine, inductively coupled plasma mass spectrometry (ICPMS) was also used to identify trace species and provide quantitative data for a range of elements.
- Finally, chemometric analysis was performed to evaluate source determination capabilities and demonstrate the capacity to link explosive samples to their source. Principal component analysis (PCA) and linear discriminant analysis (LDA) were used for the interpretation of analytical data which allowed for an objective approach to identify relationships and reveal underlying trends within the complex datasets. The use of analytical instrumentation in combination with chemometrics demonstrated the amount and type of characteristic data that could be obtained as well as the capacity to accurately discriminate between sources.

#### 7.1.1 Characterisation and source attribution of nitrate based HMEs

The investigative and analytical framework described above was used to perform a comprehensive study on the preparation, identification and source attribution of AN, UN and nitrate based party sparklers. The approach proved to be extremely successful at generating a significant amount of information with respect to each HME and their precursors. The majority of the information generated has also not been previously reported as studies exploring the preparation and characterisation of alternatively

sourced inorganic HMEs are minimal. The findings from investigations of each HME are presented within Chapters 3-5, which are summarised in the sections below.

#### 7.1.1.1 Party sparklers

Despite being a readily available and affordable pyrotechnic, limited research has been conducted on the forensic characterisation and source attribution of party sparklers. Due to their continued presence within explosive casework in WA, there is a high forensic interest in the chemical analysis of sparkler residues to provide characteristic and source information, which in turn would improve the amount of evidential value they can provide. In Chapter 3, nineteen Australian sourced party sparklers were collected and analysed using multiple analytical techniques and chemometric methods. The market study confirmed that sparkler products can easily be sourced and repurposed to prepare HME mixtures or improvised devices as a packet of 24 sparklers (~25 g of sparkler material) can be obtained for as little as \$2 (AUD), highlighting their ongoing illicit use as a HME.

Physical analysis of the nineteen brands highlighted the large range of distinct sparkler products that can be obtained, however, once the residue was ground to a powder, no distinguishing features were observed. IR spectroscopy could effectively discriminate sparkler residue from other low order inorganic explosives such as black powder and could provide a preliminary identification of the oxidising agent. Additional routine forensic procedures including IC and SEM demonstrated the capability of confirming oxidiser and fuel components but could not distinguish between sources. Although not routine within the analysis of pyrotechnics, GCMS could infer whether the sample originated from a colour coated sparkler based on the presence of resin or binding compounds.

ICPMS coupled with PCA-LDA was revealed to be extremely effective at discriminating between sources. A refined elemental profile containing elements with high discriminatory power was used to fully discriminate between eight brands of unburnt and burnt party sparklers with high predictive accuracy. However, source prediction of burnt samples was inconsistent and could not accurately be linked to unburnt samples of the same brand. These findings demonstrate that chemometrics combined with trace elemental analysis has the potential to provide additional source

information beyond identifying oxidiser and fuel components, however, additional validation procedures are required to determine whether the model can consistently distinguish between similar residue types. This method could then be implemented within a forensic investigation such that if sparkler material was recovered from a device and was also found at a clandestine lab or within other forensic samples, chemometric analysis can be used to establish links based on trace elemental profiles and support previously gathered intelligence.

#### 7.1.1.2 Ammonium nitrate

Although some restrictions have been imposed on obtaining large quantities and high purity forms of AN, it was shown that it can still be sourced and prepared from a range of readily available products. Large amounts can be prepared from products such as cold packs and fertiliser mixtures, requiring little knowledge of chemical synthesis. From the market study performed, nine distinct AN products were obtained from different sources and separated into two groups: 'pure form' and homemade. Products that were sourced in their original form and did not require any further extraction or synthesis were classed as 'pure form', which included chemical grade AN, explosive grade AN and AN obtained from cold packs. Products that were synthesised from ammonium sulfate and calcium nitrate were classed as synthesised, which included products prepared from chemical reagents or varying brands of fertiliser mixtures.

IR and Raman spectroscopy, IC, SEM and XRD were all capable of distinguishing between pure and homemade AN based on characteristic data. Therefore, given an unknown sample, some source information can be quickly obtained using several routine techniques. Source determination capabilities were subsequently assessed using data from IR, XRD and ICPMS coupled with chemometrics. PCA-LDA performed with diffraction patterns could accurately discern between pure and homemade products but could not consistently distinguish between products within each group. Using IR spectral data improved source prediction capabilities as all pure products could be identified, however, products within the homemade group could not be discerned. The capacity to rapidly distinguish between pure products is extremely beneficial within a forensic investigation, as sourcing and storing chemical or explosive grade AN may be illegal without proper licensees, whereas possession of AN based cold packs is not. Repeated analysis using trace elemental data demonstrated

that full discrimination between all pure and homemade AN products could be achieved using the concentrations from ten elements, indicating that an AN sample of questionable source can be linked back to the products used within synthesis as well as specific fertiliser brands.

#### 7.1.1.3 Urea nitrate

As UN has no legitimate uses outside of industry, it cannot be sourced directly from commercial products. However, homemade UN can easily be prepared from urea, which remains unregulated and so could become the preferred choice as a fertiliser based HME. Like AN, highly pure UN can be prepared with cold packs or fertiliser products as well as diesel exhaust fluid (DEF), which contains urea dissolved in water. In a similar fashion to the AN investigations, eight UN products were characterised using an array of analytical techniques and a substantial amount of characteristic data was reported. While IC, SEM and XRD could identify that a UN product was prepared from a fertiliser mixture, ICPMS was the only technique capable of discerning between the remaining sources based on minor variation across elemental profiles. These results showed that routine analysis can easily identify an unknown sample as UN, but more advanced instrumentation is required to provide additional source information.

Although many analytical techniques were used to provide characteristic information on several UN products, subsequent research into the identification of potential route-specific by-products is critical to improving our understanding of UN as a HME. Previous work by Oxley *et al.* has reported the identification of several by-products within synthesised UN by LCMS (75). The various urea precursors used to prepare UN may contain urea derivatives such as biuret and triuret, which have the potential to form distinctive by-products during synthesis that could be identified by LC methods and aid in distinguishing between UN sources. The capacity to effectively discriminate between UN and its precursors with techniques other than ICPMS would provide laboratories equipped with different analytical instrumentation the ability to identify the source of seized UN and aid in explosive investigations.

PCA-LDA performed with elemental data was extremely effective as all UN products could be identified across two models, using the concentration from four elements.

These results show that by applying this method to an explosive sample identified as UN, it can subsequently be linked to a specific urea product and can also discern between distinct fertiliser brands. Comparable to the source prediction of AN using elemental data, the model's predictive accuracy is limited based on a small dataset and so additional validation studies are required to improve reliability and source prediction capabilities.

Characteristic spectra and elemental profiles were also reported for seven NU products prepared from homemade UN. Although making NU is more complex and resulted in low yields, it remains a powerful HME that can be prepared from commercial products. Chemometric analysis demonstrated that the NU products could be discriminated based on the minor variation within elemental profiles, however, they did not correlate to the respective UN precursors.

### 7.1.2 Recovery and source attribution of nitrate based IEDs

In addition to the extensive investigations performed on pre-blast HMEs, Chapter 6 applied the methodologies established in previous chapters to the forensic characterisation and source determination of post-blast residues. Post-blast investigations are crucial for assessing the performance of previously established analytical protocols on real samples representative of residues that may be found at a post-blast scene. Despite their importance, few studies can be found on the chemical analysis or source determination of post-blast residues. This is partly due to several difficulties resulting from the increased risk involved, insufficient funding and the need for effective collaboration with law enforcement. Additionally, studies that have reported the analysis of post-blast residues typically focus on the identification of the explosives present with no further attempt to link them to a source. A large amount of evidentiary value could be gained from knowing the source of the explosive and precursors used to prepare an improvised explosive device (IED) and so there is a need for ongoing post-blast studies to improve source determination capabilities.

The preparation and functionality of party sparkler and UN-based IEDs are described in Chapter 6. Sparkler based devices were constructed to imitate IEDs commonly seized in WA, which were found to have high destructive potential within a confined space. It was also confirmed that UN is detonator sensitive and does not require the

need of a commercial booster or boosting material, which is an extremely valuable contribution to the intelligence of UN as a HME. The experimental design and analytical methods presented allowed for a direct comparison between the forensic characterisation of post-blast samples from low-order and high-order HMEs and highlighted the additional challenges presented in conducting post-blast experiments. A summary of the post-blast investigations is detailed below.

#### 7.1.2.1 Sparkler based IEDs

Intact post-blast material was recovered from controlled firings of several improvised devices prepared using party sparklers from four different brands. ICPMS coupled with PCA-LDA was used to demonstrate that all brands used could be discerned based on the variation observed across seven elements, indicating that the source of sparkler material can potentially be identified from analysis of post-blast debris. Furthermore, additional firings with different canister types revealed that the correct sparkler brand could still be identified. However, projection of the samples onto the unburnt sparkler model found that approximately half of the samples did not correlate to the respective unburnt sample of the same brand. Further analysis also showed that the post-blast material collected was likely to be a complex mixture of unburnt, burnt and post-blast debris, rather than being representative of a true post-blast sample. Therefore, to further assess source attribution capabilities of post-blast sparkler residues, future experiments should be performed such that alternative containers that produce higher amounts of fragmentation are used. Fragmented debris can be collected and sampled, which would be more representative of a post-blast sample recovered from a low-order device within casework.

#### 7.1.2.2 Urea nitrate based IEDs

The recovery and analysis of post-blast residues from UN based charges resulted in limited findings due to several impacting factors relating to the experimental design and environment in which experiments took place. A total of five 200g charges were prepared and detonated, each containing UN prepared from a different source of urea. Minimal amounts of residue were recovered from witness plates surrounding each charge and analysed by ICPMS to reveal only a few elements were present in quantifiable amounts that were not attributed to contamination or interference.

Subsequent PCA could not provide any additional discriminatory or source information.

Although the use of trace elemental profiles to link post-blast UN residues to a specific urea precursor proved ineffective, the experimental data presented can be used in subsequent studies to further assess source attribution capabilities of this technique. Ideally, future experiments would be performed in a sterile location with minimal environmental impact before being applied to an unconfined scene representative of a real-life scenario. The experimental design and recovery and analysis protocols will also aid future research regarding the conduct and chemical analysis of post-blast residues from high order explosives.

## **7.2 Future work and applications**

The overall investigative strategy described and outlined across Chapters 3-6 could be further adapted and applied within future pre- or post-blast investigations of any HME that is currently in frequent use or yet to emerge. Comparable to the nitrate based HMEs investigated, chlorate and perchlorate salts are often used to prepare inorganic HMEs and can be prepared from several commercial products and synthetic pathways. A chlorate based IED was most notably used in the Bali bombing attacks, which involved a homemade potassium chlorate charge mixed with sulfur and aluminium powder. Characterisation and source attribution studies performed on chlorate and perchlorate based explosives would complement the information provided within this thesis to further contribute to the forensic intelligence of explosives and improve our understanding of inorganic HMEs.

The source attribution techniques described could also benefit the investigation of peroxide based HMEs such as TATP or HMTD, which have been used in several high profile incidents and are similarly prepared from commercial ingredients including hydrogen peroxide, acetone and hexamine. The capacity to discern between brands and forms of acetone and hexamine could generate leads and introduce or eliminate specific lines of enquiry within an investigation. However, due to the sensitivity of peroxide based explosives, research of peroxides presents extreme risk and would require major collaboration with numerous law enforcement and government

agencies, meaning many research laboratories would not have the capability to prepare and analyse peroxide based HMEs.

Across investigations of each HME, it was clear that elemental profiling coupled with chemometrics was highly successful at discriminating between sources and linking HME samples to a specific precursor product. A current limitation of this method was seen in validating the discriminant models. Due to a small dataset, a 'leave one out' approach was performed and could only provide an indication of the predictive accuracy; however, a more reliable method can be performed that involves the use of a large test set completely independent from the training set. Therefore, to increase the predictive accuracy of the models generated, future work should also focus on performing additional validation procedures with a larger and more diverse dataset. Expanding the models to include more distinctly sourced products is also necessary to improve reliability and source prediction capabilities, as described below.

To improve source prediction capabilities of AN, this process should include the analysis of AN prepared from more products (e.g. alternative fertiliser mixtures), brands (e.g. alternative cold pack and fertiliser brands), different batches (fertiliser products purchased at different times), different nitrate salts, as well as common AN mixtures such as AN/sugar, ammonium nitrate fuel oil (ANFO) or AN/aluminium. For nitrate based party sparklers, more distinct brands as well as a range of pyrotechnic products and mixtures incorporating different fuel/oxidiser compositions would improve the predictive efficacy of the model. For homemade UN, in addition to expanding the model with more distinct sources of urea, future studies should also focus on preparing UN from homemade nitric acid. As the preparation of UN is limited by the availability of concentrated nitric acid, the feasibility of preparing large amounts of acid using different synthetic methods and commercial products warrants investigation. UN products prepared from distinct sources of nitric acid can also be used to expand the predictive model so that products prepared using homemade nitric acid can be identified and linked to the precursors used.

Beyond increasing the number of unique AN and UN sources, source prediction capabilities and knowledge of HME sources could further be improved by conducting large scale population surveys of key precursors over longer time frames. Although a substantial amount of characteristic data was reported for known and emerging



precursors and HMEs, long-term variation of these products was not investigated. Within Chapter 3, the discrimination of various party sparkler brands was achieved with a small number of trace elements, which may not have been intentionally added by the manufacture and therefore may change over time. Variation in manufacturing conditions or quality and availability of ingredients would alter the trace composition of batch made sparklers, and so a long-term study investigating changes in their elemental profile is essential for using this source attribution method effectively in forensic casework. This also applies to several of the AN and UN precursors investigated, in particular the fertiliser and DEF products. Within-batch and between-batch variation should be investigated over time to improve the reliability and robustness of the method described in this work.

In addition to increasing the diversity of the predictive models, combining elemental data with isotope ratio profiles from IRMS could further improve source prediction capabilities, as has been shown previously with AN (73). Despite demonstrating full discrimination could be achieved between HME sources using trace elemental data, isotopic profiling of precursors, synthesised products, and HMEs of varying purity may improve the accuracy and confidence associated with source prediction. Furthermore, this could also improve the capacity to link burnt and post-blast residues back to their original source, which was shown to be less successful. The use of multiple profiling techniques could also be particularly beneficial in the source attribution of NU, which was shown to be more difficult as little trace elemental variation existed between products after being synthesised from UN.

### **7.3 Summary**

In summary, this thesis has presented a comprehensive investigation of the preparation, forensic characterisation and source attribution of several nitrate based HMEs to address the fundamental knowledge gaps in the research literature, as well as improving investigative and analytical protocols within forensic investigations of explosive incidents. Initial studies performed into the feasibility of preparing large amounts of HME material from commercial sources provided a substantial amount of information that will assist various agencies and personnel that rely on previously established intelligence for the disruption, forensic analysis or identification of HMEs. The significant volume of pre- and post-blast chemical data and source information

that can be obtained from selected routine and non-routine analytical techniques has been highlighted. This greatly benefits the forensic chemical analysis of HMEs by reducing the uncertainty surrounding HME identification and demonstrates the capability and limitations of these techniques in providing source information. Finally, although additional data types were also explored, the source prediction capabilities of using trace elemental data with chemometrics proved the most effective at discriminating and identifying precursor sources. This technique was capable of discriminating between all HME sources investigated throughout this study and was also used to identify the source of post-blast residues recovered from sparkler based IEDs. The investigative and analytical processes presented significantly contributes to the forensic intelligence of nitrate based HMEs and lays the groundwork for future explosive related investigations to improve our understanding of energetic materials.

## **Appendix A – Supplementary figures**

**Figure A.1:** Images of party sparkler products used throughout this study. Party sparklers have been photographed in the packet as they were purchased (top row) and individually (bottom row). Party sparklers have been labelled according to their sample name as detailed in Table 3.1.



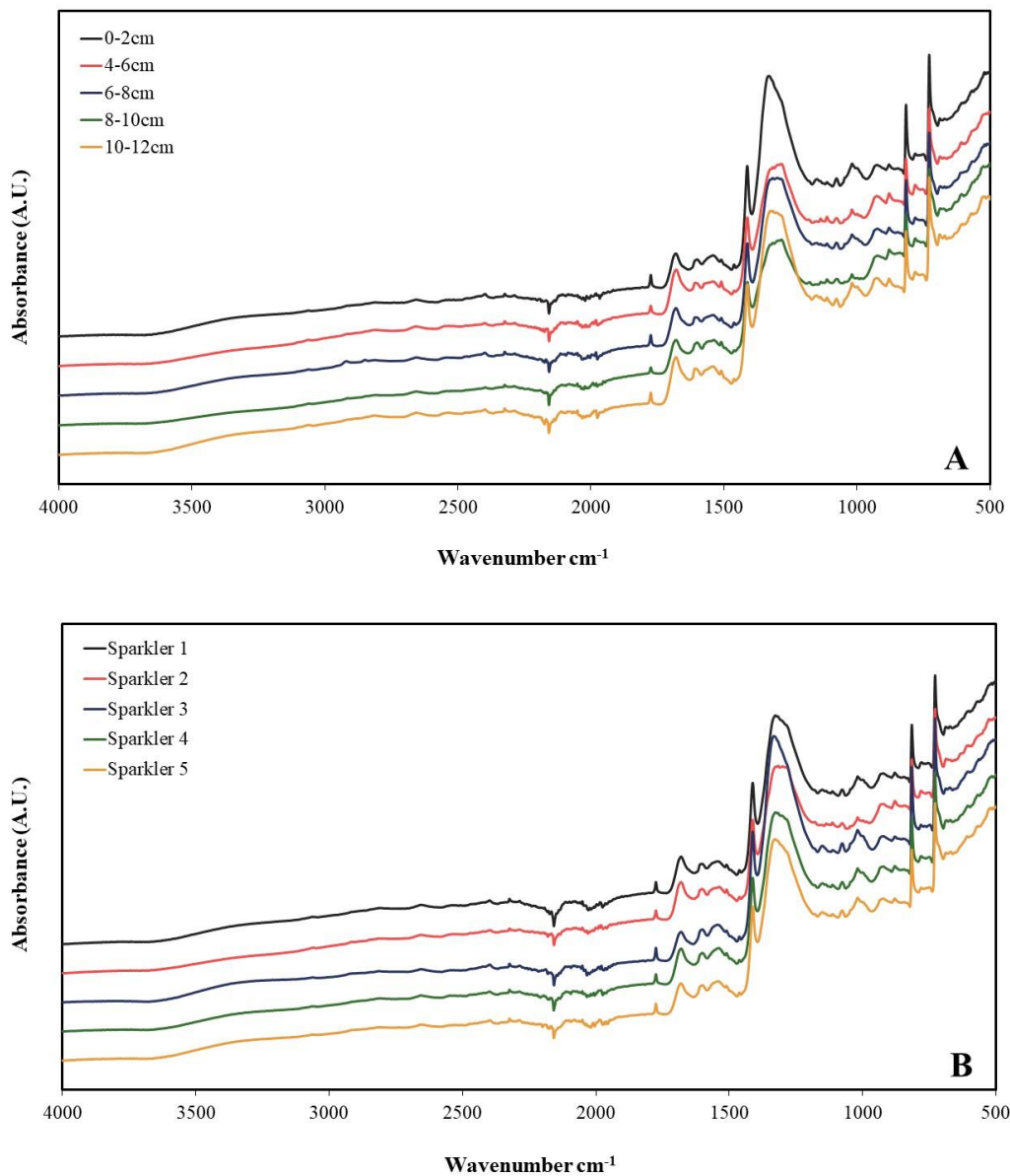


**Figure A.2:** ATR-FTIR spectra of party sparkler from the PC brand. Spectra of five two cm sections of a single sparkler (a) and of five individual sparklers from the same packet (b). Both show no discernible difference between samples. Spectra has been offset for better visualisation of individual samples.

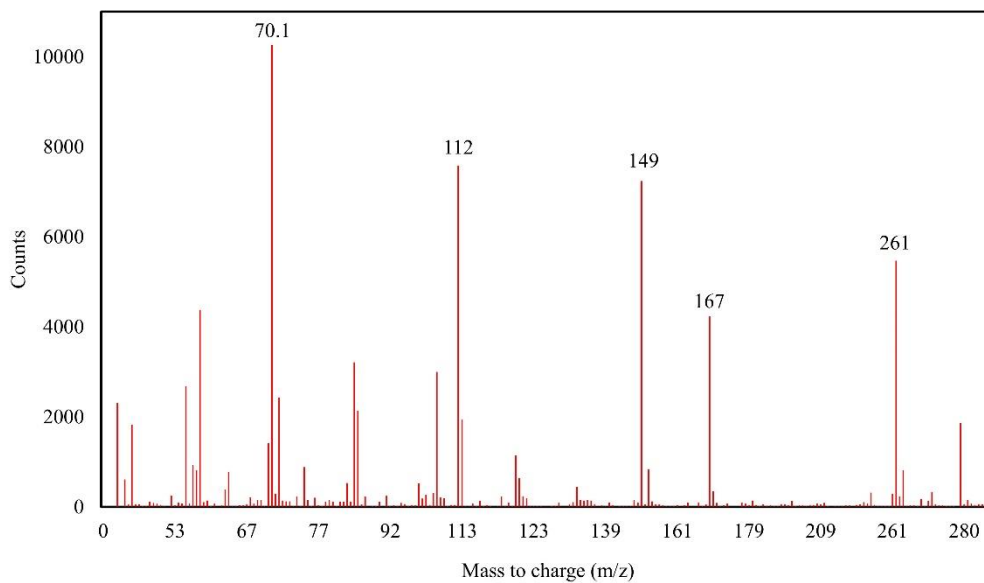


**Figure A.3:** Mass spectrum of the terephthalic acid (PTA) peak (25.1 minutes) detected from GCMS analysis of the blue, pink, purple and green Artwrap branded party sparklers.

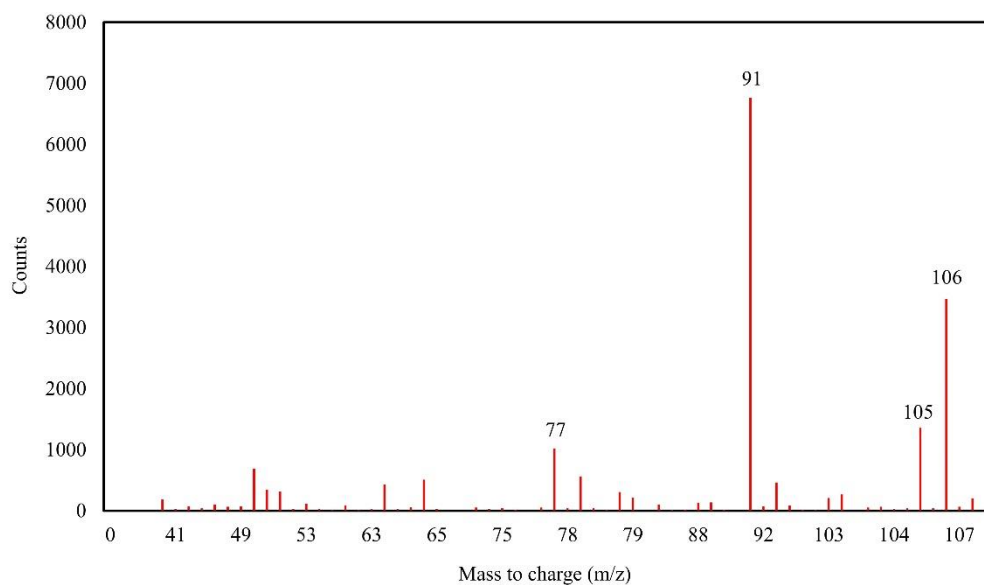


**Figure A.4:** Mass spectrum of the paraxylene peak (7.6 minutes) detected from GCMS analysis of gold coated Artwrap branded party sparkler.

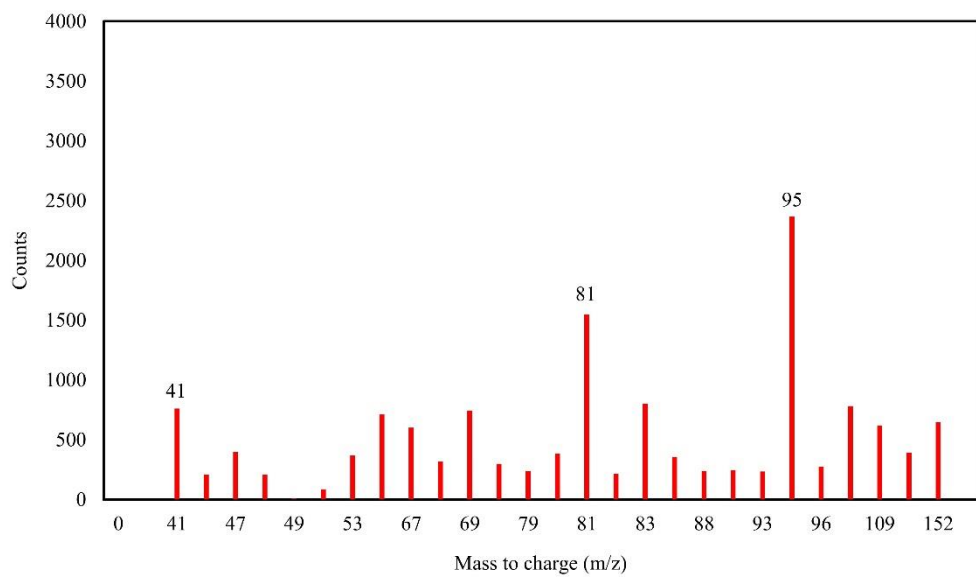


**Figure A.5:** Mass spectrum of the 2-bornanone peak (12.1 minutes) detected from GCMS analysis of silver coated Artwrap branded party sparkler.

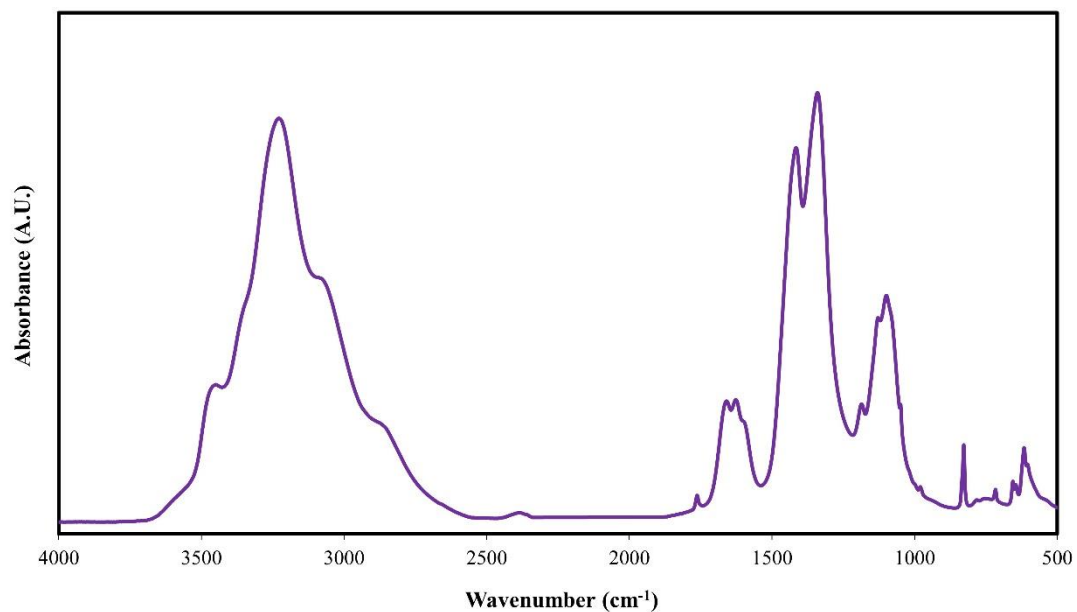


**Figure A.6:** Individual ATR-FTIR spectra of AN prepared from African Violet Food fertiliser product. The presence of several additional peaks allowed for the product prepared from this fertiliser to be discerned from other homemade AN products.

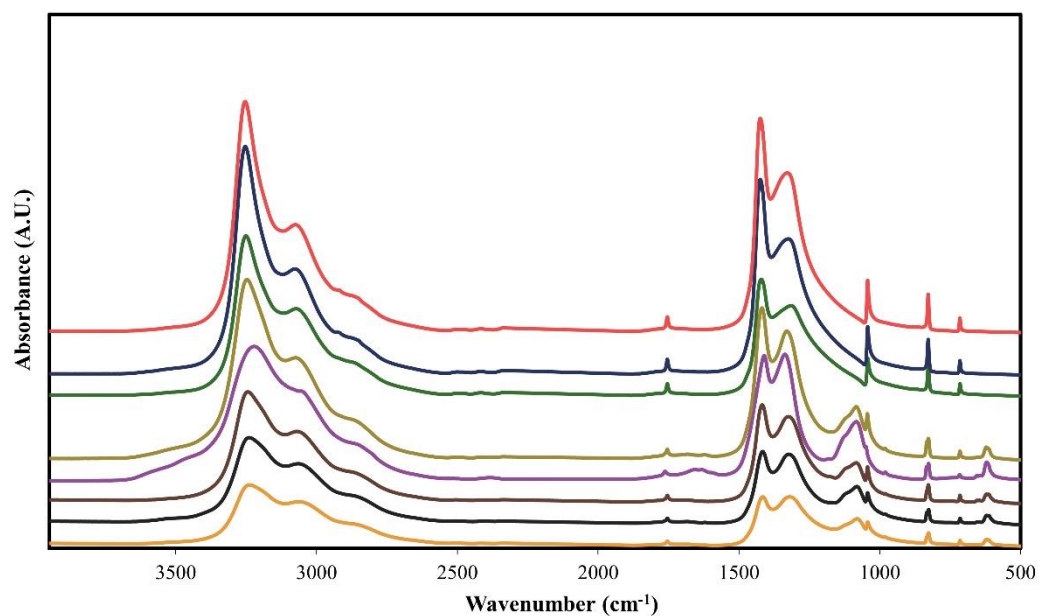


**Figure A.7:** ATR-FTIR spectra of all pure form and homemade AN products. Stacked spectra highlights additional peaks present within the homemade products within the 1100 – 600  $\text{cm}^{-1}$  region. (baseline has been offset for better visualisation of individual spectra).



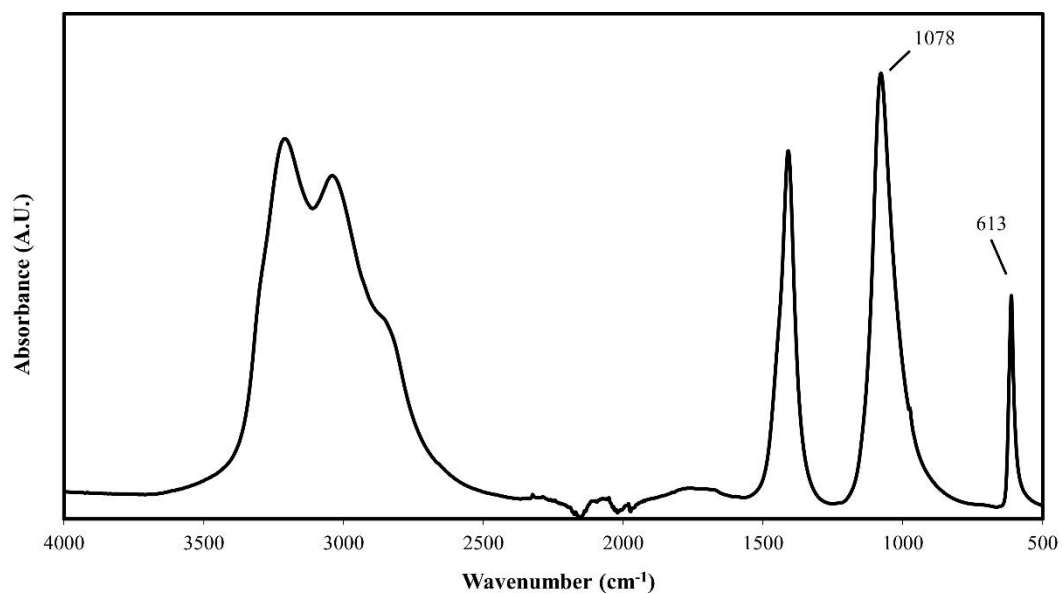


**Figure A.8:** Individual ATR-FTIR spectra of commercial (Richgro brand) sulfate of ammonia fertiliser. Labelled peaks align closely with those observed in the homemade AN products.

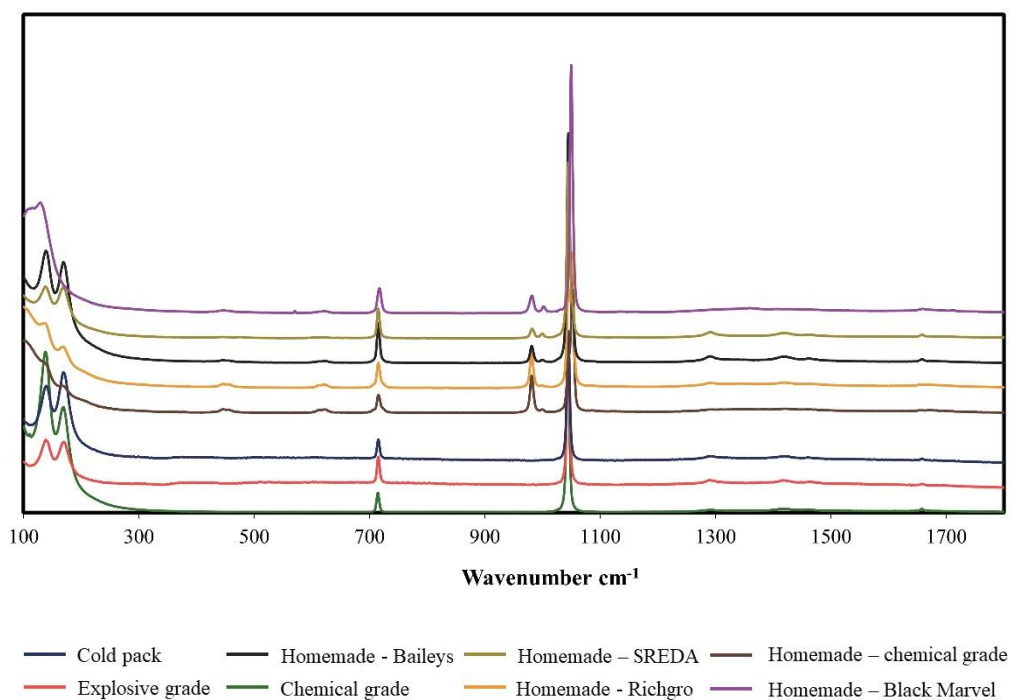


**Figure A.9:** Raman spectra of all AN products (baseline has been offset for better visualisation). Stacked spectra highlights additional peaks present within the homemade products within the 1100 – 700 cm⁻¹ region.

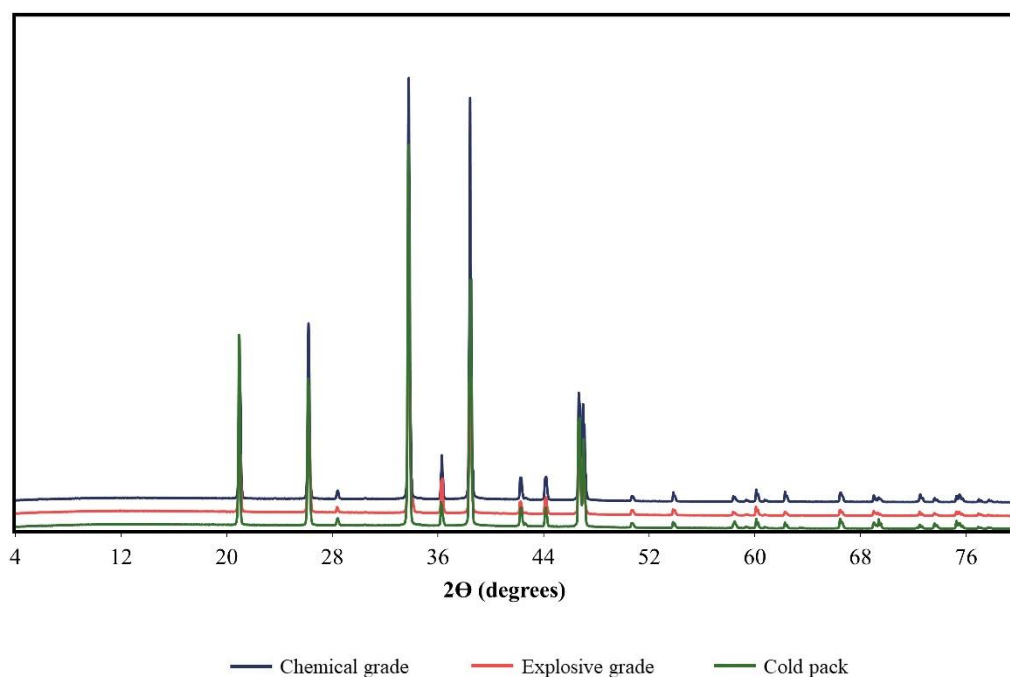


**Figure A.10:** X-ray diffraction patterns of pure form AN products (baseline has been offset for better visualisation).

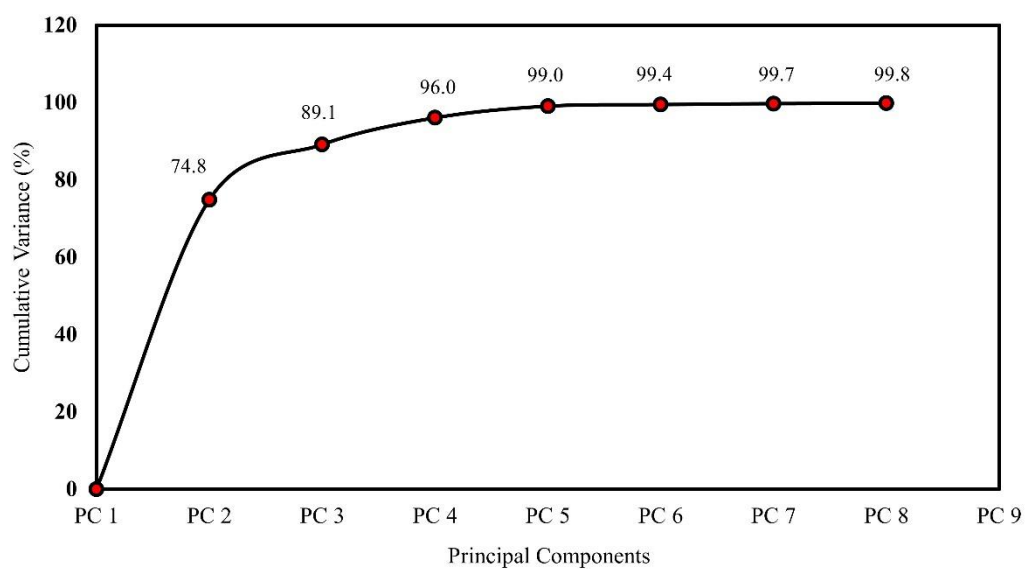


**Figure A.11:** Scree plot associated with the discriminant model generated using ATR-FTIR spectral data collected from eight AN products. The plot shows the cumulative variance accounted for by each successive PC.

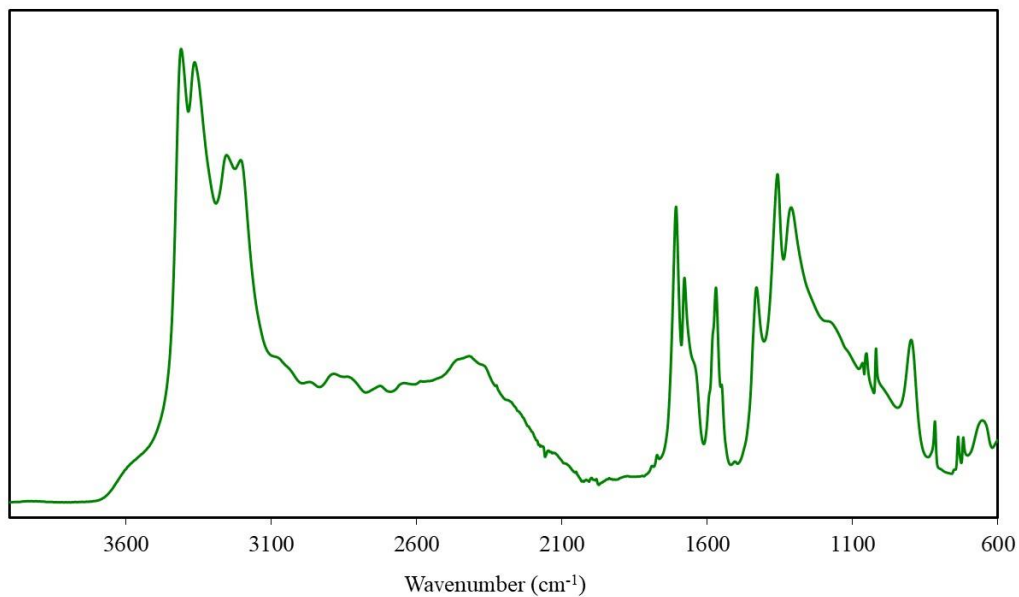


**Figure A.12:** ATR-FITR spectrum of the UN product prepared from Green Boost fertiliser. The presence of several additional peaks allowed for the product prepared from this fertiliser to be discerned from other synthesised UN products.

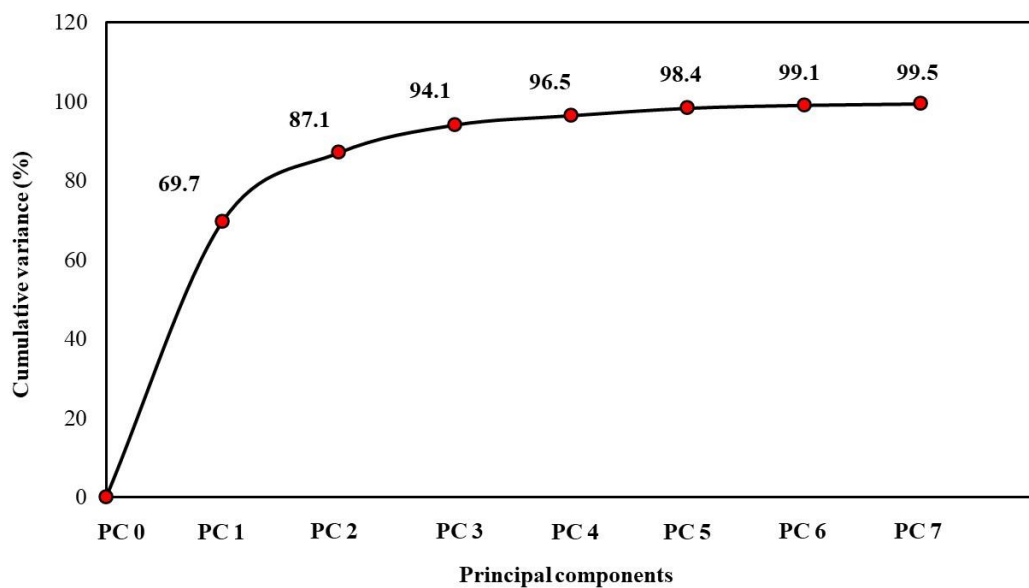


**Figure A.13:** Scree plot associated with the discriminant model generated using ATR-FITR spectral data collected from seven UN products. The plot shows the cumulative variance accounted for by each successive PC.

## **Appendix B – Supplementary table data**

**Table B.1:** Concentration of barium and nitrate ions within 100 mg of sparkler material from the ASilver brand. Eight samples were prepared and analysed from ground and unground material.

Sample number	Ionic species	
	Ba <sup>2+</sup>	NO <sub>3</sub> <sup>-</sup>
<b>Ground residue</b>		
<b>1</b>	82.5	75.4
<b>2</b>	81.0	73.6
<b>3</b>	80.1	72.8
<b>4</b>	77.5	70.2
<b>5</b>	78.7	71.1
<b>6</b>	72.4	65.9
<b>7</b>	77.5	70.1
<b>8</b>	76.8	69.6
<b>Total average</b>	78.3 ± 2.9	71.1 ± 2.7
<b>Unground residue</b>		
<b>1</b>	47.9	43.3
<b>2</b>	46.6	42.2
<b>3</b>	29.0	26.5
<b>4</b>	45.3	41.0
<b>5</b>	36.3	33.1
<b>6</b>	30.0	27.5
<b>7</b>	31.6	29.0
<b>8</b>	38.4	35.0
<b>Total average</b>	38.1 ± 7.2	34.7 ± 6.4

**Table B.2:** ICP-MS analysis of refined sparkler sample set that shows the average concentration (ppb) of elements found in 100 mg of unburnt sparkler residue. Elements that were present due to contamination or present below the calibration range were removed resulting in the concentration of 22 elements being reported.

<b>Brand</b>	<b>Ti</b>	<b>V</b>	<b>Cr</b>	<b>Mn</b>	<b>Co</b>	<b>Ni</b>	<b>Cu</b>	<b>Zn</b>
<b>WLP</b>	828 ± 32%	307 ± 6%	2.57 x 10 <sup>3</sup> ± 4%	1.26 x 10 <sup>4</sup> ± 4%	3.37 x 10 <sup>3</sup> ± 5%	757 ± 1%	1.94 x 10 <sup>3</sup> ± 3%	4.85 x 10 <sup>3</sup> ± 12%
<b>Artwrap</b>	317 ± 6%	138 ± 2%	4.63 x 10 <sup>3</sup> ± 8%	1.37 x 10 <sup>4</sup> ± 3%	3.18 x 10 <sup>3</sup> ± 1%	4.68 x 10 <sup>3</sup> ± 2%	3.88 x 10 <sup>3</sup> ± 3%	4.34 x 10 <sup>3</sup> ± 8%
<b>T2P</b>	499 ± 8%	206 ± 4%	3.78 x 10 <sup>3</sup> ± 10%	1.32 x 10 <sup>4</sup> ± 9%	2.23 x 10 <sup>3</sup> ± 4%	4.03 x 10 <sup>3</sup> ± 6%	4.65 x 10 <sup>3</sup> ± 4%	1.13 x 10 <sup>4</sup> ± 6%
<b>Korbond</b>	633 ± 12%	120 ± 4%	2.55 x 10 <sup>3</sup> ± 7%	1.45 x 10 <sup>4</sup> ± 3%	2.46 x 10 <sup>3</sup> ± 4%	689 ± 6%	2.26 x 10 <sup>3</sup> ± 8%	2.90 x 10 <sup>3</sup> ± 4%
<b>PC</b>	485 ± 9%	150 ± 3%	3.04 x 10 <sup>3</sup> ± 9%	1.21 x 10 <sup>4</sup> ± 5%	2.44 x 10 <sup>3</sup> ± 3%	743 ± 9%	3.05 x 10 <sup>3</sup> ± 3%	9.57 x 10 <sup>3</sup> ± 7%
<b>FC</b>	537 ± 25%	272 ± 11%	1.85 x 10 <sup>3</sup> ± 10%	1.13 x 10 <sup>4</sup> ± 3%	6.09 x 10 <sup>3</sup> ± 3%	503 ± 3%	1.45 x 10 <sup>3</sup> ± 2%	2.94 x 10 <sup>4</sup> ± 3%
<b>FF</b>	4.75 x 10 <sup>3</sup> ± 10%	554 ± 2%	666 ± 2%	2.59 x 10 <sup>3</sup> ± 2%	1.05 x 10 <sup>3</sup> ± 4%	633 ± 2%	2.30 x 10 <sup>3</sup> ± 2%	1.29 x 10 <sup>4</sup> ± 13%
<b>Wizard</b>	1.09 x 10 <sup>3</sup> ± 4%	204 ± 11%	3.80 x 10 <sup>3</sup> ± 9%	1.48 x 10 <sup>4</sup> ± 5%	2.16 x 10 <sup>3</sup> ± 4%	1.32 x 10 <sup>3</sup> ± 37%	2.54 x 10 <sup>3</sup> ± 13%	8.81 x 10 <sup>3</sup> ± 26%
	<b>Ga</b>	<b>Sr</b>	<b>Nb</b>	<b>Mo</b>	<b>Sn</b>	<b>Sb</b>	<b>Ba</b>	<b>La</b>
<b>WL2P</b>	121 ± 3%	7.41 x 10 <sup>3</sup> ± 6%	6.3 ± 11%	215 ± 10%	46.5 ± 5%	40.0 ± 5%	2.18 x 10 <sup>6</sup> ± 8%	25.5 ± 7%
<b>Artwrap</b>	108 ± 1%	9.46 x 10 <sup>3</sup> ± 4%	4.7 ± 4%	316 ± 8%	59.1 ± 15%	36.2 ± 5%	2.35 x 10 <sup>6</sup> ± 6%	28.1 ± 17%
<b>T2P</b>	120 ± 3%	6.64 x 10 <sup>4</sup> ± 3%	7.2 ± 10%	728 ± 13%	67.1 ± 4%	26.1 ± 3%	2.22 x 10 <sup>6</sup> ± 11%	27.0 ± 15%

<b>Korbond</b>	107 ± 4%	9.82 x 10 <sup>3</sup> ± 5%	5.8 ± 16%	233 ± 16%	73.3 ± 3%	45.1 ± 6%	2.16 x 10 <sup>6</sup> ± 12%	13.3 ± 11%
<b>PC</b>	109 ± 2%	1.64 x 10 <sup>3</sup> ± 5%	4.4 ± 17%	464 ± 36%	69.9 ± 6%	30.4 ± 11%	2.05 x 10 <sup>6</sup> ± 12%	21.0 ± 34%
<b>FC</b>	104 ± 2%	1.12 x 10 <sup>3</sup> ± 6%	6.6 ± 6%	141 ± 5%	33.9 ± 10%	13.9 ± 5%	2.28 x 10 <sup>6</sup> ± 9%	14.6 ± 10%
<b>Firefox</b>	152 ± 1%	1.72 x 10 <sup>4</sup> ± 6%	14.3 ± 11%	92 ± 1%	388 ± 2%	84.2 ± 2%	2.55 x 10 <sup>6</sup> ± 11%	23.7 ± 8%
<b>Wizard</b>	111 ± 5%	1.93 x 10 <sup>3</sup> ± 6%	7.9 ± 12%	694 ± 19%	75.5 ± 19%	33.4 ± 10%	2.73 x 10 <sup>6</sup> ± 11%	48.7 ± 10%
	Ce	Eu	Sm	Gd	W	Pb		
<b>WL2P</b>	57.8 ± 5%	20.2 ± 10%	84.5 ± 8%	12.5 ± 11%	28.4 ± 7%	64.2 ± 8%		
<b>Artwrap</b>	35.4 ± 26%	22.1 ± 10%	88.6 ± 7%	12.6 ± 5%	45.2 ± 4%	206 ± 17%		
<b>T2P</b>	67.5 ± 8%	20.6 ± 13%	84.0 ± 14%	11.9 ± 8%	26.4 ± 9%	318 ± 4%		
<b>Korbond</b>	8.2 ± 10%	20.7 ± 10%	82.5 ± 12%	11.8 ± 14%	24.0 ± 13%	393 ± 6%		
<b>PC</b>	25.9 ± 27%	20.2 ± 14%	76.8 ± 12%	11.3 ± 13%	22.1 ± 12%	383 ± 4%		
<b>FC</b>	9.0 ± 7%	22.0 ± 7%	84.4 ± 7%	12.6 ± 7%	20.1 ± 5%	347 ± 18%		
<b>Firefox</b>	29.8 ± 8%	23.8 ± 13%	93.9 ± 12%	14.5 ± 12%	213 ± 2%	182 ± 2%		
<b>Wizard</b>	95.9 ± 11%	25.0 ± 11%	101 ± 11%	14.9 ± 15%	24.1 ± 9%	113 ± 8%		

## Chapter 8. References

1. Yeager K. *Improvised Explosives Characteristics, Detection, and Analysis. Forensic Investigation of Explosions*. 2nd ed. Boca Raton, FL: CRC Press; 2012. p. 493-538.
2. Doyle S. *Improvised Explosives. Encyclopedia of Forensic Sciences*. 2 ed: Elsevier; 2013. p. 98-103.
3. Maria-Georgeta S, Emilian C. *Categories of high-explosives used in committing terrorist attacks. Physical-chemical examination of post-blast explosive residues. Forensic Science No 5*. 2017;18(113).
4. Committee, on Defeating Improvised Explosive Devices: Basic Research to Interrupt the IED Delivery Chain et al. *Countering the Threat of Improvised Explosive Devices: Basic Research Opportunities* 1ed: National Academies Press; 2007.
5. National Research Council et al. *The Principles of Science and Interpreting Scientific Data. Strengthening Forensic Science in the United States: A Path Forward*: National Academies Press; 2009. p. 111-26.
6. National Research Council et al. *Descriptions of Some Forensic Science Disciplines. Strengthening Forensic Science in the United States: A Path Forward*: National Academies Press; 2009. p. 127-82.
7. Caddy B, Cobb P. *Forensic Science. Crime Scene to Court: The Essentials of Forensic Science*. 2 ed. Cambridge, UK: Royal Society of Chemistry; 2004.
8. Strobel RA. *Recovery of Material from the Scene of an Explosion and Its Subsequent Forensic Laboratory Examination - A Team Approach Forensic Investigation of Explosions* Boca Raton, FL: CRC Press; 2012. p. 119-58.
9. Vermette J. *General Protocols at the Scene of an Explosion Forensic Investigation of Explosions* Boca Raton, FL: CRC Press; 2012. p. 79-118.
10. Royds D, Lewis SW, Taylor AM. *A case study in forensic chemistry: The Bali bombings. Talanta*. 2005;67:262-8.



11. Benson S, Speers N, Otieno-Alego V. Portable Explosive Detection Instruments Forensic Investigation of Explosions Boca Raton, FL: CRC Press; 2012. p. 691-724.
12. Tamiri T, Zitrin S. Explosives: Analysis. Encyclopedia of Forensic Sciences. 2 ed: Elsevier; 2013. p. 64-84.
13. Janesheski RS, Groven LJ, Son SF. Detonation Failure Characterization of Homemade Explosives. Propellants, Explosives, Pyrotechnics. 2014;39(4):609-16.
14. Nazarian A, Presser C. Forensic analysis methodology for thermal and chemical characterization of homemade explosives. Thermochemica Acta. 2014;576:60-70.
15. National Research Council et al. Improving Methods, Practice, and Performance in Forensic Science. Strengthening Forensic Science in the United States: A Path Forward: National Academies Press; 2009. p. 183-92.
16. Nazarian A, Presser C. Forensic methodology for the thermochemical characterization of ANNM and ANFO homemade explosives. Thermochemica Acta. 2015;608:65-75.
17. Zapata F, Garcia-Ruiz C. Chemical Classification of Explosives. Crit Rev Anal Chem. 2021;51(7):656-73.
18. Davis DTL. Properties of Explosives. The Chemistry of Powder and Explosives San Francisco: Hauraki Publishing 2016.
19. Crippin JB. Explosions. Encyclopedia of Forensic Sciences. 2 ed: Elsevier; 2013. p. 104-8.
20. Goodpaster J. Explosives. Forensic Chemistry: Fundamentals and Applications: John Wiley & Sons, Inc; 2015.
21. Jones L, Marshall M. Explosions Crime Scene to Court: The Essentials of Forensic Science. Cambridge, UK: Royal Society of Chemistry 2004. p. 241-68.
22. Akhavan J. Classification of Explosive Materials The Chemistry of Explosives 3ed. Cambridge, UK: Royal Society of Chemistry; 2011.
23. Yu HA. Novel approaches to forensic explosives recovery, storage and analysis. Perth (Australia): Curtin University; 2017.

24. Sauzier GY. Applications of Chemometrics to the Analysis and Interpretation of Forensic Physical Evidence: Curtin University; 2016.
25. Akhavan J. Combustion, Deflagration and Detonation. The Chemistry of Explosives Cambridge, UK: Royal Society of Chemistry 2011. p. 60-73.
26. Fatah AA, Arcilesi Jr RD, McClintock JA, Lattin CH, Helinski M, Hutchings M. Guide for the Selection of Explosives Detection and Blast Mitigation Equipment for Emergency First Responders U.S. Department of Homeland Security; 2008.
27. Bolz Jr F, Dudonis KJ, Schulz DP. Energetic Materials and Explosive Devices. The Counterterrorism Handbook: Tactics, Procedures, and Techniques 3ed. Boca Raton, FL: CRC Press; 2012. p. 241-60.
28. Murray SG. Military. Encyclopedia of Forensic Sciences. 2 ed: Elsevier; 2013. p. 92-7.
29. Hopler RB. The History, Development, and Characteristics of Explosives and Propellants. Forensic Investigation of Explosions Boca Raton, FL: CRC Press; 2012. p. 1-17.
30. Murray SG. Commercial. Encyclopedia of Forensic Sciences. 2 ed: Elsevier; 2013. p. 85-91.
31. Akhavan J. Introduction to Explosives. The Chemistry of Explosives Cambridge, UK: Royal Society of Chemistry; 2011. p. 1-26.
32. Beveridge AD. Improvised Explosive Devices. Encyclopedia of Forensic Sciences. 2 ed: Elsevier; 2013. p. 59-63.
33. McCurry PM. The Use of Advanced Analytical Tehcniques to Enable Batch and Source Matching of Homemade Explosives: Flinders University; 2015.
34. Marshall M, Oxley JC. Explosives: The Threats and the Materials. Aspects of Explosives Detection. Radarweg: Elsevier; 2008. p. 11-26.
35. JCAT. Triacetone Triperoxide (TATP): Indicators of Acquisition and Manufacture, and Considerattions for Response 2019.
36. Quaresma J. Homemade Explosives based in Ammonium and Urea nitrates: Universidade de Coimbra; 2013.

37. Harris HA, Lee HC. Arsons and Explosives. Introduction to Forensic Science and Criminalistics 2ed. Milton: Taylor & Francis Group; 2019.
38. Tilstone WJ. Explosions and Explosives. Forensic Science: An Encyclopedia of History, Methods and Techniques ABC-CLIO; 2006. p. 137-8.
39. National Research Council et al. Disrupting Improvised Explosive Device Terror Campaigns. 1 ed: National Academies Press; 2008.
40. Barker AD. Improvised Explosive Devices in Southern Afghanistan and Western Pakistan, 2002–2009. Studies in Conflict & Terrorism. 2011;34(8):600-20.
41. The National Academies. IED Attack Fact Sheet: Improvised Explosive Devices: Homeland Security.; 2022.
42. Collett G. An examination of the precursor chemicals used in the manufacture of explosive compositions found within Improvised Explosive Devices (IEDs): Action on Armed Violence; 2021. 44 p.
43. Glines TC. Resistance or Terrorism? The 1970 Sterling Hall Bombing. The Journal of American History 2006;93(1).
44. BBC. IRA Bomb devastates City of London: On This Day 1950-2005; 1993 [Available from: [http://news.bbc.co.uk/onthisday/hi/dates/stories/april/24/newsid\\_2523000/2523345.stm](http://news.bbc.co.uk/onthisday/hi/dates/stories/april/24/newsid_2523000/2523345.stm)].
45. Parachini JV. World Trade Center Bombers (1993): U.S. Department of Justice; 2000 [Available from: <https://www.ojp.gov/ncjrs/virtual-library/abstracts/world-trade-center-bombers-1993>].
46. Sloan S. Placing Terrorism in an Academic and Personal Context: A Case Study of the Oklahoma City Bombing. Social Science Quarterly. 2016;97(1):65-74.
47. Gimse LM. The Police: - The bomb in the Government Quarter was 950 kg. Aftenporten Norway 2011.
48. Carroll J, Batt M. Manchester Areana Bombing: Australian Strategic Policy Institute; 2017.
49. Gill P, Horgan J, Lovelace J. Improvised Explosive Device: The Problem of Definition. Studies in Conflict & Terrorism. 2011;34(9):732-48.

50. Reville J. *Improvised Explosive Devices: The Paradigmatic Weapon of New Wars*. 1 ed: Palgrave Macmillan Cham; 2016. 134 p.
51. Thurman JT. *Improvised Explosive Device Components - Pre- and Post-Blast Identification*. *Practical Bomb Scene Investigation* 2ed. Boca Raton, FL: CRC Press; 2011. p. 121-71.
52. Technical Working Group for Bombing Scene Investigation. *A Guide for Explosion and Bombing Scene Investigation* National Institute of Justice; 2000. p. 64.
53. Hoffmann SG, Stallworth SE, Foran DR. Investigative studies into the recovery of DNA from improvised explosive device containers. *Journal of Forensic Science*. 2012;57(3):602-9.
54. McCarthy D. Latent Fingerprint Recovery from Simulated Vehicle-Borne Improvised Explosive Devices. *Journal of Forensic Identification*. 2012;62(5):488-516.
55. Ramasamy S, Houspian A, Knott F. Recovery of DNA and fingermarks following deployment of render-safe tools for vehicle-borne improvised explosive devices (VBIED). *Forensic Science International*. 2011;210(1-3):182-7.
56. Sanders N. Recovery of Fingerprint Evidence from Post-Blast Device Materials. *Journal of Forensic Identification*. 2010;61(3):281-95.
57. Al-Snan NR. The recovery of touch DNA from RDX-C4 evidences. *International Journal of Legal Medicine* 2021;135(2):393-7.
58. Houck M, Siegel J. *Criminal Justice and Forensic Science Fundamentals of Forensic Science* San Diego: Elsevier Science & Technology; 2006. p. 3-26.
59. Marshall M, Oxley JC. *The Detection Problem Aspects of Explosive Detection*. Radarweg: Elsevier; 2008. p. 1-10.
60. Thurman JT. *Investigations of the Explosions Scene and Collection of Evidence*. *Practical Bomb Scene Investigation* 2ed. Boca Raton, FL: CRC Press; 2011. p. 185-278.
61. Marshall M. *Post-blast Detection Issues*. *Aspects of Explosive Detection*. Radarweg: Elsevier; 2008. p. 223-42.

62. Theron F. Explosive Precursors: Fighting the misuse of chemicals by terrorists. European Parliamentary Research Service. 2019.
63. Underwriters Laboratories. Ammonium nitrate in Australia: UL LLC; 2020 [Accessed November 24 2021]. Available from:  
<https://www.ul.com/news/ammonium-nitrate-australia>.
64. Orica. Operations - Orica Kooragang Island [Available from:  
<https://www.orica.com/Locations/Asia-Pacific/Australia/Kooragang-Island/Operations#ammonium>].
65. Dorsey Jr JJ. Pilot Plant- Ammonium Nitrate by the Stengel Process. Industrial & Engineering Chemistry. 2002;47(1):11-7.
66. Government WA. Overview of Security Sensitive Ammonium Nitrate Regulations. Department of Mines and Petroleum. 2016.
67. Mahadevan EG. Ammonium Nitrate and AN/FO. Ammonium Nitrate Explosives for Civil Applications: Slurries, Emulsions and Ammonium Nitrate Fuel Oils. Weinheim, Germany WILEY-VCH Verlag GmbH & Co. KGaA; 2013. p. 31-58.
68. Oxley JC, Smith JL, Naik S, Moran J. Decompositions of Urea and Guanidine Nitrates. Journal of Energetic Materials. 2008;27(1):17-39.
69. Eggers R. Industrial High Pressure Applications: Processes, Equipment, and Safety. 1 ed: John Wiley & Sons, Incorporated; 2012. 424 p.
70. World Urea Statistics by Region 2009-2020: International Fertilizer Association; 2021 [Available from:  
<https://www.ifastat.org/supply/Nitrogen%20Products/Urea>].
71. World Ammonium Nitrate Statistics by Region 2009-2020: International Fertilizer Association; 2021 [Available from:  
<https://www.ifastat.org/supply/Nitrogen%20Products/AN%20and%20CAN>].
72. Decision No 1348/2008/EC of the European Parliament and of the Council. Official Journal of the European Union. 2008;OJ L 348:108-12.

73. Brust H, Koeberg M, van der Heijden A, Wiarda W, Mugler I, Schrader M, et al. Isotopic and elemental profiling of ammonium nitrate in forensic explosives investigations. *Forensic Science International*. 2015;248:101-12.
74. Porter SJ. Method of Desensitizing Fertilizer Grade Ammonium Nitrate and the Product Obtained. United States Patent Office. 1968;3,366,468.
75. Oxley JC, Smith JL, Vadlamannati S, Brown AC, Zhang G, Swanson DS, et al. Synthesis and Characterization of Urea Nitrate and Nitrourea. *Propellants, Explosives, Pyrotechnics*. 2013;38(3):335-44.
76. Cui K, Xu Z, Xu G, Meng Z, Liu W, Shi X, et al. Design and Synthesis of Hydrolytically Stable N-Nitrourea Explosives. *Propellants, Explosives, Pyrotechnics*. 2015;40(6):908-13.
77. Cui K, Xu G, Xu Z, Wang P, Xue M, Meng Z, et al. Synthesis and Characterization of a Thermally and Hydrolytically Stable Energetic Material based on N-Nitrourea. *Propellants, Explosives, Pyrotechnics*. 2014;39(5):662-9.
78. Wang Z, Cao D, Xu Z, Wang J, Chen L. Thermal safety study on the synthesis of HMX by nitrourea method. *Process Safety and Environmental Protection*. 2020;137:282-8.
79. Mitchell AR, Pagoria PF, Coon CL, Jessop ES, Poco JF, Tarver CM, et al. Nitroureas 1. Synthesis, Scale-up and Characterization of K-6. *Propellants, Explosives, Pyrotechnics*. 1994;19:232-9.
80. Klapotke TM. Classification of Energetic Materials. *Chemistry of High-Energy Materials 3ed*: De Gruyter, Inc; 2015. p. 45-98.
81. Conkling JA, Mocella CJ. *Pyrotechnic Principles*. *Chemistry of Pyrotechnics*. 2 ed. Boca Raton, FL: CRC Press; 2011. p. 97-112.
82. Davis DTL. *Pyrotechnics. The Chemistry of Powder and Explosives* San Francisco: Hauraki Publishing 2016. p. 52-118.
83. Conkling JA, Mocella CJ. *Components of High-Energy Mixtures*. *Chemistry of Pyrotechnics: Basic Principles and Theory*. 2 ed. Boca Raton, FL: CRC Press; 2011. p. 59-96.

84. Akhavan J. Introduction to Propellants and Pyrotechnics. *The Chemistry of Explosives*. 3 ed: The Royal Society of Chemistry; 2011. p. 162-77.
85. Davis DTL. Black Powder. *The Chemistry of Powder and Explosives*. San Francisco: Hauraki Publishing; 2016. p. 33-51.
86. Naik V, Patil KC. High Energy Materials: A Brief History and Chemistry of Fireworks and Rocketry. *Resonance*. 2015;431-44.
87. Phillips SA. Pyrotechnic residues analysis – detection and analysis of characteristic particles by scanning electron microscopy/energy dispersive spectroscopy. *Science & Justice*. 2001;41(2):73-80.
88. Martín-Alberca C, García-Ruiz C. Analytical techniques for the analysis of consumer fireworks. *Trends in Analytical Chemistry*. 2014;56:27-36.
89. Russel MS. *The Chemistry of Fireworks*. 2 ed. Cambridge, UK: The Royal Society of Chemistry 2008.
90. Government W. Dangerous Goods Safety (Explosives) Regulations. *Dangerous Goods Safety Act 2004*. 2007;6541-717.
91. Conkling JA, Mocella CJ. *Chemistry of Pyrotechnics: Basic Principles and Theory*. 2 ed. Boca Raton, FL: CRC Press; 2011. 242 p.
92. Oxley JC, Smith JL, Bernier ET, Sandstrom F, Weiss GG, Recht GW, et al. Characterizing the Performance of Pipe Bombs. *Journal of Forensic Science*. 2018;63(1):86-101.
93. TWGFEX Laboratory Explosion Group Standards & Protocols Committee. *Recommended Guidelines for Forensic Identification of Intact Explosives 2007*. p. 4.
94. TWGFEX Laboratory Explosion Group Standards & Protocols Committee. *Recommended Guidelines for Forensic Identification of Post-Blast Explosives Residues 2007*. p. 9.
95. Zapata F, Garcia-Ruiz C. The discrimination of 72 nitrate, chlorate and perchlorate salts using IR and Raman spectroscopy. *Spectrochimica Acta Part A: Molecular and Biomolecular Spectroscopy*. 2018;189:535-42.

96. Hargadon KA, McCord BR. Explosive residue analysis by capillary electrophoresis and ion chromatography. *Journal of Chromatography*. 1992;602:241-7.
97. Johns C, Shellie RA, Potter OG, O'Reilly JW, Hutchinson JP, Guijt RM, et al. Identification of homemade inorganic explosives by ion chromatographic analysis of post-blast residues. *Journal of Chromatography A*. 2008;1182(2):205-14.
98. Hopper KG, Leclair H, McCord BR. A novel method for analysis of explosives residue by simultaneous detection of anions and cations via capillary zone electrophoresis. *Talanta*. 2005;67(2):304-12.
99. Castro K, de Vallejuelo SF-O, Astondoa I, Goñi FM, Madariaga JM. Analysis of confiscated fireworks using Raman spectroscopy assisted with SEM-EDS and FTIR. *Journal of Raman Spectroscopy*. 2011;42(11):2000-5.
100. Saiz J, Duc MT, Koenka IJ, Martin-Alberca C, Hauser PC, Garcia-Ruiz C. Concurrent determination of anions and cations in consumer fireworks with a portable dual-capillary electrophoresis system. *Journal of Chromatography A*. 2014;1372C:245-52.
101. Bezemer KDB, Forbes TP, Hulsbergen AWC, Verkouteren J, Krauss ST, Koeberg M, et al. Emerging techniques for the detection of pyrotechnic residues from seized postal packages containing fireworks. *Forensic Science International*. 2020;308:110160.
102. He N, Ni Y, Teng J, Li H, Yao L, Zhao P. Identification of inorganic oxidizing salts in homemade explosives using Fourier transform infrared spectroscopy. *Spectrochimica Acta Part A: Molecular and Biomolecular Spectroscopy*. 2019;221:117164.
103. Martin-Alberca C, Zapata F, Carrascosa H, Ortega-Ojeda FE, Garcia-Ruiz C. Study of consumer fireworks post-blast residues by ATR-FTIR. *Talanta*. 2016;149:257-65.
104. Hutchinson JP, Johns C, Breadmore MC, Hilder EF, Guijt RM, Lennard C, et al. Identification of inorganic ions in post-blast explosive residues using portable CE instrumentation and capacitively coupled contactless conductivity detection. *Electrophoresis*. 2008;29(22):4593-602.



105. Brown KE, Greenfield MT, McGrane SD, Moore DS. Advances in explosives analysis-part II: photon and neutron methods. *Anal Bioanal Chem.* 2016;408:49-65.
106. Zitrin S, Tamiri T. *Analysis of Explosives by Infrared Spectrometry. Forensic Investigation of Explosives* Boca Raton, FL: CRC Press; 2012. p. 671-87.
107. Castro K, Fdez-Ortiz de Vallejuelo S, Astondoa I, Goni FM, Madariaga JM. Are these liquids explosive? Forensic analysis of confiscated indoor fireworks. *Anal Bioanal Chem.* 2011;400:3065-71.
108. Kosanke KL, Dujay RC, Kosanke BJ. Pyrotechnic reaction residue particle analysis. *Journal of Forensic Science.* 2006;51(2):296-302.
109. Klapac DJ, Czarnopys G, Pannuto J. Interpol review of detection and characterization of explosives and explosives residues 2016-2019. *Forensic Science International: Synergy* 2. 2020;2:670-700.
110. Valdes ER, Hoang KT. *X-ray Fluorescence Spectroscopy for Analysis of Explosive-Related Materials and Unknowns.* Aberdeen Proving Ground, MD: Edgewood Chemical Biological Centre; 2017. Contract No.: ECBC-TR-1455.
111. Margui E, Van GR. *Basic Principles of X-ray Fluorescence. X-ray fluorescence spectrometry and related techniques: An introduction:* Momentum Press; 2013. p. 1-7.
112. Birkholz M. *Principles of X-ray Diffraction. Thin Film Analysis by X-ray Scattering:* Wiley-VCH; 2005. p. 1-40.
113. McCord BR, Corbin I, Bender EC. *Chromatography of Explosives. Forensic Investigation of Explosions.* Boca Raton, FL: CRC Press; 2012. p. 586-615.
114. Martin-Alberca C, de la Ossa MA, Saiz J, Ferrando JL, Garcia-Ruiz C. Anions in pre- and post-blast consumer fireworks by capillary electrophoresis. *Electrophoresis.* 2014;35(21-22):3272-80.
115. Dicinoski GW, Shellie RA, Haddad PR. Forensic Identification of Inorganic Explosives by Ion Chromatography. *Analytical Letters.* 2006;39(4):639-57.

116. de Perre C, McCord B. Trace analysis of urea nitrate by liquid chromatography-UV/fluorescence. *Forensic Science International*. 2011;211(1-3):76-82.
117. Almog J, Espino D, Tamiri T, Sonenfeld D. Trace analysis of urea nitrate in post-blast debris by GC/MS. *Forensic Science International*. 2013;224(1-3):80-3.
118. Kumar R, Sharma V. Chemometrics in forensic science. *Trends in Analytical Chemistry*. 2018;105:191-201.
119. Sauzier G, van Bronswijk W, Lewis SW. Chemometrics in forensic science: approaches and applications. *Analyst*. 2021;146(8):2415-48.
120. Popovic A, Morelato M, Roux C, Beavis A. Review of the most common chemometric techniques in illicit drug profiling. *Forensic Science International* 2019;302:109911.
121. Sharma V, Kumar R. Trends of chemometrics in bloodstain investigations. *Trends in Analytical Chemistry*. 2018;107:181-95.
122. Bueno J, Lednev IK. Advanced statistical analysis and discrimination of gunshot residue implementing combined Raman and FT-IR data. *Analytical Methods*. 2013;5(22).
123. Bueno J, Lednev IK. Raman microspectroscopic chemical mapping and chemometric classification for the identification of gunshot residue on adhesive tape. *Anal Bioanal Chem*. 2014;406(19):4595-9.
124. Karahacane DS, Dahmani A, Khimeche K. Raman spectroscopy analysis and chemometric study of organic gunshot residues originating from two types of ammunition. *Forensic Science International*. 2019;301:129-36.
125. Chang KH, Yew CH, Abdullah AF. Optimization of headspace solid-phase microextraction technique for extraction of volatile smokeless powder compounds in forensic applications. *Journal of Forensic Science*. 2014;59(4):1100-8.
126. Steffen S, Otto M, Niewoehner L, Barth M, Brożek-Mucha Z, Biegstraaten J, et al. Chemometric classification of gunshot residues based on energy dispersive X-ray microanalysis and inductively coupled plasma analysis with mass-spectrometric detection. *Spectrochimica Acta Part B: Atomic Spectroscopy*. 2007;62(9):1028-36.

127. Reese KL, Jones AD, Smith RW. Characterization of smokeless powders using multiplexed collision-induced dissociation mass spectrometry and chemometric procedures. *Forensic Science International*. 2017;272:16-27.
128. Figueroa-Navedo AM, Galán-Freyre NJ, Pacheco-Londoño LC, Hernández-Rivera SP. Chemometrics-enhanced laser-induced thermal emission detection of PETN and other explosives on various substrates. *Journal of Chemometrics*. 2015;29(6):329-37.
129. Moros J, Serrano J, Sánchez C, Macías J, Laserna JJ. New chemometrics in laser-induced breakdown spectroscopy for recognizing explosive residues. *Journal of Analytical Atomic Spectrometry*. 2012;27(12).
130. Gottfried JL, De Lucia Jr FC, Miziolek AW. Discrimination of explosive residues on organic and inorganic substrates using laser-induced breakdown spectroscopy. *Journal of Analytical Atomic Spectrometry*. 2009;24(3).
131. Zadora G. Chemometrics and Statistical Considerations in Forensic Science. *Encyclopedia of Analytical Chemistry* 2010.
132. Fernandez de la Ossa MA, Amigo JM, Garcia-Ruiz C. Detection of residues from explosive manipulation by near infrared hyperspectral imaging: a promising forensic tool. *Forensic Science International*. 2014;242:228-35.
133. Almeida MR, Logrado LPL, Zacca JJ, Correa DN, Poppi RJ. Raman hyperspectral imaging in conjunction with independent component analysis as a forensic tool for explosive analysis: The case of an ATM explosion. *Talanta*. 2017;174:628-32.
134. Suppajariyawat P, Elie M, Baron M, Gonzalez-Rodriguez J. Classification of ANFO samples based on their fuel composition by GC-MS and FTIR combined with chemometrics. *Forensic Science International* 2019;301:415-25.
135. Fraga CG, Mitroshkov AV, Mirjankar NS, Dockendorff BP, Melville AM. Elemental source attribution signatures for calcium ammonium nitrate (CAN) fertilizers used in homemade explosives. *Talanta*. 2017;174:131-8.
136. Ribaux O, Margot P, Julian R, Kelty SF. Forensic Intelligence. *Encyclopedia of Forensic Sciences*. 2 ed: Elsevier; 2013. p. 298-302.

137. Bruenisholz E, Prakash S, Ross A, Morelato M, O'Malley T, Raymond MA, et al. The Intelligent Use of Forensic Data: An Introduction to the Principles. *Forensic Science Policy & Management: An International Journal*. 2016;7(1-2):21-9.
138. Ribaux O, Walsh SJ, Margot P. The contribution of forensic science to crime analysis and investigation: forensic intelligence. *Forensic Science International*. 2006;156(2-3):171-81.
139. Wilson LE, Gahan ME, Lennard C, Robertson J. The forensic intelligence continuum in the military context. *Australian Journal of Forensic Sciences*. 2018;52(1):3-15.
140. Morelato M, Beavis A, Tahtouh M, Ribaux O, Kirkbride P, Roux C. The use of forensic case data in intelligence-led policing: the example of drug profiling. *Forensic Science International*. 2013;226(1-3):1-9.
141. Legrand T, Vogel L. The landscape of forensic intelligence research. *Australian Journal of Forensic Sciences*. 2014;47(1):16-26.
142. Vane MA, Quantock DE. Countering the Improvised Explosive Device Threat. *Army*. 2011;61(3).
143. Pierce KM, Hope JL, Johnson KJ, Wright BW, Synovec RE. Classification of gasoline data obtained by gas chromatography using a piecewise alignment algorithm combined with feature selection and principal component analysis. *J Chromatogr A*. 2005;1096(1-2):101-10.
144. Johnson KJ, Synovec RE. Pattern recognition of jet fuels : comprehensive GCxGC with ANOVA-based feature selection and principal component analysis. *Chemometrics and Intelligent Laboratory Systems*. 2002;60:225-37.
145. Bezemer K, Woortmeijer R, Koeberg M, Schoenmakers P, van Asten A. Multicomponent characterization and differentiation of flash bangers - Part I: Sample collection and visual examination. *Forensic Science International*. 2018;290:327-35.
146. Nic Daeid N, Waddell RJH. The analytical and chemometric procedures used to profile illicit drug seizures. *Talanta*. 2005;67:280-5.
147. Dujourdy L, Dufey V, Besacier F, Miano N, Marquis R, Lock E, et al. Drug intelligence based on organic impurities in illicit MA samples. *Forensic Science International* 2008;177:153-61.

148. Yang S, Li P, Liu J, Bi X, Ning Y, Wang S, et al. Profiles, source identification and health risks of potentially toxic metals in pyrotechnic-related road dust during Chinese New Year. *Ecotoxicology and Environmental Safety*. 2019;184:109604.
149. Sabatini JJ. A Review of Illuminating Pyrotechnics. *Propellants, Explosives, Pyrotechnics*. 2017;43(1):28-37.
150. Betha R, Balasubramanian R. Particulate Emissions from Commercial Handheld Sparklers: Evaluation of Physical Characteristics and Emission Rates. *Aerosol and Air Quality Research*. 2013;13(1):301-7.
151. McManus HD, Wiqal VF, Long RS. Sparkler composition. Patent 3862865. 1975.
152. Danali SM, Palaiah RS, Raha KC. Developments in Pyrotechnics. *Defense Science Journal*. 2010;60(2):152-8.
153. Henderson IK, Saari-Nordhaus R. Analysis of commercial explosives by single-column ion chromatography. *Journal of Chromatography*. 1992;602:149-54.
154. Kolla P. Gas Chromatography, liquid chromatography and ion chromatography adapted to the trace analysis of explosives. *Journal of Chromatography A*. 1994;674:309-18.
155. Gaurav D, Malik AK, Rai PK. High-Performance Liquid Chromatographic Methods for the Analysis of Explosives. *Critical Reviews in Analytical Chemistry*. 2007;37(4):227-68.
156. Yinon J, Zitrin S. Modern methods and applications in analysis of explosives. *Trends in Analytical Chemistry*. 1994;13(3).
157. Coffee KR, Panasci-Nott AF, Stewart BJ, Olivas JA, Williams AM, Reynolds JG. Trace Compound Analysis in TATB by Liquid Chromatography coupled with Spectroscopic and Spectrometric Detection. *Propellants, Explosives, Pyrotechnics*. 2022;47(4).
158. Botti S, Cantarini L, Palucci A. Surface-enhanced Raman spectroscopy for trace-level detection of explosives. *Journal of Raman Spectroscopy*. 2010;41(8):866-9.

159. Vermeij E, Duvalois W, Webb R, Koeberg M. Morphology and composition of pyrotechnic residues formed at different levels of confinement. *Forensic Science International* 2009;186(1-3):68-74.
160. Ewing RG, Atkinson DA, Eiceman GA, Ewing GJ. A critical review of ion mobility spectrometry for the detection of explosives and explosive related compounds. *Talanta*. 2001;54:515-29.
161. López-López M, García-Ruiz C. Infrared and Raman spectroscopy techniques applied to identification of explosives. *Trends in Analytical Chemistry*. 2014;54:36-44.
162. Peng L, Hua L, Wang W, Zhou Q, Li H. On-site rapid detection of trace non-volatile inorganic explosives by stand-alone ion mobility spectrometry via acid-enhanced evaporation. *Scientific Reports* 2014;4:6631.
163. Sokol E, Jackson A, Cooks R. Trace detection of inorganic oxidants using desorption electrospray ionization (DESI) mass spectrometry. *Central European Journal of Chemistry* 2011;9(5):790-7.
164. Eastman. High-solids polyester resins for appliance and general metal coatings. N-321D. 2013;2(13):1-6.
165. Benson SJ, Lennard CJ, Maynard P, Hill DM, Andrew AS, Roux C. Forensic analysis of explosives using isotope ratio mass spectrometry (IRMS)--discrimination of ammonium nitrate sources. *Science & Justice*. 2009;49(2):73-80.
166. Zygmunt B, Buczkowski D. Agriculture Grade Ammonium Nitrate as the Basic Ingredient of Massive Explosive Charges. *Propellants, Explosives, Pyrotechnics*. 2012;37(6):685-90.
167. Lotspeich E, Petr V. The Characterization of Ammonium Nitrate Mini-Prills. In: Song B, Casem D, Kimberley J, editors. *Dynamic Behavior of Materials, Volume 1: Proceedings of the 2014 Annual Conference on Experimental and Applied Mechanics*. Cham, Switzerland: Springer; 2015. p. 319-24.
168. Marlair G, Kordek MA. Safety and security issues relating to low capacity storage of AN-based fertilizers. *Journal of Hazardous Materials*. 2005;123(1-3):13-28.

169. Fabin M, Jarosz T. Improving ANFO: Effect of Additives and Ammonium Nitrate Morphology on Detonation Parameters. *Materials (Basel)*. 2021;14(19).
170. Zygmunt B, Buczkowski D. Influence of Ammonium Nitrate Prills' Properties on Detonation Velocity of ANFO. *Propellants, Explosives, Pyrotechnics*. 2007;32(5):411-4.
171. Presles H-N, Vidal P, Khasainov B. Experimental study of the detonation of technical grade ammonium nitrate. *Comptes Rendus Mécanique*. 2009;337(11-12):755-60.
172. Hu C, Mei H, Guo H, Yu Z, Zhu J. Purification of ammonium nitrate via recrystallization for isotopic profiling using isotope ratio mass spectrometry. *Forensic Science International*. 2021;328:111009.
173. Kaniewski M, Hoffmann K, Hoffmann J. Influence of selected potassium salts on thermal stability of ammonium nitrate. *Thermochimica Acta*. 2019;678.
174. Sinditskii VP, Egorshv VY, Levshenkov AI, Serushkin VV. Ammonium Nitrate: Combustion Mechanism and the Role of Additives. *Propellants, Explosives, Pyrotechnics*. 2005;30(4):269-80.
175. Gromov AA, Popenko EM, Sergienko AV, Slyusarsky KV, Nalivaiko AY, Ozherelkov DY, et al. Characterization of Aluminum Powders: IV. Effect of Nanometals on the Combustion of Aluminized Ammonium Nitrate-Based Solid Propellants. *Propellants, Explosives, Pyrotechnics*. 2021;46(3):450-9.
176. Izato Y-i, Miyake A, Date S. Combustion Characteristics of Ammonium Nitrate and Carbon Mixtures Based on a Thermal Decomposition Mechanism. *Propellants, Explosives, Pyrotechnics*. 2013;38(1):129-35.
177. Kohga M. Thermal Decomposition Behaviors and Burning Characteristics of Ammonium Nitrate/Polytetrahydrofuran/Glycerin-based Composite Propellants Supplemented with MnO<sub>2</sub> and Fe<sub>2</sub>O<sub>3</sub>. *Propellants, Explosives, Pyrotechnics*. 2017;42(6):665-70.
178. Anderson EK, Short M, Jackson SI. Cylinder test wall velocity profiles and product energy for an ammonium nitrate and aluminum explosive. *American Institute of Physics Conference Proceedings* 2017;1793.

179. Preston DN, Brown GW, Sandstrom MM, Pollard CJ, Warner KF, Remmers DL, et al. Small-Scale Safety Testing of Ammonium Nitrate and Mixtures. *Propellants, Explosives, Pyrotechnics*. 2016;41(1):9-13.
180. Wharton RK, Royle HJ. Factors that affect the impact sensitiveness of ammonium nitrate - fuel oil (ANFO) explosives containing aluminium. *Journal of Energetic Materials*. 2000;18(2-3):177-205.
181. Tan L, Xia LH, Wu QJ, Xu S, Liu DB. Detonation characteristics of ammonium nitrate and activated fertilizer mixtures. *Combustion, Explosion, and Shock Waves*. 2016;52(3):335-41.
182. Chiquito M, Castedo R, Lopez LM, Santos AP, Mancilla JM, Yenes JI. Blast Wave Characteristics and TNT Equivalent of Improvised Explosive Device at Small-scaled Distances. *Defense Science Journal*. 2019;69(4):328-35.
183. Kavicky V, Figuli L, Jangl S, Ligasová Z. Analysis of the field test results of ammonium nitrate: fuel oil explosives as improvised explosive device charges. *Structures Under Shock and Impact XIII2014*. p. 297-309.
184. Phillips SA, Lowe A, Marshall M, Hubbard P, Burmeister SG, Williams DR. Physical and Chemical Evidence Remaining After the Explosion of Large Improvised Bombs. Part 1: Firings of Ammonium Nitrate/Sugar and Urea Nitrate. *Journal of Forensic Science*. 2000;45(2):324-32.
185. Johnson Jr CM. Counterterrorism: U.S. Agencies Face Challenges Countering the Use of Improvised Explosive Devices in the Afghanistan/Pakistan Region. United States Government Accountability Office. 2012.
186. Yang M, Chen X, Wang Y, Yuan B, Niu Y, Zhang Y, et al. Comparative evaluation of thermal decomposition behavior and thermal stability of powdered ammonium nitrate under different atmosphere conditions. *Journal of Hazardous Materials*. 2017;337:10-9.
187. Skarlis SA, Nicolle A, Berthout D, Dujardin C, Granger P. Combined experimental and kinetic modeling approaches of ammonium nitrate thermal decomposition. *Thermochimica Acta*. 2014;584:58-66.
188. Chaturvedi S, Dave PN. Review on Thermal Decomposition of Ammonium Nitrate. *Journal of Energetic Materials*. 2013;31(1):1-26.



189. Izato Y-i, Miyake A. Thermal decomposition mechanism of ammonium nitrate and potassium chloride mixtures. *Journal of Thermal Analysis and Calorimetry*. 2015;121(1):287-94.
190. Oxley JC, Smith JL, Rogers E, Yu M. Ammonium nitrate: thermal stability and explosivity modifiers. *Thermochimica Acta*. 2002;384:23-45.
191. Sun J, Sun Z, Wang Q, Ding H, Wang T, Jiang C. Catalytic effects of inorganic acids on the decomposition of ammonium nitrate. *Journal of Hazardous Materials*. 2005;127(1-3):204-10.
192. Turcotte R, Lightfoot PD, Fouchard R, Jones DEG. Thermal hazard assessment of AN and AN-based explosives. *Journal of Hazardous Materials*. 2003;101(1):1-27.
193. Ettouney RS, El-Rifai MA. Explosion of ammonium nitrate solutions, two case studies. *Process Safety and Environmental Protection*. 2012;90(1):1-7.
194. Babrauskas V. Explosions of ammonium nitrate fertilizer in storage or transportation are preventable accidents. *Journal of Hazardous Materials*. 2016;304:134-49.
195. Dechy N, Bourdeaux T, Ayrault N, Kordek MA, Le Coze JC. First lessons of the Toulouse ammonium nitrate disaster, 21st September 2001, AZF plant, France. *Journal of Hazardous Materials*. 2004;111(1-3):131-8.
196. Pittman W, Han Z, Harding B, Rosas C, Jiang J, Pineda A, et al. Lessons to be learned from an analysis of ammonium nitrate disasters in the last 100 years. *Journal of Hazardous Materials*. 2014;280:472-7.
197. Ur Rehman S, Ahmed R, Ma K, Xu S, Aslam MA, Bi H, et al. Ammonium nitrate is a risk for environment: A case study of Beirut (Lebanon) chemical explosion and the effects on environment. *Ecotoxicology and Environmental Safety*. 2021;210:111834.
198. Mahadevan EG. Functional Safety during Manufacture of AN Explosives. *Ammonium Nitrate Explosives for Civil Applications: Slurries, Emulsions and Ammonium Nitrate Fuel Oils*. Weinheim, Germany WILEY-VCH Verlag GmbH & Co. KGaA; 2013. p. 163-77.

199. Zapata F, de la Ossa MAF, Gilchrist E, Barron L, Garcia-Ruiz C. Progressing the analysis of Improvised Explosive Devices: Comparative study for trace detection of explosive residues in handprints by Raman spectroscopy and liquid chromatography. *Talanta*. 2016;161:219-27.
200. Banas A, Banas K, Lim SK, Loke J, Breese M. Broad Range FTIR Spectroscopy and Multivariate Statistics for High Energetic Materials Discrimination. *Anal Chem*. 2020;92(7):4788-97.
201. Schachel TD, Stork A, Schulte-Ladbeck R, Vielhaber T, Karst U. Identification and differentiation of commercial and military explosives via high performance liquid chromatography - high resolution mass spectrometry (HPLC-HRMS), X-ray diffractometry (XRD) and X-ray fluorescence spectroscopy (XRF): Towards a forensic substance database on explosives. *Forensic Science International*. 2020;308:110180.
202. Soldate AM, Noyes RM. X-Ray Diffraction Patterns for the Identification of Crystalline Constituents of Explosives. *Analytical Chemistry*. 1947;19(7):442-4.
203. Bezemer K, McLennan L, van Duin L, Kuijpers CJ, Koeberg M, van den Elshout J, et al. Chemical attribution of the home-made explosive ETN - Part I: Liquid chromatography-mass spectrometry analysis of partially nitrated erythritol impurities. *Forensic Science International*. 2020;307:110102.
204. Bezemer KD, Koeberg M, van der Heijden AE, van Driel CA, Blaga C, Bruinsma J, et al. The Potential of Isotope Ratio Mass Spectrometry (IRMS) and Gas Chromatography-IRMS Analysis of Triacetone Triperoxide in Forensic Explosives Investigations. *Journal of Forensic Science*. 2016;61(5):1198-207.
205. Chajistamatiou A, Angelis Y, Kiouisi P, Tsivou M, Bakeas E. Discrimination of tetryl samples by gas chromatography – Isotope ratio mass spectrometry. *Forensic Chemistry*. 2019;12:42-5.
206. Benson S, Lennard C, Maynard P, Roux C. Forensic applications of isotope ratio mass spectrometry - A review. *Forensic Science International*. 2006;157(1):1-22.

207. Alvarez A, Yanez J, Contreras D, Saavedra R, Saez P, Amarasiriwardena D. Propellant's differentiation using FTIR-photoacoustic detection for forensic studies of improvised explosive devices. *Forensic Science International*. 2017;280:169-75.
208. Ceto X, AM OM, Wang J, Del Valle M. Simultaneous identification and quantification of nitro-containing explosives by advanced chemometric data treatment of cyclic voltammetry at screen-printed electrodes. *Talanta*. 2013;107:270-6.
209. Manutec. African Violet Food - Soluble. Material Safety Data Sheet. 2014.
210. Biessikirski A, Pytlik M, Kuterasiński Ł, Dworzak M, Twardosz M, Napruszewska BD. Influence of the Ammonium Nitrate(V) Porous Prill Assortments and Absorption Index on Ammonium Nitrate Fuel Oil Blasting Properties. *Energies*. 2020;13(15).
211. Goel V, Mishra SK, Sharma C, Sarangi B, Aggarwal SG, Agnihotri R, et al. A Non-destructive FTIR Method for the Determination of Ammonium and Sulfate in Urban PM2.5 Samples. *Journal of Metrology Society of India* 2018;33(3):209-15.
212. Kadam SS, Mesbah A, van der Windt E, Kramer HJM. Rapid online calibration for ATR-FTIR spectroscopy during batch crystallization of ammonium sulphate in a semi-industrial scale crystallizer. *Chemical Engineering Research and Design*. 2011;89(7):995-1005.
213. Schlack TR, Beal SA, Corriveau EJ, Clausen JL. Detection Limits of Trinitrotoluene and Ammonium Nitrate in Soil by Raman Spectroscopy. *ACS Omega*. 2021;6(25):16316-23.
214. Farrell ME, Holthoff EL, Pellegrino PM. Surface-enhanced Raman scattering detection of ammonium nitrate samples fabricated using drop-on-demand inkjet technology. *Applied Spectroscopy* 2014;68(3):287-96.
215. Diaz D, Hahn DW. Raman spectroscopy for detection of ammonium nitrate as an explosive precursor used in improvised explosive devices. *Spectrochim Acta A Mol Biomol Spectrosc*. 2020;233:118204.
216. Dunuwille M, Yoo CS. Phase diagram of ammonium nitrate. *Journal of Chemical Physics*. 2013;139(21):214503.

217. Fontana MD, Ben Mabrouk K, Kauffmann TH. Raman spectroscopic sensors for inorganic salts. *Spectroscopic Properties of Inorganic and Organometallic Compounds. Spectroscopic Properties of Inorganic and Organometallic Compounds* 2013. p. 40-67.
218. Sherrill WM. *Synthesis, Characterization and Sensitivity Analysis of Urea Nitrate (UN)*. US Army Research Laboratory; 2015. Contract No.: ARL-TR-7250.
219. Worsham Jr JE, Busing WR. The Crystal Structure of Uronium Nitrate (Urea Nitrate) by Neutron Diffraction. *Acta Crystallographica Section B*. 1969;25:572-8.
220. Elbasuney S, El-Sherif AF. Instant detection and identification of concealed explosive-related compounds: Induced Stokes Raman versus infrared. *Forensic Science International*. 2017;270:83-90.
221. Almog J, Klein A, Tamiri T, Shloosh Y, Abramovich-Bar S. A Field Diagnostic Test for the Improvised Explosive Urea Nitrate. *Journal of Forensic Science*. 2005;50(3).
222. de Perre C, Prado A, McCord BR. Rapid and specific detection of urea nitrate and ammonium nitrate by electrospray ionization time-of-flight mass spectrometry using infusion with crown ethers. *Rapid Communications in Mass Spectrometry*. 2012;26(2):154-62.
223. Menzel ER, Schwierking JR. Fluorescence Detection of the Explosive Urea Nitrate with p-DMAC. *Journal of Forensic Identification*. 2006;56(3):325-32.
224. Rozin R, Almog J. Colorimetric detection of urea nitrate: the missing link. *Forensic Science International*. 2011;208(1-3):25-8.
225. Lemberger N, Almog J. Structure elucidation of dyes that are formed in the colorimetric detection of the improvised explosive urea nitrate. *Journal of Forensic Science*. 2007;52(5):1107-10.
226. Wang G, Cai Z, Dou X. Colorimetric logic design for rapid and precise discrimination of nitrate-based improvised explosives. *Cell Reports Physical Science*. 2021;2(2).
227. Kunduru KR, Basu A, Abtew E, Tsach T, Domb AJ. Polymeric sensors containing P-dimethylaminocinnamaldehyde: Colorimetric detection of urea nitrate. *Sensors and Actuators B: Chemical*. 2017;238:387-91.

228. Harkema S, Feil D. The crystal structure of urea nitrate. *Acta Crystallographica*. 1969;25:589-91.
229. Désilets S, Brousseau P, Chamberland D, Singh S, Feng H, Turcotte R, et al. Degradation mechanism and thermal stability of urea nitrate below the melting point. *Thermochimica Acta*. 2011;521(1-2):176-83.
230. Li S, Li Q, Wang K, Zhou M, Huang X, Liu J, et al. Pressure-Induced Irreversible Phase Transition in the Energetic Material Urea Nitrate: Combined Raman Scattering and X-ray Diffraction Study. *The Journal of Physical Chemistry C*. 2012;117(1):152-9.
231. Tsai CW, Midey A, Wu C, Yost RA. Analysis of Ammonium Nitrate/Urea Nitrate with Crown Ethers and Sugars as Modifiers by Electrospray Ionization-Mass Spectrometry and Ion Mobility Spectrometry. *Analytical Chemistry* 2016;88(19):9435-42.
232. Tamiri T. Characterization of the improvised explosive urea nitrate using electrospray ionization and atmospheric pressure chemical ionization. *Rapid Communications in Mass Spectrometry* 2005;19(14):2094-8.
233. Almog J, Burda G, Shloosh Y, Abramovich-Bar S, Wolf E, Tamiri T. Recovery and detection of urea nitrate in traces. *Journal of Forensic Science*. 2007;52(6):1284-90.
234. Tamiri T, Rozin R, Lemberger N, Almog J. Urea nitrate, an exceptionally easy-to-make improvised explosive: studies towards trace characterization. *Anal Bioanal Chem*. 2009;395(2):421-8.
235. Corbin I, McCord B. Detection of the improvised explosives ammonium nitrate (AN) and urea nitrate (UN) using non-aqueous solvents with electrospray ionization and MS/MS detection. *Talanta*. 2013;115:533-9.
236. Aranda R, Stern LA, Dietz ME, McCormick MC, Barrow JA, Mothershead RF, 2nd. Forensic utility of isotope ratio analysis of the explosive urea nitrate and its precursors. *Forensic Science International*. 2011;206(1-3):143-9.
237. Scotts. Osmocote plus trace elements total all purpose. *Material Safety Data Sheet*. 2015;228170i(2).

238. Manutec. Green Boost for Foliage & Growth. Material Safety Data Sheet. 2021.
239. Nagli L, Gaft M, Fleger Y, Rosenbluh M. Absolute Raman cross-sections of some explosives: Trend to UV. *Optical Materials*. 2008;30(11):1747-54.
240. Grant B, Sauzier G, Lewis SW. Discrimination of automotive window tint using ATR-FTIR spectroscopy and chemometrics. *Forensic Science International*. 2020;313:110338.
241. Martín-Alberca C, Ferrando JL, García-Ruiz C. Anionic markers for the forensic identification of Chemical Ignition Molotov Cocktail composition. *Science & Justice*. 2013;53(1):49-54.
242. Martín-Alberca C, Sáiz J, Ferrando JL, García-Ruiz C. Qualitative determination of inorganic anions in incendiary device residues by capillary electrophoresis. *Analytical Methods*. 2012;4(9).
243. Wu JY. Determination of Titanium Content as Principal Components in Pyrotechnic Compositions Used for Fireworks and Firecrackers Based on Inductively Coupled Plasma Optical Emission Spectrometric Approach (ICP-OES). *Applied Mechanics and Materials*. 2014;608-609:1010-4.
244. Awasthi S, Kumar R, Rai AK. In situ Analysis of Fireworks Using Laser-Induced Breakdown Spectroscopy and Chemometrics. *Journal of Applied Spectroscopy*. 2017;84(5):811-5.
245. Doyle JM, Miller ML, McCord BR, McCollam DA, Mushrush GW. A Multicomponent Mobile Phase for Ion Chromatography Applied to the Separation of Anions from the Residue of Low Explosives. *Analytical Chemistry*. 2000;72:2302-7.
246. Hutchinson JP, Evenhuis CJ, Johns C, Kazarian AA, Breadmore MC, Macka M, et al. Identification of Inorganic Improvised Explosive Devices by Analysis of Postblast Residues Using Portable Capillary Electrophoresis Instrumentation and Indirect Photometric Detection with a Light-Emitting Diode. *Analytical Chemistry*. 2007;79:7005-13.
247. Government SA. Explosives (Fireworks) Regulations. Regulations under the explosives act 1936. 2001;245.

248. Government NSW. List of authorised explosives and categories of prohibited explosives in NSW. Explosives Regulation 2013. 2022.
249. Udupa MR. Thermal Behaviour of Urea Nitrate. *Thermochimica Acta*. 1982;55:359-62.
250. Hiyoshi RI, Brill TB, Kohno Y, Takahashi O, Saito K. Experimental and Computational Study of the Thermal Decomposition of Uronium Nitrate (Urea Nitrate). 12th International Detonation Symposium, San Diego, CA. 2002.
251. Kohno Y, Takahashi O, Hiyoshi RI, Nakamura J, Saito K. Theoretical Study of the Initial Decomposition Process of the Energetic Material Urea Nitrate. *Journal of Physical Chemistry A*. 2003;107(33):6444-50.
252. Tokmakov IV, Alavi S, Thompson DL. Urea and Urea Nitrate Decomposition pathways: A Quantum Chemistry Study. *J Phys Chem A*. 2006;110(8):2759-70.
253. Désilets S, Brousseau P, Chamberland D, Singh S, Feng H, Turcotte R, et al. Analyses of the thermal decomposition of urea nitrate at high temperature. *Thermochimica Acta*. 2011;521(1-2):59-65.
254. Clark S, Francis PS, Conlan XA, Barnett NW. Determination of urea using high-performance liquid chromatography with fluorescence detection after automated derivatisation with xanthidrol. *Journal of Chromatography A*. 2007;1161(1-2):207-13.
255. Cagan A, Lu D, Cizek K, La Belle J, Wang J. Reliable, rapid and simple voltammetric detection of urea nitrate explosive. *Analyst*. 2008;133(5):585-7.

To whom it may concern

I, **Joshua D'Uva**, contributed conceptualization, investigation, methodology, visualization, writing-original draft, writing-review & editing to the following paper:

D'Uva, J. A., D. DeTata, C. D. May, and S. W. Lewis. 2020. "Investigations into the source attribution of party sparklers using trace elemental analysis and chemometrics." *Analytical Methods* 12 (41): 4939-4948.

I as a Co-Author, endorse that this level of contribution by the candidate indicated above is appropriate.

**David DeTata**

**Christopher May**

**Simon W. Lewis**



To whom it may concern

I, **Joshua D’Uva**, contributed conceptualization, visualization, writing-original draft, writing-review & editing to the following book chapters:

**Joshua A. D’Uva**, David DeTata. Improvised explosive devices. *Encyclopedia of Forensic Sciences*. 3<sup>rd</sup> ed; Elsevier Ltd; 2022. p. 224-231.

David DeTata, Ryan Fillingham, **Joshua A. D’Uva**. Overview of explosives. *Encyclopedia of Forensic Sciences*. 3<sup>rd</sup> ed; Elsevier Ltd; 2022. p. 356-390.

I as a Co-Author, endorse that this level of contribution by the candidate indicated above is appropriate.

**David Detata**

**Ryan Fillingham**

**Simon W. Lewis**

To whom it may concern

I, **Joshua D'Uva**, contributed conceptualization, investigation, methodology, visualization, writing-original draft, writing-review & editing to the following paper:

D'Uva, J., D. DeTata, R. Fillingham, R. Dunsmore, and S. Lewis. 2021. "Synthesis and characterisation of homemade urea nitrate explosive from commercial sources of urea." *Forensic Chemistry* 26: 100369-100369.

I as a Co-Author, endorse that this level of contribution by the candidate indicated above is appropriate.

**David DeTata**

**Ryan Fillingham**

**Robert Dunsmore**

**Simon W. Lewis**

To whom it may concern

I, **Joshua D'Uva**, contributed conceptualization, investigation, methodology, visualization, writing-original draft, writing-review & editing to the following paper:

D'Uva, J., D. DeTata, and S. W. Lewis. 2022. "Source determination of homemade ammonium nitrate using ATR-FTIR spectroscopy, trace elemental analysis and chemometrics." *Forensic Chemistry* 28: 100411-100411.

I as a Co-Author, endorse that this level of contribution by the candidate indicated above is appropriate.

**David DeTata**

**Simon W. Lewis**